THE MEASUREMENT OF GAMMA-RADIATION BY SCINTILLATION COUNTING.

A Thesis submitted to the
University of London for the
Degree of Doctor of Philosophy
in Physics

by

E. H. Belcher, M.A.

Physics Department,
Royal Cancer Hospital,
S. W. 3.

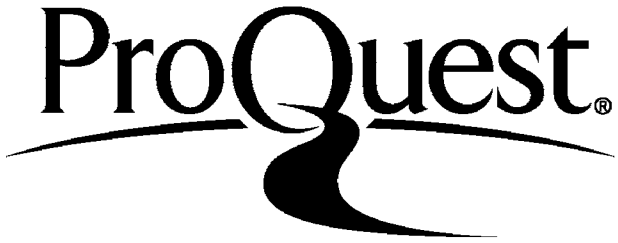

ABSTRACT.

This thesis is concerned with the application of the technique of scintillation counting to the detection of gamma radiation. In counters of this type the scintillations produced in a luminescent medium are detected by means of a photo-multiplier tube and the electrical pulses at the output of the latter are amplified and counted electronically. An attempt is made to interpret the behaviour of such counters and to relate the observed counting rates to the physical processes occuring in the luminophor.

Following a brief historical review of the scintillation counting technique, a theoretical analysis of the gamma scintillation counter is developed. This analysis describes how the number and energy distribution of the secondary electrons produced in a luminophor of known composition and dimensions subjected to a known flux of gamma radiation can be calculated. It shows that, providing the luminescent decay of the luminophor is rapid, each secondary electron will produce a single scintillation the intensity of which will be proportional to the energy of the electron. When the

luminophor has a slow decay, on the other hand, this simple behaviour is not to be expected. The amplitude distribution of the resulting electrical pulses will be modified by statistical processes in the photo-multiplier tube, and by the resolving time of the amplifying and counting equipment.

Experimental studies designed to test the validity of the theoretical analysis are described. The first part of these studies is an investigation of the statistics of the type 1P21 photo-multiplier tube, stimulated by both continuous and pulsed light. The results of this investigation are in good accord with the theoretical predictions.

The crystalline luminophors investigated experimentally included calcium tungstate, thallium-activated potassium iodide, and thallium-activated sodium iodide. Following some preliminary studies on the effect of resolving time on counting rate, the absolute counting rates obtained when specimens of each of these luminophors were irradiated under scatter-free conditions with the gamma radiation from sodium$_{24}$, cobalt$_{60}$, bromine$_{82}$, iodine$_{131}$ and gold$_{198}$ were measured. These rates were then compared with the calculated rates of production of secondary electrons in the media. In the case of calcium tungstate under appropriate conditions, good

agreement between counting rate and rate of secondary electron production was obtained. In the alkali halide luminophors, on the other hand, counting rates were abnormally high because of their relatively slow phosphorescent decay. These findings were confirmed by the study of the pulse amplitude distributions obtained with the luminophors under various experimental conditions.

Studies on the variation in luminescent efficiency with temperature of each of these luminophors, and on the spectral distributions of the emitted light are also described.

Comparative measurements on a large number of liquid luminescent systems were made, with particular reference to the variation in luminescent efficiency with concentration of solute. These variations are interpreted in terms of a general theory due to Johnson and Williams. The system p-terphenyl-benzene was selected for more detailed study and the absolute counting rates obtained in this medium when irradiated by the gamma rays from each of the five radio-isotopes already mentioned were measured. When a correction is applied for the electrons scattered into the medium from the walls of the containing vessel, the observed rates are found to be in good agreement with the calculated rates of production of secondary electrons.

It was observed in the course of the above studies that both pure liquids such as water and transparent solids such as Perspex luminesce under gamma irradiation, and this luminescence is shown to be often explicable in terms of the Čerenkov effect. Detailed studies of this effect in Perspex were carried out, and the angular distributions and relative intensities of the emission due to each of the radio-isotopes: sodium$_{24}$, cobalt$_{60}$, bromine$_{82}$ and iodine$_{131}$ were measured. Good agreement is obtained between the observed results and the classical theory due to Frank and Tamm for the effect.

Finally, experimental studies made on the luminescent decay of a copper-activated zinc sulphide phosphor of long afterglow following excitation by gamma radiation from each of the five radio-isotopes mentioned are described. The decay is shown to be non-exponential in form, but provided that certain precautions are observed, the counting rate at a known time after irradiation can be related to the gamma radiation flux through the phosphor during the exposure.

The thesis ends with a critical discussion of the experimental results and an assessment of their implications, together with some suggestions for future research in this field. Four appendices are included: Appendix I consists of tables of linear absorption coefficients for gamma radiation in various media.

The values of these coefficients have been calculated by the author and are required for the development and application of the theoretical analysis. Appendix II gives values of the ranges of mono-energetic electrons in unit density material. Appendix III gives values for the maximum energies of the Compton recoil electrons produced by gamma radiation of various energies. Appendix IV describes in detail the method used for calculating the rate of production of secondary electrons in a luminophor of known composition and dimensions, subjected to a known flux of gamma radiation.

INDEX TO TEXT

SECTION I - INTRODUCTION.

1. The scintillation counter, which uses a photo-multiplier tube or similar device coupled to an amplifier and recorder to detect the small light pulses produced by ionising radiations in various media, has found increasing favour in the past five years as a sensitive instrument for the measurement of gamma-radiation. In particular, for measurements requiring a high sensitivity to gamma-radiation and a low resolving time, this type of counter may be superior to the more conventional devices at present available to the physicist - the Geiger-Müller counter, the proportional counter, and the ionisation chamber. It has already proved of value in such diverse fields of research as the study of radio-isotope decay schemes, the measurement of extremely short time intervals in nuclear processes, and the clinical dosimetry of radio-isotopes, to mention but a few of its applications.

The scintillation counter must here be clearly distinguished from the "crystal counters" in which the conductivity pulses induced by ionisating radiations in photo-conducting phosphors are amplified

electrically and counted. Such counters have been described by Van Heerden (1945), Frerichs and Warminsky (1946), Jentschke (1947), Wooldridge et al. (1947), and are the subject of a review by Hofstadter (1949 a, b,).

Since the publication by Kallman (1947 a, b, c) of the first reports of the extension of the scintillation counting technique to the measurement of gamma-radiation, a considerable volume of literature describing the design and application of these counters has appeared. The work so described has been mainly empirical in nature; attention has been directed towards the development of improved luminophors and the classification of their properties, rather than towards the better understanding of the physical processes responsible for the production of scintillations in certain media. In an excellent review, Jordan and Bell (1949) write: "It is difficult to survey the published data and decide what phosphors have the highest efficiency. Some investigators have made measurements on powdered crystals, others on single crystals. Absolute efficiency measurements are rare; usually the phosphor is compared to

anthracene or naphthalene."

In any measuring device for gamma-radiation, and especially in one to be used for clinical dosimetry, a knowledge of absolute efficiency is of fundamental importance. It is desirable always to be able to relate the observed readings to the absolute flux of gamma-radiation through the sensitive volume of the instrument. The studies described in this thesis were accordingly initiated by Mayneord in 1948, and extended by the author, in an effort to elucidate the physical principles of scintillation counting. The general form of these studies will be described in section I.3 below, but first it will be of value briefly to review the state of the technique at the time these studies began, and its progress since that time.

2. SHORT HISTORICAL REVIEW:-

It was known to the early workers on radio-activity that alpha-particles produced scintillations in many materials. In the spinthariscope of Crookes (1903) and Regener (1908) this principle was utilised to detect such particles, the flashes produced when

they impinged on a zinc sulphide screen being observed and counted in a low-power microscope. Rutherford (1913) refers frequently to such measurements. However, the technique was tedious and restricted to low counting rates; because of this, the device was soon to be abandoned in favour of the proportional counter.

Becquerel (1899) was aware that fast electrons also exerted luminescence in many materials, but it was not until the development of a sensitive detector in the shape of the photo-multiplier tube that the small scintillations produced by beta- and gamma-radiation could be individually observed and counted. Following the work of Zworykin and his co-workers (1936) and of Allen (1939) on secondary electron-multipliers, and the discovery by Görlich (1936) of the antimony-alkali photo-sensitive cathode, the design of compact photo-multiplier tubes of high gain became possible. In 1940 the construction of such a tube - the R.C.A. type 931^{A} - was described by Rajchman and Snyder. This photo-multiplier was to be the prototype of several others,

such as the types I P 21 and I P 28, differing from it in spectral response and overall gain; the latter have been described by Morton and Mitchell (1948) and by Rodda (1949). All these are nine-stage photo-multipliers, having the photo-cathode mounted inside the glass envelope. More recently, ten- and eleven-stage tubes of various designs have become available, which have the photo cathode deposited on the envelope, permitting a more efficient optical coupling between the luminophor and the photo-sensitive surface; examples of this mode of construction are the R.C.A. type 5819 and the E.M.I. type 5311.

The application of the photo-multiplier to the measurement of very low light levels was discussed in detail by Engström (1947 a), who emphasized the necessity for cooling the tube to low temperatures in order to reduce the dark current due to thermionic emission from the photo-cathode, if low intensities of visible light are to be detected. The same author described a suitable refrigerator using liquid air as the cooling medium (Engstrom 1947 b).

In 1945, Blau and Dreyfus used a zinc sulphide screen in conjunction with a type 931 A photo-multiplier to detect alpha-particles, taking the change in current through the photo-multiplier as a measure of the indident radiation. Two years later Kallmann (1947 a, b, c) first reported the extension of the technique to the detection of gamma-radiation; like Blau and Dreyfus, he used polycrystalline screens of luminophors, but showed that individual scintillations, amplified by the photo-multiplier, could be observed in an oscilloscope or counted electronically. He investigated the behaviour of zinc sulphide, zinc silicate, calcium tungstate and naphthalene to alpha-, beta-, and gamma-radiation, and found naphthalene to be the most useful substance for scintillation counting. In these comparative studies, Kallmann distinguished between:

(i) the "physical light yield" of the luminophor - that is, the amount of light produced <u>within</u> the luminophor, and

(ii) its "technical light yield" - that is, the amount of light <u>emerging from</u> the luminophor layer. He showed that (ii) will usually be lower than (i) because of absorption of light within the layer and scattering at the faces of the many small crystals

of which it is formed. It is interesting to record that Kallmann was unable to detect any light pulses from calcium tungstate irradiated by gamma-rays, probably because he used powdered mineralogical specimens (Scheelite) of doubtful purity.

Kallmann's pioneer work was confirmed by Coltman and Marshall (1947), and by Deutsch (1947), and awakened great interest. It was soon realised that the "technical light yield" of the luminophor would be greatly improved if large single crystals could be used instead of polycrystalline screens; so began a search for improved luminophors that could be produced as single crystals. Moon (1948) showed that pure calcium tungstate is particularly useful in this respect, and being also of high density and high mean atomic number is peculiarly suited to the detection of gamma-radiation. Bell (1948) irradiated single crystals of pure anthracene with the gamma-radiation from $cobalt_{60}$, and obtained pulses three times as large as those produced in naphthalene. Hofstadter (1948) also obtained large pulses from thallium-activated alkali halide luminophors,

notably from sodium iodide containing up to one per cent of thallium iodide. Among the other substances recommended have been lithium fluoride (Farmer et al., 1949), cadmium tungstate (Gillette, 1950), stilbene (Gittings et al., 1949), chrysene (Schillinger et al., 1949), p-terphenyl (Hofstadter, Liebson and Elliot, 1950), and diphenylacetylene (Ravilious et al., 1950). Comprehensive studies of the relative properties of various luminophors have been conducted by Kallmann (1949), Hofstadter (1949 c) and Jordan and Bell (1949).

One of the advantages of the scintillation counter over the Geiger-Müller counter is its short resolving time; this depends on the time required for the light to be emitted by the luminophor following the passage through it of an ionising particle. The form of the decay of the emitted light in various phosphors has been the subject of numerous investigations (Collins, 1948; McIntyre, 1949; Elliot et al., 1950 a, b; Liebson and Elliot, 1950; Post and Shiren, 1950; Lundby, 1950; Liebson et al., 1950; Morrish and Dekker, 1950.) In general, the decay of organic luminophors appears

exponential in form and very fast (decay time < 0.1 microseconds), whereas that of inorganic luminophors is often non-exponential and may occupy hundreds of microseconds. Examples of the use of scintillation counters using organic luminophors as devices of short resolving time are furnished by the work of de Benedetti et al. (1948) and McIntyre (1951) on the measurement of short-lived radioisotopes, and that of Kraushaar et al. (1950) on the π-μ meson decay.

Jordan and Bell (1949) showed that the amplitude of the light pulses produced in a given luminophor by monoenergetic secondary electrons is linearly proportional to the energy of the electrons. They indicated how this principle could be used in the measurement of gamma- and beta-ray energies in the "scintillation spectrometer". This application of the technique has been extended by Johansson (1950 a, b), Pringle et al. (1950 a, b, c), Hofstadter and McIntyre (1950 a, b, c, d, e), and Cavanagh (1950).

While it was early recognised that the scintillation counter can give higher absolute counting efficiencies towards gamma-radiation than the Geiger-Müller counter, a satisfactory discussion

of the relationship between the observed counting rate and the gamma-radiation flux through the luminophor is yet to be published. The general principles of this relationship have been indicated by Mayneord and Belcher (1950 a), and some absolute measurements on calcium tungstate by Mayneord and Belcher (1950 b) and on potassium iodide by Belcher (1950 a) have been reported. Smeltzer (1950) has shown the proportionality between the light emission of a naphthalene crystal irradiated by X-radiation in the energy range 0.25 - 1.2 MeV. and the dosage rate in röntgens/minute. However, he measured the total light emission in terms of the direct current through the photo-multiplier, and not the number of scintillations produced; for this reason, his measurements cannot properly be described as scintillation counting. Ramler and Freedman (1950 a, b) studied the counting efficiency of thin anthracene crystals towards low energy electrons in the range 0 - 20 keV., and showed that a counting efficiency of almost 100% could be achieved for electron energies greater than 10 keV.

Turning now to the design of practical counters, it was early realised that maximum sensitivity

towards gamma-radiation can only be achieved if steps are taken to reduce the background counting rate due to thermionic emission at the cathode of the photo-multiplier tube. This can be achieved most easily by cooling, and where such a method is adopted, it is often desirable to locate the luminophor at a distance from the photo-multiplier, placing a "light guide" between them to conduct the emitted light to the photo-cathode. This "light guide" may be a hollow tube of highly polished metal, but more often is a solid rod of perspex or quartz. Such arrangements have been described by Blizard and de Benedetti (1949), Cassen and Curtis (1949) and Timmerhaus et al. (1950), and are valuable in the design of probe units and directional counters for the "in vivo" localisation of clinically-administered radio-isotopes. (Belcher and Evans, 1951).

Coincidence counters have also been described (Morton and Robinson, 1949; Kallmann and Accardo, 1950; Wiegand, 1950) which obviate the necessity for cooling the photo-multiplier tube in order to reduce the background counting rate. In such arrangements, two photo-multipliers are stimulated by light from the

same crystal, their outputs being connected to a coincidence circuit such that only pulses appearing simultaneously at both photo-multiplier outputs register in the recorder. A considerable improvement in performance over that of a single uncooled tube may be achieved in this way, but because of random coincidences between the two tubes, the background of such a counter is higher than that due to a single photo-multiplier cooled in liquid nitrogen.

In conclusion, two recent developments of the scintillation counting technique must be mentioned. The first is the use of liquid luminescent media instead of solid luminophors. Because of the difficulty in growing large single crystals of luminophors, the possibility of using glass cells filled with liquids in their place is an attractive one. In 1949, Ageno, Chiozzoto and Querzoli demonstrated luminescence in solutions of naphthalene in xylene exerted by gamma-radiation; their work led to the study of many liquid systems. Reynolds et al. (1950 a, b) showed p-terphenyl in xylene to be as efficient as crystalline naphthalene. Kallmann and

Furst (1950) investigated a very wide variety of solutions, but found none superior to p-terphenyl. Belcher (1951) recommended $\alpha\alpha'$-dinaphthyl in benzene as a scintillating medium. It seems probable that still more efficient liquid luminophors will be discovered with the further study of liquid-state luminescence.

The other new development is the use by Mandeville and his co-workers (1950 a, b, c, d, e, f) of a photo-sensitive Geiger-Müller tube in place of a photo-multiplier tube to detect the scintillations in the luminophor. The latter is chosen in this case to emit light, not in the region of maximum spectral sensitivity of the photo-multiplier, but in the near ultra-violet portion of the spectrum. It seems unlikely that this technique can give such high sensitivities towards gamma-radiation as the conventional scintillation counter, and the advantage of short resolving time is of course lost. Nevertheless, since the associated electronic equipment is considerably simplified, and the necessity for cooling or complex coincidence arrangements to reduce the photo-multiplier background is overcome, it may prove of value in certain applications.

3. PLAN OF THESIS.

In this thesis, a physical theory of the scintillation counting of gamma-radiation will be developed, and experimental studies designed to test the validity of this theory and to widen the scope of the technique will be described. In section II, which follows immediately, the general principles of this theory are outlined; sub-sections deal successively with:-

1. The basic principles of scintillation counting.
2. The calculation of the rate of production of secondary electrons within the luminophor.
3. The energy distribution of the secondary electrons.
4. Current theories of luminescent emission.
5. The detection and amplification of the light pulses.
6. Statistical processes within the photo-multiplier tube.

Section III deals with the methods and instrumentation used in the experimental studies. Sub-sections describe in detail:-

1. The photo-multiplier and luminophor mountings.
2. The associated electronic equipment.
3. Methods of calibration of the electronic equipment.
4. The luminophors investigated.
5. The sources of gamma-radiation used in the studies.

The experimental results are described in section IV. The sub-sections are devoted to the following topics:-

1. Statistical studies on the type I P 21 photo-multiplier tube.
2. Preliminary experiments with crystalline luminophors.
3. The measurement of absolute counting rates in crystalline luminophors.
4. The measurement of pulse-height distributions in crystalline luminophors.
5. The measurement of the variation of efficiency with temperature in crystalline luminophors.

6. Spectrographic studies on the emission of various luminophors under gamma-radiation.
7. Comparative studies on luminescence induced in liquid luminophors by gamma-radiation.
8. The measurement of absolute counting rates in liquid luminophors.
9. Studies on the Čerenkov effect in scintillation counters.

A critical discussion of the experimental results, and an assessment of their implications, together with some suggestions for future research in this field, are given in Section V.

Four appendices are included. Appendix I consists of tables of linear absorption coefficients for gamma-radiation in a wide variety of liquid and solid media. The values of the coefficients have been calculated by the author according to a method

to be described in sub-section II.2, and are required for the development and application of the theory of section II. Appendix II gives values of the ranges of mono-energetic electrons in unit density material for various electron energies; these are derived from the collected data of Kamen (1950). Appendix III gives values calculated by the author for the maximum energies of the Compton recoil electrons produced by gamma-radiation of various energies. In Appendix IV, the method outlined in sub-section II.2 for calculating the rate of production of secondary electrons in a luminophor of known composition and dimensions subjected to a known flux of gamma-radiation is described in detail.

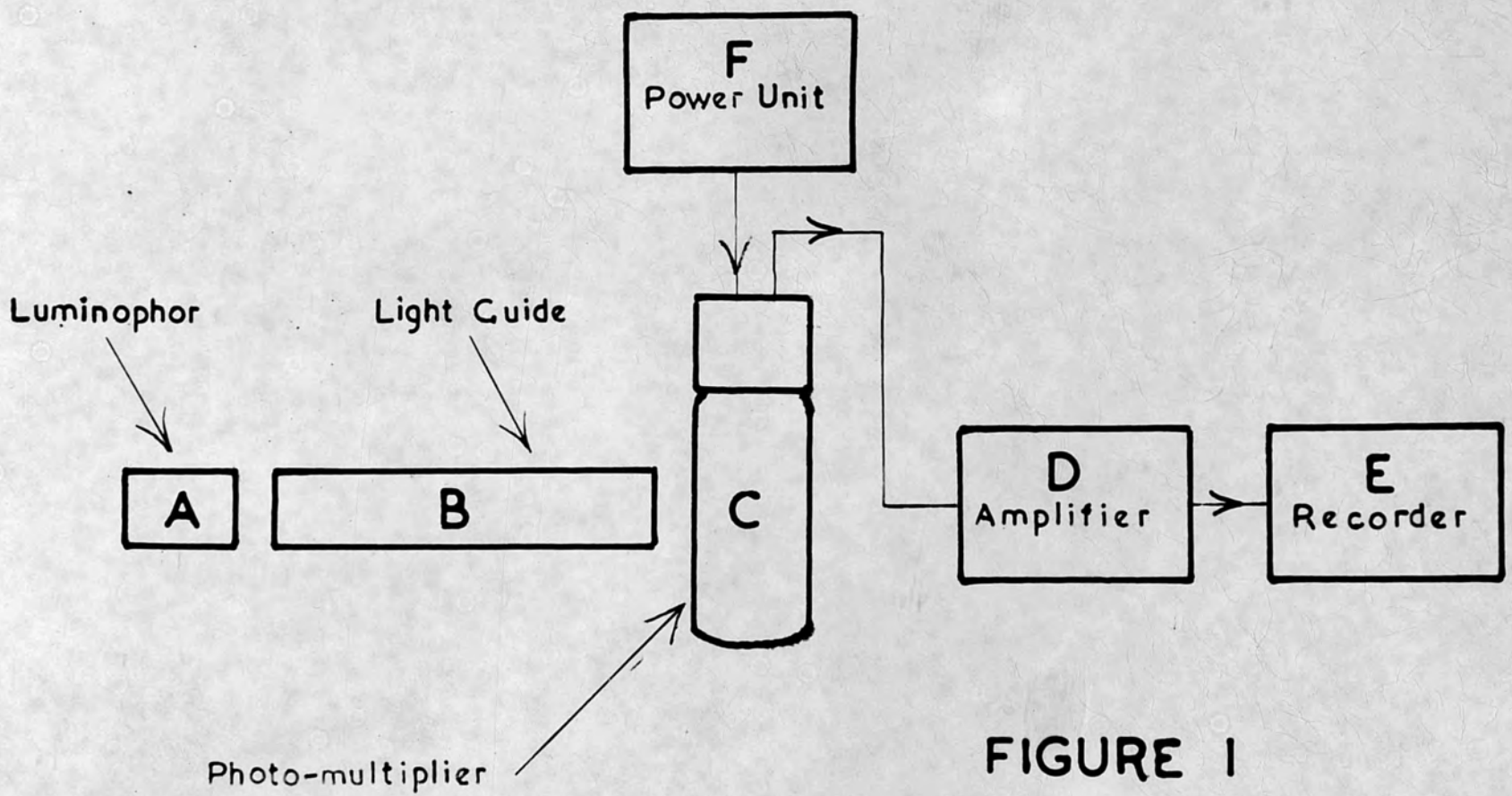

FIGURE 1

Elements of Scintillation Counter

SECTION II - GENERAL THEORETICAL CONSIDERATIONS.

1. THE BASIC PRINCIPLES OF SCINTILLATION COUNTING.

In figure 1, the scintillation counter in its simplest form is shown diagrammatically. Alpha-, beta- or gamma-radiation impinges upon a luminophor A, which may be a single crystal, a polycrystalline screen, or a cell containing a liquid luminophor. With alpha- or beta-radiation, the whole of the energy of the incident particles will normally be dissipated within the luminophor, whereas in the case of gamma-radiation, only the energy of the secondary electrons is so dissipated. It is with the gamma-scintillation counter that these studies are concerned.

The secondary electrons may be produced in the luminophor by the photo-electric absorption process, by Compton absorption, or by electron-positron pair production. In the first type of process, the secondary electrons carry almost the entire energy of the absorbed gamma quantum; in the second, they may have any energy between zero and a value given by the expression $\frac{E_\gamma}{1 + \frac{0.51}{2E_\gamma}}$, where E_γ is the

energy of the absorbed gamma-quantum in MeV; in the third type of process, an energy of ($E_\gamma - 1.02$) is shared between the two members of the electron-positron pair. The mean energy of the secondary electrons is thus considerably less than the energy of the incident gamma-quanta.

The secondary electrons produced by absorbed gamma-quanta travel through the luminophor, losing energy by collisional encounters, and exciting electrons in the lattice, or in the molecules of the luminophor, to higher energy states. Electrons in excited states may then return to the ground state with the emission of visible light. In many luminophors, this emission process is almost instantaneous; in such cases, each gamma-quantum absorbed will produce a single short scintillation containing many photons of visible light. In other luminophors, in which electron-trapping levels are present, the emission may occur as a slow phosphorescence lasting many minutes, and a single absorption event may produce many discrete scintillations, each consisting of a single photon of visible light. Between these two extreme types of system are luminophors of intermediate type, in which an absorbed gamma-quantum

produces an initial scintillation followed by a slow phosphorescent decay.

It will be apparent that the maximum attainable efficiency of the scintillation counter towards gamma-radiation is limited by the number of secondary electrons released, and hence, by the fraction of the incident gamma-quanta absorbed in the luminophor.

The number of luminescent centres activated, and hence, the total intensity of the emitted light, depends upon the energy of the secondary electrons, which in turn is related to the energy of the incident gamma-radiation.

An optical system B, links the luminophor to the photo-cathode of the photo-multiplier tube C. This optical system may be a "Perspex" light-guide, an arrangement of lenses and mirrors, or a combination of both systems. In some counters, the luminophor is placed in direct contact with the photo-multiplier envelope. Whatever be the arrangement adopted, a fraction of the light produced in the luminophor determined by the optical efficiency of the system falls upon the photo-cathode, and of these incident light quanta, a fraction determined by the quantum

efficiency of the photo-cathode release photo-electrons that actuate the photo-multiplier. The amplified pulses at the photo-multiplier output are fed to a linear amplifier D, and thence to a recording device E, which may be a scaling counter, or a rate-meter. A power unit F maintains the required potentials between the photo-multiplier dynodes.

The amplitude of the electrical pulse at the amplifier output depends upon the intensity of the light pulse that produces it, but is subject to statistical variations due to effects in both the optical system and the photo-multiplier tube. The fractional spread in pulse height introduced in this way increases as the mean pulse height decreases.

2. CALCULATION OF RATE OF PRODUCTION OF SECONDARY ELECTRONS WITHIN THE LUMINOPHOR.

The number of secondary electrons produced per second in a luminescent medium of known atomic composition and linear dimensions irradiated by a known flux of gamma-radiation can be calculated, provided that the total linear absorption coefficient

of the medium towards gamma-radiation of the appropriate energy is known (Mayneord and Belcher, 1950). For consider a luminophor of cross-section a sq. cm. and thickness t cm., irradiated by gamma-radiation from a source of strength S millicuries emitting 1 gamma-ray of energy E_γ MeV. per disintegration, and distant x cms. from the front face of the luminophor. The number of quanta incident upon the luminophor per second is:-

$$\frac{3{\cdot}7.10^7.S.a}{4\pi x^2}$$

Provided that x is large compared with the dimensions of the luminophor, these may be considered as forming a parallel beam of radiation, in which case the number of quanta absorbed per second, and hence the rate of production of secondary electrons is:-

$$N_e = \frac{3{\cdot}7.10^7.S.a}{4\pi x^2}\left(1 - e^{-\mu_\gamma t}\right) \quad 2.1$$

where μ_γ is the total linear absorption coefficient for gamma radiation of energy E_γ. Where each secondary electron produces a single scintillation, as in the first class of luminophors considered in section II.1 above, this will also be the rate of production of scintillations.

Where the emission of the source is not monochromatic, it is necessary to calculate N_e for each separate gamma-ray energy, and obtain the total rate by summation, making allowance for the emission probability of each type of gamma-quantum:-

$$N_e = \frac{3.7.10^7.S.a}{4\pi x^2} \sum_{\gamma} (1 - e^{-\mu_\gamma t}).f_\gamma \qquad 2.2$$

where f_γ is the mean number of gamma-quanta of energy E_γ emitted per disintegration. Corrections for internal conversion must be included in f_γ where necessary.

The values of the total linear absorption coefficient μ_γ for a medium of known density and atomic composition may be evaluated using the relationship:-

$$\mu_\gamma = \tau_\gamma + \sigma_\gamma + \pi_\gamma \qquad 2.3$$

where τ_γ , σ_γ , π_γ , are the linear absorption coefficients for photo-electric absorption, total Compton absorption, and pair production respectively. The coefficient σ_γ should be carefully distinguished from the coefficient for Compton recoil $\sigma_{a\gamma}$.

The partial coefficients τ_γ, σ_γ and π_γ may be calculated from first principles for gamma-radiation of a given energy using the theories of Fowler and Hulme (1935), Klein and Nishina (1929), and Bethe and Heitler (1934), but in view of the complexity of such calculations, it is preferable to derive their values from the corresponding values for a medium whose absorption coefficients are well established, e.g. lead. This may be done for an absorbing medium which is also a pure atomic species using the relationships:-

$$\tau_{\gamma_M} = \tau_{\gamma_{Pb}} \cdot \frac{\rho_M}{\rho_{Pb}} \cdot \frac{A_{Pb}}{A_M} \cdot \left(\frac{Z_M}{Z_{Pb}}\right)^4 \qquad 2.4$$

$$\sigma_{\gamma_M} = \sigma_{\gamma_{Pb}} \cdot \frac{\rho_M}{\rho_{Pb}} \cdot \frac{A_{Pb}}{A_M} \cdot \left(\frac{Z_M}{Z_{Pb}}\right) \qquad 2.5$$

$$\pi_{\gamma_M} = \pi_{\gamma_{Pb}} \cdot \frac{\rho_M}{\rho_{Pb}} \cdot \frac{A_{Pb}}{A_M} \cdot \left(\frac{Z_M}{Z_{Pb}}\right)^2 \qquad 2.6$$

where the subscripts M, Pb, refer to the absorbing medium and lead respectively, ρ is density in gms./cm^3, A atomic weight, and Z atomic number.

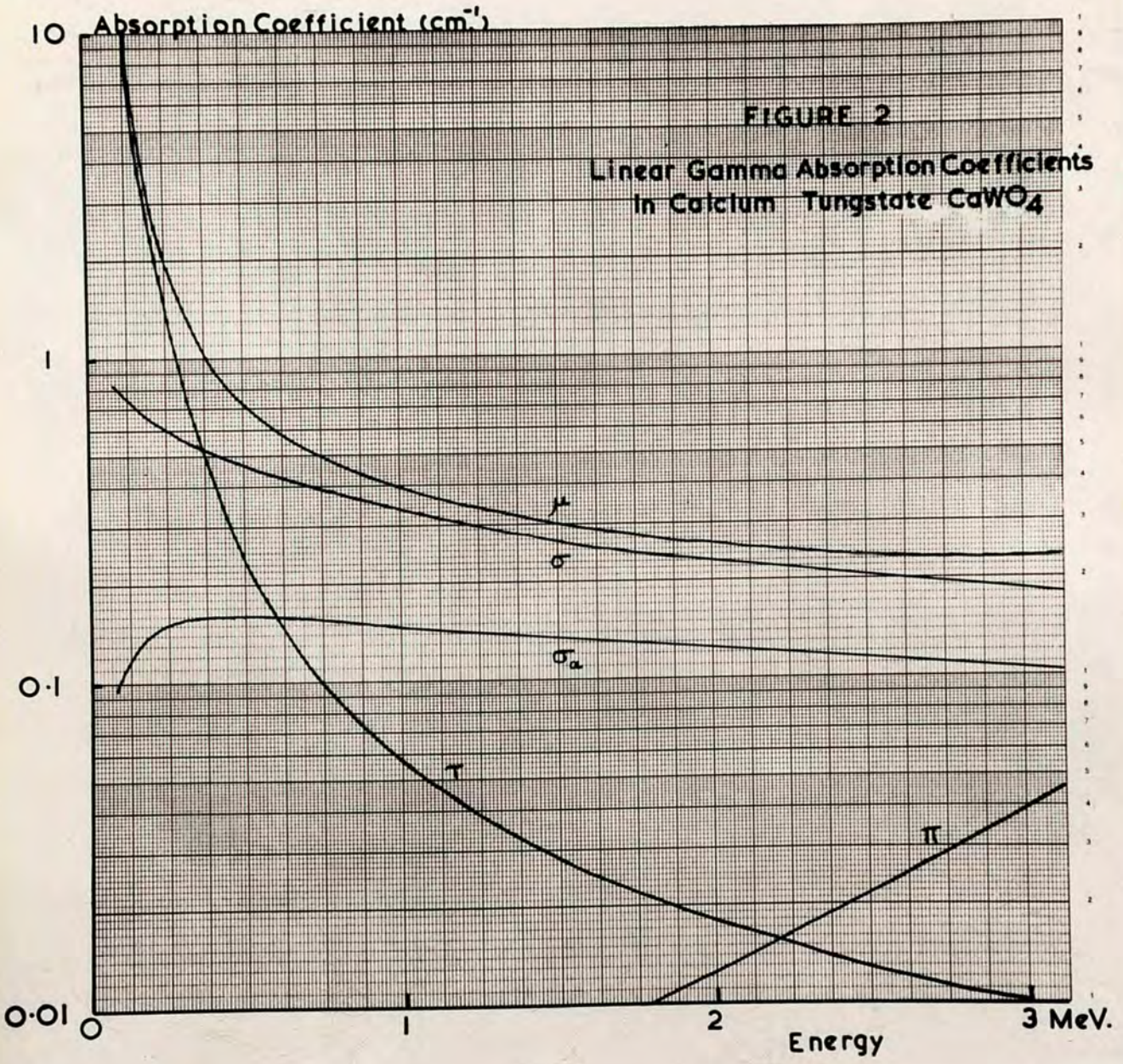

FIGURE 2

Linear Gamma Absorption Coefficients in Calcium Tungstate $CaWO_4$

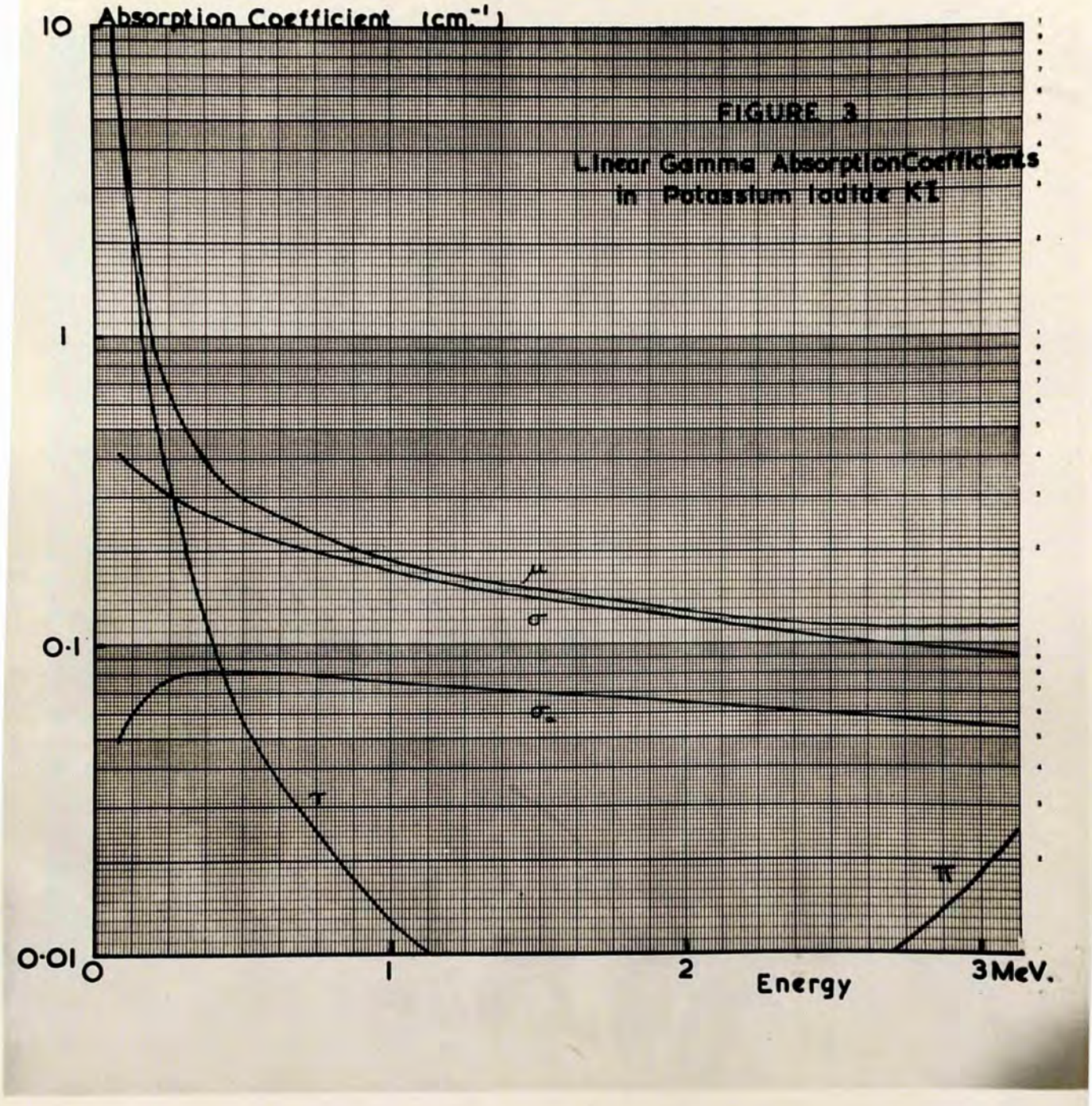

FIGURE 3

Linear Gamma Absorption Coefficients in Potassium Iodide KI

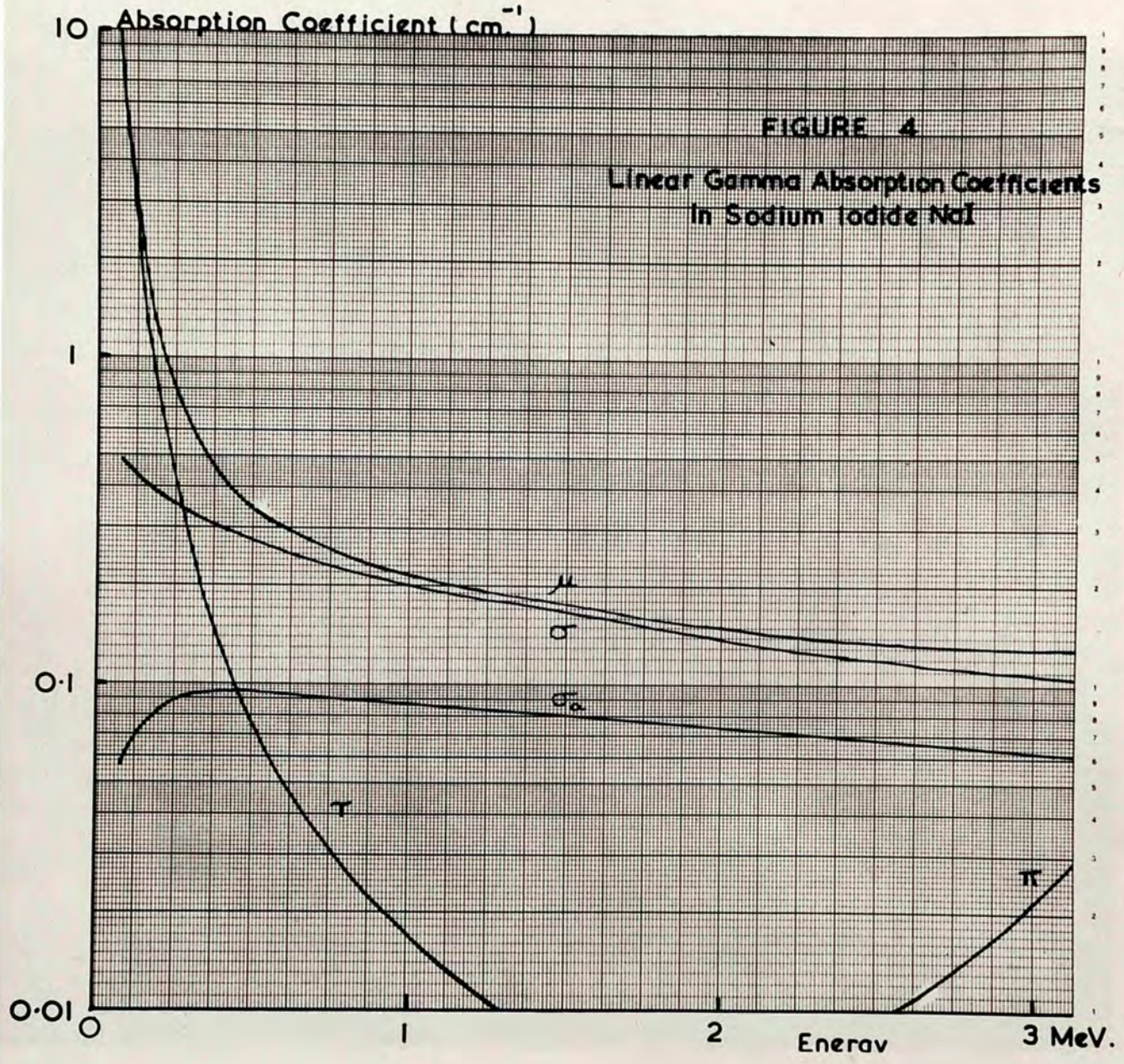

FIGURE 4

Linear Gamma Absorption Coefficients In Sodium Iodide NaI

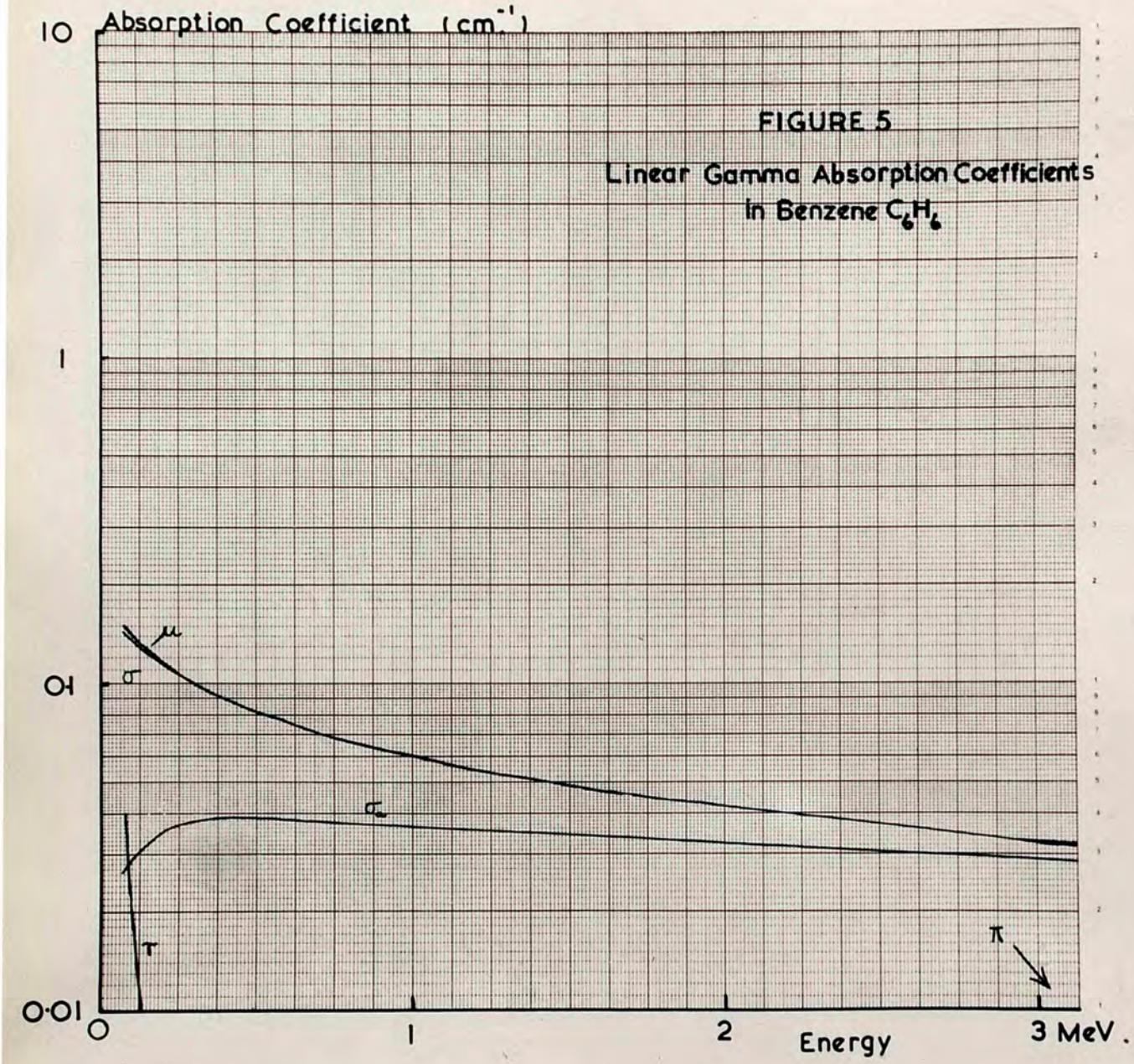

FIGURE 5

Linear Gamma Absorption Coefficients in Benzene C_6H_6

It will normally be the case that the absorbing medium will not be a pure element; it is then necessary to sum the effects due to each constituent atomic species considered separately, weighting each according to its atomic abundance. This procedure may be illustrated by considering the case of calcium tungstate, $CaWO_4$:-

$CaWO_4$:- Density 6.06 gms./cm^3, Molecular Weight 288

Pb :- Density 11.35 gms./cm^3, Atomic Weight 207.2

$$\tau_{\gamma\, CaWO_4} = \tau_{\gamma\, Pb} \cdot \frac{6.06}{11.35} \cdot \frac{207.2}{288} \cdot \left[\left(\frac{20}{82}\right)^4 + \left(\frac{74}{82}\right)^4 + 4\left(\frac{8}{82}\right)^4 \right]$$

$$= 0.256\, \tau_{\gamma\, Pb}$$

$$\sigma_{\gamma\, CaWO_4} = \sigma_{\gamma\, Pb} \cdot \frac{6.06}{11.35} \cdot \frac{207.2}{288} \cdot \left[\left(\frac{20}{82}\right) + \left(\frac{74}{82}\right) + 4\left(\frac{8}{82}\right) \right]$$

$$= 0.590\, \sigma_{\gamma\, Pb}$$

$$\pi_{\gamma\, CaWO_4} = \pi_{\gamma\, Pb} \cdot \frac{6.06}{11.35} \cdot \frac{207.2}{288} \cdot \left[\left(\frac{20}{82}\right)^2 + \left(\frac{74}{82}\right)^2 + 4\left(\frac{8}{82}\right)^2 \right]$$

$$= 0.350\, \pi_{\gamma\, Pb}$$

In figures 2, 3, 4 and 5, values of μ, τ, σ, σ_a, and π calculated in this manner for gamma-quantum energies between 0.1 and 3 MeV. are shown for

calcium tungstate, potassium iodide, sodium iodide and benzene. The values of σ, τ, and π for lead, on which these calculations are based, have all with the exception of those for τ at gamma-quantum energies below 0.5 MeV. been obtained from "The Science and Engineering of Nuclear Power", Volume I, and are also quoted by Siri (1949). Those for τ at low energies are due to Mayneord (private communication).

In Appendix I, are tabulated the results of these and similar calculations for numerous materials whose linear absorption coefficients were required during these investigations. Values for the mean energy, $\overline{E}_e$, of the secondary electrons produced in the medium, evaluated from the expression:-

$$\overline{E}_e = \frac{E_\gamma.(\tau_\gamma + \sigma_{a_\gamma}) + (E_\gamma - 1.02).\pi_\gamma}{\tau_\gamma + \sigma_\gamma + \pi_\gamma} \qquad 2.7.$$

have also been included in these tables.

3. ENERGY DISTRIBUTION OF THE SECONDARY ELECTRONS.

It was pointed out in section II.1 that the secondary electrons produced in an absorbing medium by gamma-radiation are not mono-energetic. Those

that are produced by photo-electric absorption carry the whole energy of the absorbed gamma-quantum less the binding energy of the ejected electron; since the latter is small compared with E_γ for $E_\gamma >$ 0.1 MeV., the photo-electrons may be assumed all to have energy E_γ . The secondary electrons produced by Compton absorption may have any energy between zero and a value given by $\dfrac{E_\gamma}{1 + \dfrac{0.51}{2E_\gamma}}$. The pair production process, where it occurs ($E_\gamma >$ 1.02 MeV.), produces electron-positron pairs with a total energy of (E_γ - 1.02). It may be assumed that both members of the pair are equally efficient in activating luminescent centres, and each pair may thus be considered equivalent to a single secondary electron of energy (E_γ - 1.02). The complete secondary electron spectrum due to monochromatic gamma-radiation therefore consists of two sharp peaks at E_γ and (E_γ - 1.02) respectively, and a continuum extending from zero to $\dfrac{E_\gamma}{1 + \dfrac{0.51}{2E_\gamma}}$.

The exact form of this continuum may be derived

from a consideration of the relativistic theory of Compton scattering due to Klein and Nishina (1929).

These authors showed that the intensity of scattering of gamma-radiation of quantum energy $h\nu$ by a single free electron at an angle ϕ to the direction of incident radiation is given by the expression:-

$$_eI_\phi = I_e(1+\alpha\,\mathrm{vers}\,\phi)^{-3}\left[1+\frac{\alpha^2\,\mathrm{vers}^2\phi}{(1+\cos^2\phi)(1+\alpha\,\mathrm{vers}\,\phi)}\right] \qquad 2.8.$$

where $\alpha = \frac{h\nu}{m_0c^2}$ and I_e is the intensity of scattering by a single electron predicted by the classical theory of Thomson. I_e is given by the expression:-

$$I_e = I\frac{e^4}{2r^2m^2c^4}(1+\cos^2\phi) \qquad 2.9.$$

where I is the intensity of the incident radiation, r the radius of the circumscribing sphere at the surface of which the scattered intensity is measured, the other symbols having their conventional significance.

Hence from 2.8 and 2.9:-

$$_eI_\phi = I\frac{e^4}{2r^2m^2c^4}(1+\cos^2\phi)(1+\alpha\,\mathrm{vers}\,\phi)^{-3}\left[1+\frac{\alpha^2\,\mathrm{vers}^2\phi}{(1+\cos^2\phi)(1+\alpha\,\mathrm{vers}\,\phi)}\right] \qquad 2.10.$$

The total power scattered between ϕ and $(\phi+d\phi)$ is therefore given by the expression:-

$$ {}_eP_\phi = {}_eI_\phi \cdot 2\pi r^2 \sin\phi \cdot d\phi $$

$$ = I \frac{\pi e^4}{m^2c^4} \sin\phi(1+\cos^2\phi)(1+\alpha \operatorname{vers}\phi)^{-3} \qquad 2.11. $$

$$ \left[1 + \frac{\alpha^2 \operatorname{vers}^2\phi}{(1+\cos^2\phi)(1+\alpha\operatorname{vers}\phi)}\right] . d\phi $$

Now the well-known treatment of Compton (1923), based on considerations of conservation of energy and momentum, shows that if an incident quantum of energy $h\nu$ is scattered at an angle ϕ, the energy of the scattered quantum $h\nu'$, and of the secondary electron, E_e, will be given by the expressions:-

$$ h\nu' = \frac{h\nu}{(1+\alpha\operatorname{vers}\phi)} \qquad 2.12. $$

$$ E_e = \frac{h\nu . \alpha \operatorname{vers}\phi}{(1+\alpha\operatorname{vers}\phi)} \qquad 2.13. $$

From 2.11. and 2.12., the total number of quanta scattered per electron per incident quantum between the limits ϕ and $(\phi + d\phi)$ is clearly:-

$$ {}_eN_\phi = \frac{\pi e^4}{m^2c^4} \sin\phi(1+\cos^2\phi)(1+\alpha\operatorname{vers}\phi)^{-2}\left[1 + \frac{\alpha^2\operatorname{vers}^2\phi}{(1+\cos^2\phi)(1+\alpha\operatorname{vers}\phi)}\right] . d\phi \qquad 2.14. $$

This is also the number of secondary electrons emitted with energies between the limits E_e and $(E_e + dE)$, where dE is obtained from 2.13:-

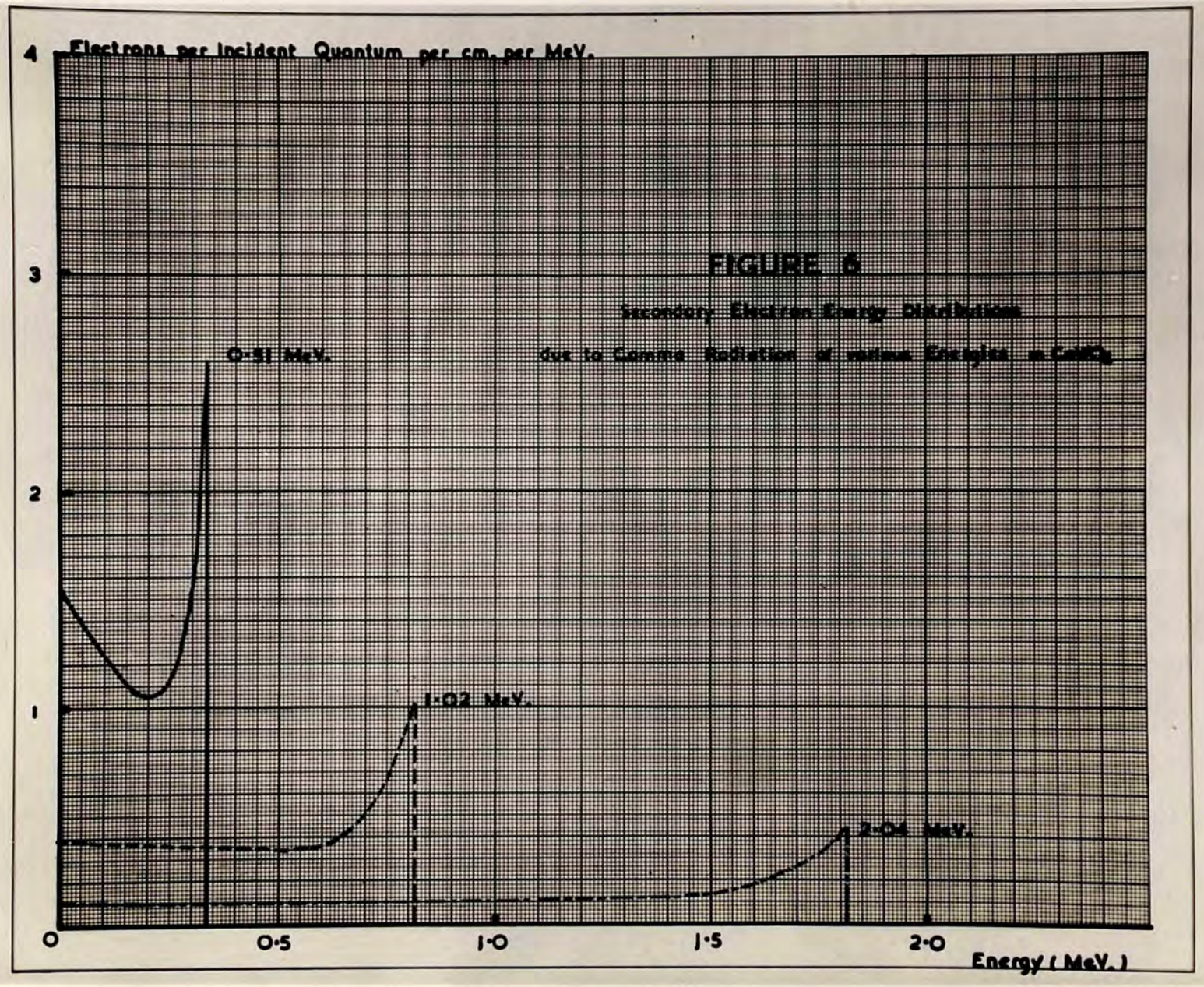

FIGURE 6

Secondary Electron Energy Distributions

due to Gamma Radiation of various Energies in $CaCO_3$

$$\frac{dE_e}{d\phi} = h\nu \frac{\alpha \sin\phi}{(1+\alpha \operatorname{vers}\phi)^2} \qquad 2.15.$$

$$d\phi = \frac{(1+\alpha \operatorname{vers}\phi)^2}{h\nu . \alpha \sin\phi} . dE_e$$

From 2.14. and 2.15, it follows that:-

$$_eN_{E_e} = \frac{\pi e^4}{m^2 c^4} \cdot \frac{1}{\alpha . h\nu} \cdot \left[(1+\cos^2\phi) + \frac{\alpha^2 \operatorname{vers}^2\phi}{(1+\alpha \operatorname{vers}\phi)}\right] . dE_e \qquad 2.16.$$

where N_{E_e} is the number of secondary electrons emitted per electron per incident quantum per MeV. having energies between the limits E_e and $(E_e + dE_e)$. The corresponding expression per cm.$^{-1}$ in a medium that is a pure element is:-

$$N_{E_e} = {}_eN_{E_e} \frac{6.023 . 10^{23} . \rho . Z}{A} \qquad 2.17.$$

When the medium is not a pure atomic species, the effects of the various atoms present may be added in a similar manner to that described in section II.2.

In figure 6, the calculated distributions of secondary electrons in calcium tungstate corresponding to E_γ = 0.5, 1 and 2 (α = 0.51, 1.02, and 2.04 MeV.) are shown. A check on the accuracy of the calculations is provided by the fact that:-

$$\int_0^{E_{e\,Max.}} N_E . dE = \sigma \qquad 2.18.$$

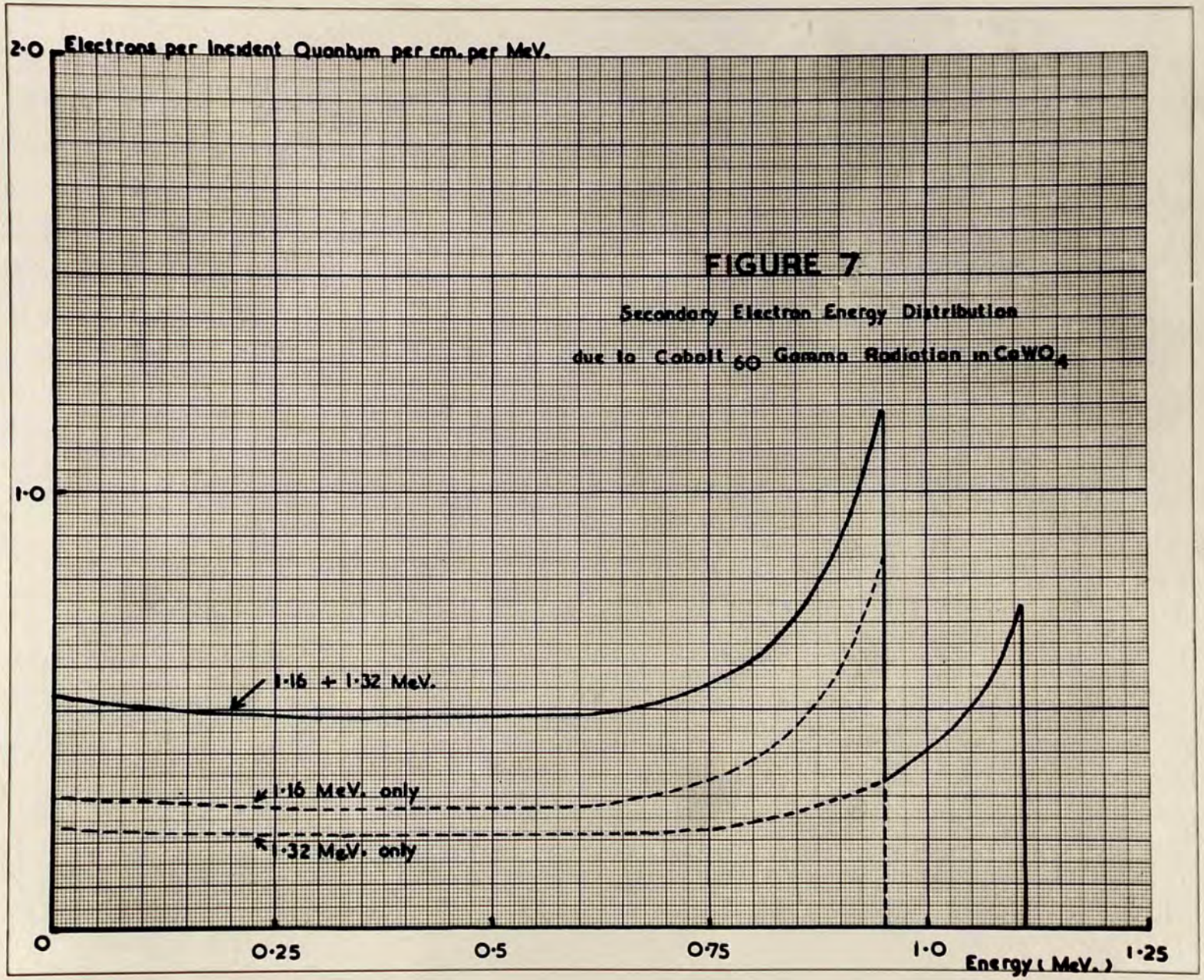

FIGURE 7

Secondary Electron Energy Distribution

due to Cobalt 60 Gamma Radiation in $CaWO_4$

In Table I, the values for σ obtained by graphical integration of the distributionsof figure 6 are compared with the derived values obtained from the data of figure 2. There is seen to be excellent agreement between the two sets of figures:-

Table I

Calculated Values of σ in Calcium Tungstate.

Method	E_γ (MeV.)		
	0.51	1.02	2.04
Graphical Integration Of Distribution of N_E	0.46	0.34	0.23
Calculation from Value for Pb	0.46	0.34	0.23

In figure 7, the corresponding distribution for the secondary electron spectrum produced in calcium tungstate by the gamma-radiation of cobalt$_{60}$ is shown. In this case, the complete spectrum comprises the superimposed effects of two gamma-quantum energies of 1.16 and 1.32 MeV. respectively.

Studies on the range-energy relationship of homogeneous beta-radiation in absorbing media (Schonland, 1925; Madgwick, 1927; Marshall and Ward, 1937) show that the range of mono-energetic electrons in a wide variety of materials is linearly proportional to their energy over the energy range 0.5 - 3 MeV. Experimental data on this topic, collected by Kamen (1950) are presented in Appendix II. At electron energies below 0.5 MeV., there is some departure from linearity, but only below 0.1 MeV. does the non-proportionality of range and energy become considerable. This implies that the loss of energy per unit length is constant along the track of an electron; hence the total number of luminescent centres excited by a secondary electron travelling through a luminescent medium may be expected to be proportional to the range of the electron in the medium, and so to its energy, provided that the electron is brought to rest within the volume of the luminophor. The total intensity of emitted light due to a single electron should therefore be linearly proportional to its energy. If this light

is emitted in the form of a single scintillation or pulse of short duration, the pulse amplitude distribution of all the scintillations produced when gamma-radiation is absorbed by the luminophor should correspond to the energy distribution of the secondary electrons developed above.

This simple treatment of the problem ignores such effects as the escape of secondary electrons from the sensitive volume of the luminophor before they have expended all their available energy, the multiple scattering of gamma-radiation within the luminophor, and radiative energy losses by secondary electrons. All these effects will be shown in later sections measureably to influence the experimental results.

4. CURRENT THEORIES OF LUMINESCENT EMISSION.

The duration and intensity of the luminescent emission and the wavelength of light emitted after activation of the luminophor by a single secondary electron may vary widely with the type of medium. The nature of the luminescent process is still only incompletely understood, but it will be of value at

this point briefly to review the current theories regarding such processes in the light of their application to scintillation counting:-

Consider first the conditions for luminescence to occur in crystalline solids. The first requisite is the existence of certain localities in the crystal where radiative processes can take place following the absorption of energy; the structure of these luminescent centres provides shielding from lattice vibrations which would otherwise remove the energy by thermal dissipation (Peierls, 1932). It was shown by Randall (1939) that in some cases, these centres could be specified; thus in the pure tungstate phosphors, the seat of emission is most probably the WO_4^{--} ion. The electronic transitions responsible for absorption and emission in pure crystalline luminophors of this type have been explained by Seitz (1939) and von Hippel (1936) in a theory based on graphical representation of the potential energies of the normal and excited states of the luminescent centre in terms of some configurational co-ordinate of the centre. Similar methods have been adopted by Bowen (1946) and

by Weiss (1942) to explain the luminescence of pure organic substances such as anthracene in the solid state. In pure luminophors of these types, in which the luminescent process is confined to the emission centre, the emission is usually of very short duration, and shows an exponential decay of intensity with time; the presence of small amounts of impurities is sufficient severely to reduce, if not completely to quench the emission of visible light. The behaviour of such systems is capable of relatively precise theoretical treatment.

Only a few solids however are luminescent in the pure state, and in the majority of luminophors the luminescent centres consist of impurity atoms or molecules present in the matrix lattice, the luminescence process involving motion of electrons in the matrix between absorption and emission. Such materials often show photo-conductivity; the emission of light may persist for many seconds after an absorption event, and rarely obeys a simple exponential decay law. Examples of luminophors of this class are the alkali

halides activated by the addition of small amounts of thallium, and zinc sulphide activated by copper.

The theoretical model best suited to explain the behaviour of such luminophors was first developed by Johnson (1939) for zinc sulphide phosphors, and is based on the zone theory of solids originally postulated by Bloch (1928). This author showed that whereas in an isolated atom the energy states consist of discrete levels defined by Schrödinger's equation and separated by regions of forbidden energies, when such atoms or ions are arranged in a crystal lattice, their levels are disturbed by mutual inter-action. As a result, the discrete states of isolated atoms are broadened into bands of allowed energy, separated by bands of forbidden energy, this system of bands bearing little resemblance to the original arrangement of atomic levels. In photo-conducting phosphors, the bands extend throughout the crystal lattice, so that electrons can travel through the lattice without requiring any activation energy to do so. In an insulator, the allowed bands for electrons are either completely occupied or completely empty; in order to produce photo-conductivity, electrons must be raised from a

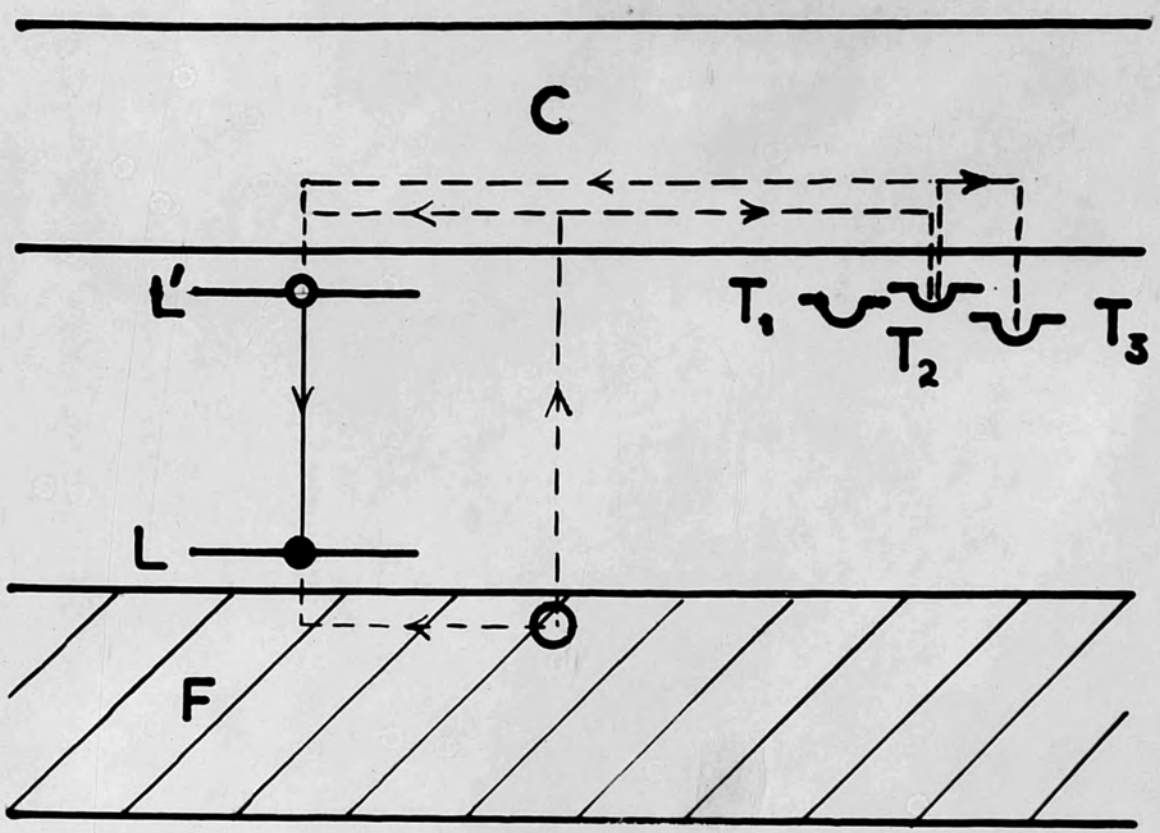

FIGURE 8

Energy Levels of Impurity-activated Luminophor

full band to a higher empty band - usually referred to as a conduction band.

When the periodicity of the crystal lattice is destroyed or disturbed by lattice defects or traces of impurities, additional and usually discrete electron levels are produced, which may lie in the region between the highest filled band and the conduction band. Such an energy-level scheme is shown in figure 8 which represents an impurity-activated photo-conducting phosphor. Between the filled band F, and the conduction band C, lie additional allowed levels, L and L^1, shown here as discrete; these represent the normal and excited states respectively of the impurity luminescent centres. Other lattice disturbances provide extra levels T_1, T_2, T_3 lying just below the bottom of the conduction band. When these are unoccupied, they may capture electrons from the latter band, and because of this property, they are referred to as "electron-traps". At least two possible modes of activation of this system are possible, viz:-

(1) Absorption at the luminescent centres followed by almost instantaneous emission - this is the same process as has already been described for pure crystalline phosphors.

(2) Absorption in the matrix with the elevation of an electron to the conduction band. The resulting "positive hole" may wander through the filled band until it is filled from a normal luminescent centre. The electron travels through the conduction band until it is captured by an empty excited luminescent centre. Emission then occurs as above, but may be delayed by the trapping and eventual release of the electron by electron trapping levels. In view of the low activator concentrations, absorption in the matrix certainly predominates under conditions of gamma-excitation.

There is some evidence that a third process described by Frenkel (1931) may occur, in which electrons are elevated from the filled to the conduction band, but remain bound to their positive holes.

This model has been used successfully by

Randall and Wilkins (1945) and Garlick and Gibson (1946, 1948) to explain the phosphorescent decay of many impurity activated phosphors. In general a long period phosphorescence is a disadvantage in a luminophor to be used in scintillation counting, and it is desirable that the period of phosphorescent decay should be small compared with the resolving time of the recording device used. But, as suggested by Mayneord and Belcher (1950a), in certain applications it might be possible to use the phosphorescence of a luminophor of very long decay time as a measure of radiation flux, bu observing the counting rate at a fixed time interval after the end of the excitation period.

In figure 8, the normal and excited states of the luminescent centres have been depicted as discrete levels, but more probably they should be themselves drawn as band structures. The spectrum of the emitted light is thus not sharp, but forms a diffuse band extending over 100 Å or more of wavelength; this is true for both pure and impurity-activated luminophors. In choosing a luminophor for a scintillation counter, it is advisable to select a substance whose emission corresponds as nearly as possible to the peak spectral sensitivity of the photo-multiplier tube to be used.

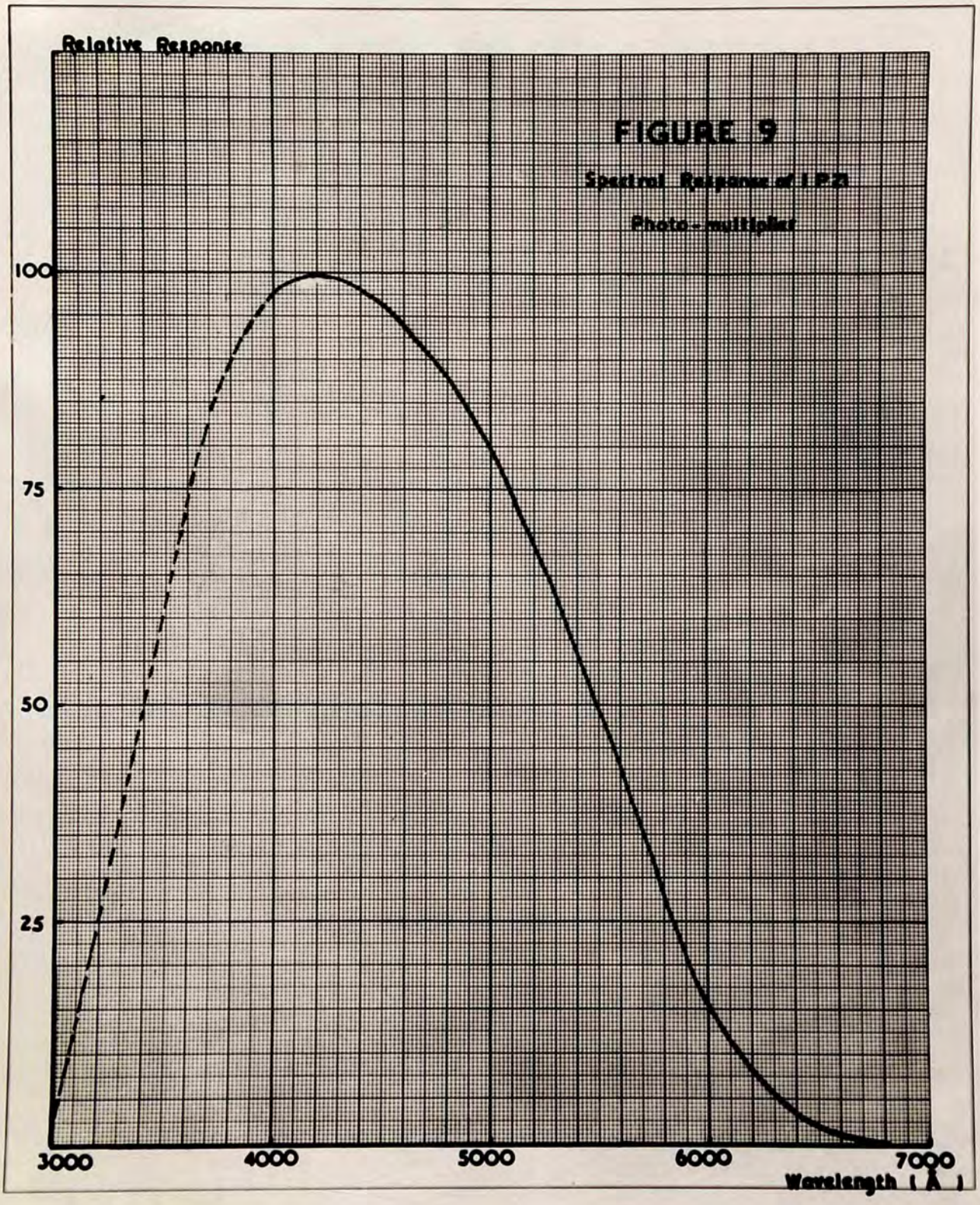

FIGURE 9

Spectral Response of I.P.21 Photo-multiplier

In the case of the R.C.A. type I P 21 photo-multiplier, used throughout these studies, this maximum sensitivity will be seen from figure 9 to occur at 4200 Å .

In table II, the more important characteristics of the luminophors used in the present investigations are listed; the data shown have been collected from the published reports of Jordan and Bell (1949), Kallmann (1949), and Hofstadter (1950). In this table, the values for relative light yield refer to the total light emission, anthracene being considered as unity; the values are uncorrected for the response of the photo-multiplier tube, (type 5319). Only the more important peaks in the emission and absorption spectra have been indicated. The decay constants quoted are those which appear in the expression $e^{-t/\tau}$, if an exponential luminescent decay is assumed.

Table II

Properties of Luminophors.

Luminophor	Emission Spectrum (Å)	Absorption Spectrum (Å)	Relative Light Yield for Beta Particle	Decay Constant ($\times 10^8 sec^{-1}$)	Density (gm/cm^3)	Melting Point (°C)	Remarks
Calcium Tungstate $CaWO_4$	4300	Starts at 4000	~ 1.0	Long	6.06	1325	Good small crystals readily obtained.
Thallium-activated Potassium Iodide KI/Tl	4100	2870, 2360	~ 0.5	> 100	3.13	582	Excellent crystals readily obtained
Thallium-activated Sodium Iodide NaI/Tl	4100	2930, 2340	~ 2.0	25	3.67	651	Excellent crystals obtained; deliquescent.
Anthracene $C_{14}H_{10}$	4400	Starts at 4050	1.0	3.0 ± 0.5 (300°K) 1.2 ± 0.2 (77°K)	1.25	217	Good crystals rather difficult to obtain
Naphthalene $C_{10}H_8$	3450	-	0.25	6.0	1.15	80	Good crystals readily obtained; sublime.

5. DETECTION AND AMPLIFICATION OF THE LIGHT PULSES.

It has been shown in section II.3. that a secondary electron released and brought to rest in a luminescent medium will cause the emission of a number of light quanta proportional to its initial energy. Owing to the quantum nature of the emission process, the exact number of quanta emitted by a given secondary electron will be subject to statistical variations, but suppose that the mean number produced by secondary electrons of energy E_e is m_1. If the average optical efficiency of the system is m_2, then ($m_1 . m_2$) quanta will be incident upon the photo-multiplier cathode. If the mean quantum efficiency of the latter for light of the wavelength concerned is m_3, then ($m_1 . m_2 . m_3$) photo-electrons will be released there.

Now it has been demonstrated by Morton and Mitchell (1948) that not all the photo-electrons released at the photo-cathode arrive at the first dynode; a proportion, depending on the area of the cathode irradiated, is lost because of poor focussing. If the fraction that does arrive is designated by m_4, and if the multiplier has n stages and an inter-stage gain of R_m, then the average

total number of electrons arriving at the collector following the release of a single secondary electron of energy E_e in the luminophor is:-

$$m_1 . m_2 . m_3 . m_4 . R_n^n$$

All of the quantities in this expression with the exception of n are subject to statistical variation which will be considered in the next section. First it is necessary to consider the form of the output pulse resulting from the arrival of this charge at the photo-multiplier collector.

Reference to table II shows that the duration of the light pulse in the luminophor may be as short as 10^{-8} seconds (anthracene) or as long as 10^{-6} seconds (potassium iodide). Papp (1948) and Morton (1949) state the resolving time of a I P 21 photo-multiplier to be of the order of 10^{-9} seconds, and thus it is probable that it would resolve the individual quanta arriving at the photo-cathode during a single scintillation. Charge would thus arrive at the collector in a succession of discrete packets each corresponding to the release of a single photo-electron at the photo-cathode. However it is not to be expected that these packets would be

FIGURE 10

Effect of Circuit Constants on Pulse Shape

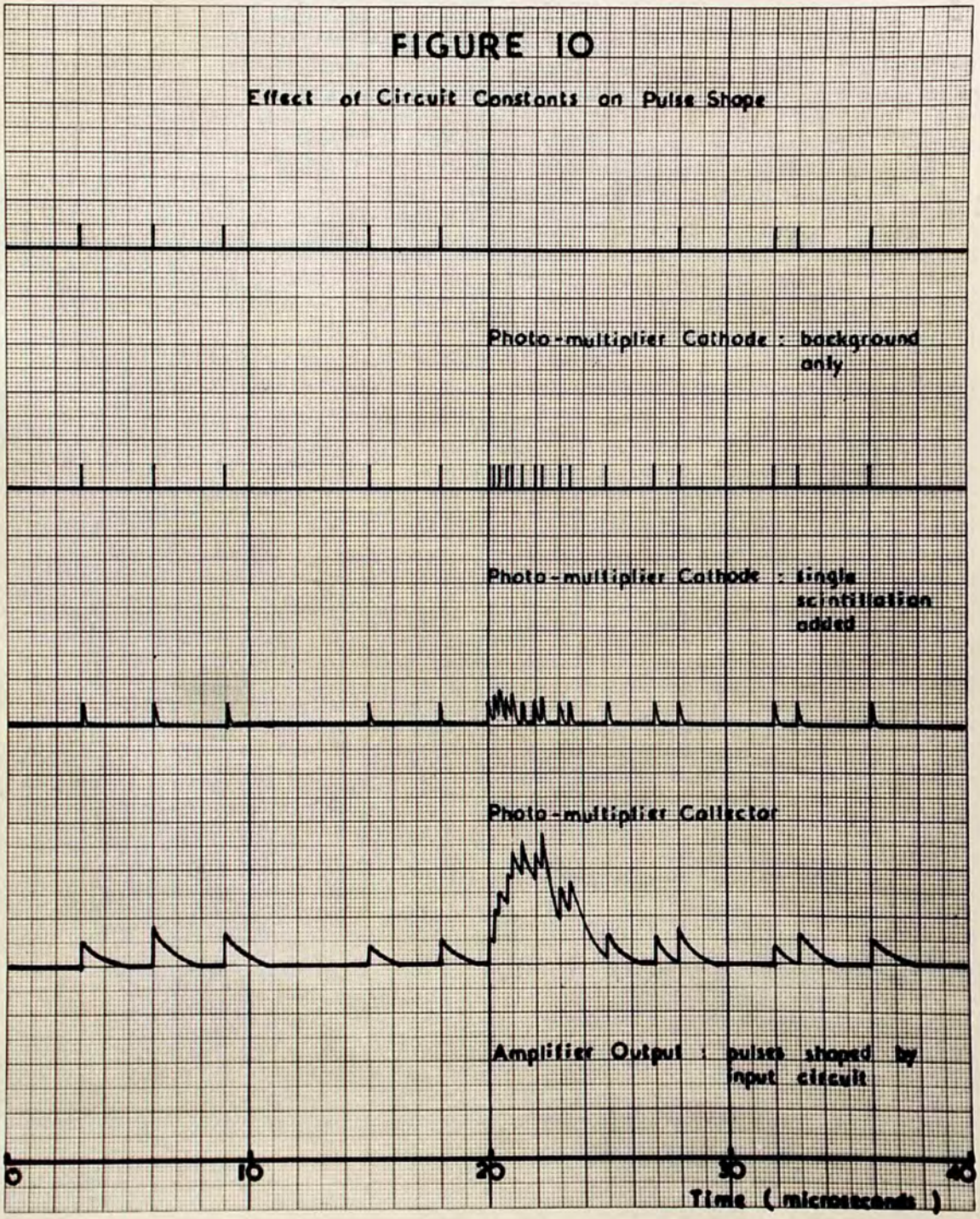

resolved by the linear amplifier and recording system.

The form of the final pulse at the amplifier output is determined by the form and duration of the original scintillation, the efficiency of the optical system, and the resolving times of the photo-multiplier and amplifier. These effects are shown qualitatively in figure 10 (after Marshall, Coltman and Bennett (1948).

Owing to the random distribution of light quanta during a single scintillation, an exact mathematical analysis of the form of the output pulse is difficult. An approximate treatment can be given where the luminophor shows no delayed phosphorescence due to electron trapping levels, if it is assumed that charge arrives uniformly at the photo-multiplier collector during the duration of the scintillation - a reasonable assumption provided that the quantity $(m_1 \cdot m_2 \cdot m_3 \cdot m_4)$ is large (> 10).

In this case, the analysis of Wynn-Williams and Ward (1931) shows that if charge arrives uniformly at the collector during a scintillation lasting from time 0 until time T, then the potential V_t across the amplifier input at an instant t ($< T$) is given by:-

$$V_t = \frac{R_q}{T}\left(1 - e^{-t/RC}\right) \qquad 2.19.$$

where q is the total charge arriving during the pulse, and RC is the time constant of integration of the input circuit. The potential at an instant t' $(> T)$ is given by:-

$$V_{t'} = \frac{Rq}{T}(1 - e^{-T/RC}) \cdot e^{-(t'-T)/RC} \qquad 2.20.$$

The maximum potential across the amplifier input is thus:-

$$V_T = \frac{Rq}{T}(1 - e^{-T/RC}) \qquad 2.21.$$

and if the voltage gain of the amplifier is G, the amplitude A_T of the pulse at the amplifier output is:-

$$A_T = \frac{GRq}{T}(1 - e^{-T/RC}) \qquad 2.22.$$

where q is of course given by:-

$$q = m_1 \cdot m_2 \cdot m_3 \cdot m_4 \cdot R_m^n$$

If the duration of the scintillation is short compared with the time constant of the amplifier ($T << RC$), this reduces to:-

$$A_0 = \frac{Gq}{C} \qquad 2.23.$$

It will be seen that in all cases, the proportionality between A and q is preserved. For scintillations of equal duration, the amplitude of

the output pulse is always proportional to the charge arriving at the photo-multiplier collector, and hence to the energy of the secondary electron in the luminophor, subject only to the statistical variations to be considered in the section that follows. A more detailed analysis of linear pulse amplifiers has been given by Gillespie (1947, 1948).

6. STATISTICAL PROCESSES WITHIN THE PHOTO-MULTIPLIER TUBE.

It has been shown that the mean amplitude of output pulses produced in a scintillation counter by mono-energetic secondary electrons released in the luminophor is proportional to the energy of the secondary electrons. However, because of the statistical variations already mentioned, the output pulse amplitude distributions produced by gamma-radiation may be very different to the secondary electron energy distribution of figures 6 and 7.

The problem of determining the magnitude of these statistical effects is seen to be that of combining the successive distributions due to variations in the number of light quanta produced in the luminophor, in the optical efficiency of the system, in the quantum efficiency of the photo-cathode, in the number of electrons lost

between the cathode and the first dynode, and in the gain of each stage of the photo-multiplier.

Problems involving successive probability distributions of this nature may be conveniently treated by the use of the appropriate "probability generating functions". These functions are the subject of a paper by Jörgensen (1948) and their properties have been excellently summarised by Seitz and Müller (1950); use is made of them in the work of both Morton and Mitchell (1948) and Sauter (1949).

Briefly, if in any series of observations, p_n is the probability that any one observation yields a score of n, then a function $F(x)$ defined by:-

$$F(x) = p_0 x^0 + p_1 x^1 + p_2 x^2 + \cdots \cdots + p_n x^n + \cdots \qquad 2.24.$$

where x is a "hilfbuchstabe" and can take any arbitrary value, is termed a probability generating function for p_n.

It can be shown that:-

$$F(0) = p_0 \quad , \quad F(1) = 1 \qquad 2.25.$$

and that if m, V, are the mean and variance of a series of single observations defined by:-

$$m = \sum_n n p_n \quad , \quad V = \sum_n p_n (n-m)^2 = \sum_n p_n n^2 - m^2$$

it can be further shown that:-

$$m = \left| \frac{dF}{dx} \right|_{x=1} \qquad 2.26$$

$$V = \left| \frac{d^2F}{dx^2} + \frac{dF}{dx} - \left(\frac{dF}{dx}\right)^2 \right|_{x=1} \qquad 2.27.$$

$$= \left| \frac{d^2F}{dx^2} \right|_{x=1} + m - m^2$$

For a Poisson distribution, defined by:-

$$p_n = \frac{\mu^n}{\lfloor n} e^{-\mu}$$

where μ is the mean value of n over all the observations, the appropriate generating function is:-

$$F(x) = e^{\mu(x-1)}$$

whence:-

$$m = \mu \ , \quad V = \mu \qquad 2.28.$$

For a simple choice between two alternatives, e.g. tossing a coin, the appropriate generating function is:-

$$F(x) = (1-p) + px$$

where p is the probability of obtaining a "hit", whence:-

$$m = p \ , \quad V = p - p^2 \qquad 2.29.$$

The usefulness of probability generating functions is still further increased by the following properties.

Suppose that instead of making one observation, two are made; then the probability of making a total score of n is of course:-

$$P_0 P_n + P_{(n-1)} P_1 + P_{(n-2)} P_2 + \cdots \cdots + P_n P_0$$

This is seen to be the coefficient of x^n in the expansion of $F^2(x)$, which is thus the generating function appropriate to the probability distribution for two observations. We can extend this principle to obtain the distribution for three, four, or more observations. For r observations, the generating function will be:-

$$F^r(x) \qquad 2.30.$$

and if m_r, v_r are the mean and variance for r observations, it follows that:-

$$m_r = rm \quad , v_r = rv \qquad 2.31.$$

where m, v, are the mean and variance for single observations of the same type.

Consider now the case of two successive probability distributions, each event of the first type being succeeded by one of the second type. The appropriate generating function can be shown to be:-

$$F_1(F_2(x)) \qquad 2.32.$$

where $F_1(x)$, $F_2(x)$ are the generating functions for the two distributions considered individually; this is clear if we write $F_1(F_2(x))$ in the form:-

$$p_0 F_2^0(x) + p_1 F_2'(x) + p_2 F_2^2(x) + \cdots \quad \cdots + p_n F_2^n(x) \cdots$$

where p_n is defined by:-

$$F_1(x) = p_0 x^0 + p_1 x^1 + p_2 x^2 + \cdots \quad \cdots + p_n x^n \cdots$$

It will be seen that the term in $F_2^n(x)$ which represents the generating function for a set of n similar observations of the second type is weighted by the factor p_n which is the probability that a single observation of the first type will give a score of n .

From this it follows that if M , V , are the mean and variance of the combined distribution due to two successive types of event, then:-

$$M = m_1 . m_2 , \quad V = v_1 m_2^2 - v_2 m_1 , \qquad 2.33.$$

where m_1 , m_2 ; v_1 , v_2 are the means and variances for single observations of each type considered separately. This principle can obviously be extended to account for any number of

successive distributions; for r distributions, the appropriate generating function will be:-

$$F_1(F_2(F_3 \cdots (F_r(x)) \cdots) \qquad 2.34.$$

One may now apply the relationships deduced above to the scintillation counter. One must first decide what are the generating functions appropriate to each distribution involved in the production of the pulse at the photo-multiplier output; these distributions will therefore be considered in turn:-

If the production of light quanta in the luminophor by particles of a given energy were governed only by random statistics, the resulting distribution would be of the Poisson form. In any practical case, the distribution will be somewhat distorted by the fact that certain of the particles may escape from the luminophor before expending all their energy. However this effect will be small provided that the linear dimensions of the luminophor are large compared with the range of the particles within it. As a first approximation, one may assume this to be the case, and assume a Poisson distribution (2.28) for the number m_1, of light quanta produced per scintillation for particles of equal energy.

The probability m_2 , that a quantum of light produced in the luminophor falls on the photo-multiplier cathode is determined by the statistics of simple choice (2.29). It is assumed here that the optical efficiency of the system is constant for light emitted at all points within the luminophor; if this is not so, the final distribution will be broadened.

The probability m_3 , that a quantum of light falling on the photo-cathode releases an electron, and the probability m_4 , of this electron being captured by the first dynode, are also determined by the statistics of simple choice (2.29).

If the emission of electrons at each successive dynode of the photo-multiplier is governed by random statistics, and if there is no loss of electrons after the first dynode, one may assume a Poisson distribution at each stage. Combining n such stages after the manner of equation 2.33, the mean gain and variance of the photo-multiplier dynode system are found to be:-

$$m = R^n, \quad v = R^n(R^{(n-1)} + R^{(n-2)} + R^{(n-3)} + \cdots \cdots + 1)$$
$$= \frac{R^n(R^n - 1)}{(R-1)} \qquad 2.35.$$

This expression has been derived by Sauter (1948) and, incorrectly, by Morton and Mitchell (1948). If $R > 2$

and n is large, as is the case in practice, one may write

$$V \simeq \frac{R^{2n}}{(R-1)} \qquad 2.36.$$

One may now construct a table showing the means and variances of the various distributions, as follows:

Table III

Statistics of Scintillation Counters.

	Generating Function	Mean	Variance
Luminophor	$F_1(x) = e^{m_1(x-1)}$	m_1	m_1
Optical System	$F_2(x) = (1-m_2) + m_2 x$	m_2	$(m_2 - m_2^2)$
Photo-cathode quantum efficiency	$F_3(x) = (1-m_3) + m_3 x$	m_3	$(m_3 - m_3^2)$
Loss of electrons between photo-cathode and first dynode.	$F_4(x) = (1-m_4) + m_4 x$	m_4	$(m_4 - m_4^2)$
Photo-multiplier.	$F_5(x) = G_1(G_2(G_3 \cdots (G_n(x)) \cdots)$ where $G(x) = e^{R(x-1)}$	R^n	$\frac{R^{2n}}{(R-1)}$

Combining the means and variances in the manner of equation 2.33, one obtains for the mean amplitude and variance M , V , of the output pulse from the photo-multiplier:-

$$M = m_1 . m_2 . m_3 . m_4 . R^n \qquad 2.37$$

$$V = m_1 . m_2 . m_3 . m_4 . R^{2n} \left(1 + \frac{1}{(R-1)}\right) \qquad 2.38$$

and the fractional variance $\frac{V}{M^2}$ is seen to be given by:-

$$\frac{V}{M^2} = \frac{\left(1 + \frac{1}{(R-1)}\right)}{(m_1 . m_2 . m_3 . m_4)} \qquad 2.39$$

The quantity $(m_1 . m_2 . m_3 . m_4)$ in the denominator of this expression is of course the mean number of electrons reaching the first dynode of the photo-multiplier during any one pulse.

For single electrons emitted at the photo-cathode, the corresponding expressions are:-

$$M_1 = m_4 . R^n \qquad 2.40$$

$$V_1 = m_4 . R^{2n} \left(1 - m_4 + \frac{1}{(R-1)}\right) \qquad 2.41$$

$$\frac{V_1}{M_1^2} = \frac{\left(1 - m_4 + \frac{1}{(R-1)}\right)}{m_4} \qquad 2.42$$

It will be seen from equations 2.38 and 2.39 that the variance of the output pulse distribution may be expected to increase with increasing mean pulse amplitude, but that the fractional variance of the distribution decreases with increasing mean pulse amplitude. In measurements in which it is required to resolve the distributions produced by secondary electrons of different energies e.g. gamma-ray spectroscopy or gamma-ray absorption studies, the product $(m_1 . m_2 . m_3 . m_4)$ must therefore be made as high as possible. This requires a luminophor of high light output matched to the spectral response of the photo-multiplier, and an optical system of high efficiency.

Because of the non-Gaussian character of the output pulse distributions produced by secondary electrons of a single energy, they cannot easily be combined with known secondary electron energy distributions, such as those of figures 6 and 7. An approximation to the combined distribution can be obtained if the assumption is made that the distributions due to mono-energetic secondary electrons are normal, but have the fractional variances given in equation 2.39.

The error implicit in this assumption will be small provided that the quantity $(m_1 \cdot m_2 \cdot m_3 \cdot m_4)$ is greater than 5.

The ordinates of the normal curve of error are derived from the expression:-

$$y = \frac{1}{\sqrt{2\pi}} e^{-x^2/2} \qquad 2.43$$

where the values of x are measured in units of σ, the standard deviation, given of course by $\sigma = V^{1/2}$. From equation 2.38, the pulse amplitude distribution at the photo-multiplier output resulting from uniform light pulses in the luminophor, each containing (m_1), quanta, has a standard deviation of:-

$$\sigma = R^2 \cdot (m_1 \cdot m_2 \cdot m_3 \cdot m_4)^{1/2} \cdot \left(1 + \frac{1}{(R-1)}\right)^{1/2} \qquad 2.44$$

From equations 2.43 and 2.44, the normal distribution appropriate to any mono-energetic group of secondary electrons can be found. As an example of this method, consider now the secondary electron distribution for $cobalt_{60}$ gamma-radiation in calcium tungstate shown in figure 7. If this distribution is divided into

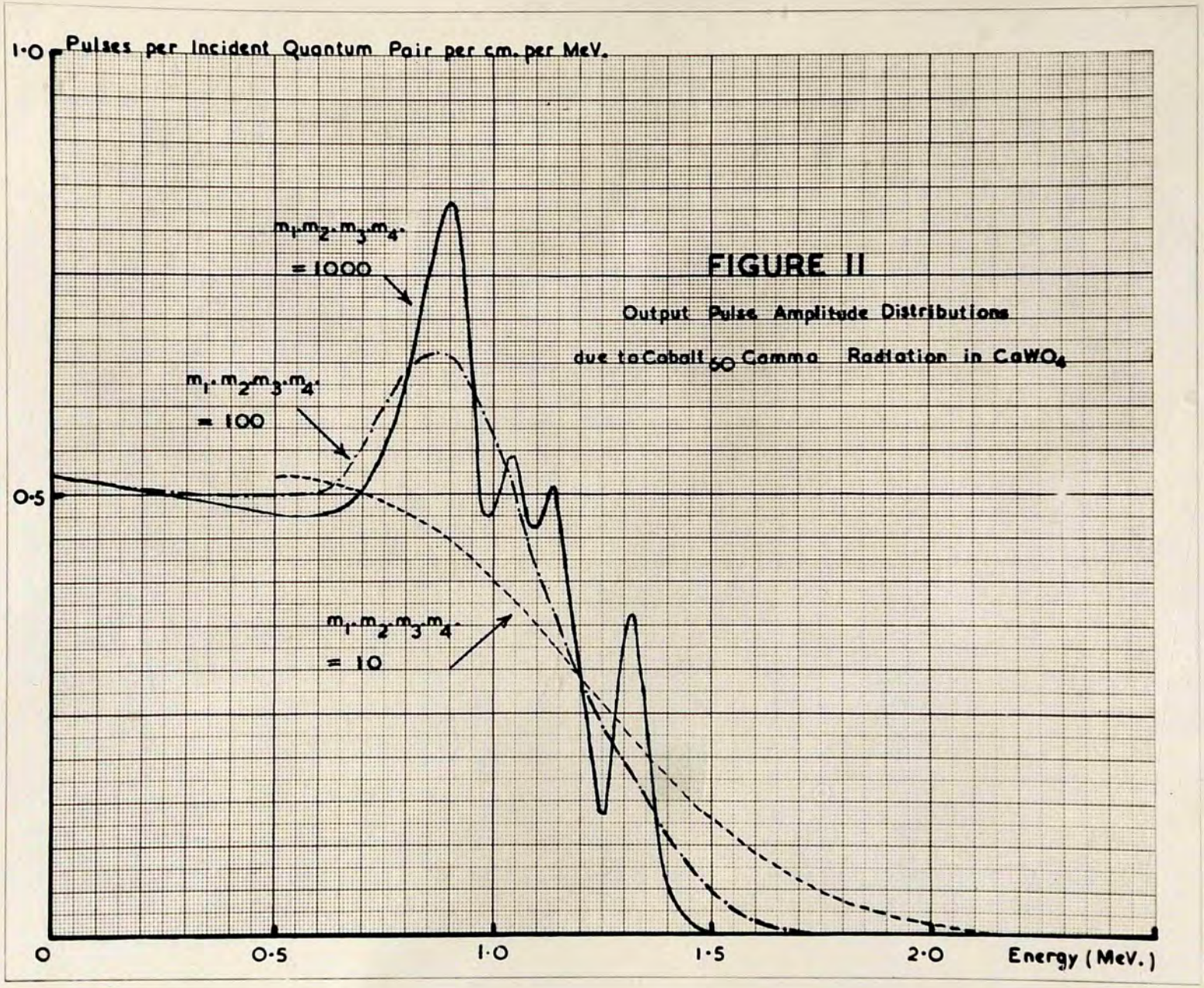

FIGURE II

Output Pulse Amplitude Distributions due to Cobalt $_{60}$ Gamma Radiation in $CaWO_4$

sections of 0.05 MeV., and each section is replaced by a normal distribution about its mid-point whose standard deviation satisfies equation 2.44 and whose ordinates are those given by equation 2.43 weighted appropriately, the distributionsof figure 11 result. These three distributions represent the complete output pulse amplitude distributions due to cobalt$_{60}$-radiation in calcium tungstate, when the release of a 1 MeV. secondary electron in the luminophor results in the arrival at the first dynode of the photo-multiplier of 10, 100, and 1000 electrons respectively. The distribution for $(m_1 \cdot m_2 \cdot m_3 \cdot m_4) = 10$ is not continued below $E_e = 0.5$ MeV because the errors implicit in the assumption of a Gaussian distribution become large in this case at low secondary electron energies. The dependence of resolution on optical efficiency is well illustrated.

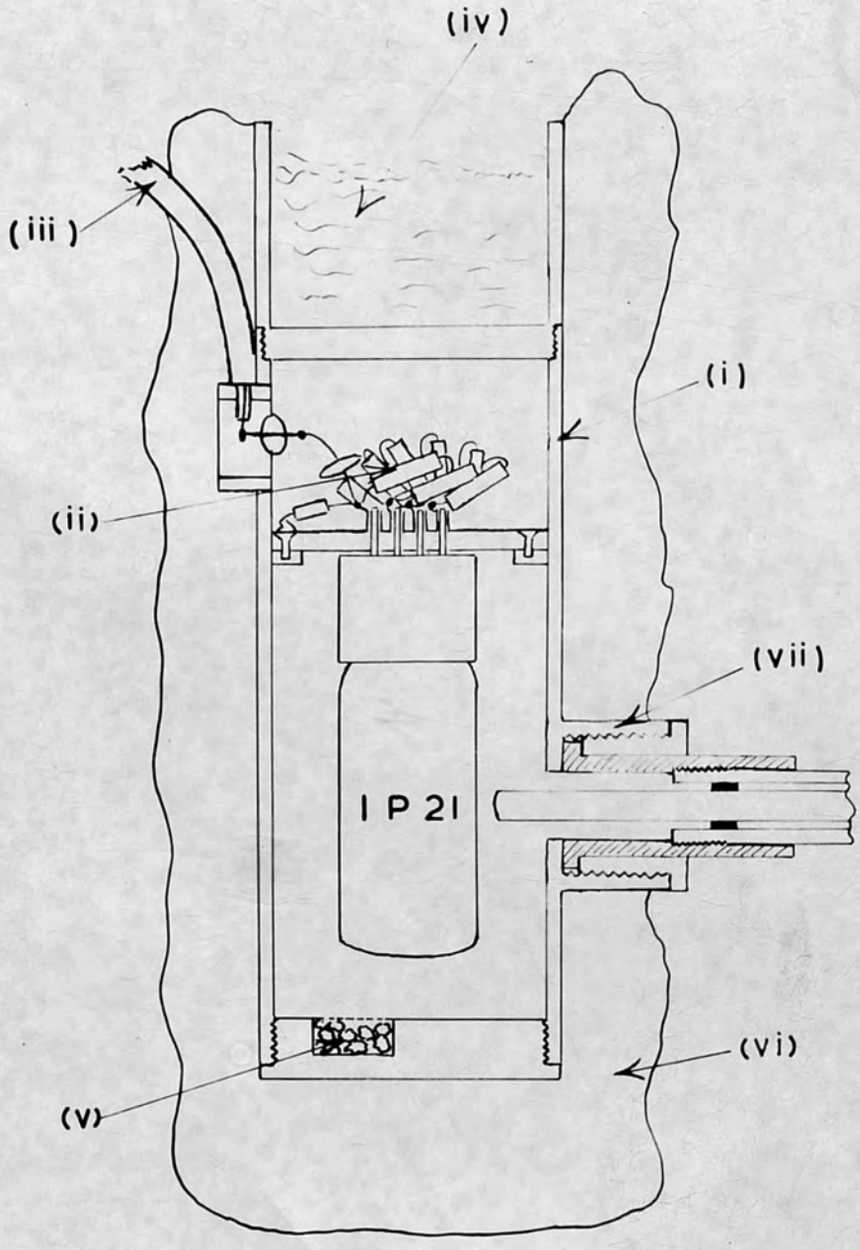

FIGURE 12

TYPE 1P21 PHOTO-MULTIPLIER MOUNTING

SECTION III. EXPERIMENTAL METHODS AND INSTRUMENTATION.

1. PHOTO-MULTIPLIER AND LUMINOPHOR MOUNTINGS:

(a) Type of Photo-Multiplier Used:-

The photo-multiplier used throughout these investigations was an R.C.A. type I P 21 tube, having nine multiplying stages and a rated overall voltage gain of 2×10^6 at an inter-stage potential of 100 volts. The photo-cathode of such tubes is of the antimony-caesium type with a maximum spectral sensitivity at about 4200 Å. and a rated sensitivity of 20 micro-amperes/lumen. Owing to the fact that the envelope is of glass, the spectral sensitivity curve falls rapidly for wavelengths below 3500 Å. (see figure 9).

(b) Photo-multiplier mounting:-

This tube was mounted as shown in figure 12 inside a heavy cylindrical brass case (i), which also contained the resistance chain (ii), through which the dynode potentials were maintained. Cables (iii), passing through light-tight insulated bushes supplied power to the dynodes and fed the photo-multiplier output pulses to the amplifying and recording equipment. The upper

FIGURE 13

LUMINOPHOR MOUNTINGS

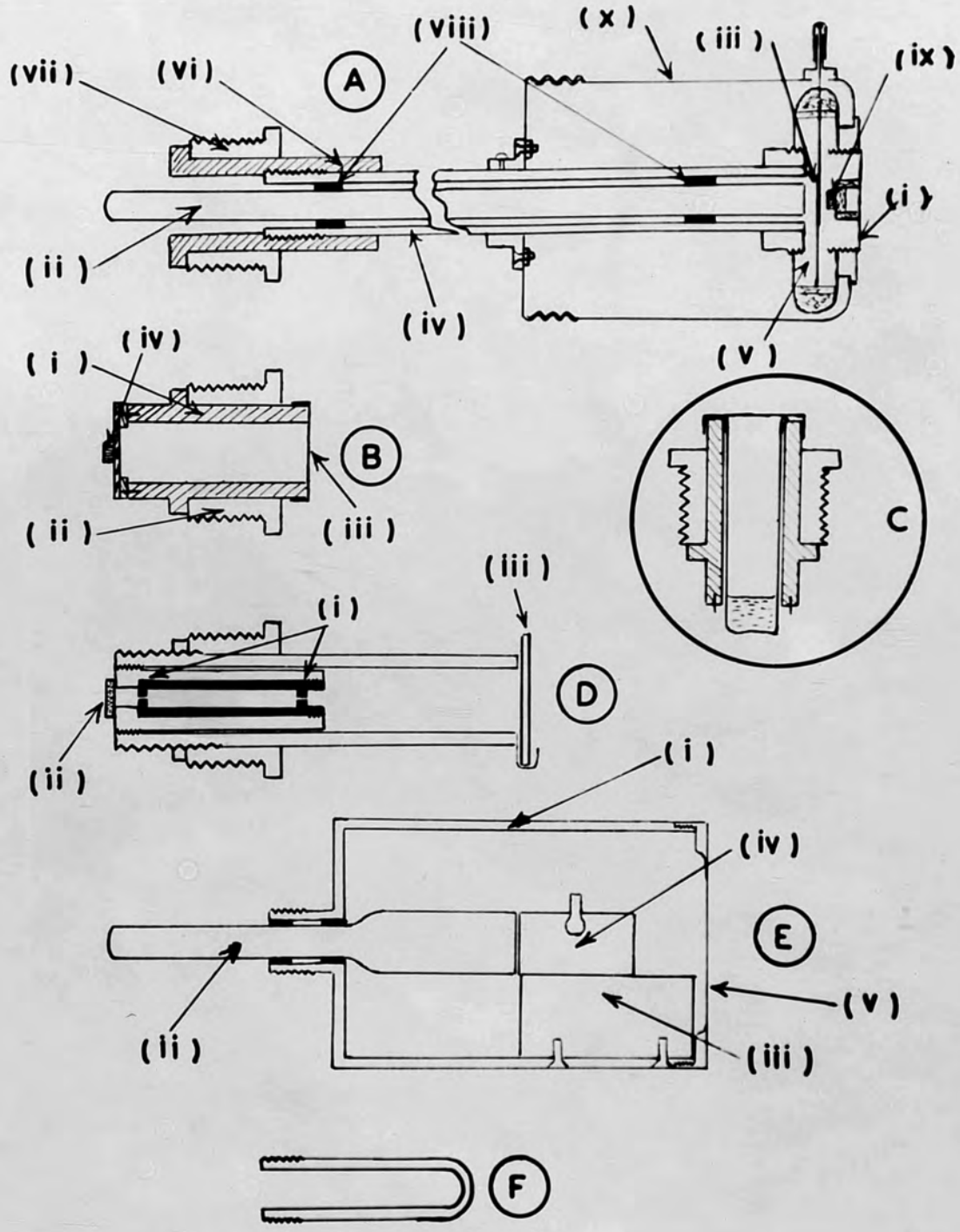

section of this brass case was in the form of a cup (iv), into which a cooling agent (liquid nitrogen or solid carbon dioxide) could be introduced in order to cool the photo-multiplier by conduction. A drying agent (v), (silica gel) placed in a small container in the lower portion of the case prevented frosting of the photo-multiplier envelope and other optical surfaces during cooling. The whole case was heavily lagged with cotton wool (vi), to ensure temperature stability and it was found that thermal equilibrium was reached approximately one hour after the initiation of cooling, whether by liquid nitrogen or by solid carbon dioxide.

A short side tube (vii), was mounted at right angles to the axis of the case directly opposite the cathode of the photo-multiplier, and into this tube could be screwed various interchangeable luminophor mountings and other devices. A number of these devices are shown in figure 13. Extreme care was needed to ensure that all screwed joints were completely light-tight since the presence of even a very low intensity of extraneous light would be sufficient to invalidate the results of investigations of the type under discussion.

(c) <u>Absolute Measurements on Crystals</u>:-

Measurements of the absolute counting rates

obtained in solid crystalline luminophors were made with the arrangement shown in figure 13 (inset A) screwed into the photo-multiplier holder. This consisted of a crystal holder (i), mounted at the end of a Perspex light guide 0.5 inches in diameter (ii), but separated from it by a camera shutter (iii). The end of the light guide nearest the crystal was ground and polished flat; that presented towards the photo-multiplier was convex and of such a curvature as to focus the transmitted light on to a small area of the photo-cathode. The light guide was enclosed in a tube of Dural (iv), on one end of which was mounted the camera shutter assembly (v). A short thermal-insulating section of Keramot tube (vi), separated the Dural tube from the threaded brass collar (vii), and prevented cooling of the crystal by conduction down the Dural during experiments in which the photo-multiplier tube was cooled. Small collars (viii), mounted on the light-guide preserved an air space between it and the Dural rod, since it was found that the light transmitting properties of the guide were impaired wherever there was a face contact between it and other surfaces. The crystal

holder (i), was screwed into the camera shutter assembly and consisted of a short cylinder of thin brass across which two balsa-wood guides were cemented, the whole being covered and made light tight by a diaphragm of black paper. A light-tight hood (x), surrounded both crystal holder and camera shutter assembly. The crystals themselves were mounted on thin slips of balsa-wood (ix), which fitted exactly into the space between the guides in the crystal holder, the thickness of the slips being adjusted to the size of the crystals in such a way that the front face of every crystal, when inserted, was flush with the end of the holder. A selection of crystals thus mounted is seen in figure 14. By taking counting rates first with the camera shutter open and then with the shutter closed, it was possible to correct for the background effects and obtain the true counting rate due to the scintillations produced in the crystal.

Studies using the above device were made with the light guide horizontal and the photo-multiplier case mounted vertically on an optical bench, as seen in figure 15. This bench consisted of a rigid wooden table, two feet above which was fixed the crystal and

Figure 15.

Experimental Arrangement for Absolute Measurements on Crystals.

1.7.50 D.855

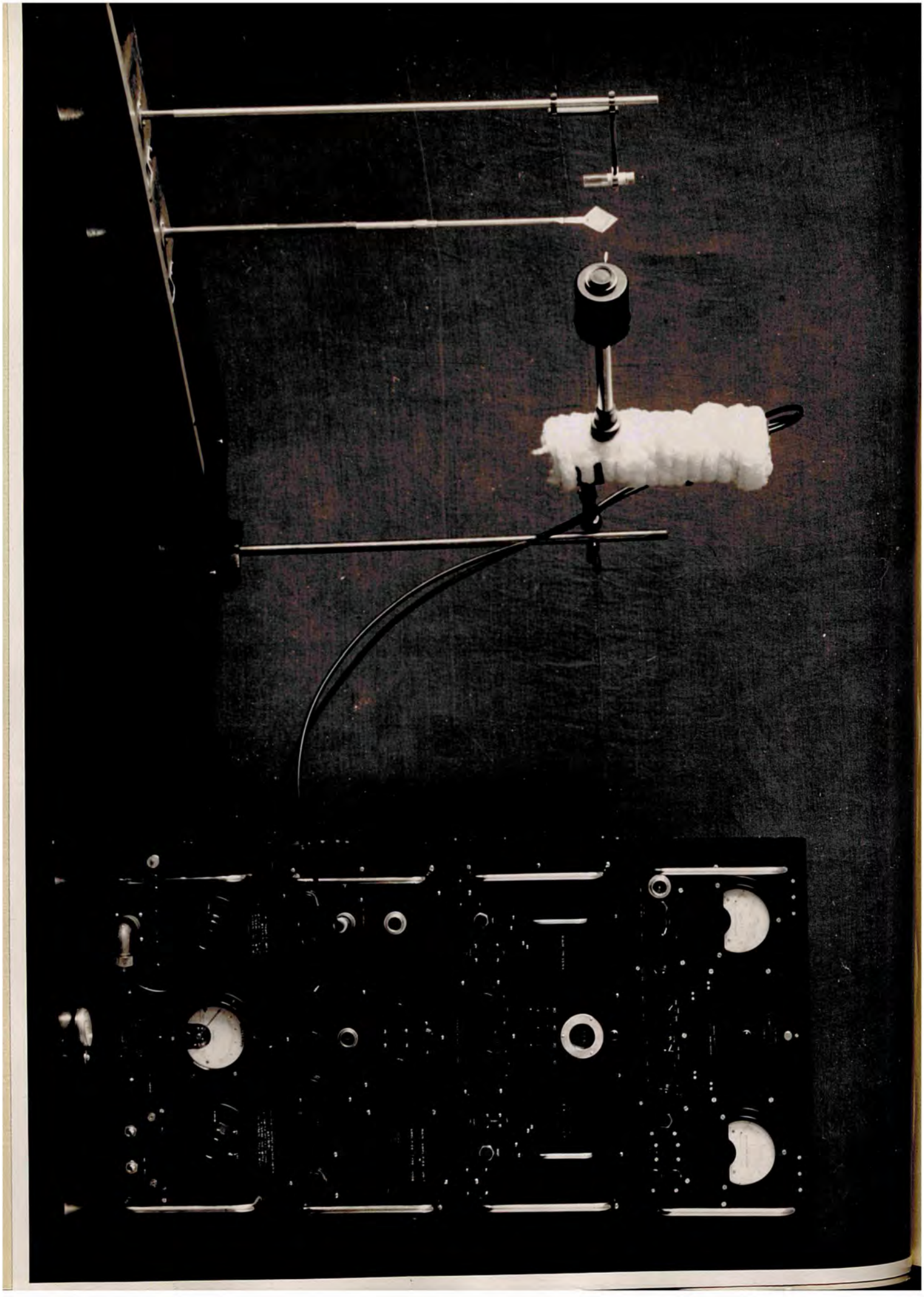

photo-multiplier mounting. Source and filter holders of telescopic Dural tube moving along a calibrated slide made possible the positioning of sources and absorbers at measured distances from the crystal along the axis of the light guide. The whole optical bench was placed well clear of the walls of the laboratory. Under these conditions, excitation of the crystal by scattered radiation was reduced to a minimum. Since the crystal mounting consisted of very light material of low mean atomic number, the only appreciable source of degenerate radiation was back-scatter from the shutter assembly, the light guide, and the photo-multiplier and its case. This should be only slight for high energy gamma-radiation ($>$ 0.2 MeV.) which is scattered mainly in the forward direction. Preliminary experiments with lead blocks and strips placed around the crystal holder confirmed this. In no case could scattered radiation account for more than 5% of the total counting rate observed in single crystals.

(d) Comparative Measurements on Crystals:-

In certain applications, notably the study of pulse amplitude distributions, it was required to mount the crystal in close proximity to the photo-

multiplier envelope, this could be conveniently achieved with the holder shown in figure 13 (inset B). The latter consisted of a short length of Keramot tube (i), over which fitted a threaded brass collar (ii), the whole being closed by a diaphragm of thin black paper held in place by a Dural locking ring (iii). The crystal, on its balsa-wood mount, was held in position by two steel pins (iv), driven into the Keramot. Measurements with this device were usually made with the photo-multiplier case mounted in an upright position on the optical bench as already indicated.

(e) Comparative Measurements on Liquids:-

If however the photo-multiplier case were mounted horizontally the device just described could be used for measurements on liquid samples, a small cylindrical glass phial being mounted as shown in figure 13 (inset C). The length of this phial was such that when in position its flat base was at the same level with respect to the photo-multiplier as the nearest face of the crystals in the previous application. Its outside diameter ($\frac{1}{2}$ inch) was slightly smaller than the inside diameter of the Keramot tube, so that a 1 ml. sample of the liquid under investigation gave a depth of 0.5 cm. It should be pointed out that the arrangements shown as insets B and C,

unlike that of inset A, cannot be considered scatter-free, since in the former the luminophor is mounted inside the heavy brass case in close proximity to the photo-multiplier.

(f) Study of Photo-multiplier Characteristics:-

In experiments in which it was desired to excite the photo-multiplier with continuous or pulsed light from an external source, the device shown in figure 13 (inset D) was used. This consisted of a double pin-hole collinator (i), terminating at one end in a small ground glass screen (ii) and having a fitting at the other end into which light filters of the Ilford "Spectrum" type could be clipped (iii). The complete collimator could be screwed directly into the photo-multiplier case by means of a threaded brass collar, or indirectly through a short brass adaptor into the light guide assembly of inset A in place of the crystal holder. In either case, the position occupied by the ground glass screen with respect to the photo-multiplier was the same as that occupied by the nearest face of the crystals in the corresponding arrangements of insets A and B.

(g) Absolute Measurements on Liquids:-

In measurements on the absolute counting rates

obtained in liquid luminophors, a more scatter-free arrangement than that of inset C was required, and accordingly, the device shown in figure 13 (inset E) was designed. This consisted of a light-tight Dural cylinder (i), containing a short light guide of tapered perspex rod (ii), which could be screwed into the Keramot tube of the assembly of inset A in place of the light guide and camera shutter unit. Perspex knife-edges (iii) supported one of several cylindrical cells (iv) of varying capacity which could be filled with the liquid under investigation, and then placed with one face close against the flat polished end of the light guide. The latter had a diameter of 1 inch at this point, slightly larger than the outside diameter of the cells, but tapered to 0.5 inch before entering the photo-multiplier case. The unit was closed by a screwed cap of thin Dural.

(h) Measurement of Photo-multiplier Background:-

Finally where it was desired to measure the background of the unstimulated photo-multiplier, a Dural plug (figure 13, inset F) could be screwed into the Keramot tube of the assembly shown in inset A.

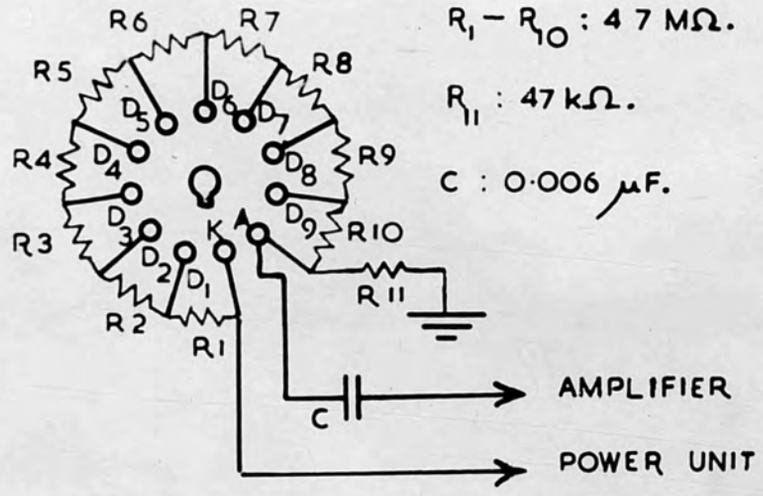

FIGURE 16

CIRCUIT OF PHOTO-MULTIPLIER

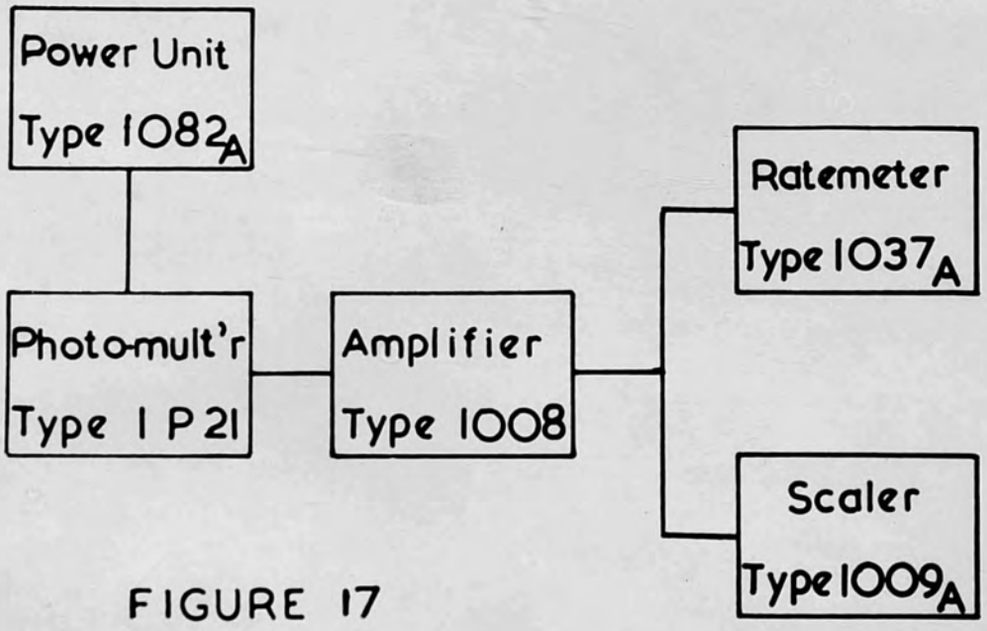

FIGURE 17

SCHEMATIC DIAGRAM OF COUNTER

2. ASSOCIATED ELECTRONIC EQUIPMENT:

(a) Photo-multiplier unit:-

The electrical circuit of the photo-multiplier unit is shown diagrammatically in figure 16, and in figure 17 a schematic diagram of the associated electronic equipment is given. It will be observed that no cathode follower was mounted on the photo-multiplier unit, the output being fed directly over a 4.0 foot length of "Uniradio 32" concentric cable to the linear amplifier. This resulted in some loss of pulse amplitude and shape owing to the high input capacity of the system.

(b) Linear Amplifier:-

The amplifier was an Amplifier Type 1008, having a rated overall gain of 16,000 and a band-width of 20 c/s.- 500 kc/s. Both low impedance and high impedance input circuit are available in this unit; in the present application, the high impedance circuit was used, for which the input capacity is stated to be 20 pF., and the input impedance 500 KΩ. The amplifier has a switched attenuator giving a 10 : 1 cut in signal at its input and consists of two three-stage amplifying units separated by a second attenuator giving a variable attenuation between 0 dB. and 20 dB.

in 2 dB. steps. A total range of attenuation between 0 and 40 dB. could thus be covered in 2 dB. steps by manipulation of these two controls, the minimum overall gain being 160. The gain stability is rated at ± 1% for a mains variation of ±10%.

(c) Counting Rate Meter:-

The output of the amplifier was fed to a ratemeter type 1037 A and to a scaler type 1009 A in parallel. In the former, counting rates are read directly on a meter whose deflection is linearly proportional to counting rate . An overall range of 0 to 100,000 counts/second is covered in six ranges by a switch, the full scale deflections of these ranges corresponding to 1, 10, 100, 1000, 10,000 and 100,000 counts/second respectively. A series of integrating times is provided on each range, selected by a switch which varies the integrating capacity of the circuit; capacities of 8, 2, 0.5, 0.1 or 0.02 μF may be chosen. When used with a random source of pulses, the counting rate meter reading fluctuates about its mean value in a manner determined by the mean pulse rate and the integrating time selected. The R.M.S. value of the fluctuations is given by the formula:-

$$\text{R.M.S. fluctuation} = \pm \frac{100}{\sqrt{2n\tau}} \% \text{ of mean reading} \qquad 3.1.$$

where n = mean pulse rate

τ = integrating time in seconds.

The integration time can be changed during measurement without affecting the meter reading; thus it is possible to use a short time constant at first to obtain an approximate reading, and then switch to progressively longer time constants to obtain a more accurate value with smaller fluctuations. In measurements with this ratemeter it was found desirable always to use a final integration time such that the R.M.S. fluctuation of the meter reading determined by formula 3.1 was at all times less than the scale reading error - estimated at $\pm \frac{1}{2}$ scale division. The latter corresponds to an error of 1% in counting rates giving full scale deflection of the meter, and 10% in rates giving 1/10 full scale deflection. Choosing a sufficiently long integrating time in this way, the error in observed counting rate was always determined by the scale reading errors and not by the R.M.S. fluctuation of the meter reading.

(d) Scaler:-

The scaler type 1009 A consists of two scale-of-ten circuits followed by a mechanical register. The latter moves one unit for every hundred pulses, the tens and units being recorded on neon indicators.

Counting is started and stopped manually by a panel key. If the mean number of counts recorded in a given time is N, then the standard deviation assuming a random distribution of pulses in time is $N^{\frac{1}{2}}$ (see equation 2.28). Hence the percentage standard error in any given estimate of counting rate with the scaler is:-

$$\text{Percentage error} = \frac{100}{N^{\frac{1}{2}}} \% \text{ of observed rate.} \qquad 3.2.$$

where N is the recorded number of counts. It will be seen from 3.2 that a percentage error of less than 1% requires the counting of at least 10,000 pulses. In experiments with the scaler at least this number of pulses were counted wherever possible.

In the study of the absolute counting rates obtained in various materials, the true counting rate in the luminophor was usually obtained as the difference between two rates, the total counting rate and the background. In such a case, the percentage standard error in the true rate can be shown to be given by the well-known expression:-

$$\text{Percentage error} = \frac{100\,(N_1+N_2)^{\frac{1}{2}}}{(N_1 - N_2)} \% \text{ of observed rate} \qquad 3.3.$$

where N_1 , N_2 are the number of counts recorded in measuring the total rate and background respectively.

(e) Pulse Discriminator Circuits of Ratemeter and Scaler:-

Both the scaler and ratemeter incorporate calibrated pulse discriminator circuits, which select for counting only pulses of amplitude greater than a given value. In the case of the ratemeter, this amplitude is continuously variable from 5 to 50 volts by means of a single potentiometer control, the voltage being displayed on a panel voltmeter. In the scaler, a switch selects a range of amplitude from 5 to 10, 10 to 20, 20 to 30, 30 to 40, or 40 to 50 volts, and a continuously variable potentiometer calibrated from 0 to 10 volts gives control over the selected range, the voltage being read on the calibrated dial of the potentiometer.

Owing to overheating within the unit, the levels of pulse discrimination of the scaler type 1009 A were found in practice to be subject to considerable drift; moreover the potentiometer calibration was found to be unreliable, especially at readings between 0 and 1 and between 9 and 10 volts. For these reasons, wherever it was required to plot accurate pulse amplitude distributions, it was preferred to use the ratemeter

type 1037 A; the latter unit was found completely steady and free from drift.

(f) Variable Resolving Time Circuits of Ratemeter and Scaler:-

Both these units also incorporate a variable resolving time circuit (Cooke-Yarborough, 1949) which makes them insensitive for a short period after each recorded pulse. The paralysis time is selected by a switch and in each unit the following values are available:-

"OFF" (approximately 1 microsecond), 5, 10, 20, 50, 100, 200, 500, 1 K., 2 K., 5 K., 10 K. microseconds. These values are stated to be correct to ± 5%.

In measurements with a counter of finite resolving time, the observed counting rates must be corrected to allow for pulses uncounted because they arrive during the time for which the circuit is insensitive. The appropriate correction for devices which cannot be re-excited during their cycle of operation has been developed by Ruark and Brammer (1937) and by Skinner (1935). If the observed counting rate is n' counts/sec, the true rate n counts/sec. and the resolving time of the counter τ, then assuming a random distribution of pulses in time:-

$$\frac{n}{n'} = \frac{1}{1+n\tau}$$

whence

$$\frac{1}{n} = \frac{1}{n'} - \tau \qquad 3.4.$$

Using tables of reciprocals, the true rates can be quickly computed from equation 3.3., provided that the appropriate value of the resolving time of the counter is known.

(g) Power Units:-

The amplifier type 1008, ratemeter type 1037 A and scaler type 1009 A have their own built-in power supplies. The photo-multiplier dynode potentials were maintained from a Power Unit type 1082 A; this gives a voltage output continuously variable up to 3 kV., and stabilised to ± 1% for mains variations of ± 10%. Connection to the photo-multiplier resistance chain was made over a 4 foot length of "Uniradio 32" cable, and the photo-multiplier was normally operated at an inter-dynode potential of 108 volts.

(h) Stop-watch:-

In all measurements with the scaler type 1009 A a single stop watch with a 60 second dial was used: this was checked frequently against the Post Office "Talking Clock" (TIM) and on no occasion showed an error greater than 0.2%.

3. METHODS OF CALIBRATION OF THE ELECTRONIC EQUIPMENT.

(a) Calibration of Linear Amplifier Gain:

The gain of the Amplifier type 1008 was determined at regular intervals during the experimental studies by feeding into it rectangular pulses derived from a calibrated Pulse Generator type 200, and measuring the amplitude of the output pulses on a calibrated Cossor oscilloscope. The pulse generator in question is designed to give single or double rectangular pulses. Two channels of single pulses (channels A and B) are provided, both giving pulses of amplitude variable between 1 and 100 volts. These are combined in channel C, in which double pulses with a separation variable between 0 and 110 microseconds and an amplitude between 10 microvolts and 50 volts are available. The pulse width can be varied between 0.1 and 10 microseconds in all cases and the pulse recurrence frequency between 50 and 50,000 pulses/second.

In this application, pulses from channel C were selected, the pulse width being 1 microsecond and the pulse recurrence frequency 250 pulses/second.

For each attenuator setting of the amplifier, the input voltage required to produce an output of 10 volts was determined. A typical set of results are summarised in Table IV; since the error in measuring the pulse amplitude of the pulse generator is stated to be ± 5%, the values of voltage gain quoted may be assumed correct within similar limits.

Table IV.

Calibration of Attenuators: Amplifier Type 1008, S/No. 121.

Input Attenuator Setting	Variable Attenuator Setting	Overall Gain	Attenuation (dB)
0	0	12400	0
0	2	10000	1.9
0	4	8330	4.1
0	6	6250	6.0
0	8	4760	8.3
0	10	3840	10.2
0	12	3030	12.2
0	14	2440	14.1
0	16	2000	15.8
0	18	1590	17.8
0	20	1280	19.7
20	0	1060	21.4
20	2	901	23.4
20	4	667	25.4
20	6	500	27.9
20	8	400	29.8
20	10	322	31.7
20	12	256	33.7
20	14	204	35.7
20	16	170	37.2
20	18	135	39.2
20	20	109	41.1

(b) Calibration of Pulse Discriminator Circuits:

The pulse discriminator circuits on both scaler and ratemeter were similarly calibrated using single pulses of width 1 microsecond from channel B of the Pulse Generator type 200. In these measurements, the output of the pulse generator was fed directly into the recording unit under test. The discriminator control of the latter was set a selected value, and the pulse generator amplitude control was then adjusted until the observed counting rate was half the pulse recurrence frequency. In practice the counting rate rose very sharply from zero to its maximum value, and it was sufficient to adjust the amplitude control until counting just occurred. Measurements were made at a nominal resolving time of 10 microseconds.

Typical sets of results are shown in Tables V and VI below. The errors in pulse amplitude for channel B of the pulse generator are stated as $\pm$ 4% or $\frac{1}{2}$ scale division which ever is the greater; in these results they may be taken in all cases as $\pm$ 4%

Table V.

Calibration of Pulse Discriminator: Ratemeter Type 1037[A], S/No. E.4.

Discriminator Volts.		5	10	15	20	25	30	35	40	45	50
P	500/sec.	5.7	11	17	22	28	33.5	39	44	50	55
R	5000/sec.	5.4	11	17	22	28	33.5	39	44	50	55
F	50000/sec.	5.5	12	18	23	29	35	40	46	52	57

Table VI.

Calibfation of Pulse Discriminator: Scaler Type 1009[A], S/No. 161.

Discriminator Volts.		5	10	15	20	25	30	35	40	45	50
P	500/sec.	5.5	12	18	24	30	35	41	46	51	57
R	5000/sec.	5.6	12	18	24	30	35	41	46	52	57
F	50000/sec.	5.7	12	19	25	30	37	42	48	53	59

(c) Calibration of Variable Resolving Time Circuits:

The variable resolving time circuits were calibrated using two separate methods, by measuring the fall in counting rate from a standard source as the resolving time is increased from its lowest

value, and by using the double pulses from channel C of the Pulse Generator type 200.

The first method is only suitable for the determination of resolving times of 100 microseconds or more. Where the true counting rate of the source is not known, some method of increasing it in a known ratio must be devised in order to determine the resolving time. This has been achieved by observing the decay of a radioactive source of known half-life (Flammersfelt, 1939), the use of multiple weak sources (Lifschutz and Duffendack, 1938 a, b), and by the use of two sources of nearly equal strength (Beers, 1942), but none of these methods is capable of giving sufficient accuracy within a reasonable measuring time. However, in the case of circuits of the type under consideration here, the true counting rate may be taken as the counting rate observed when the resolving time is set at the lowest value (approximately 1 microsecond). The resolving time at any other setting can then be calculated from the expression:-

$$\tau = \frac{1}{n'} - \frac{1}{n} = \frac{(n - n')}{nn'} \qquad 3.5.$$

derived from equation 3.4., n being the counting rate observed at the lowest resolving time, and n' that observed at a resolving time of τ . The value of τ obtained in this way is subject to a percentage error equal to the root mean square of the errors in n , n' , and ($n - n'$). In the case of the scaler, this will be:-

$$100 \left[\frac{1}{N} + \frac{1}{N'} + \frac{(N + N')}{(N - N')^2} \right]^{1/2} \qquad 3.6.$$

where N , N' are the corresponding numbers of counts recorded. It is clear that the percentage error can be reduced by increasing N , N'. In the ratemeter on the other hand, the errors in n , n' are determined by the scale reading error of the instrument and cannot be so reduced.

In measurements using this method, the photo-multiplier, cooled in liquid nitrogen and excited by a source of approximately 1 millicurie of cobalt 60 at 50 cms. distance, was used as a source of random pulses. The linear amplifier was operated at full gain, and the pulse discriminator of the scaler or ratemeter adjusted to give a suitable counting rate at minimum resolving time. Counts were taken with

the scaler over 5 minute periods, and measurements with the ratemeter were made using the longest available integration time.

For the settings of resolving time up to and including 100 microseconds, the second method was preferred. In this, double pulses from channel C of the pulse generator were fed directly into the scaler or ratemeter, at a pulse recurrence frequency of 250 pulses/second; the pulse separation was then adjusted until the twin pulses were just resolved and the observed counting rate rose sharply to 500 pulses/second. The pulse separation read off the calibrated dial of the pulse generator then equalled the resolving time. The error in determining this value is stated to be $\pm \frac{1}{2}$ scale division, that is $\pm$ 0.1 microsecond on the the 0 - 10 microsecond range of pulse separation, and $\pm$ 1 microsecond on the 10 - 110 microsecond range. For these measurements, the pulse amplitude was set at 20 volts and the pulse width at 1 microsecond. The pulse discriminator setting of the scaler or ratemeter was 10 volts.

At resolving times greater than 100 microseconds, it was still possible to use pulse separation as a measure

of resolution. The method used in such cases was to feed in single pulses of 20 volts amplitude and 1 microsecond width at a high pulse recurrence frequency and to adjust the latter until the observed rate fell below that indicated on the dial of the pulse generator. The separation between adjacent pulses determined by the latter rate then equalled the resolving time. The error in measurement of counting rate is stated to be $\pm$ 50 pulses/second over the 500 - 5000 pulses/second range and $\pm$ 500 pulses over the 5000 - 50000 pulses/second range. The correct value of pulse separation could be verified by observing the pulses on a calibrated Cossor Oscillograph (type 1035); the accuracy of the latter was not known, but its error was probably not greater than 3%.

The results of both types of measurement are summarised in Tables VII and VIII. It will be observed that the errors for the loss of counts method are considerably higher for the ratemeter than for the scaler, for the reason outlined above, but that the nominal values of resolving time are in most cases correct within the limits of experimental error.

Table VII

Calibration of Resolving Times: Ratemeter Type 1037[A], S/No. E.4.

Nominal Resolving Time (Microseconds)	5	10	20	50	100	200	500	1 K	2 K	5 K	10 K
Resolving Time by Loss of Counts Method (Microseconds)	-	-	-	52	105	203	511	1020	2140	5950	10800
Percentage Error	-	-	-	175	88.8	47.4	20.5	1188	7.56	6.51	3.17
Resolving Time by Pulse Separation Method (Microseconds)	5.5	12	22	52	104	190	500	1050	2200	5900	10800
Percentage Error	1.82	8.33	4.54	1.92	0.96	3.00	3.00	3.00	3.00	3.00	3.00

Table VIII.

Calibration of Resolving Time: Scaler Type 1009[A], S/No. 161.

Nominal Resolving Time (Microseconds)	5	10	20	50	100	200	500	1 K	2 K	5 K	10 K
Resolving Time by Loss of Counts Method (Micro-seconds)	-	-	-	62	126	239	485	1090	2100	5650	10400
Percentage Error ±	-	-	-	22.5	11.4	6.01	3.14	1.60	1.04	0.779	0.815
Resolving Time by Pulse Separation Method (Microseconds)	5.4	12	22	55	101	185	470	1100	2100	6200	11300
Percentage Error ±	1.85	8.33	4.54	1.82	0.99	3.00	3.00	3.00	3.00	3.00	3.00

4. LUMINOPHORS USED IN THE EXPERIMENTAL STUDIES.

(a) Calcium Tungstate:

Early experiments with calcium tungstate were made with opaque polycrystalline specimens of Scheelite of doubtful purity. These were found to be very variable in performance and of low efficiency; their use was therefore discontinued. All measurements of absolute counting rates in this material were made with artificial crystals of pure calcium tungstate obtained from the Linde Air Products Co. Ltd. of New York. These crystals were obtained as $\frac{1}{8}$ inch diameter rods up to 1 inch in length and of great clarity. They could be cleaved with a sharp knife blade at right angles to their length, into sections of any desired thickness, which were then mounted upright on balsa-wood slips by means of a drop of cellulose cement. They proved extremely stable to atmospheric conditions and showed no apparent deterioration after two years' use.

(b) Thallium-activated Potassium Iodide:

Thallium-activated potassium iodide (up to 1% thallium) was obtained in the form of clear cubic crystals of edge up to 2 cms. from Mr. J. Sharpe of A.E.R.E. Harwell. These crystals could be readily cleaved with

a razor blade into rectangular sections of any desired size, and mounted on balsa-wood. Although readily soluble in water, they were stable to atmospheric conditions in the laboratory, but showed some yellow discolouration after six months' use, possibly due to surface oxidation with the liberation of small amounts of free iodine.

(c) Thallium-activated Sodium Iodide:

Towards the end of the research programme described in this thesis, single crystals of thallium-activated sodium iodide (up to 1% thallium) were obtained in the form of cubic crystals of edge up to 2 cms. from Messrs. Adam Hilger Ltd. These crystals were partially clear at first, but extremely unstable owing to the rapid deliquescence of sodium iodide. A cleaved surface became opaque in a few minutes at room temperature in the open laboratory, but it was possible to preserve clear cleaved specimens indefinitely in a dessicator or on a hotplate (60°C). Crystals could be conveniently worked on such a hotplate using hot instruments, and sections of suitable size mounted on balsa-wood. Numerous varnishes were tested in efforts to find a suitable coating to protect crystals mounted in this way. Canada balsam in xylene, Perspex in benzene or chloroform, shellac

in chloroform, and Formvar in chloroform were found valueless, the crystal becoming yellow or brown with the liberation of free iodine and absorbing appreciable amounts of water within a few days. The most suitable coating appeared to be Vaseline (50 gm.) dissolved in benzene (100 ml.) and liberally applied to all surfaces of the crystal; absorption of light in the resultant coating was slight, and crystals so treated showed no significant deterioration after seven days in the open laboratory. Even so, it was found desirable to store such mounted specimens in the dessicator.

(d) Organic hydrocarbons:

Single crystals of pure anthracene and of naphthalene containing 0.5% anthracene, were obtained from Dr. G. H. J. Garlick of Birmingham University in the form of small flakes and needles up to 2 cms. long and of varying clarity. They could be readily cut with a razor blade and mounted on balsa-wood, but sublimed in the open laboratory, so that it was necessary to store them in tightly stoppered containers if constancy of size and mass was to be maintained. This was particularly true of the anthracene-activated naphthalene specimens.

5. SOURCES OF GAMMA-RADIATION.

(a) Description of Sources:

The sources of gamma-radiation used in these studies were obtained from pile-irradiated materials from A.E.R.E. Harwell; the radioactive isotopes used were sodium$_{24}$, cobalt$_{60}$, bromine$_{82}$, iodine$_{131}$ and gold$_{198}$. In the case of all the isotopes except cobalt$_{60}$, the active materials were dissolved in water and diluted to give solutions of specific activity approximately 1 millicurie/millilitre; portions of these solutions containing approximately 1 millicurie were then pipetted into small cylindrical glass phials approximately 2 inches long and $\frac{1}{2}$ inch in diameter, which were used as gamma-ray sources.

The cobalt$_{60}$ sources consisted of several discs of irradiated cobalt metal 1 inch in diameter and 1/32 inch in thickness, each containing approximately 1 millicurie of the active isotope, and a number of quartz ampoules of cobalt chloride solution containing varying amounts of activity from 1 up to 5 millicuries.

(b) Measurement of Source Strength:

The absolute strengths of the sources used were estimated in terms of the dosage rates in röntgens/hour

at a given distance from the source, measured by means of an ionisation chamber system. The relationship between these quantities can be shown in the following way:-

It has been shown by Mayneord (1946) that if E_f is the energy flux of incident radiation in ergs per sq. cm. per röntgen, then the energy absorbed per gram-röntgen in air is:-

$$E_{gm.} = E_f (\tau + \sigma_a + \pi) = 84 \text{ ergs.} \qquad 3.7.$$

where τ , σ_a , π are the appropriate linear absorption coefficients for photo-electric absorption, Compton recoil, and pair production.

Now if the curie is defined as $3.7 - 10^{10}$ disintegrations/second, the intensity of radiation (I) at a distance of 1 cm. from a point source of radiation of strength 1 curie is given by:-

$$I = \frac{1}{4\pi} (3.7.10^{10}.3600.E_\gamma.1.59.10^{-6}) \text{ ergs/cm}^2\text{./hour.}$$

where the source is assumed to emit one gamma-quantum of energy E MeV. per disintegration. Hence:-

$$I = 1.685.10^7.E_\gamma \text{ ergs/cm}^2\text{./hour.} \qquad 3.8.$$

If the quantity k is defined as the dosage rate in röntgens/hour at 1 cm. distance in air from a source of 1 millicurie, then from 3.8.:-

$$k = \frac{1.685 \cdot 10^4 \cdot E_\gamma}{E_f} \qquad 3.9.$$

and from 3.7.:-

$$k = \frac{1.685 \cdot 10^4 \cdot E_\gamma}{84} (\tau + \sigma_a + \pi)$$

$$= 2.005 \cdot 10^2 \cdot E_\gamma (\tau + \sigma_a + \pi) \qquad 3.10.$$

By using this factor, k, Mayneord has shown the relationship between dosage rate in röntgens/hour and source strength in millicuries in various isotopes. For consider two sources of different radioisotopes A and B of strength S_A, S_B. The ratio of the dosage rates D_A, D_B, in röntgens/hour at equal distances from the two will be given by:-

$$\frac{D_A}{D_B} = \frac{S_A \cdot k_A}{S_B \cdot k_B} \qquad 3.11.$$

where k_A, k_B are the appropriate k factors which can be calculated from the expression 3.10. above. Where a radio-isotope emits more than one gamma-quantum per disintegration its k factor is the sum of the k factors for the individual gamma-ray energies, weighted according to the probability of emission of each. Corrections must be made where necessary for internal conversion effects,

The relative dosage rate at a known distance

from each source was measured in terms of that due to a standard radium needle with $\frac{1}{2}$ mm. platinum filtration whose strength was known from N.P.L. calibration to be 2.09 millicuries, using an experimental arrangement due to Sinclair (1950). This consisted of a 5 millimetre carbon ionisation chamber connected to a F.P. 54 valve electrometer circuit with mirror galvanometer display. The ionisation chamber was mounted on an optical bench provided with adjustable source holders. Since a carbon chamber is very nearly "air-wall" (Gray, 1936), the galvanometer deflections obtained with this system are to a close approximation linearly proportional to the dosage rates in röntgens/hour at the chamber. Making due allowance for inverse square law effects, if α_I , α_{Ra} are the observed galvanometer deflections due to an unknown radio-isotopic source I and the radium standard at distances d_I , d_{Ra} respectively from the carbon chamber, and if k_I , k_{Ra} ; S_I , S_{Ra} are the appropriate k-factors and source strengths, it follows from equation 3.11. that:-

$$S_I = \frac{\alpha_I \cdot k_{Ra} \cdot d_I^2}{\alpha_{Ra} \cdot k_I \cdot d_{Ra}^2} \qquad 3.12.$$

In practice, several measurements were made on each individual source. k_{Ra} has been determined by Mayneord and Roberts (1937) and may be taken to equal 8.3 röntgens/hour for a source filtered by 0.5 mm. of platinum. Thus it is only necessary to know k_I, which can be readily evaluated if the decay scheme of the radio-isotope is known, in order to calculate S_I.

Two small corrections must be made to the values thus calculated, the first for absorption of gamma-radiation in the wall of the chamber and the second for self-absorption in the source. These effects have been studied by Sinclair, who has calculated the factor by which the calculated source strength must be multiplied to correct for each of them.

(c) Correction of Measured Source Strengths for Absorption Effects:

The correction for absorption in the chamber wall has been determined by Sinclair by the extrapolation to zero thickness of the experimental curve of ionisation current against wall thickness in carbon chambers for the radio-isotope concerned.

The required factor is the ratio of the correction for the radio-isotope to that for radium, and for this reason is close to unity; in fact, absorption in the wall can be ignored for all the radio-isotopes studied here with the exception of iodine$_{131}$ and gold$_{198}$.

No correction is required for self-absorption in the radium standard, since the k-factor used (8.3 röntgens/hour) is correct for a source filtered by 0.5 mm. of platinum. Also in the case of the cobalt$_{60}$ disc sources, self-absorption may be ignored. However for the liquid sources, the effect is not negligible, and has been considered in detail by Evans and Evans (1948). These authors give the following formula for self-absorption in a liquid source enclosed in a cylindrical vessel:-

$$N = N_0 e^{-\left[\frac{8}{3\pi}\mu_{a(l)}R + \mu_{a(g)}t\right]} \qquad 3.13.$$

where N = number of quanta leaving source in unit time

N_0 = number of quanta produced in unit time

R = radius of volume of liquid

t = thickness of wall of containing vessel

$\mu_{a(l)}$ = total linear absorption coefficient of liquid

$\mu_{a(g)}$ = total linear absorption coefficient of glass

and $\mu_a = \tau + \sigma_a + \pi$

Values of $\mu_{a(\ell)}$ for water are to be found in Appendix I, while $\mu_{a(g)}$ may be estimated as $\frac{2.5\,\mu_{a(\ell)}}{1.11}$, allowing for the difference in density and atomic constitution of the two materials.

For the phials used to hold the liquid sources, R = 0.54 cm., t = 0.1 cm., and hence, substituting these values in expression 3.13.

$$N = N_0 e^{-0.73\mu_{a(\ell)}}$$

For a complex source, it is sufficient to use in this expression the value of $\mu_{a(\ell)}$ corresponding to the mean gamma-ray energy of the emitted radiation.

In Table IX, the values of both correction factors calculated by Sinclair are listed. It will be observed that in no case does the total correction amount to more than 5%. The ~~probable~~ standard error in the measured source strengths after correction in this way is stated by Sinclair to be ± 4%.

Table IX

Correction Factors for 5 mm. Carbon Ionisation Chamber System.

Isotope	Self Absorption Correction Factor	Carbon Wall Correction Factor	Total Correction Factor
Au_{198}	1.026	1.023	1.05
I_{131}	1.026	1.023	1.05
Br_{82}	1.025	1.00	1.02
Co_{60}	1.022	1.00	1.02
Na_{24}	1.020	1.00	1.02

5. RADIO-ISOTOPE DECAY SCHEMES:

(a) In order to calculate the rate of release of secondary electrons in a luminophor of known composition by a radio-isotope source of gamma-radiation, it is necessary to know both the strength of the source in millicuries and the decay scheme of the radio-isotope (see sub-section II.2). The strength may be determined experimentally as described in the previous sub-section (III.4), but this determination requires a knowledge of the k factor for the radio-isotope, which must also be evaluated from the decay scheme. It has therefore been necessary for

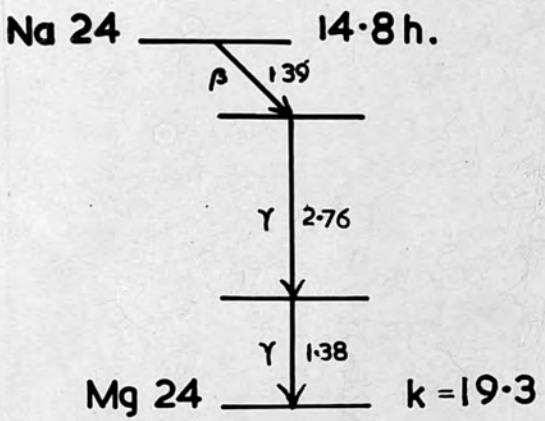

FIGURE 18

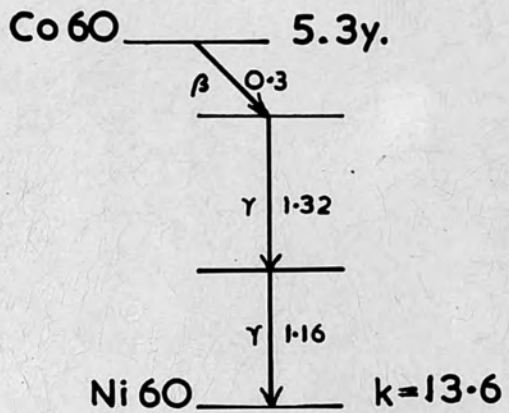

FIGURE 19

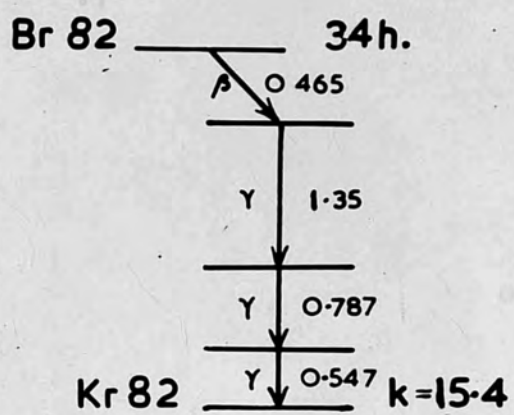

FIGURE 20

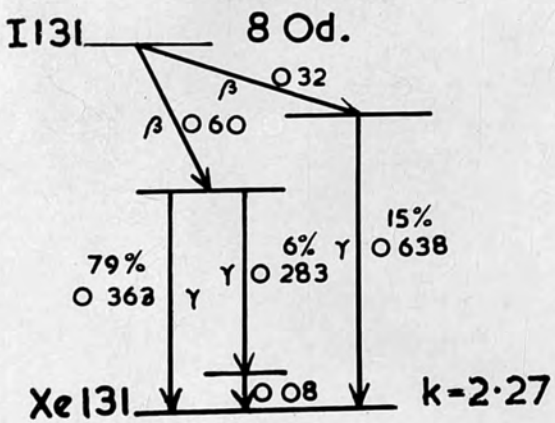

FIGURE 21

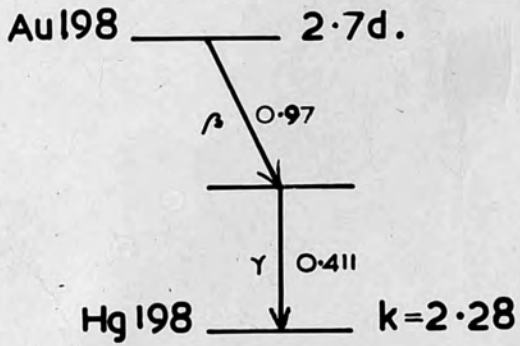

FIGURE 22

DECAY SCHEMES OF RADIO-ISOTOPES

the purpose of these studies to assume decay schemes for the radio-isotopes studied; all the calculations in the sections that follow have been based on the schemes shown in figures 18 - 22. The values for the half-lives are those quoted in Seaborg and Perlman's tables (1948); it is these values that have been used where necessary to correct the measured source strengths for radioactive decay. Also included are the k-factors calculated from the assumed decay schemes as described in sub-section III.4. It will be of value at this point briefly to review the historical evidence on which these data are based.

(b) Sodium 24: (Na 24 $\xrightarrow{\beta}$ Mg 24.):

This disintegration has been studied by numerous workers and is well substantiated. The latest determination was by Siegbahn (1947) who found one beta-ray group of end point energy 1.39 MeV. and two gamma-rays of equal intensity at 1.38 and 2.76 MeV. Robinson, Ter-Pogossian and Cook (1949) found the gamma-ray energies to be 1.380 and 2.765 MeV. Coincidence studies (Mitchell, 1948) showed that the

decay consists of the beta-ray group followed by the two gamma-rays in cascade.

Recent measurements by Solomon (1950), Sinclair and Holloway (1951) and Sreb (1951) indicate a value of 15.04 hours for the half-life, rather than that of 14.8 hours quoted by Seaborg and Perlman. Since sources were rarely studied for more than five hours after measurement, the errors introduced by the use of the latter value are small.

(c) Cobalt 60: (Co 60 $\xrightarrow{\beta}$ Ni 60):

The 5.3 year isomer of this transition was studied by Deutsch, Elliott and Roberts (1945) who showed it to emit one beta-ray of 0.308 MeV. followed by two gamma-rays in cascade at 1.10 and 1.30 MeV. Jensen, Laslett and Pratt (1949 a) gave the gamma-ray energies as 1.156 and 1.317 MeV. More recent determinations have suggested values nearer to 1.17 and 1.33 MeV. (Jensen, Laslett and Pratt, 1949 b; Alburger, 1949; Lind, Brown, and du Mond, 1949). Deutsch and Siegbahn (1950) showed that internal conversion of Co 60 gamma-radiation amounted to less than 0.001%.

(d) Bromine 82: (Br 82 $\xrightarrow{\beta}$ Kr 82):

The spectrum of bromine 82 was originally worked

out by Roberts, Downing and Deutsch (1941). They found one beta-ray group of maximum energy 0.465 MeV. followed by three gamma-rays in cascade at 0.547, 0.787, and 1.35 MeV. More recently, Siegbahn, Hedgman and Deutsch (1949) have shown the decay to be much more complicated, with as many as six gamma-rays all internally converted. It seems likely that the decay scheme proposed by these workers will eventually require still further revision. In view of this fact, and in the interests of simplicity, the earlier scheme has been accepted here, internal conversion being neglected. Measurements by Sinclair and Holloway (1951) suggest a half-life of 36 hours for the isotope rather than the value of 34 hours given by Seaborg and Perlman. The errors introduced in this work by the use of the latter value are small.

(e) Iodine 131: (I 131 $\xrightarrow{\beta}$ Xe 131):

The earliest study on this disintegration by Downing, Deutsch and Roberts (1947) was carried out with extremely weak sources, and is unreliable. The scheme shown in figure 21 is that of Metzger and Deutsch (1948) who found gamma-rays at 0.08, 0.283,

0.363 and 0.638 MeV., and beta-ray groups at 0.60 and 0.32 MeV. maximum energy. More recent measurements by Owen, Moe and Cook (1949); Kern, Mitchell and Zaffarano (1949), and Lind et al. (1949) showed that some modification of this scheme might be necessary, although the wavelengths of the main gamma-rays remained essentially the same. Moe, Owen and Cook (1949), and Kern, Mitchell and Zaffarano (1949) found some evidence of a weak gamma-ray at 0.163 MeV. This was attributed by Cork et al. (1949) to a meta-stable state of Xe_{131}.

In the interests of uniformity with other laboratories in this country, the scheme of Metzger and Deutsch was adopted for these studies. The three low energy gamma-rays are all internally converted, and in Table X the conversion coefficients based on the decay schemes of Metzger and Deutsch (Putman, 1949) and of Kern, Mitchell and Zaffarano (Mitchell, 1950) are shown. The high figure of the conversion coefficient for the 0.08 MeV. gamma-ray based on the scheme of Metzger and Deutsch suggests that the latter is probably in error. However the difference between

the two schemes is very small in practice; the substitution of Kern, Mitchell and Zaffarano's scheme would involve an increase of 3% in the k-factor for iodine; and an increase of 1% in the calculated counting rates in luminophors due to 1 millicurie of the radioisotope at 1 metre. The nett effect on the ratio of the observed counting rate due to 1 millicurie at 1 metre to the calculated rate will be negligible.

Table X.

Internal Conversion of Gamma-Rays from Iodine 131.

Gamma-ray Energy	N_e/N_γ (Mitchell)	N_e/N_γ (Putman)
0.08 MeV.	17%	80%
0.283 MeV.	7.9%	5%
0.363 MeV.	1.8%	1.9%

(f) Gold 198: ($Au\ 198 \xrightarrow{\beta} Hg\ 198$):

The spectrographic results of Levy and Greuling (1948), indicating several gamma-rays and two beta-ray groups in this disintegration are probably unreliable, and may be due to impurities. Later results by Peacock and Wilkinson (1948), Siegbahn and Hedgran

(1949), and coincidence measurements by Durney (1948) are in good agreement. A simple beta-ray group of maximum energy 0.97 MeV. is followed by a single gamma-ray at 0.411 MeV., internally converted. The conversion coefficient was given by du Mond, Lind and Watson (1948) as 4.3%.

Scintillation spectrometer studies by Pringle (1950) and by Hofstadter (1950) showed some evidence of a higher energy gamma-ray at approximately 1.05 MeV., and an emission probability of approximately 1%, with possibly a further component at 0.68 MeV. These rays, if present, are not of sufficient intensity significantly to affect the experimental results on absolute counting rate.

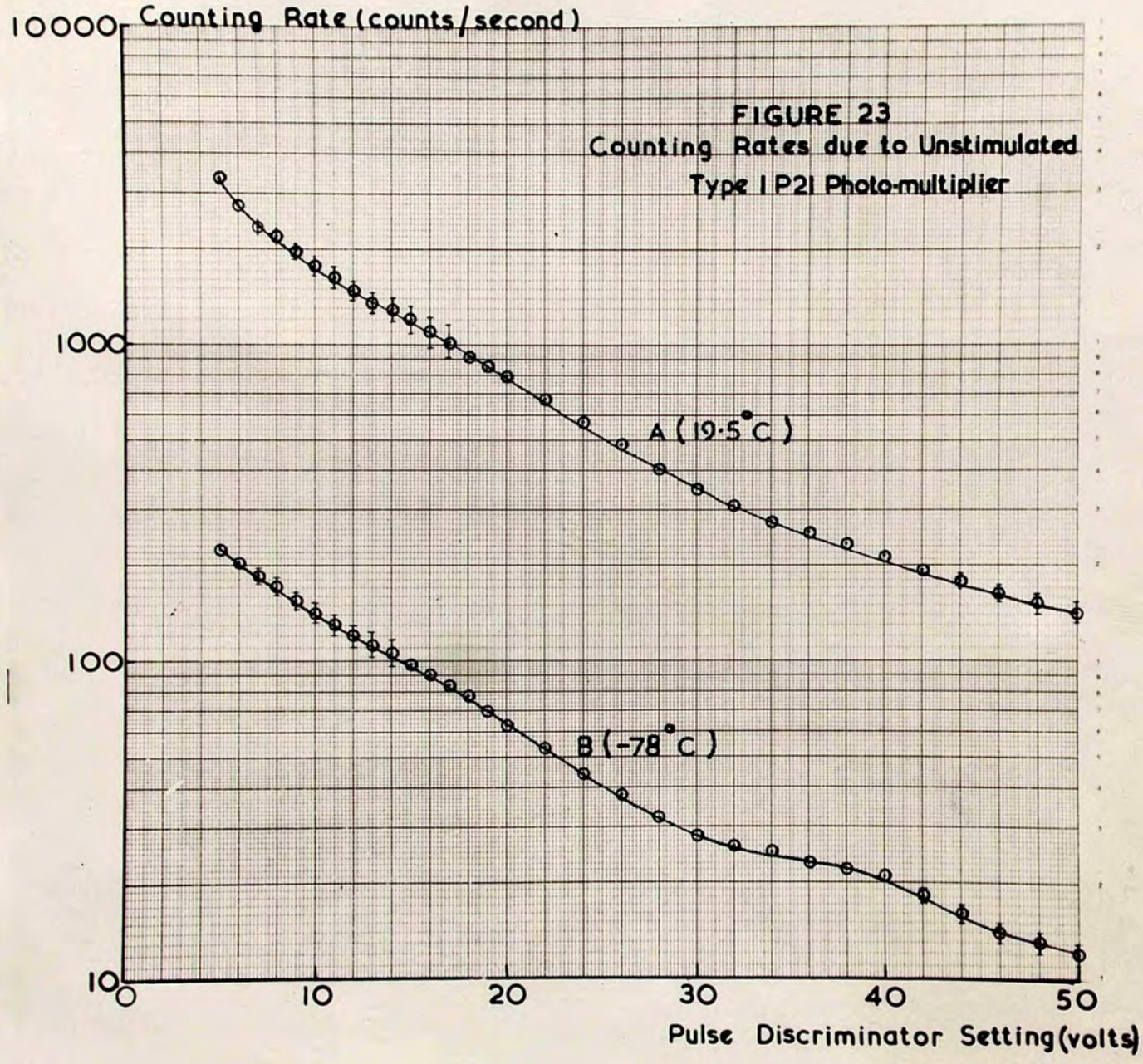

FIGURE 23
Counting Rates due to Unstimulated
Type IP21 Photo-multiplier

SECTION IV : EXPERIMENTAL RESULTS.

1. STATISTICAL STUDIES ON THE TYPE I P 21 PHOTO-MULTIPLIER TUBE.

(a) Photo-multiplier Dark Current Pulse Amplitude Distribution:

Initial experiments were concerned with measuring the pulse amplitude distribution of the photo-multiplier dark current pulses. It was anticipated that these distributions would show a peak corresponding to the emission of single electrons at the cathode of the photo-multiplier.

Measurements were made with the unstimulated photo-multiplier case mounted upright, closed by the stop shown in figure 13 (inset F). The inter-dynode potential was 108 volts and the amplifier attenuation 10 dB (nominal). Counting rates were observed with the ratemeter, the resolving time of the latter being set at 100 microseconds (nominal).

In figure 23 are shown curves of observed counting rate plotted as a function of pulse discriminator setting for the unstimulated photo-multiplier. Curve A shows measurements made at room temperature

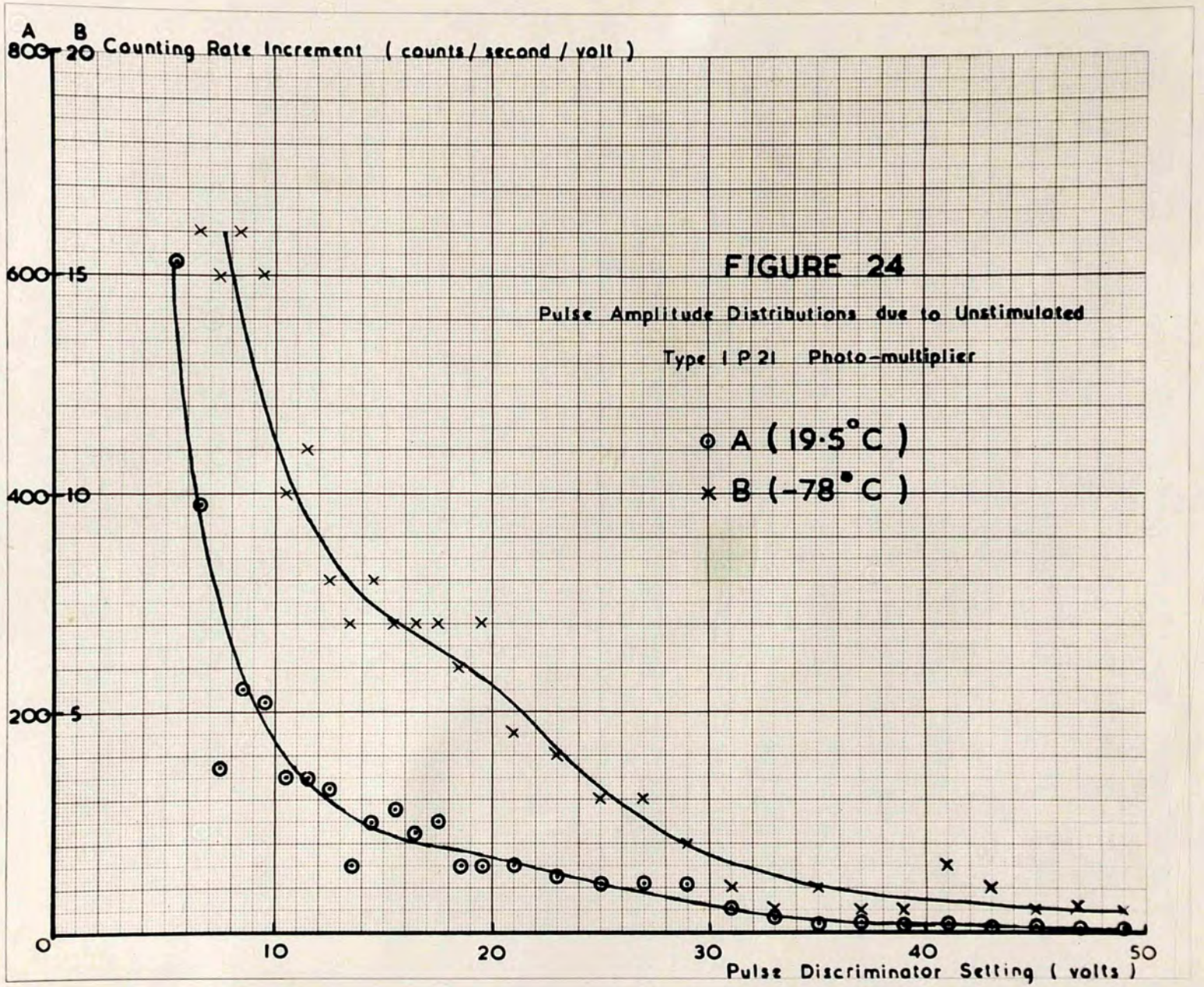

FIGURE 24

Pulse Amplitude Distributions due to Unstimulated

Type I P 21 Photo-multiplier

(19.5°C) whilst the measurements of curve B were made with the photo-multiplier cooled with solid carbon dioxide over a period of several hours, all counting rates being corrected for resolving time losses. In figure 24, differential curves of pulse amplitude distribution derived from the data of figure 23 are shown; these distributions were obtained by taking the increment in counting rate over each one-volt step in pulse-discriminator setting in the integral curves. Some evidence of a peak in the neighbourhood of 18 volts pulse discrimination is apparent, but the dark current distributions are seen to include many very small pulses; particularly is this true at room temperature. These small pulses may be due to electron emission from the dynodes succeeding the photo-cathode, to gas-ion effects, or to leakage currents across the photo-multiplier base.

(b) Pulse Amplitude Distributions under Stimulation by Continuous Light:

Measurements under stimulation by continuous light were made using the pinhole collimator shown in figure 13 (inset D). In order to observe the small pulses produced by single photons incident upon

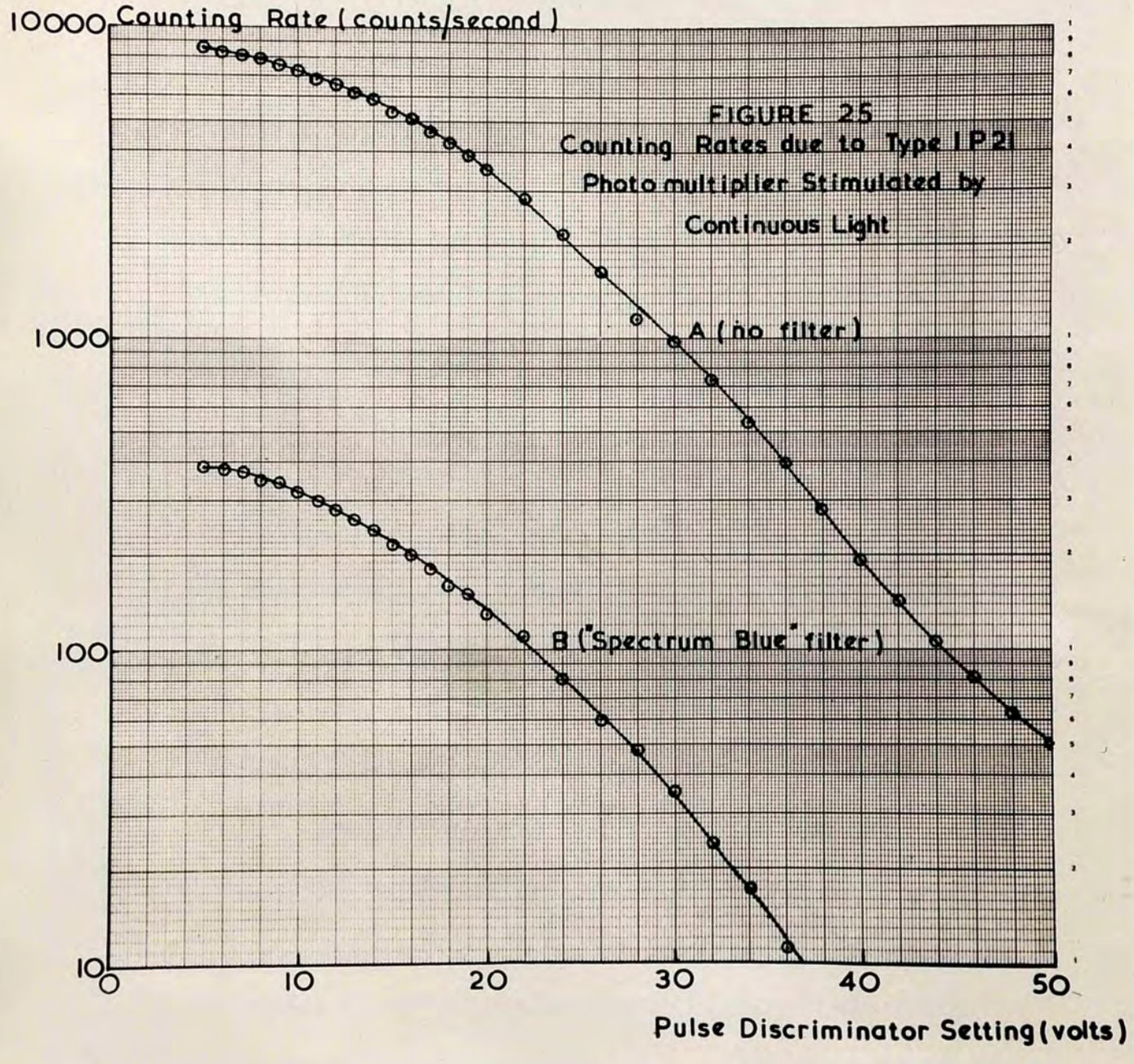

FIGURE 25
Counting Rates due to Type IP21
Photomultiplier Stimulated by
Continuous Light

the photo-cathode, it was found necessary to cool the photo-multiplier. Under these conditions, the collimator could not be mounted directly on to the photo-multiplier case, since frosting was then found to obscure the pinhole; for this reason the second arrangement described in sub-section III.1. in which the collimator is screwed into the light guide assembly of figure 13 (inset A) was preferred. The light source was a white cardboard diffuser placed on the axis of the collimator and illumined by a 40 watt incandescent light bulb several metres distant. The photo-multiplier was cooled with liquid nitrogen for several hours before measurements were commenced, the counting rate due to the unstimulated tube being then less than 1 count/second at 5 volts pulse discrimination, and at all times less than 1% of the observed rates under light stimulation.

Curve A of figure 25 is an integral curve of observed counting rate plotted as a function of pulse discriminator setting when no filter was present between light source and collimator; curve B shows the observed counting rates when an Ilford "Spectrum Blue" filter was interposed. Both sets of observations

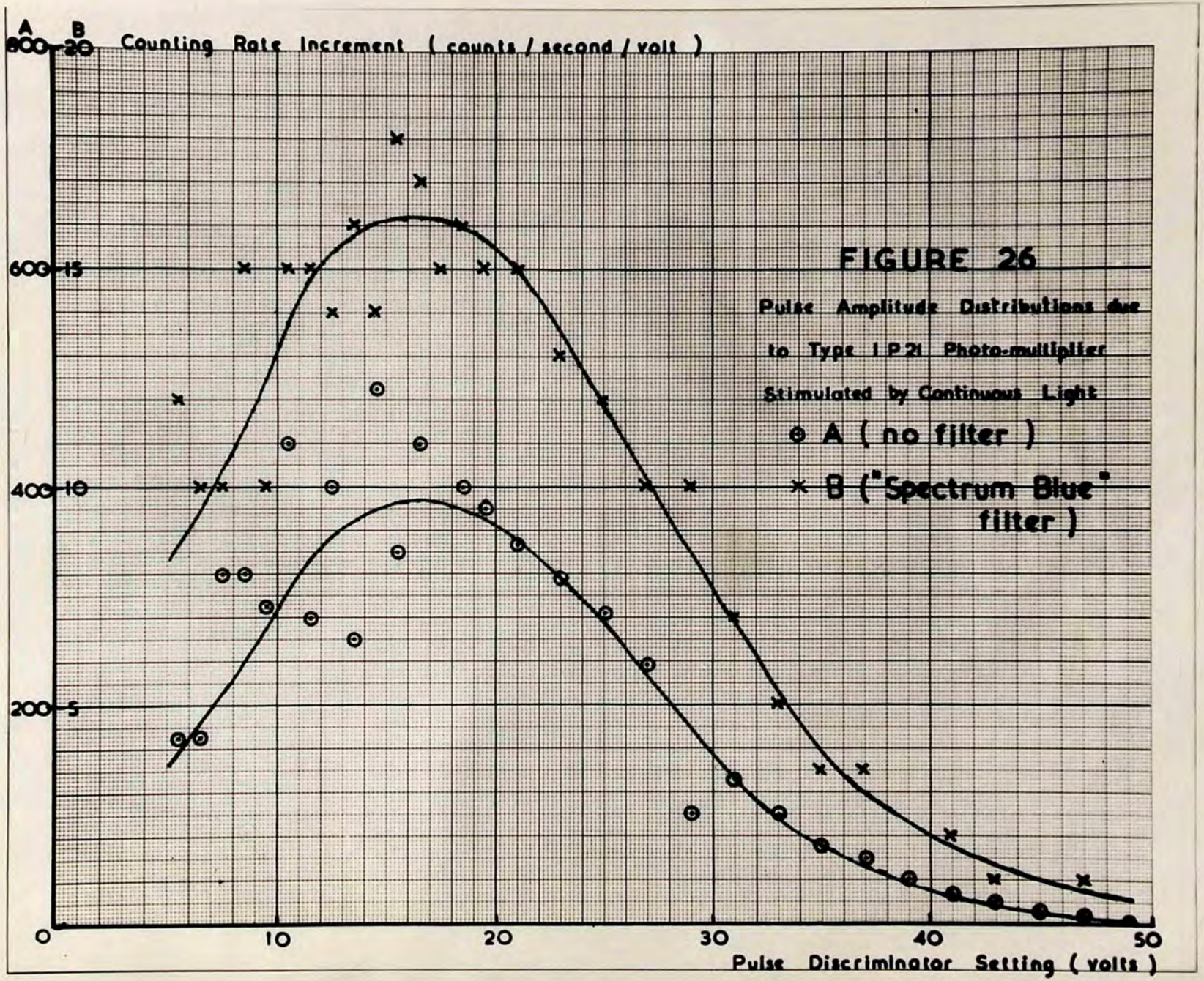
A
B
800
20
Counting Rate Increment (counts / second / volt)
600
15
400
10
200
5
0
10
20
30
40
50
Pulse Discriminator Setting (volts)
FIGURE 26
Pulse Amplitude Distributions due to Type 1P21 Photo-multiplier Stimulated by Continuous Light
⊙ A (no filter)
× B ("Spectrum Blue" filter)

were made with an inter-dynode potential of 108 volts, and an amplifier attenuation of 10 dB, and are corrected for resolving time losses in the ratemeter. In figure 26 the derived differential curves are seen; it will be noted that these distributions show a distinct peak at approximately 18 volts discrimination.

Figures 27 and 28 show the effect of varying the inter-dynode potential whilst keeping the light stimulation constant, with the Ilford "Spectrum Blue" filter in position. The amplifier attenuation was maintained at 10 dB. during this series of measurements, except for those plotted at a pulse discriminator setting of 1.6 volts; the latter were in fact made at an attenuation of 0 dB., and a pulse discriminator setting of 5 volts, and facilitate extrapolation of the observed distribution to a discrimination of 0 volts. An examination of the integral curves of figure 27 suggests that as the inter-dynode voltage is reduced, an increasing number of photo-electrons are lost in the multiplier and fail to be recorded.

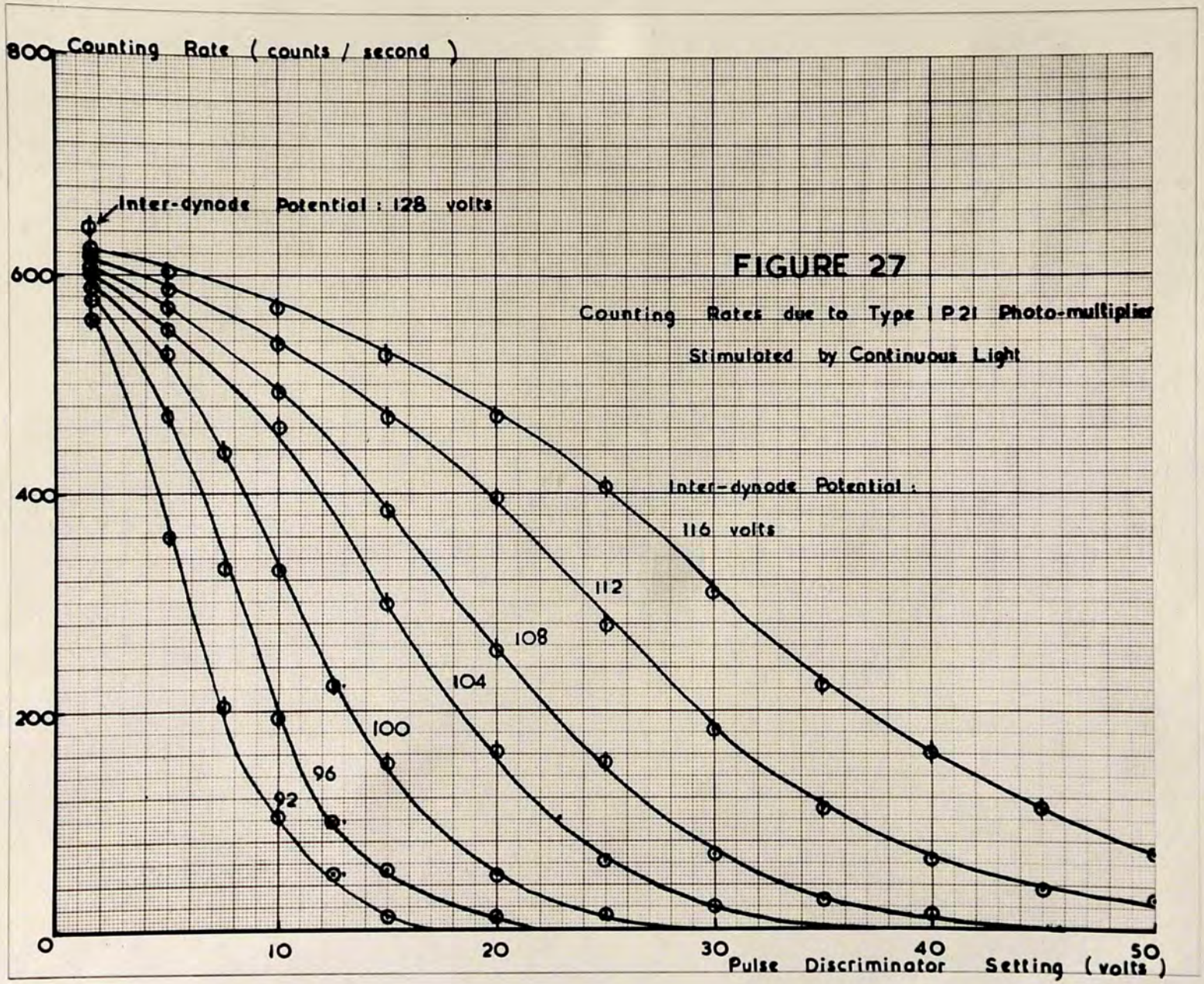

FIGURE 27

Counting Rates due to Type I P 21 Photo-multiplier Stimulated by Continuous Light

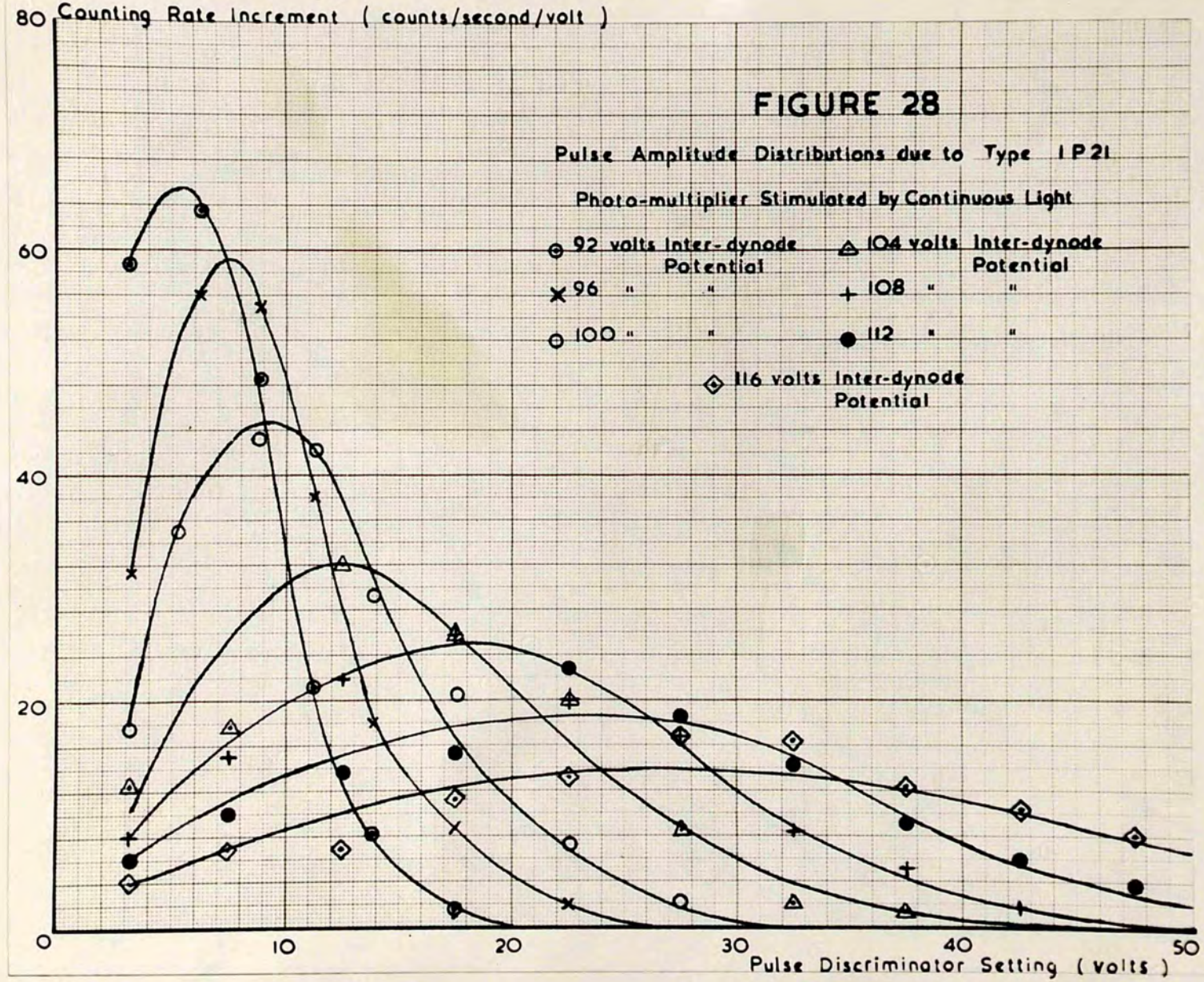
Counting Rate Increment (counts/second/volt)
80
60
40
20
0
10
20
30
40
50
Pulse Discriminator Setting (volts)
FIGURE 28
Pulse Amplitude Distributions due to Type 1P21
Photo-multiplier Stimulated by Continuous Light
92 volts Inter-dynode Potential
96 " "
100 " "
104 volts Inter-dynode Potential
108 " "
112 " "
116 volts Inter-dynode Potential

The effect of varying the wavelength of the light source was studied by interposing various filters between the light source and the collimator, the light intensity being adjusted for each set of observations to give an approximately constant maximum counting rate of 300 counts/second. The amplifier attenuation was maintained at 10 dB. and the inter-dynode potential at 108 volts throughout these measurements. No significant difference between the forms of the distributions could be observed; it may be inferred therefore that the distributions obtained in practical scintillation counters will not depend upon the wavelength of the light emitted by the luminophor, except in so far as the quantum efficiency (η_3) of the photo-cathode depends on this wavelength.

(c) Pulse Amplitude Distributions under Stimulation by Pulsed Light:

Measurements under stimulation by pulsed light were made both with the photo-multiplier uncooled, the collimator being screwed directly into the brass case, and with the photo-multiplier cooled, the collimator being screwed into the light guide assembly as just

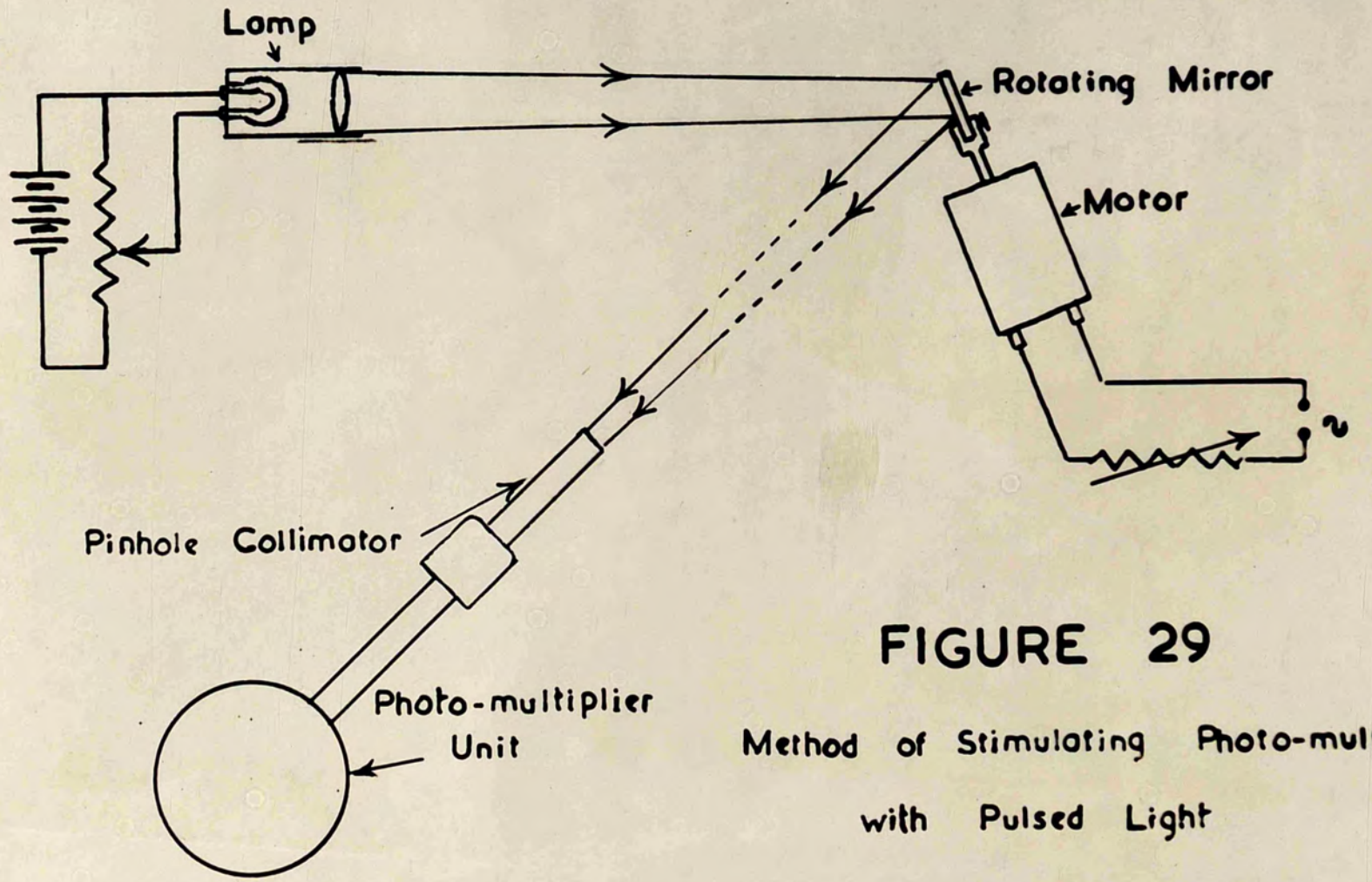

FIGURE 29

Method of Stimulating Photo-multiplier with Pulsed Light

described. The light pulses were produced mechanically by the method shown in figure 29. A converging beam of light from a tungsten lamp mounted in a housing was directed on to a small (2 cm. x 1 cm.) mirror mounted on the shaft of a high speed motor. The reflected beam traversed an optical path of some 170 cms., after which it came to a focus in the plane of the first pinhole of the collimator. Its intensity could be varied by adjusting the current through the tungsten lamp, its duration by adjusting the dimensions of the light spot passing across the collimator, and its frequency by adjusting the speed of rotation of the motor. The form and duration of the pulses produced at the output of the linear amplifier were observed in a double beam Cossor Oscillograph (type 1035). In all the measurements quoted here, the speed of rotation of the motor was 88 revs./second, and the diameter of the light spot in the plane of the pinhole 0.8 cm.; these values correspond to a light pulse of duration 4.3 microseconds, in good agreement with the observed value of 5.0 microseconds for the rise time of the output

FIGURE 30

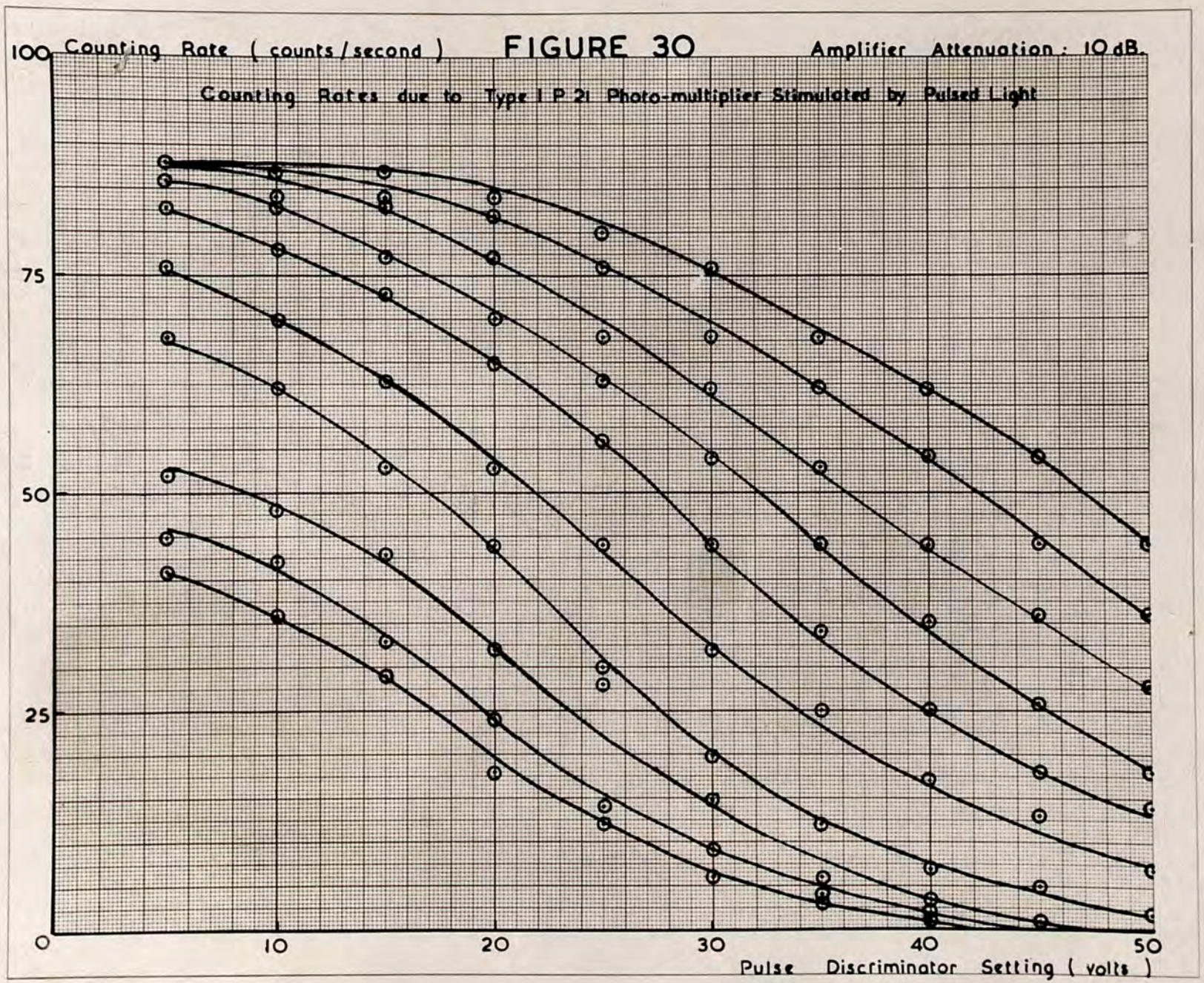
Counting Rate (counts / second)
Amplifier Attenuation : 10 dB.
Counting Rates due to Type I P 21 Photo-multiplier Stimulated by Pulsed Light
100
75
50
25
0
10
20
30
40
50
Pulse Discriminator Setting (volts)

FIGURE 31

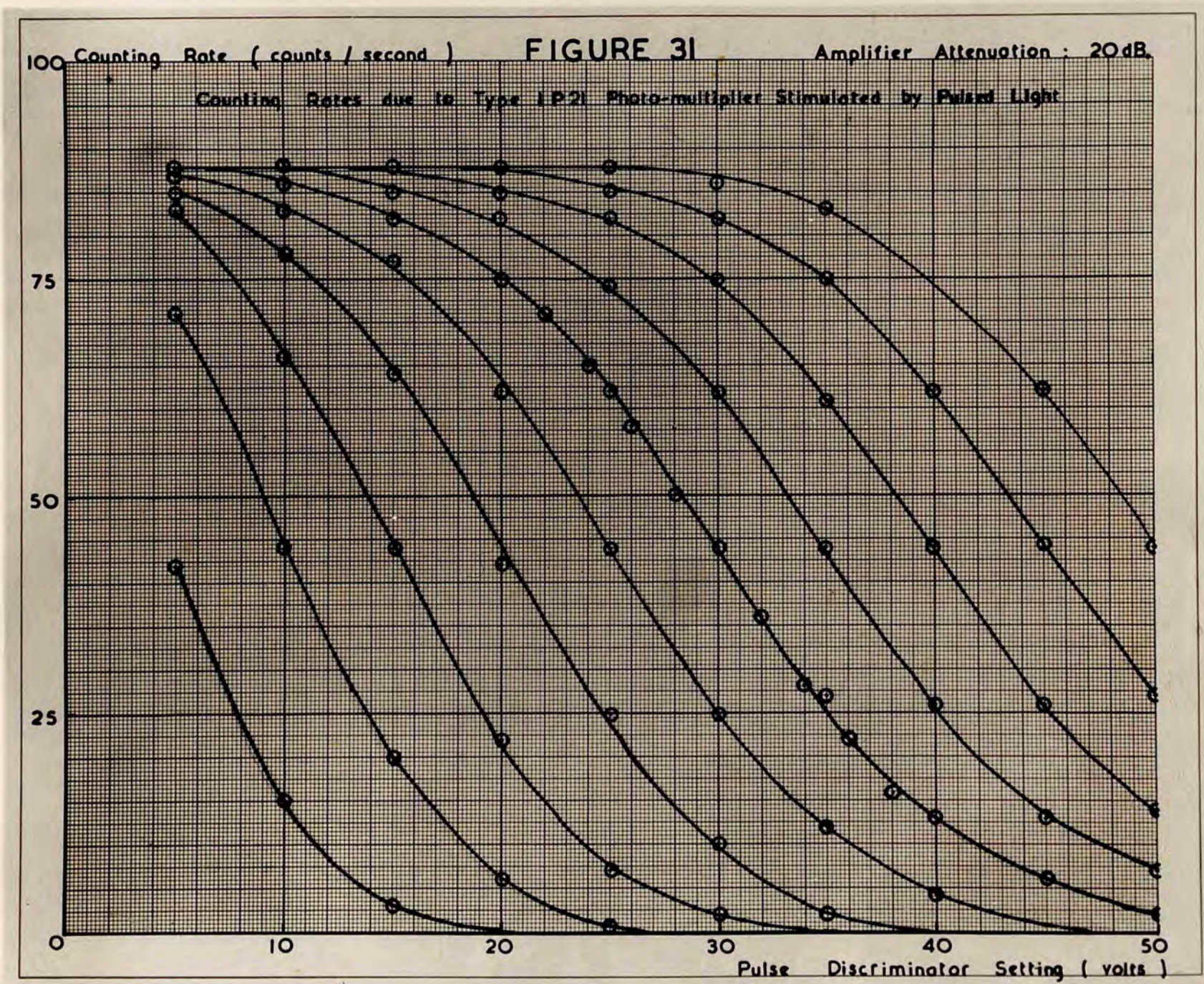
Counting Rate (counts / second)
Amplifier Attenuation : 20 dB.
Counting Rates due to Type 1P21 Photo-multiplier Stimulated by Pulsed Light
100
75
50
25
0
10
20
30
40
50
Pulse Discriminator Setting (volts)

FIGURE 32

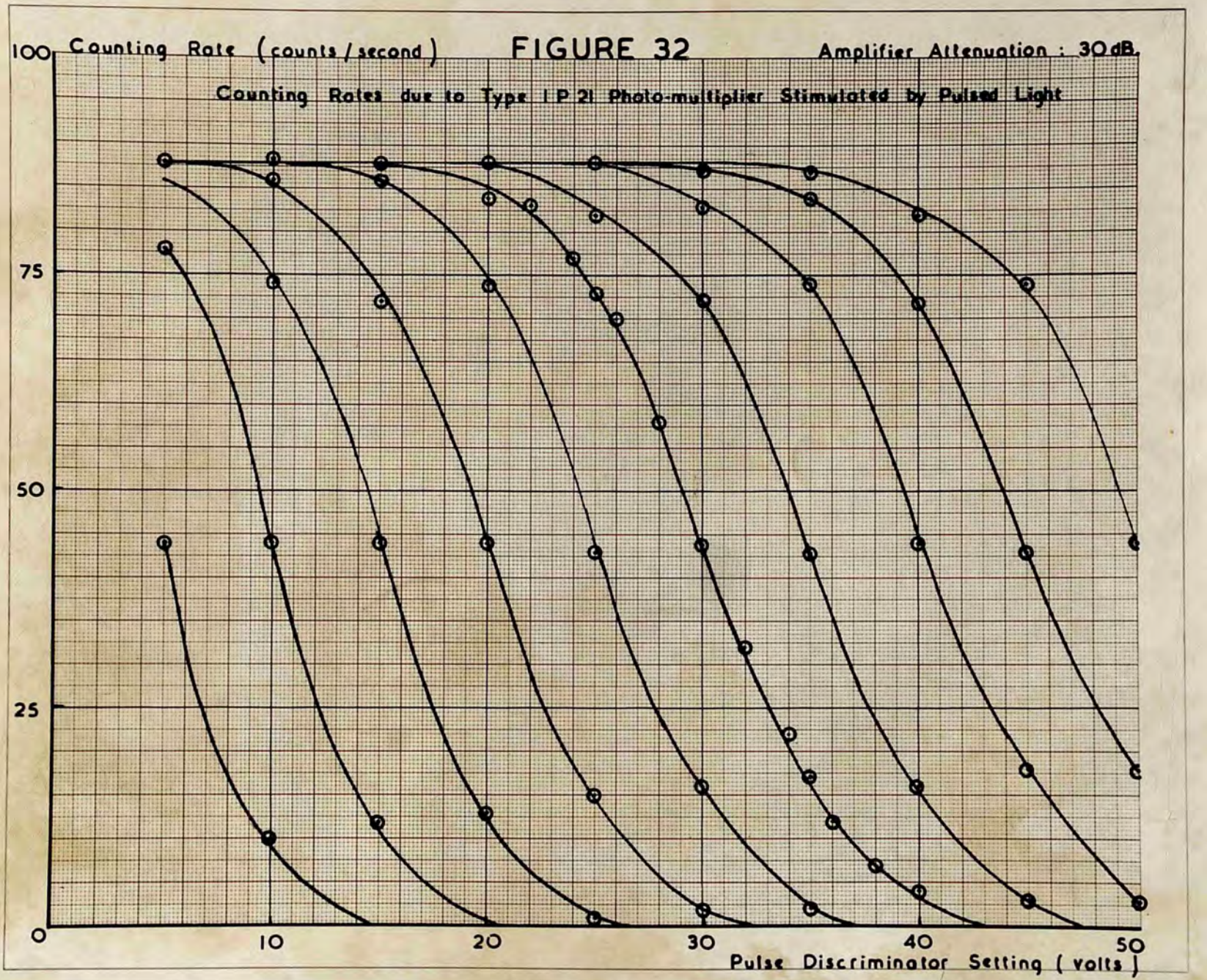
Counting Rate (counts / second)
Amplifier Attenuation : 30 dB.
Counting Rates due to Type IP 21 Photo-multiplier Stimulated by Pulsed Light
100
75
50
25
0
10
20
30
40
50
Pulse Discriminator Setting (volts)

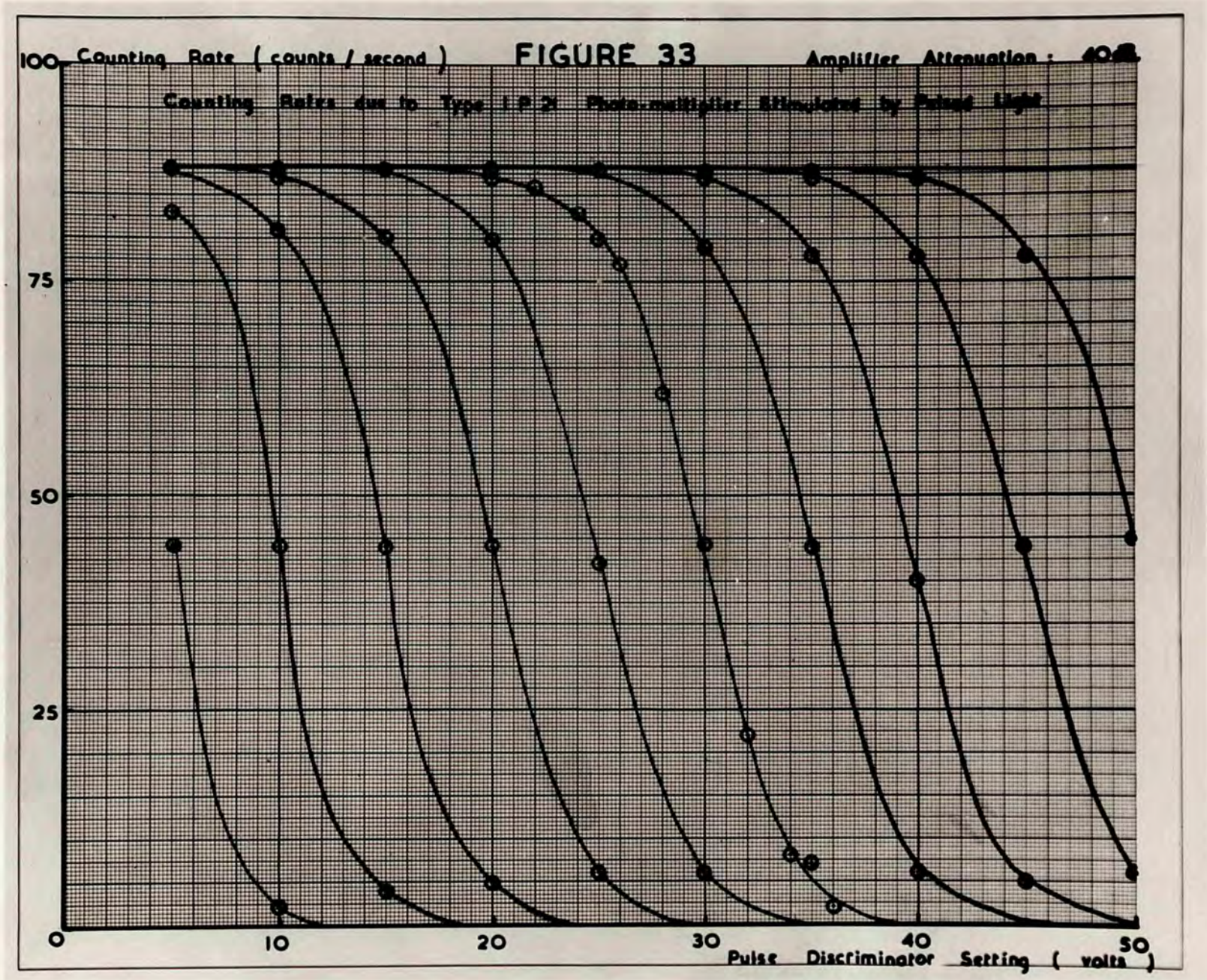
FIGURE 33
Counting Rate (counts / second)
Amplifier Attenuation : 40dB
Counting Rates due to Type 1 P 21 Photo-multiplier Stimulated by Pulsed Light
100
75
50
25
0
10
20
30
40
50
Pulse Discriminator Setting (volts)

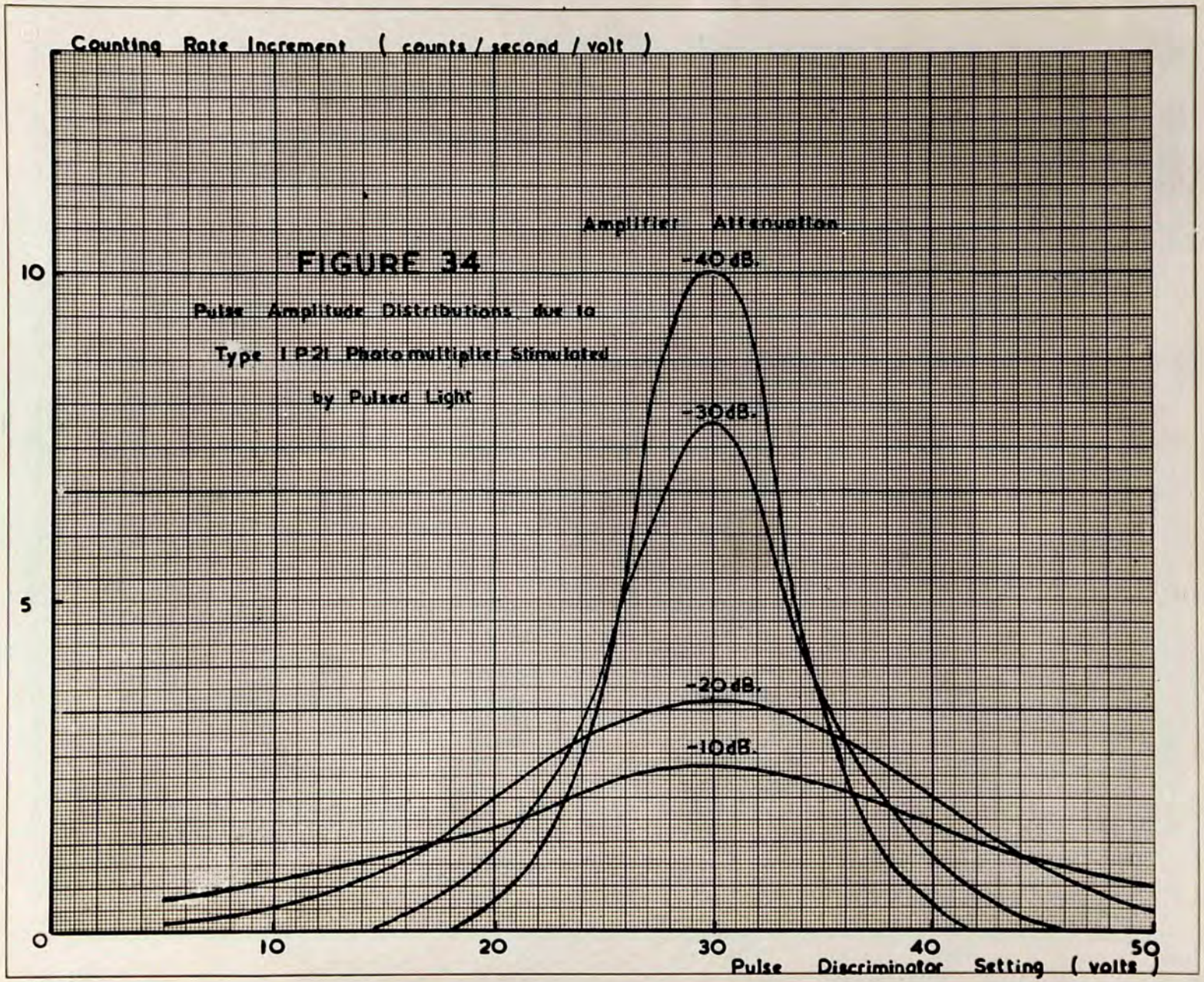

FIGURE 34

Pulse Amplitude Distributions due to Type 1P21 Photomultiplier Stimulated by Pulsed Light

pulse on the oscillograph. The Ilford "Spectrum Blue" filter was interposed between the mirror and collimator during all these experiments, and the inter-dynode potential was fixed at 108 volts.

Measurements were made on the cooled photo-multiplier at settings of amplifier attenuation of 10, 20, 30, and 40 dB; at each value of attenuation a family of curves of counting rate as a function of pulse discriminator setting was obtained by making observations at different levels of light source intensity. Such families are shown in figures 30 - 33; all counting rates being corrected for background effects and for losses due to the resolving time of the ratemeter. The increase in the spread of the output pulse amplitude distribution that accompanies a reduction of the mean pulse amplitude is clearly shown in figure 34, where the differential curves for the distributions centred on 30 volts in figures 30 - 33 are compared. Similar sets of observations were made with the uncooled photo-multiplier but measurements could not in this case be made at lower attenuations than 20 dB because of the high background.

(d) Discussion of Results:

The mean amplitude of pulse produced at the output of the linear amplifier when one electron is released at the photo-multiplier cathode may be calculated from equation 2.23. The relevant data are as follows:-

Current amplification of photo-multiplier type I P 21 at inter-dynode potential of 108 volts (stated) . . . . . $3.3.10^6$

Input capacity of amplifier type 1008 . . . . . 122 pF

(Output capacity of photo-multiplier type I P 21 (stated)	6 pF
4.0 feet "Uniradio 32" cable at 21 pF./foot	84 pF
Amplifier type 1008 input capacity (stated)	30 pF
Stray capacities	2 pF
	122 pF

Voltage gain of amplifier type 1008 at 10 dB attenuation (measured). . . . . $3.84.10^3$

1 coulomb = $6.28.10^{18}$ units of electronic charge.

Substituting these values in equation 2.23, it is found that:-

$$A_o = \frac{3.3.10^6 . \ 3.84.10^3}{6.28.10^{18} . \ 1.22.10^{-10}} \text{ volts} \qquad 4.1.$$

$$= 16.5 \text{ volts}$$

In view of the uncertainty in the value for the amplification of the photo-multiplier tube, this agrees well with the peaks observed at approximately 16 volts in figure 26. Similar values can be calculated for the amplitude of the output pulses corresponding to the release of single electrons at the photo-cathode for other inter-dynode potentials, and in Table XI the output pulse amplitude obtained in this manner is compared with the observed positions of the peaks of the various distributions of figure 28. There is seen to be reasonable agreement between experiment and theory.

Table XI

Mean Pulse Amplitudes due to Single Photo-electrons.

Inter-dynode Potential (volts)	Photo-multiplier Gain $R^9/10^6$	Output Pulse Amplitude (volts) Calculated	Observed
92	1.15	5.7	5.5
96	1.5	7.4	7.5
100	2.0	9.9	9.5
104	2.6	12.9	13
108	3.3	16.5	17
112	4.2	20.9	22
116	5.3	26.4	28

Considering now the form of the distribution curves of figure 26, it is instructive to compare the observed fractional variances, evaluated from the expression:

$$\frac{V}{M^2} = \left[\frac{\Sigma f X^2}{N} - M^2 \right] \Big/ M^2 \qquad 4.2$$

with the theoretical values calculated from equation 2.42.

If first only those electrons are considered which, released at the photo-cathode, reach the first dynode; or in other words, if m_4 is equated to unity in the theoretical expression for the variance, and those photo-electrons which fail to record are ignored in evaluating the observed variance, the values quoted in Table XII are obtained. There is seen to be good agreement between the observed and calculated variances in this table. These results are in contradiction to those of Morton and Mitchell (1948) who also measured the distribution of output pulses due to single electrons in photo-multipliers of this type but found the observed variance of the distribution to be greater than the calculated value by a factor of two. This discrepancy is apparently due to an error in their choice of units of pulse height (Morton: private communication).

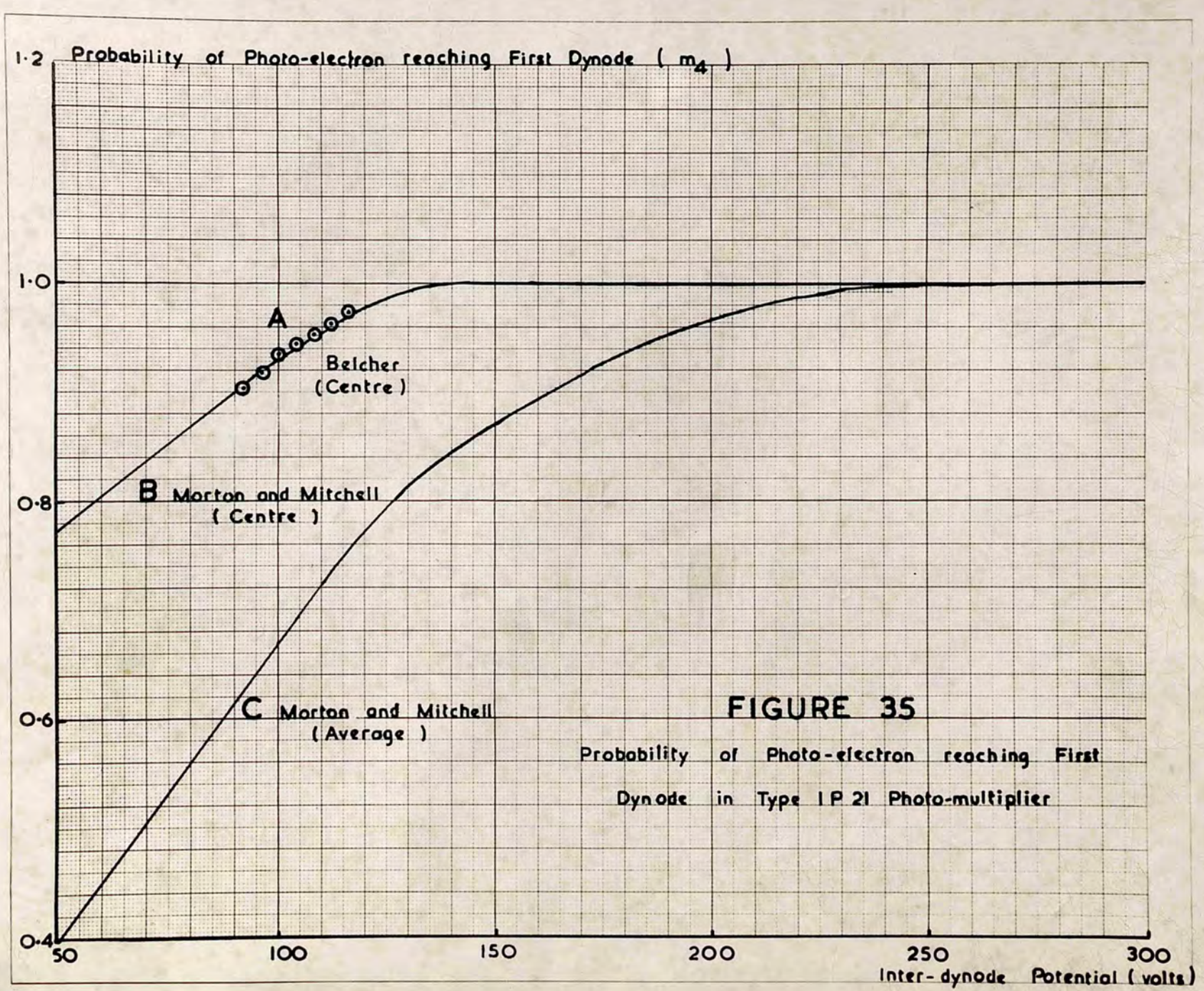

FIGURE 35

Probability of Photo-electron reaching First Dynode in Type IP 21 Photo-multiplier

However, an inspection of the integral curves of figure 28 shows that especially at lower inter-dynode potentials a significant fraction of the photo-electrons emitted at the photo-cathode may fail to produce pulses at the amplifier output. This effect is more clearly demonstrated in figure 35. The ratios of the extrapolated values at zero discrimination of the distributions of figure 28 to the maximum counting rate at an inter-dynode potential of 128 volts (assuming 100% collection of photo-electrons at the latter potential) give the probabilities (m_4) that an electron emitted at the photo-cathode will produce an avalanche in the photo-multiplier. In figure 35, these ratios are plotted as a function of inter-dynode potential (curve A). Curves B and C are obtained from the published data of Morton and Mitchell (1948) for stimulation of the central area and the whole of the photo-cathode respectively, and are included for comparison.

If the value of(m_4) obtained from figure 35 is included in the theoretical expression for the variance, and an appropriate number of (hypothetical) pulses of zero amplitude included in the distribution when evaluating the observed variance, the values of Table XIII are obtained. Here again, good agreement between theory and experiment is found.

Table XII

Fractional Variances of Output Pulse Amplitude Distributions due to Single Photo-electrons Reaching First Dynode.

Inter-dynode Potential (volts)	Photo-multiplier Gain $R^9/10^6$	Inter-stage Gain R	Fractional Variance Calculated $\left[\frac{1}{R-1}\right]$	Observed
92	1.15	4.71	0.27	0.27
96	1.5	4.86	0.26	0.25
100	2.0	5.01	0.25	0.28
104	2.6	5.16	0.24	0.24
108	3.3	5.30	0.23	0.23
112	4.2	5.44	0.22	0.25
116	5.3	5.59	0.22	0.22

Table XIII

Fractional Variances of Output Pulse Amplitude Distributions due to all Single Photo-electrons.

Inter-dynode Potential (volts)	Photo-multiplier Gain $R^{9/10}$	Inter-stage Gain R	Fraction of Photo-electrons Recording σ_4	Fractional Variance Calculated $\left[\frac{1-\sigma_4+\frac{1}{R-1}}{\sigma_4}\right]$	Fractional Variance Observed
92	1.15	4.71	0.90	0.40	0.40
96	1.5	4.86	0.92	0.37	0.36
100	2.0	5.01	0.93	0.34	0.37
104	2.6	5.16	0.94	0.31	0.34
108	3.3	5.30	0.95	0.29	0.30
112	4.2	5.44	0.96	0.27	0.30
116	5.3	5.59	0.97	0.25	0.24

Considering now the performance under stimulation by pulsed light, the variance of the distributions of figure 34 may be compared with those calculated from expression 2.39. In order to calculate the theoretical variances from the latter expression, the value of the quantity ($m_1 \cdot m_2 \cdot m_3 \cdot m_4$) must be known in each case; as pointed out on page 54 this is equivalent to the mean number of photo-electrons reaching the first dynode during any one pulse. If the duration of the pulse were short compared with the time constant of the amplifier ($T \ll RC$ in equation 2.22), ($m_1 \cdot m_2 \cdot m_3 \cdot m_4$) would be quite simply the ratio of the observed mean pulse amplitude to the mean pulse amplitude for pulses due to single electrons, given in Table XI, due allowance being made for changes in amplifier gain.

But since the input time constant of the linear amplifier in the arrangement used was 5.5 microseconds ($C = 122$ pF., $R = 45{,}400\ \Omega$.), and the measured duration of the light pulse 5.0 microseconds, the condition $T \ll RC$ is satisfied for single electron pulses but not for the light pulses. For the latter,

it is clear from equations 2.22 and 2.23 that the amplitude of the output pulses will be reduced in the ratio A_T/A_o where:-

$$\frac{A_T}{A_o} = \frac{RC}{T}\left(1 - e^{-T/RC}\right) \qquad 4.3$$

Substituting the appropriate values in the above expression, it is found that

$$\frac{A_T}{A_o} = \frac{4.545.10^6.1.22.10^{-10}}{5.10^{-6}}\left(1 - e^{-\frac{5.10^{-6}}{4.545.10^6.1.22.10^{-10}}}\right) \qquad 4.4$$

$$= 0.67$$

Applying a correction based on the above figure to the observed data, the values quoted in Table XIV are found for the mean numbers of photo-electrons arriving at the first dynode and leaving the photo-cathode per pulse for the distributions of figure 34. Care must be taken in calculating the latter figures to use the appropriate value for m_4; in experiments where the Perspex rod assembly was used, the value of 0.95 derived from curve A of figure 35 applies. But in experiments in which the collimator was screwed directly into the photo-multiplier case, and the whole of the photo-cathode was stimulated, a value of 0.66 derived from the experimental data of Morton and Mitchell (1948) (curve C of figure 35) has been adopted.

Table XIV

Mean Number of Photo-electrons per Pulse.

Amplifier Attenuation (dB) (nominal)	Mean Amplitude of Output Pulse (volts)	Mean Number of Photo-electrons per Pulse. At First Dynode ($m_1 . m_2 . m_3 m_4$)	At Photo-cathode ($m_1 . m_2 . m_3$)	
			No Perspex Rod	Perspex Rod Assembly
0	30	0.765	1.16	0.806
10	30	2.42	3.67	2.55
20	30	7.65	11.6	8.06
30	30	24.2	36.7	25.5
40	30	76.5	116	80.6

In Table XV, the values of the fractional variances evaluated from the distributions of figure 34 are compared with those calculated from expression 2.39, using the values of ($m_1 . m_2 . m_3 . m_4$) given in Table XIV.

Table XV

Fractional Variances of Output Pulse Amplitude Distributions due to Pulsed Light.

Amplifier Attenuation (dB) (nominal)	Mean Amplitude of Output Pulse (volts)	Fractional Variance Calculated $\frac{(1 + \frac{1}{R-1})}{(m_1 . m_2 . m_3 . m_4)}$	Observed No Perspex Rod	Observed Perspex Rod Assembly
10	30	0.508	-	0.29
20	30	0.161	-	0.11
30	30	0.0508	0.036	0.037
40	30	0.0161	0.013	0.014

It will be noted that whilst there is reasonable agreement between observation and theory for the measurements made at an amplifier attenuation of 40 dB, the ratio of observed to the calculated value falls significantly for pulses of lower amplitude. This apparent anomaly may be explained by the assumption made on page 44 that charge arrives uniformly at the

photo-multiplier collector during each pulse, whereas it in fact arrives in a series of discrete packets each initiated by the arrival of a single electron at the first dynode. The error involved in this assumption will be small when $(m_1 . m_2 . m_3 . m_4)$ exceeds 10 , but the assumption is no longer valid when the number of photo-electrons per pulse is small. In the latter case, not only will a small statistical spread be introduced in the height of the pulses at the amplifier output, due to random variations in the time of arrival of the electron avalanches within the duration of each pulse, but also the ratio A_T/A_o will no longer be constant for pulses of different amplitude. The variation of this ratio will be such as to increase the mean height of all pulses of smaller amplitude than the mean, and to reduce the height of all those greater than the mean, that is, to reduce the variance of the distribution. While it is difficult to make a quantitative correction for these effects, the observed discrepancies do not appear to invalidate the simple theoretical treatment. It should be noted that where the duration of a pulse is small

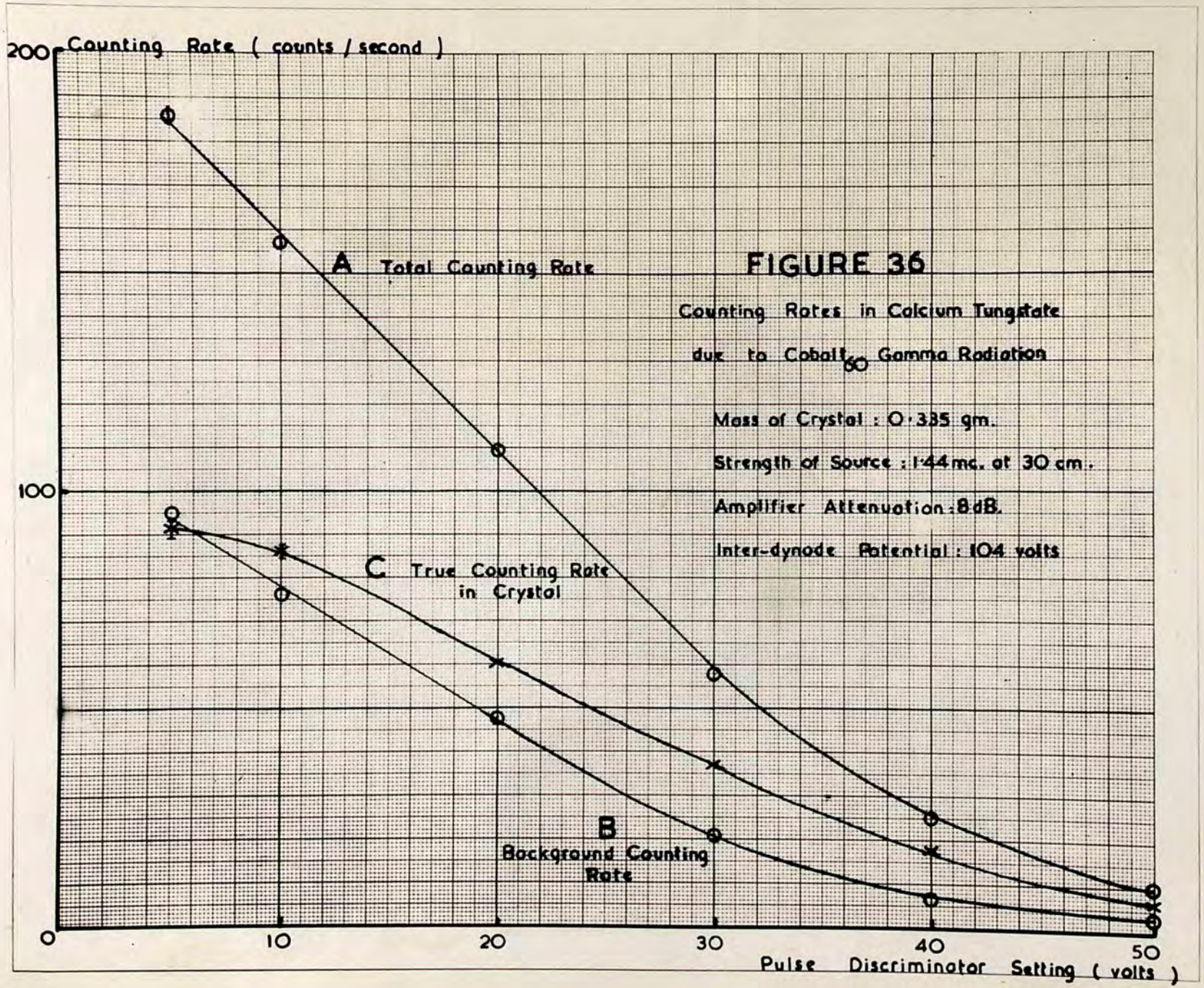

FIGURE 36

Counting Rates in Calcium Tungstate due to Cobalt$_{60}$ Gamma Radiation

Mass of Crystal : 0·335 gm.

Strength of Source : 1·44 mc. at 30 cm.

Amplifier Attenuation : 8 dB.

Inter-dynode Potential : 104 volts

compared with the time constant of the amplifier, as will be the case with the majority of practical scintillation counters, A_T/A_0 will approach unity for all pulses. The simple theory of equation 2.23. will then apply.

2. PRELIMINARY EXPERIMENTS WITH CRYSTALLINE LUMINOPHORS.

Initial experiments with crystalline luminophors were performed using the photo-multiplier cooled with liquid nitrogen, in conjunction with the Perspex rod and camera shutter assembly shown in figure 13 (inset A). Small mounted crystals of calcium tungstate were placed in the crystal holder and irradiated by the gamma-radiation from a cobalt$_{60}$ source. A filter consisting of a 2 cm. x 2 cm. square of copper foil 0.055 cm. thick was interposed between source and crystal to prevent any beta-radiation from falling on the latter. Counting rates were measured with the scaler, counts being taken over 100-second periods.

In figure 36, typical integral curves of counting rate as a function of pulse discriminator setting are seen. For this series of measurements,

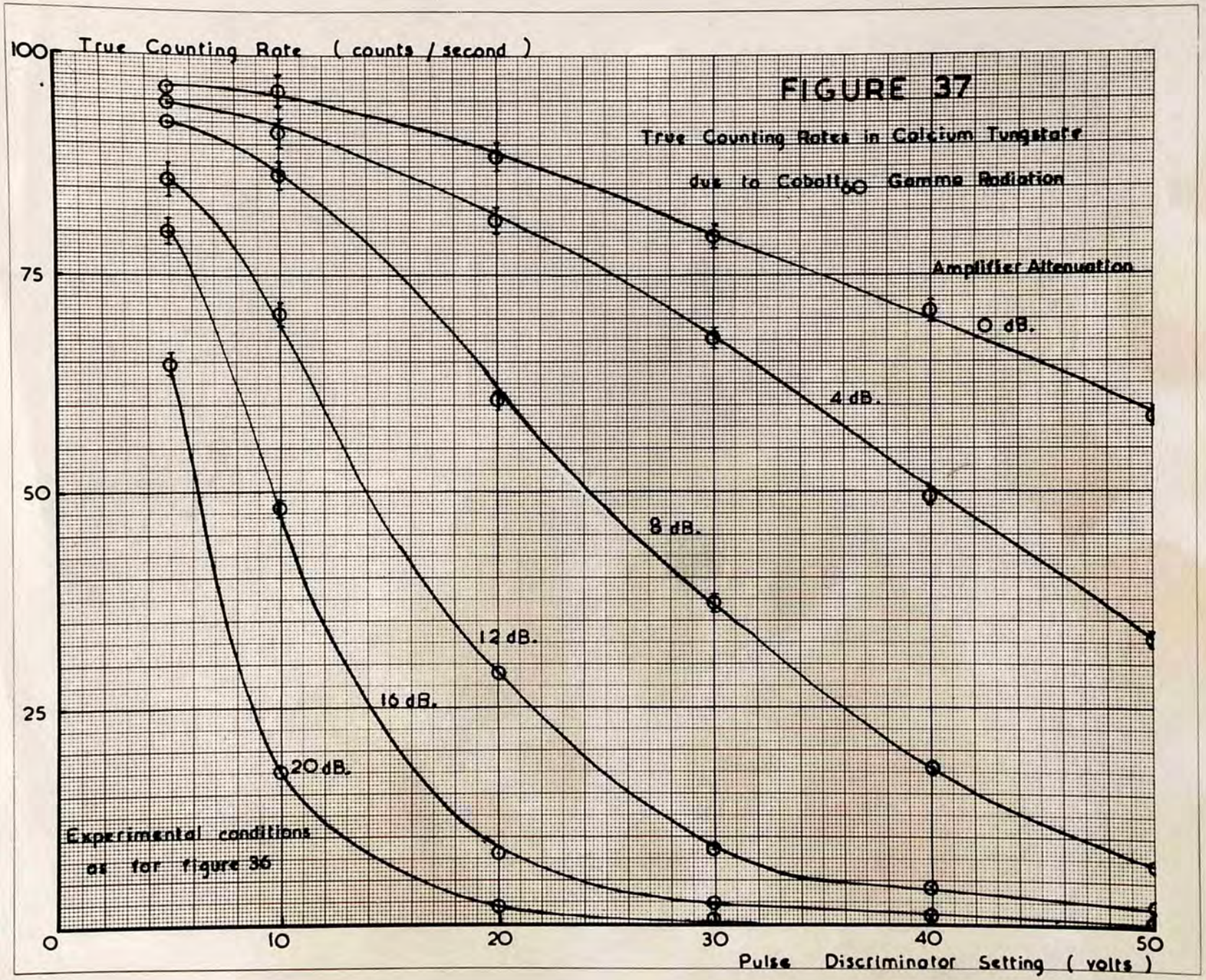

FIGURE 37

True Counting Rates in Calcium Tungstate due to Cobalt$_{60}$ Gamma Radiation

the amplifier attenuation was 8 dB (nominal) and the inter-dynode potential 108 volts. The crystal was of calcium tungstate of mass 0.124 gms., and the gamma-ray source was a 1.5 millicurie cobalt$_{60}$ disc at approximately 30 cms. from the crystal. Curve A shows the total counting rate observed with the shutter open, whilst curve B shows the background due to the direct effect of gamma-radiation on the light guide and the photo-multiplier. The latter effect is seen to be considerable at low pulse discrimination. Curve C gives the true counting rate due to scintillations in the crystal, obtained by difference. All counting rates are corrected for the background with the source absent, and for losses due to the measured resolving time of the scaler (100 microseconds nominal).

Families of curves of true counting rate against pulse discriminator setting, obtained in the above manner for various levels of amplifier attenuation, can be plotted. Such a family is presented in figure 37; the experimental conditions for these observations were identical with those for figure 36

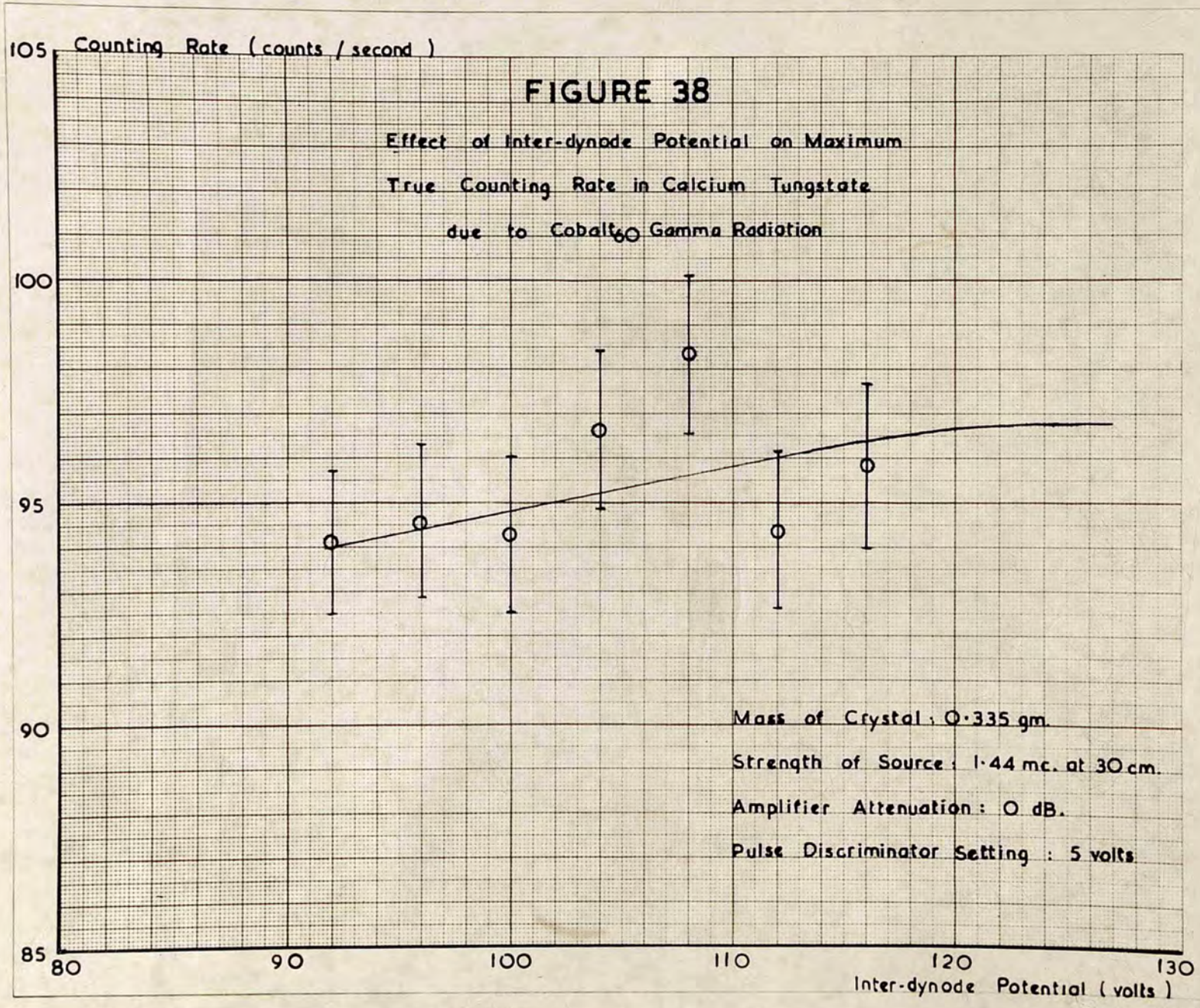

FIGURE 38

Effect of Inter-dynode Potential on Maximum True Counting Rate in Calcium Tungstate due to Cobalt$_{60}$ Gamma Radiation

save that the amplifier attenuation was varied. The true counting rate is seen to tend towards a maximum limiting value at zero pulse discrimination and high gain; this maximum counting rate represents the condition when every scintillation in the crystal which releases one or more photo-electrons at the cathode of the photo-multiplier is being counted. Once this state has been realised, a further increase in overall gain cannot result in an increase in counting rate, since a scintillation which for statistical reasons fails to release a photo-electron at the cathode can never be counted. The scintillation counter is then working under conditions comparable to those of a Geiger-Müller counter operating on its plateau; a comparatively large change in inter-dynode potential results in a slight change in counting rate. This is demonstrated by figure 38, which shows the effect of varying the inter-dynode potential on the maximum true counting rate (amplifier attenuation 0 dB, pulse discrimination 5 volts) observed in the experiment of figure 37.

Further studies served to establish the validity

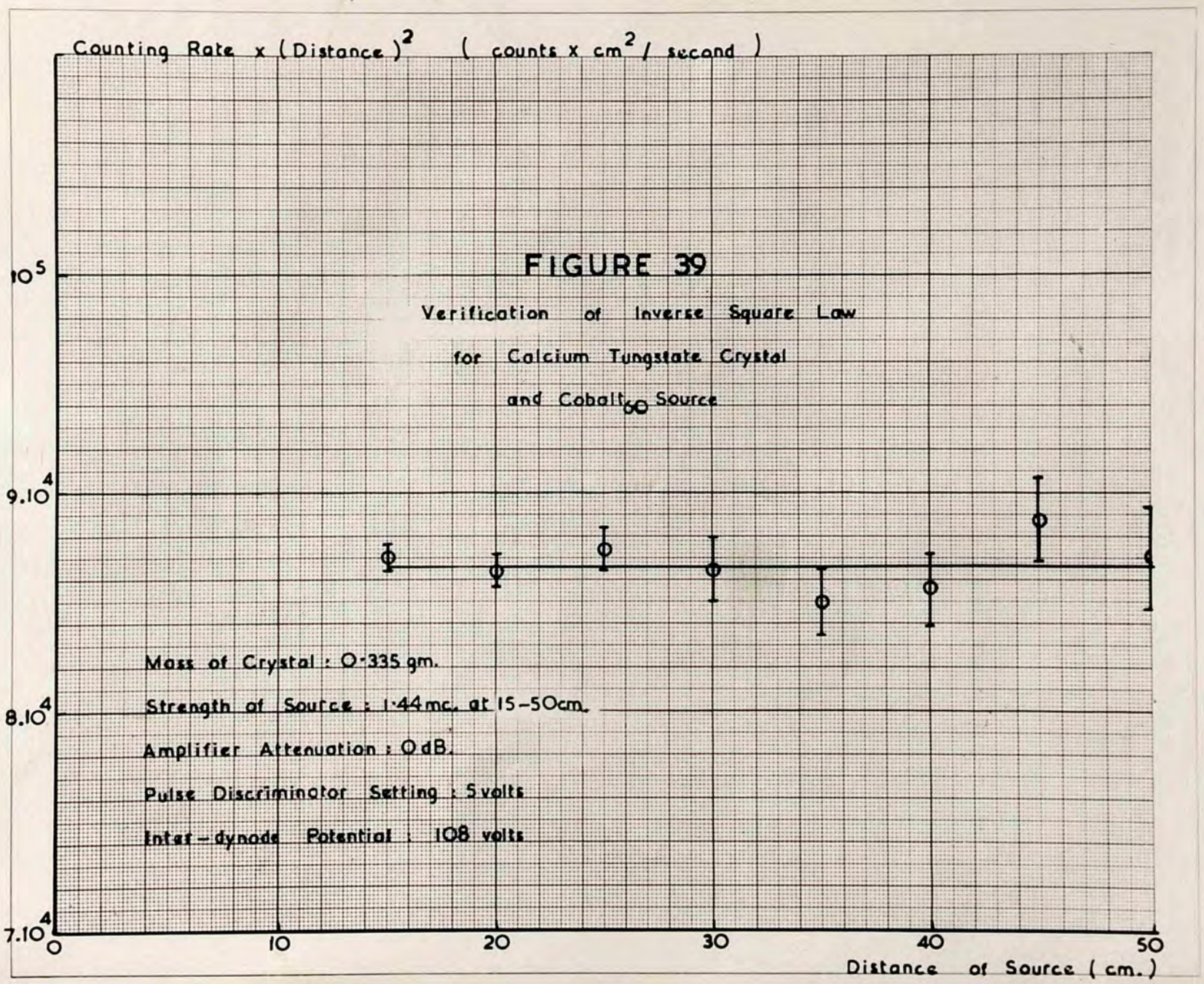

FIGURE 39

Verification of Inverse Square Law for Calcium Tungstate Crystal and Cobalt$_{60}$ Source

FIGURE 40

Effect of Orientation of Source on Maximum True Counting Rate in a Calcium Tungstate Crystal due to Cobalt Gamma Radiation

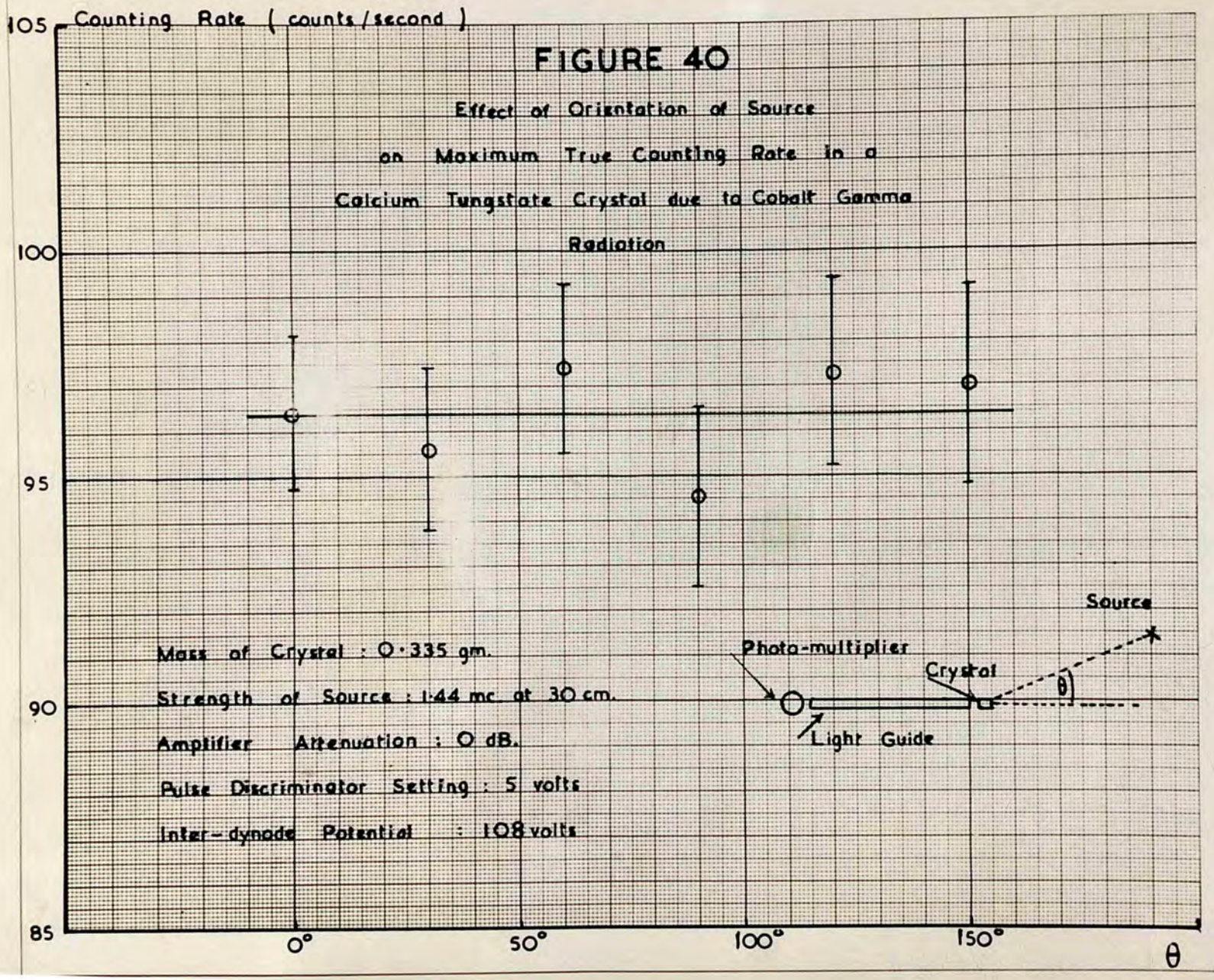

of the inverse square law and the non-directional character of the response of the crystal to gamma-radiation. Figure 39 shows the variation in maximum true counting rate, corrected for background and resolving time effects, as a source of cobalt$_{60}$ is moved along the axis of the light guide. Figure 40 shows the variation in maximum true counting rate as the source is moved in a circle at a fixed distance from the crystal. No evidence of abnormal behaviour was observed in either case.

3. MEASUREMENTS OF ABSOLUTE COUNTING RATES IN CRYSTALLINE LUMINOPHORS:

(a) Methods of Measurement:

Following the preliminary experiments described in the previous sub-section, measurements were made of the maximum true counting rates obtained in crystalline luminophors of measured dimensions. These luminophors were irradiated by a known flux of gamma-radiation from each of the five radioisotopes: sodium$_{24}$, cobalt$_{60}$, bromine$_{82}$, iodine$_{131}$ and gold$_{198}$. The

counting rates appropriate to 1 millicurie of each radioisotope at 1 metre distance were then compared with the calculated rates production of secondary electrons in the crystals, evaluated as described in sub-section II.2 .

The crystals studied were of calcium tungstate, thallium-activated potassium and sodium iodides and pure anthracene. They were weighed, and mounted on balsa wood strips in the manner described on page and in figure 14. Their cross-sectional dimensions were measured with a micrometer gauge, the mean of several measurements being taken; their thicknesses could then be estimated from the measured weights and cross-sections, assuming the values for the densities quoted in Table II.

The photo-multiplier tube was cooled with liquid nitrogen, and was used in conjunction with the Perspex rod and camera shutter assembly already described. The inter-dynode potential was standardised at 108 volts, the amplifier was operated at full gain, and the scaler pulse discrimination control was set at its minimum value of 5 volts; these conditions corresponded to the measurement of maximum counting rate of figure 37.

The strengths of the gamma-ray sources were measured against a radium standard on the 5 mm. carbon ionisation chamber system described in sub-section III.5., and were of the order of 1 millicurie.

The method of measurement of counting rate was as follows:- a mounted crystal was placed in the crystal holder and the background counting rate measured in the absence of any source, first with the shutter open, and then with the shutter closed. A source was next mounted in the source holder, at such a distance from the luminophor that the maximum true counting rate was approximately 100 counts/second, this distance being measured on the scale of the optical bench. A filter was interposed between the source and the crystal to screen the latter from beta-radiation. In the case of all the radioisotopes studied, save sodium$_{24}$, this filter was a 2 cm. x 2 cm. square of copper foil, 0.055 cm. thick; with sodium$_{24}$ sources, which emit energetic beta-particles of maximum energy 1.38 MeV., this thickness was doubled to 0.110 cm. The source and filter being in position, counting rates were again measured with the shutter open and closed. This procedure was repeated with each of the five radioisotopes studied.

All counting rates were measured over 100-second periods, duplicate measurements being made in every case. The photo-multiplier background in the absence of a source was of the order of 1 count/second; the background due to the crystal depended on its size and nature, but was usually also of this order. Appropriate corrections were made for these background effects, and for the resolving time of the scaler. From the known strength of each source, corrected for radioactive decay, and its distance from the mid-point of the crystal, the maximum true counting rate appropriate to 1 millicurie of the radioisotope at 1 metre distance could then be deduced.

The corresponding rate of production of secondary electrons in the crystal was calculated from its known dimensions as described in sub-section II.2., assuming the decay schemes of figures 18 - 22. In these calculations, it was necessary to treat each gamma-ray in the spectrum of each radioisotope separately; the method of setting out the somewhat laborious calculation of these rates for a single crystal of calcium tungstate is shown in Appendix IV.

Corrections were included in these calculations for internal conversion of the emitted gamma-radiation, self-absorption in the source, and absorption in the beta-ray filter.

The ratio of the observed maximum true counting rate to the calculated rate of production of secondary electrons could thus be studied. If each secondary electron produced a single scintillation, and if every scintillation recorded a single count in the scaler, then this ratio, henceforth referred to as ε, would of course be equal to unity.

(b) Effect of Scaler Resolving Time on Counting Rate:

It was soon realised, however, that changes in the resolving time of the scaler may profoundly modify the observed counting rates, even though these are corrected for random counting losses in the manner described on page 71 . This may be anticipated from the theoretical discussion of page 39 . Where the decay time of the luminophor is short compared with the shortest resolving time used, no more than one count per secondary electron can be recorded. On the other hand, in luminophors with a phosphorescent decay of long period a single secondary electron may

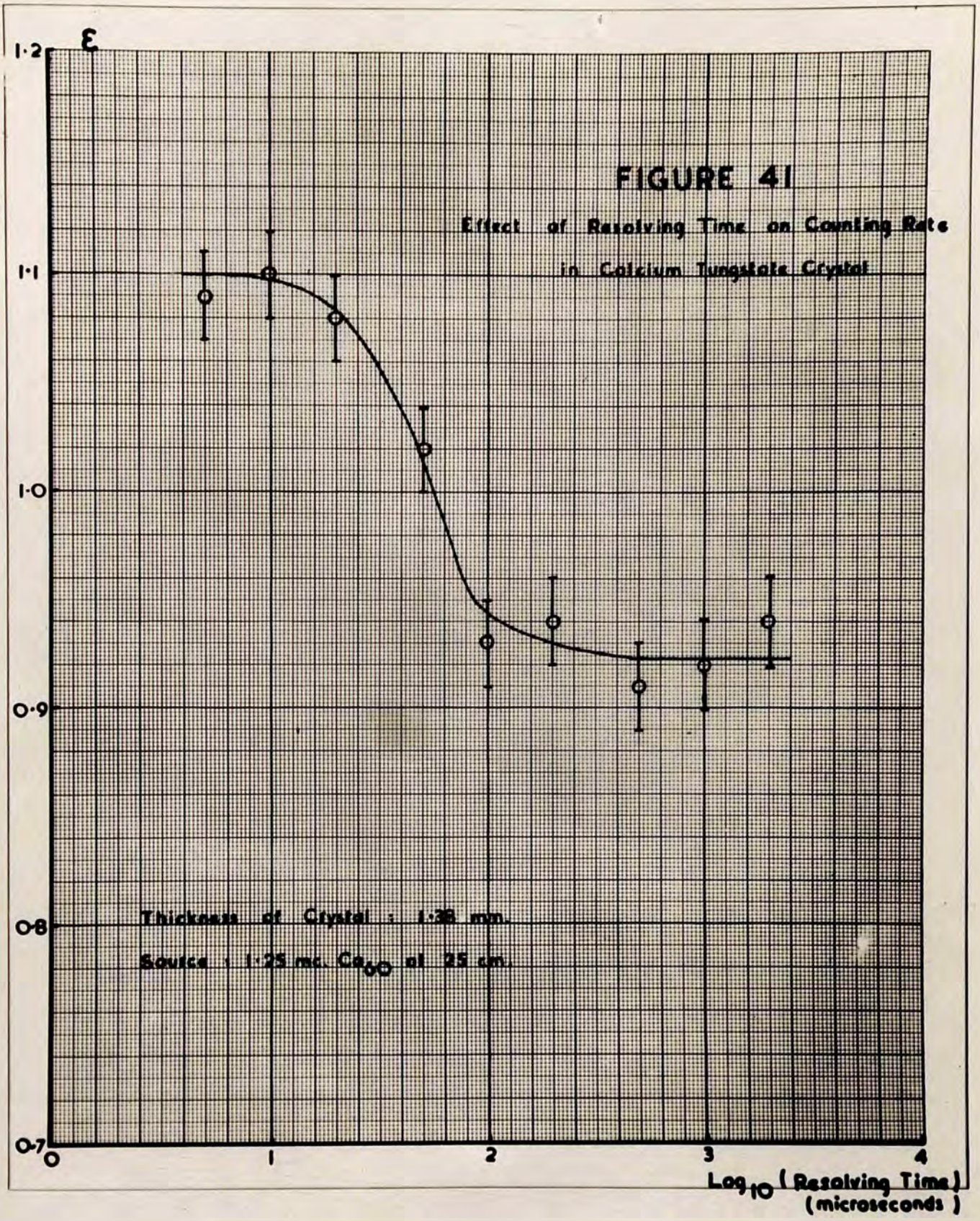

FIGURE 41

Effect of Resolving Time on Counting Rate in Calcium Tungstate Crystal

cause the emission of photons over a period many times greater than the resolving time of the system, and may then be counted many times over.

The form of the curve of ε against scaler resolving time may be expected to approximate to the decay curve of the luminophor, the observed counting rates tending towards a constant value at resolving times long compared with the luminophor decay time. These effects were studied in small crystals of each of the materials listed above, irradiated by the gamma-radiation from a cobalt ^{60} source; the experimental results are shown in figures 41 - 45.

Figure 41 shows the variation in counting rate with scaler resolving time for a crystal of calcium tungstate of mass 0.335 gms. The ratio ε, of observed counting rate to rate of production of secondary electrons is seen to be slightly greater than unity at very low resolving times, but has fallen to a constant value at a resolving time of 100 microseconds. These effects would be explained if calcium tungstate showed a phosphorescent decay of about 50 microseconds duration; such a decay has already been reported by

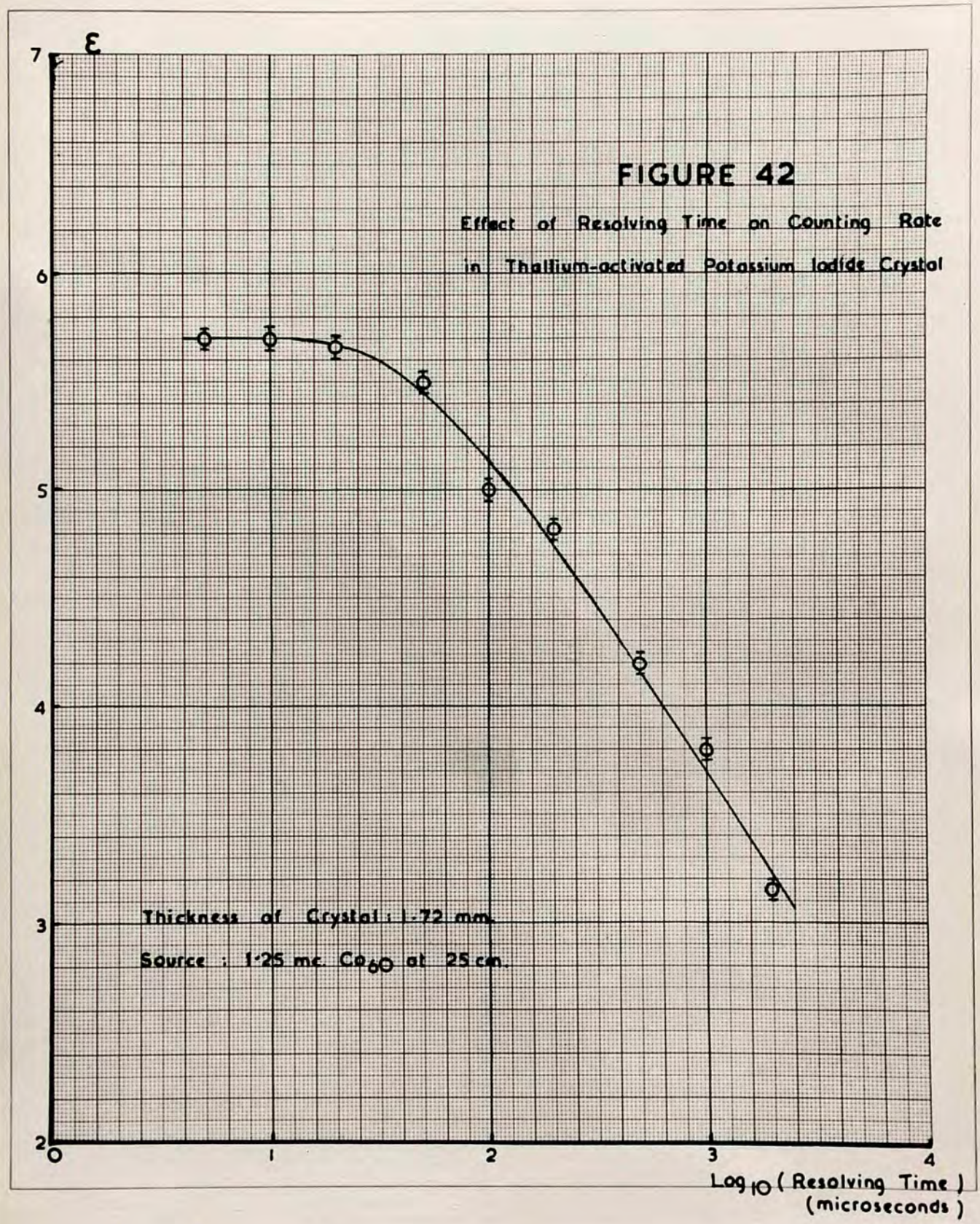

FIGURE 42

Effect of Resolving Time on Counting Rate in Thallium-activated Potassium Iodide Crystal

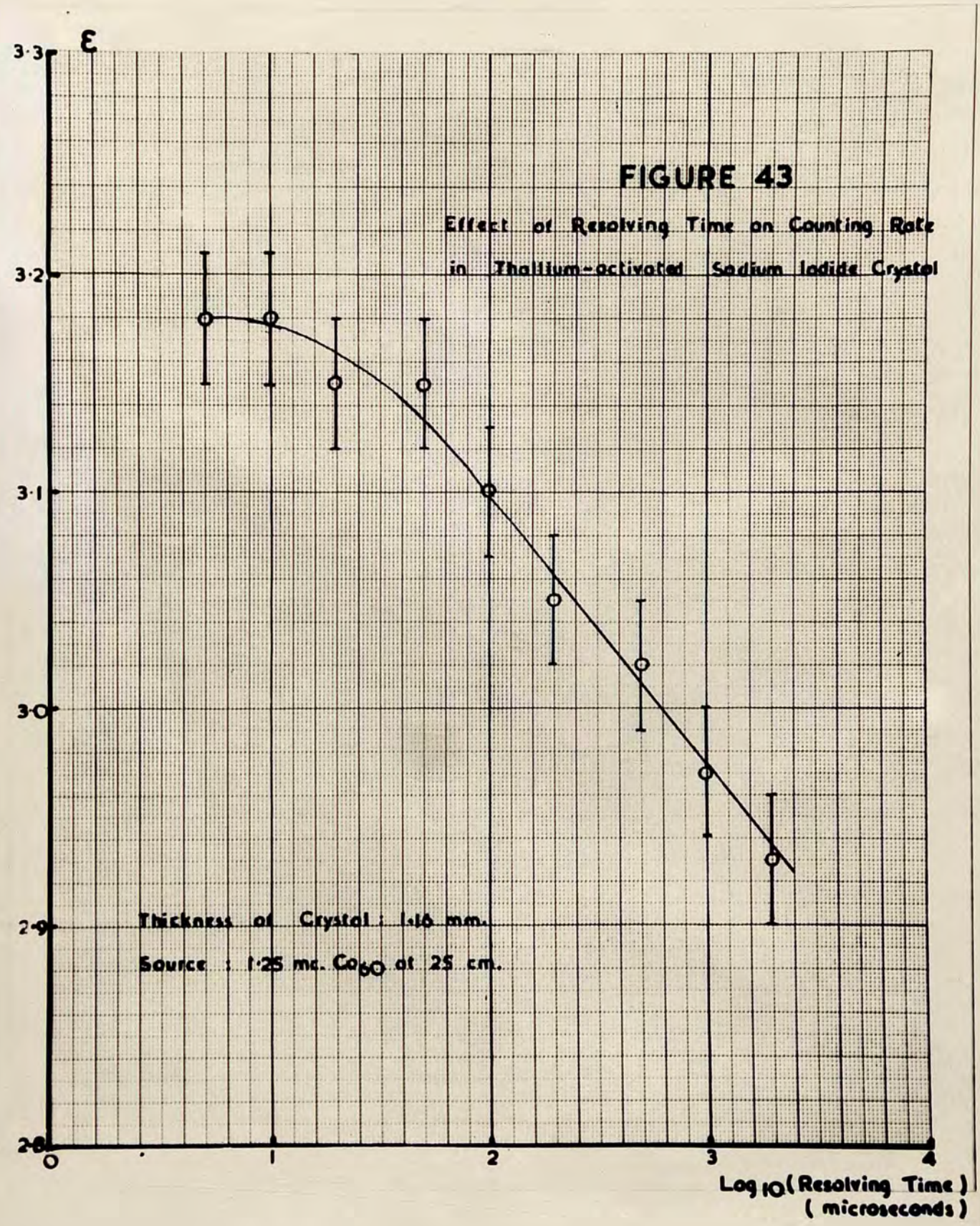

FIGURE 43

Effect of Resolving Time on Counting Rate in Thallium-activated Sodium Iodide Crystal

Garlick (1949), who observed it to be exponential in form.

In the case of thallium-activated potassium-iodide, (figure 42) the experimental results show a very different picture. Counting rates are many times greater than the calculated rate of secondary electron production and the ratio has not reached a constant value even at resolving times of 10 milliseconds. These results indicate an intense phosphorescence with a non-exponential decay lasting many milliseconds. Anomalously high scintillation counting rates in this material have also been reported by Smaller, May and Freedman (1950).

Crystals of thallium-activated potassium-iodide exposed to daylight or to intense fluxes of gamma-radiation showed a temporary increase in background owing to the long "tail" of this non-exponential decay, but recovered within a few minutes. No significant change in background counting rates were observed, however, at the low levels of radiation flux used in these experimental studies.

In thallium-activated sodium-iodide, (figure 43) the phosphorescent decay proved to be of even longer duration. Measurements with this luminophor were

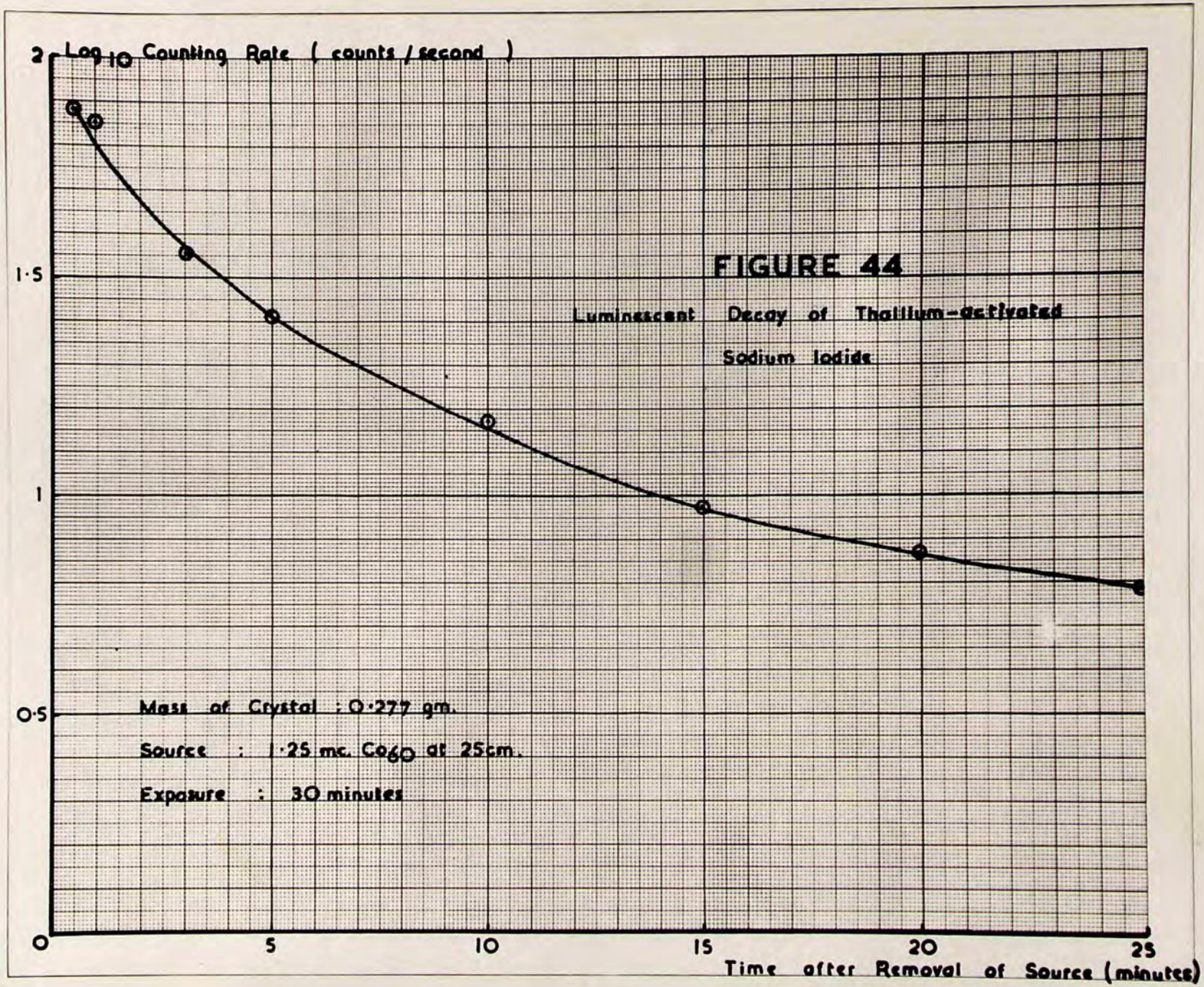

FIGURE 44

Luminescent Decay of Thallium-activated Sodium Iodide

difficult to make, firstly because of its instability under normal atmospheric conditions referred to in sub-section III.4 , and secondly because of this phosphorescent decay. Because of the latter effect, when a crystal of sodium-iodide was exposed to a constant flux of gamma-radiation, the counting rate at first rose slowly, and continued to rise as the phosphorescence built up, only reaching a steady state some thirty minutes after the initial exposure. If the source of radiation were then removed, the ensuing decay could readily be followed on the rate-meter. As will be seen from an inspection of figure 44, it is non-exponential in form. Similar effects followed exposure to visible light.

Because of these effects, it was necessary to expose crystals of sodium-iodide to each source for at least thirty minutes before measuring the counting rate, and to allow a like period of recovery before attempting another measurement with the same crystal. Only if these precautions were observed could reproducible results be obtained.

In figure 45 the relationship between observed counting rate and resolving time in a crystal of pure

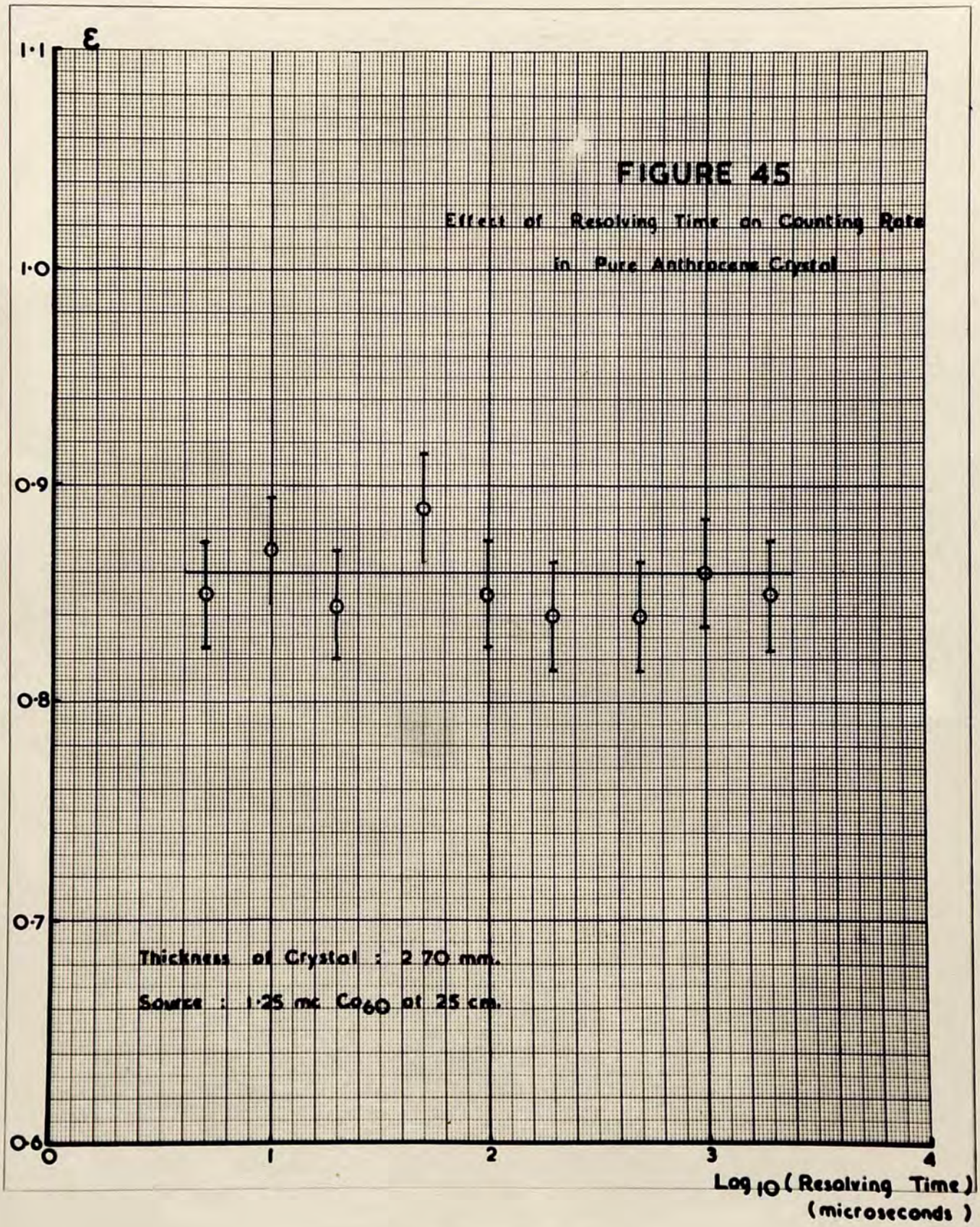

FIGURE 45

Effect of Resolving Time on Counting Rate in Pure Anthracene Crystal

anthracene is shown. The counting rate was in this case found to be independent of resolving time within the limits of experimental error over the range studied, indicating a decay time of less than 1 microsecond in the luminophor. This result is in keeping with the known extremely short decay time of organic crystalline luminophors.

The errors indicated in figures 41 - 45 represent the standard errors due to counting statistics only. Errors in the measurement of source strength and source-counter distance, and errors in the decay schemes and in the values of linear absorption coefficients and crystal dimensions used in the calculation of the rates of secondary electron production also affect the experimental values of ε. However, these are systemic errors, which are constant for each series of measurements.

A precise treatment of these systemic errors is difficult. Since they may affect both the observed counting rate and the calculated rate of secondary electron production in the same sense, their nett effect on ε may be small. For example, an error in the assumed decay scheme for a radio-isotope may lead to a positive error in the calculated

k-factor for the radioisotope, so that the measured source strength will have a negative error. The observed counting rate when corrected for 1 millicurie at 1 metre will thus also be subject to a positive error. Similar considerations apply to the measurement of crystal dimensions. The weights of the crystals are known to a high degree of accuracy. A positive error in measurement of cross-section will therefore be accompanied by a negative error in calculated crystal thickness; the nett effect on the calculated rate of secondary electron production will be small.

The quantities most likely to cause error in the experimental values for ε are the measured source strengths and the calculated absorption coefficients. Taking the standard error in the former as $\pm$ 4%, and that of the latter as $\pm$ 5% and allowing a further standard error of $\pm$ 7% for all other effects, including those due to scattered radiation, the absolute values of ε obtained are unlikely to be in error by more than $\pm$ 10%.

In calculating the absorption coefficients for thallium-activated potassium and sodium iodides, the presence of the small percentage (0.5 - 1.0%) of

thallium activator was not taken into account; the error due to this approximation is negligible in the gamma-energy range under consideration.

(c) Experimental Results: Calcium Tungstate.

Detailed studies of the counting rates observed in calcium tungstate were made at scaler resolving times of 10 and 100 microseconds. Reference to figure 41 shows that the latter condition satisfies the requirement that the resolving time should be long compared with the decay time of the luminophor; at 10 microseconds resolving time this condition is not satisfied.

The crystals used in these investigations were cylindrical in form, of cross sectional area 0.05 cm^2. approximately, and of thicknesses up to 0.5 cm. They were mounted with a basal plane presented towards the light guide. Background counting rates in these crystals in the absence of a source were in all cases less than 1 count/second.

In Table XVI, the results of a series of observations and calculations for a single crystal of thickness 0.138 cm. are presented, the resolving time of the scaler being in this case 100 microseconds. There is seen to be reasonable agreement between the observed rates and the calculated rates of production

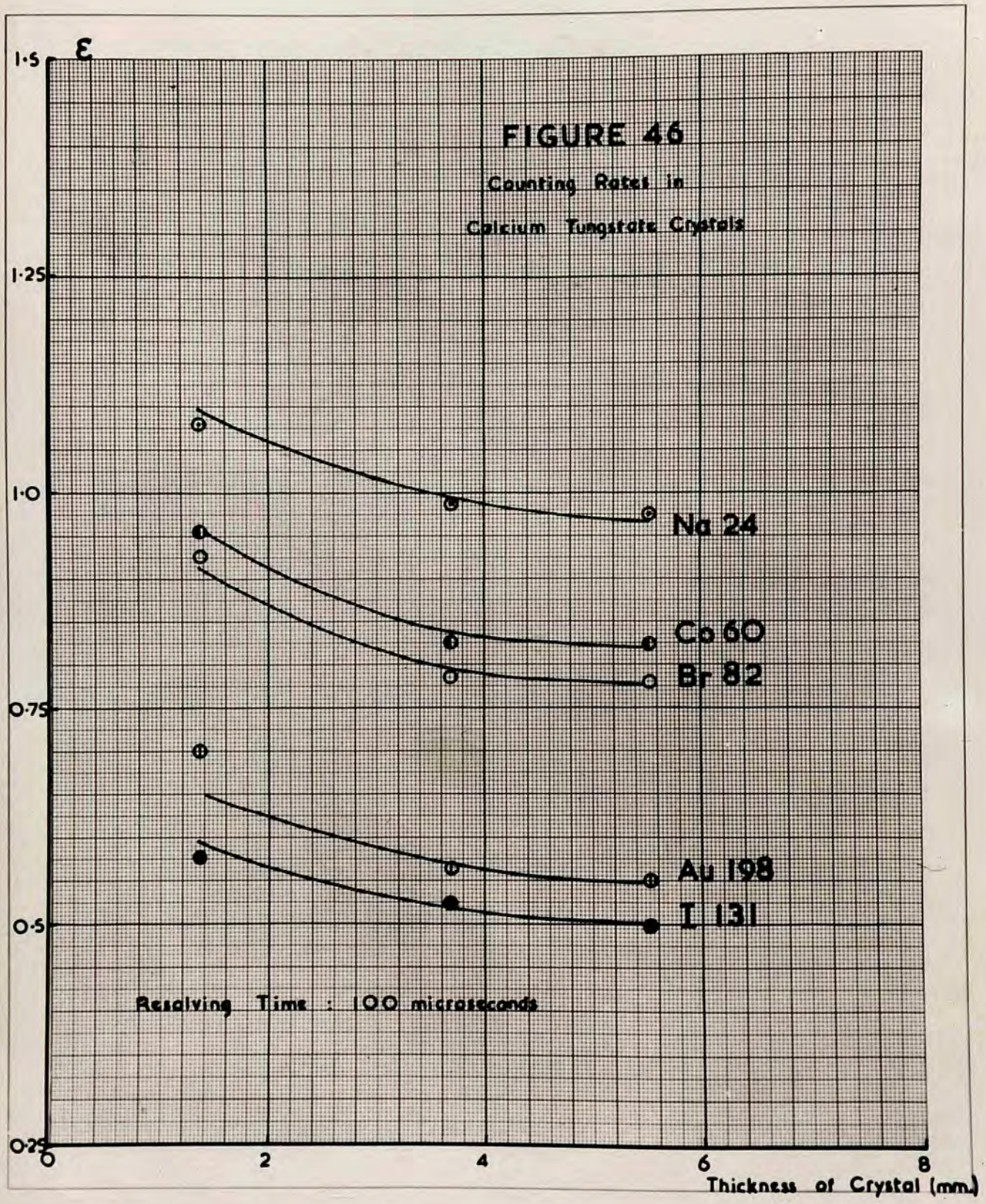

FIGURE 46

Counting Rates in Calcium Tungstate Crystals

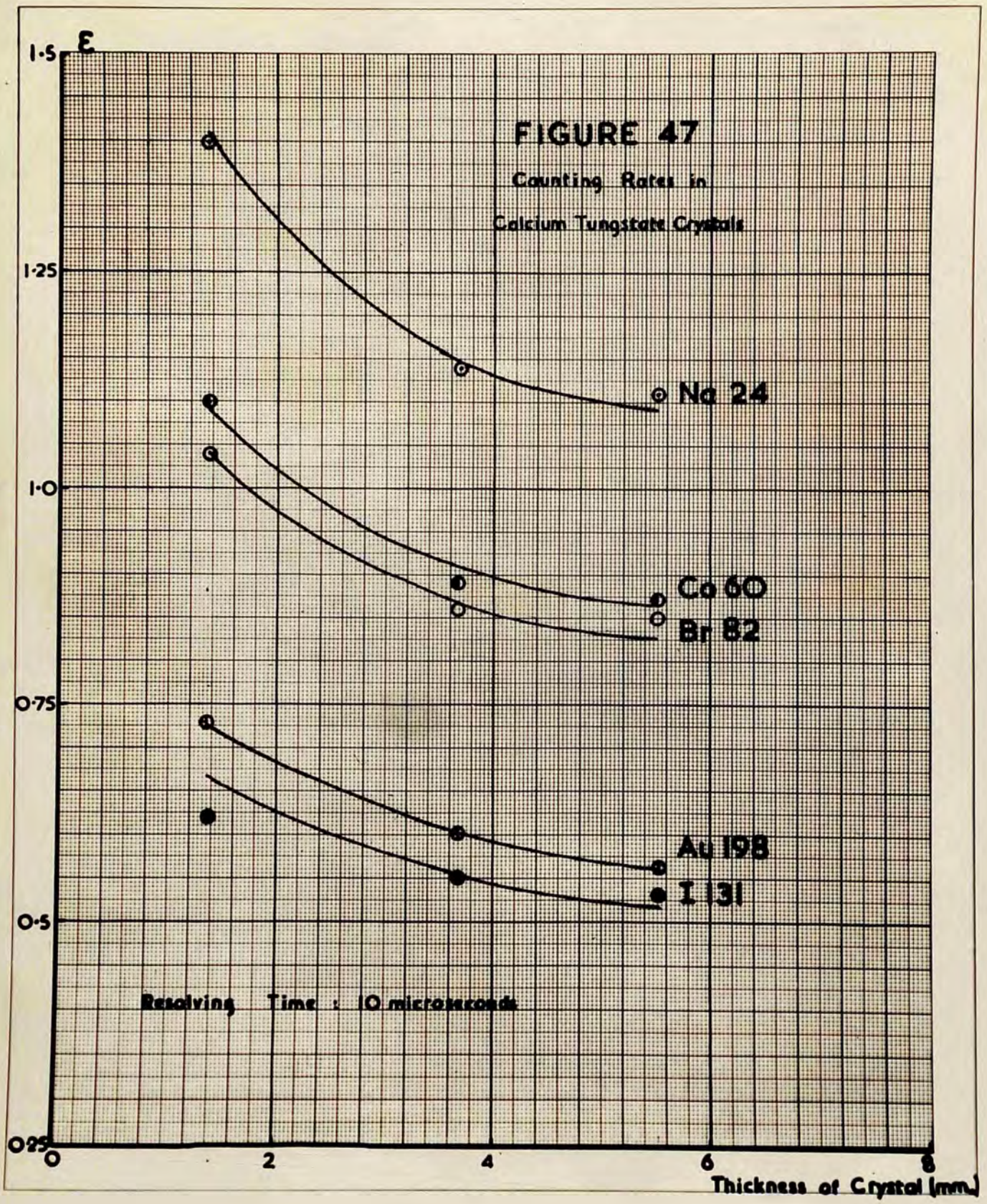
FIGURE 47
Counting Rates in
Calcium Tungstate Crystals
ε
1·5
1·25
1·0
0·75
0·5
0·25
0
2
4
6
8
Thickness of Crystal (mm.)
Na 24
Co 60
Br 82
Au 198
I 131
Resolving Time : 10 microseconds

of electrons for sodium$_{24}$ and cobalt$_{60}$ gamma-rays, but the ratio, ε, of the two rates falls off rapidly at lower gamma-ray energies.

Table XVI.

Maximum True Counting Rates in Calcium Tungstate of Thickness 0.138 cms. due to 1 millicurie of various Radioisotopes at 1 metre.

Radioisotope.	Observed Counting Rate counts/sec.	Calculated Rate of Production of Secondary Electrons electrons/sec.	ε
Sodium 24	3.32	3.16	1.05
Cobalt 60	3.98	4.19	0.95
Bromine 82	7.55	8.12	0.93
Iodine 131	3.23	5.67	0.57
Gold 198	3.27	4.67	0.70

These results are to be expected because of the increased probability that the small scintillations produced by low energy gamma-radiation will fail to release an electron at the photo-multiplier cathode, and thus fail to be recorded.

Similar measurements were made on crystals of thickness 0.370 cm. and 0.553 cm., and in figures 46 and 47, the ratio ε is plotted as a function of

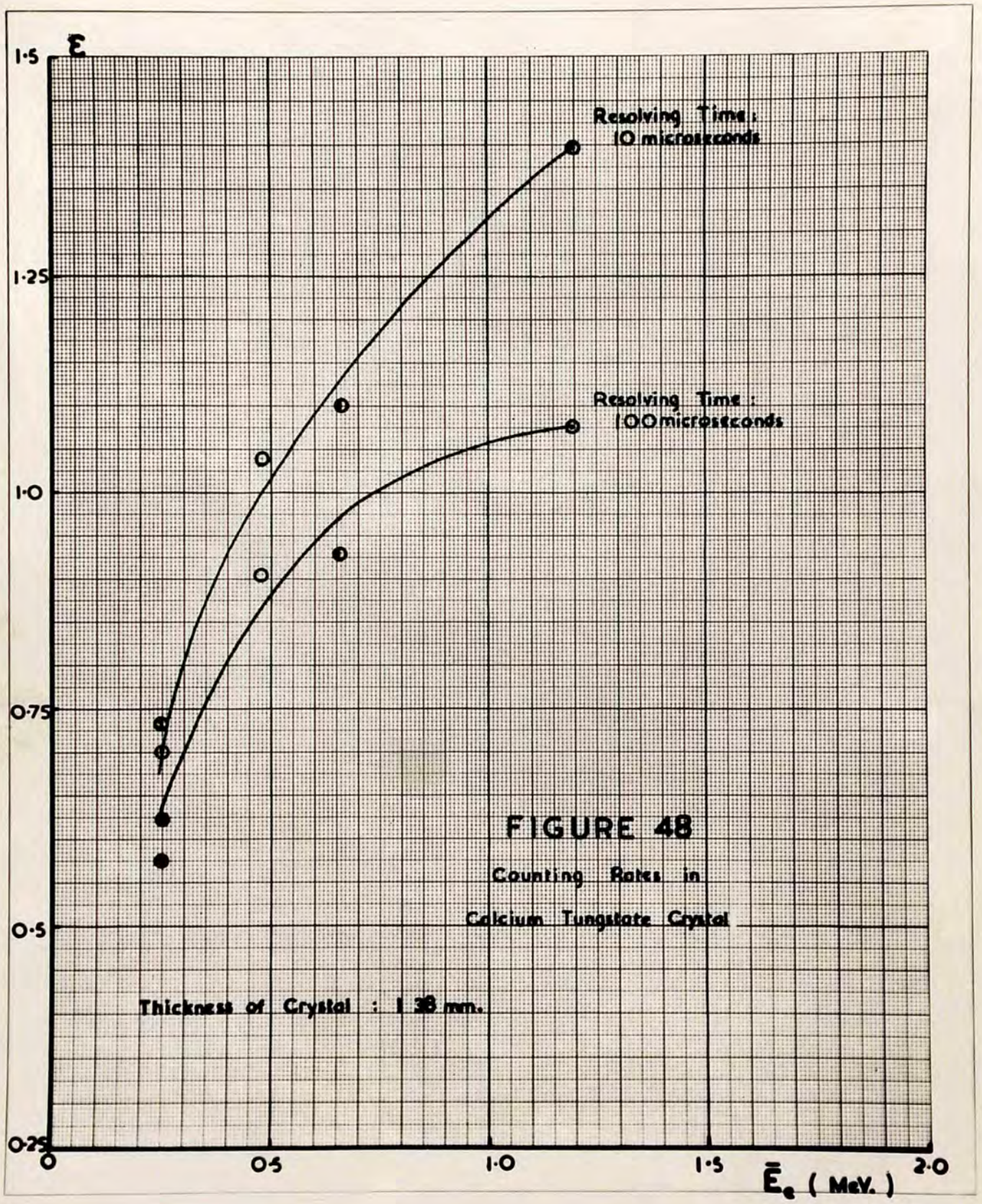

FIGURE 48

Counting Rates in

Calcium Tungstate Crystal

crystal thickness for each of the five radioisotopes studied, at resolving times of 100 microseconds and 10 microseconds respectively. All counting rates at 10 microseconds resolving time are higher by approximately 10% because of multiple counting of secondary electrons. At 100 microseconds resolving time, there is reasonable agreement between the observed and calculated rates due to sodium$_{24}$, cobalt$_{60}$, and bromine$_{82}$ if the curves of figure 46 are extrapolated to zero crystal thickness. In the case of the thicker crystals studied, there is some loss in counting rate with these radioisotopes because of the reduced optical efficiency of the system towards visible photons emitted at the back of the crystal. With the low energy gamma-radiation from iodine$_{131}$ and gold$_{198}$, a significant fraction of secondary electrons produced fail to register, even in thin crystals of calcium tungstate.

In figure 48, the values of $\mathcal{E}$ given in Table XVI are plotted as a function of the mean energy, $\overline{E}_e$, of the secondary electron produced in the crystal by the various radioisotopes studied. The values of were calculated from the data of Appendix II and from the assumed decay schemes of the radioisotopes. From

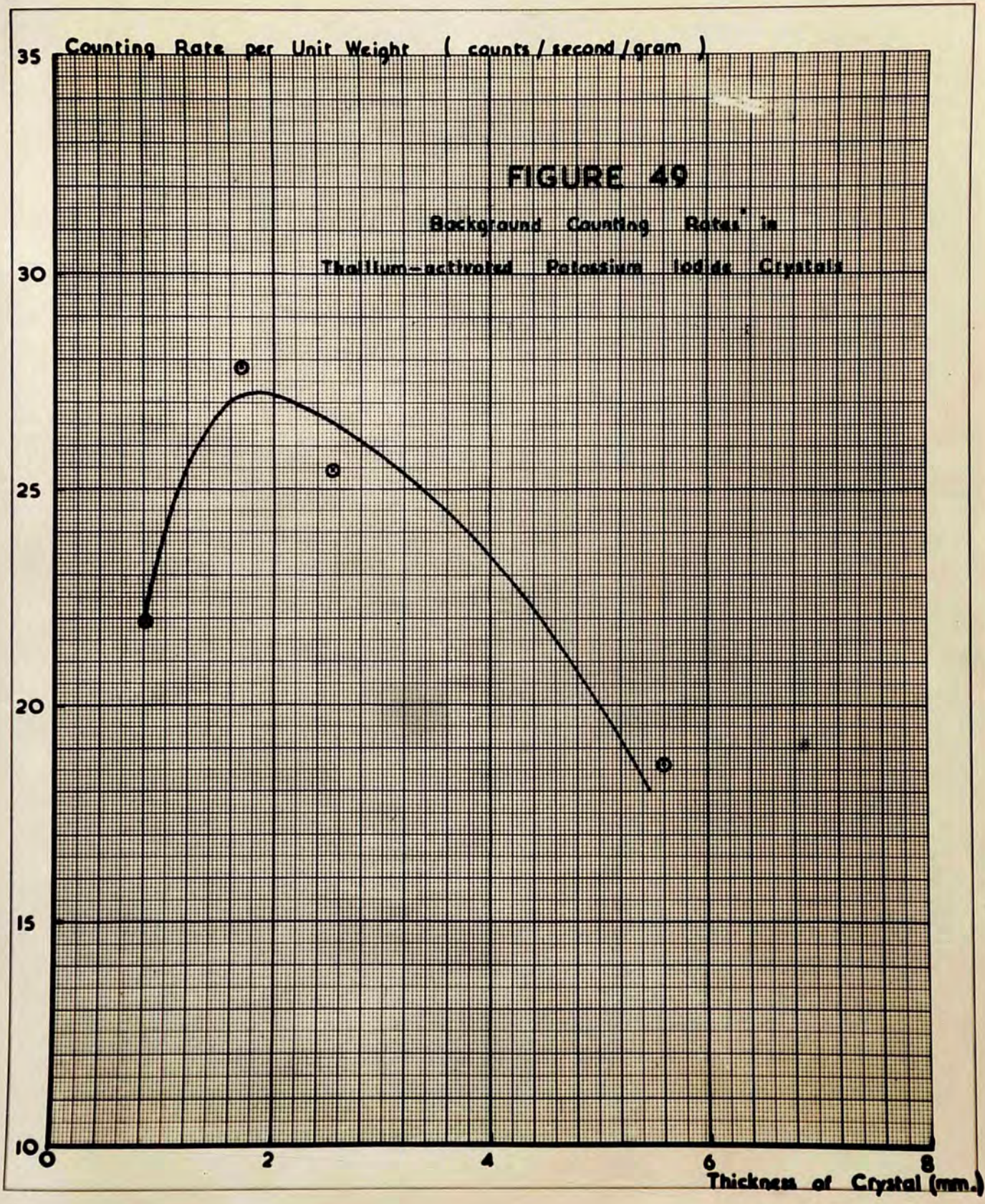

FIGURE 49

Background Counting Rates* in Thallium-activated Potassium Iodide Crystals

such a curve as figure 48, the expected value of ε can be found for any radioisotope whose decay scheme is known.

In these measurements, and in those that follow, the standard error in the absolute values of ε obtained may be estimated as $\pm$ 10%.

(d) Experimental Results: Thallium-Activated Potassium Iodide:

Similar measurements to those just described on calcium tungstate were made on thallium-activated potassium iodide. Of this luminophor, the crystals used were rectangular parallelopipeds of cross-section approximately 0.16 cm^2 and thicknesses up to 0.559 cm. The background counting rates in these crystals in the absence of any source were very much higher than those observed with crystals of calcium tungstate of similar size. In figure 49, these backgrounds, corrected for photo-multiplier background, are plotted as a function of crystal thickness. To some extent these effects may be explained by the anomalously high efficiency of the luminophor towards high energy gamma-radiation which has already been mentioned. Nevertheless, a considerable fraction

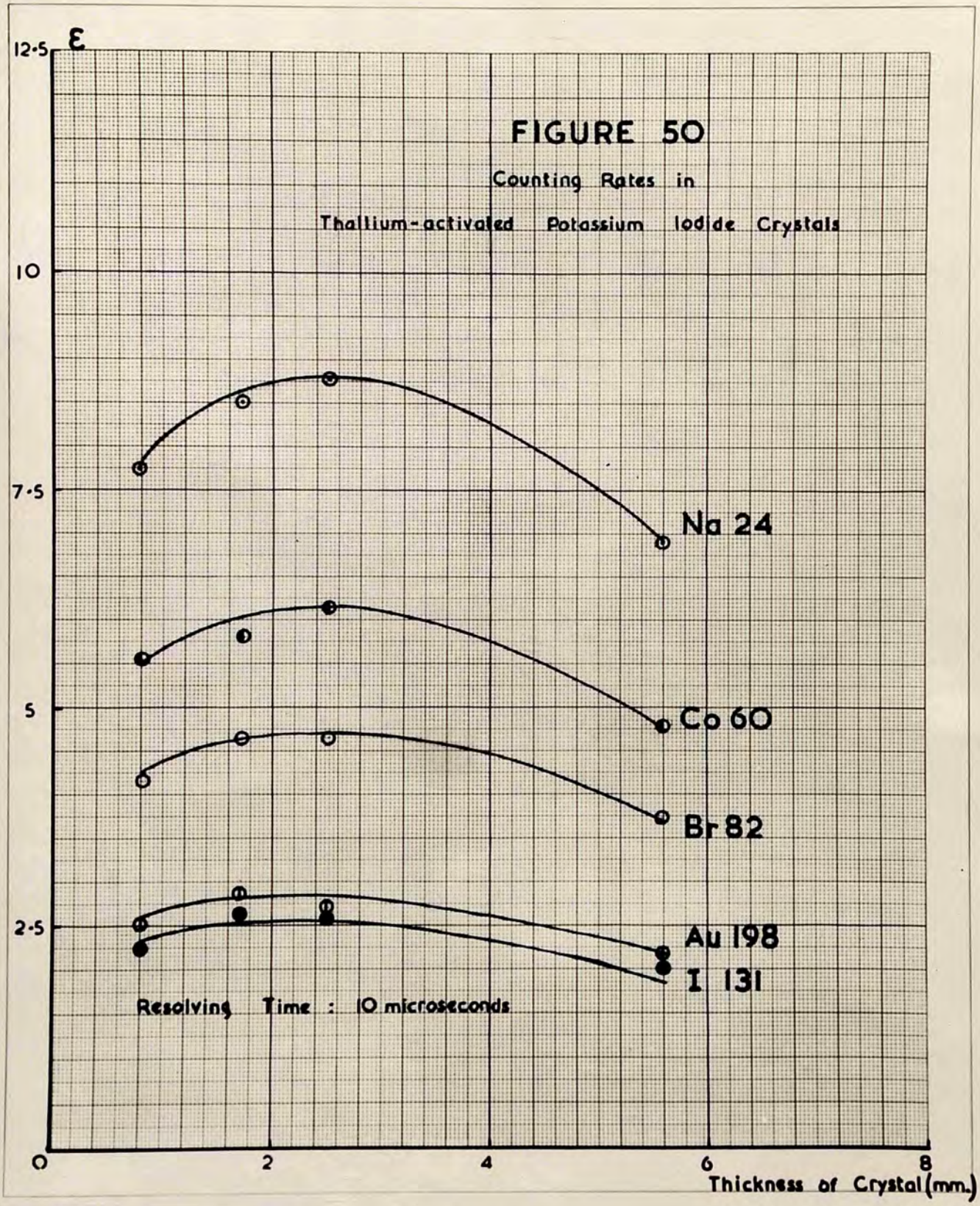

FIGURE 50

Counting Rates in

Thallium-activated Potassium Iodide Crystals

of the observed rates must also be due to the presence of the naturally occurring radioactive isotope of potassium, K_{40}. This matter will be discussed in detail on a later page.

In figure 50, results of counting rate measurements made at a resolving time of 10 microseconds in potassium iodide are shown. The ratio ε is seen to be in all cases greater than unity, and to increase rapidly with gamma-ray energy. Its diminution with increasing crystal thickness may be explained qualitatively in terms of the reduction in the optical efficiency of the system for events occurring at the back of the crystal. Its fall in the case of the thinnest crystal studied, on the other hand, is probably due to the escape of some of the more energetic secondary electrons from the lattice before they have expended all their available energy in exciting phosphorescent centres.

The number of luminescent centres excited by a given secondary electron, and hence the number of phosphorescent counts recorded per secondary electron ($\varepsilon - 1$), may be expected to be linearly proportional

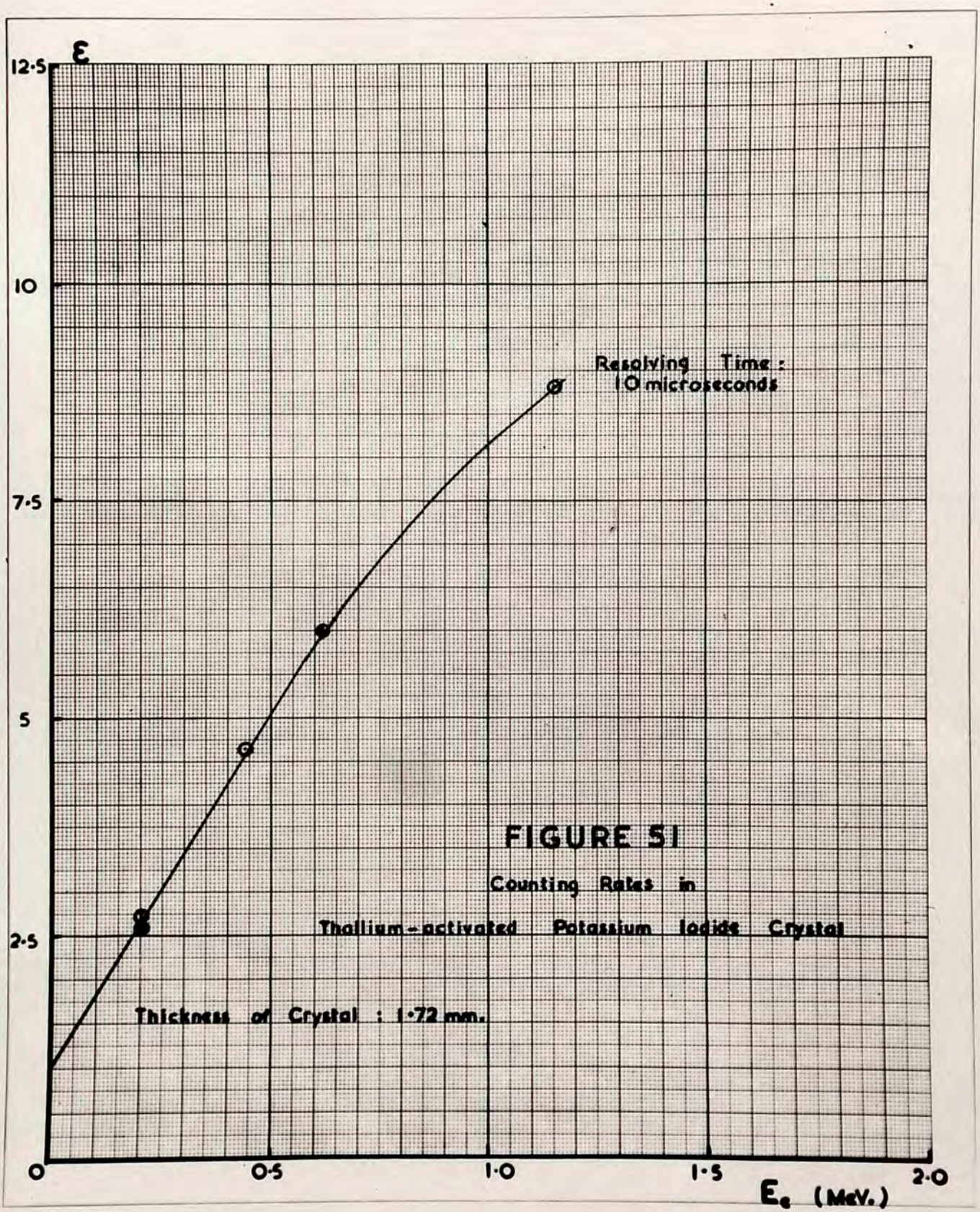

FIGURE 51

Counting Rates in Thallium-activated Potassium Iodide Crystal

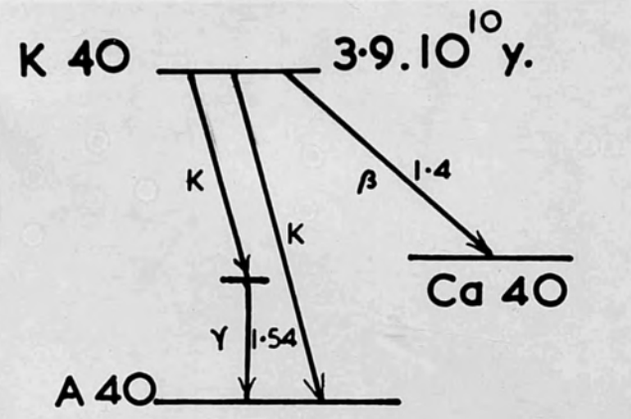

FIGURE 52

to its energy. This is agreeably borne out by the approximately linear plot of $\mathcal{E}$ against calculated mean secondary electron energy, $\overline{E}_e$, shown in figure 51 for a crystal of thickness 0.172 cm. On extrapolation, this plot intersects the y-axis approximately at unity, as expected:- in the hypothetical case in which the secondary electron energy was zero, the counting rate due to phosphorescent emission would of course vanish.

Returning now to the high backgrounds observed in crystals of potassium iodide, the date of figure 51 may be used to evaluate the expected background counting rate due to the K_{40} content of the luminophor. The radio-activity of K_{40} has been the subject of a large number of recent investigations. The most probable decay scheme is that proposed by Hirzel and Wäffler (1946) and shown in figure 52. The branching ratio $\lambda_\gamma / \lambda_\beta$ has been given as 0.05 by Floyd and Borst (1949). Since only a small fraction of the emitted gamma-quanta will be scattered or absorbed within the luminophor in crystals of the dimensions used in these studies, contribution of the gamma-ray branch can be ignored

in evaluating the expected counting rates. The decay constant of the radio-isotope has been determined by Borst and Floyd (1948), who obtained a value of $3.9 \cdot 10^{-10}$ year^{-1}. The isotope concentration of K_{40} in non-enriched activity has recently been found by Nier (1950) to be $1{\cdot}19 \cdot 10^{-4}$.

From these values, the number per second per gram of potassium iodide of those disintegrations which produce a beta-particle is given by

$$n_\beta = \frac{1{\cdot}19 \cdot 10^{-4} \cdot 6{\cdot}023 \cdot 10^{23} \cdot 3{\cdot}9 \cdot 10^{-10} \cdot 0{\cdot}95}{166 \cdot 365 \cdot 24 \cdot 3600} = 5{\cdot}1 \qquad 4.5.$$

Taking the mean energy of the beta-particles as $1{\cdot}4/3 = 0.47$ MeV. figure 51 gives a value of ε of 4.75 for this radiation in a crystal of thickness 0.172 cm. The counting rate per gm. of potassium iodide due to K_{40} should thus be $5.1 \cdot 4.75 = 24.2$ counts/second; in view of the standard errors in the values used for the decay constant and isotopic concentration of K_{40}, this value is subject to an error of $\pm$ 20%. The observed background counting rate in a crystal of thickness 0.172 cm., derived from figure 49, is 27.8 counts/second/ gm. Such a

value is consistent with the theory that the increased background rates observed in this luminophor are due to the K_{40} content.

Uncertainty regarding the magnitude and energy distribution of the external background prevents an accurate verification of the decay constant of the radio-isotope from the experimental data. This external background was large because of considerable amounts of radio-active materials stored in the vicinity of the laboratory. Measurements on crystals of calcium tungstate and thallium-activated sodium iodide, similar in size to the potassium iodide crystals studied, suggest however that an upper limit of 5 counts/second/gm.can be assigned to the background counting rates due to radiation from external sources in the latter crystals. Within the limits of experimental error, therefore, the observed rates confirm the value quoted by Borst and Floyd for the decay content of K_{40}. Similar measurements have been made by Smaller, May and Freedman (1950) using a coincidence counting arrangement; no correction for external background appears to have been made by these workers.

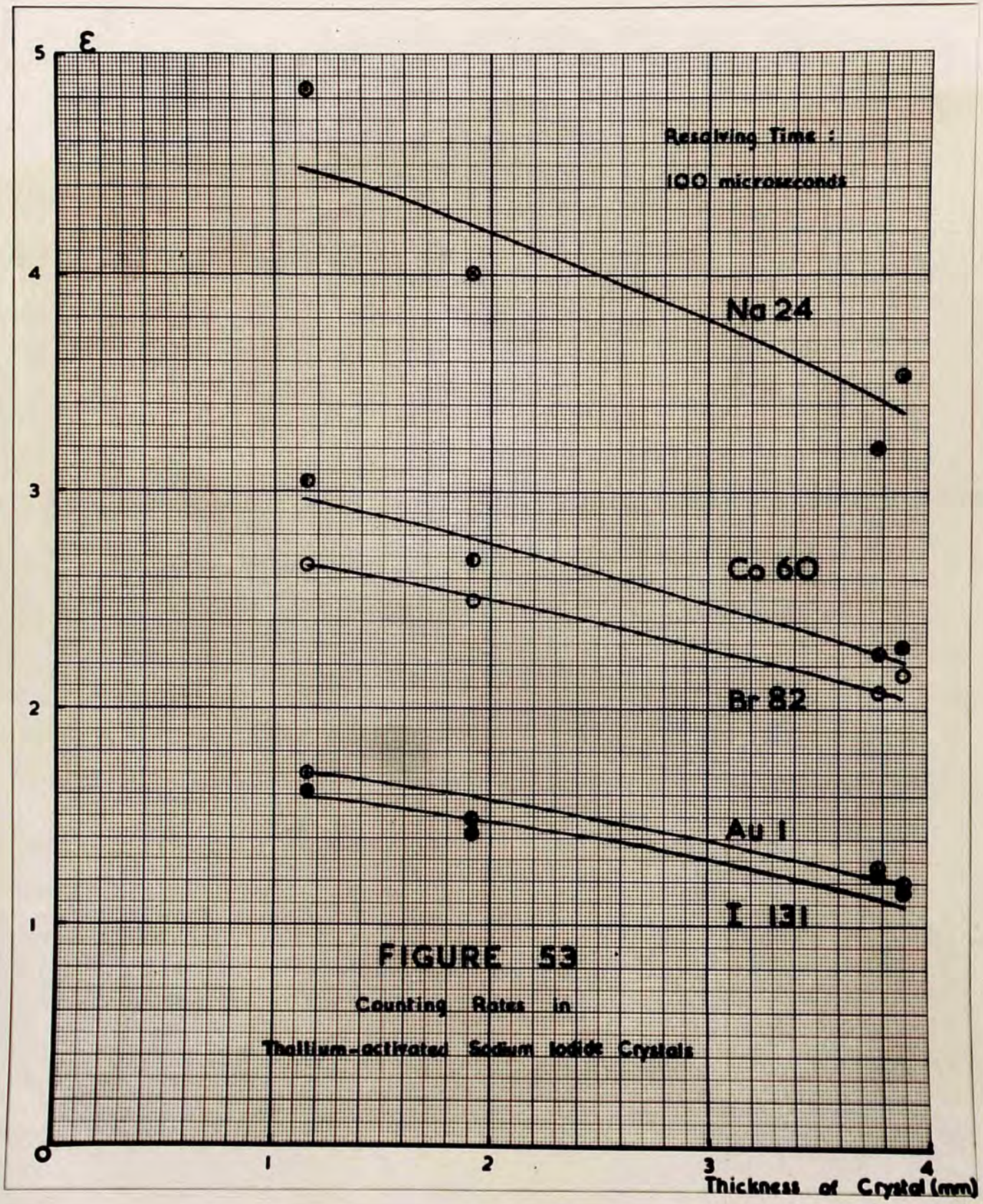

FIGURE 53

Counting Rates in

Thallium-activated Sodium Iodide Crystals

(e) Experimental Results: Thallium-activated Sodium Iodide:

Measurements were made on crystals of sodium iodide of similar form and size to those of potassium iodide studied, the precautions described on page 128 being carefully followed. The background counting rates in these crystals were in all cases less than 2 counts/second, there being no evidence of any internal background effects.

The results with radio-active sources followed the same general pattern as those already described for potassium iodide. Observed counting rates were in all cases considerably greater than the calculated rates of secondary electron production; in figure 53 are seen the values of ε derived from a series of measurements made at a scaler resolving time of 100 microseconds. Figure 54 shows the corresponding plot of ε against $\bar{E}_e$ for a crystal of thickness 1.91 cm. As in the case of potassium iodide, this plot is seen to be approximately linear and to intersect the y-axis on extrapolation at unity.

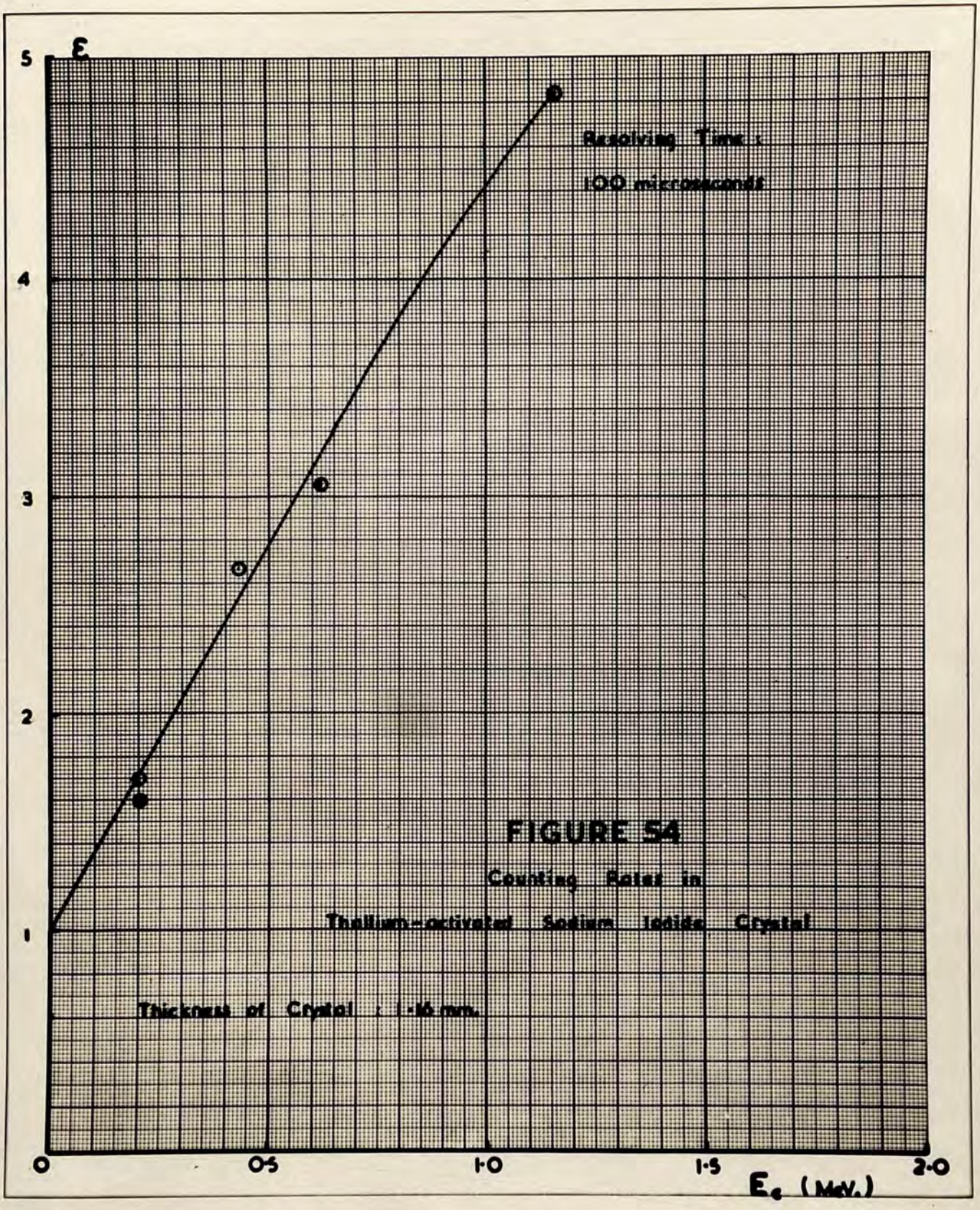

FIGURE 54

Counting Rates in Thallium-activated Sodium Iodide Crystal

4. MEASUREMENT OF PULSE-AMPLITUDE DISTRIBUTIONS IN CRYSTALLINE LUMINOPHORS:

(a) Methods of Measurement:

The experimental curves of counting rate as a function of pulse discriminator setting observed with the Perspex rod and camera shutter of figure 13 (inset A) and reported in figure 37 show no evidence of any discontinuities corresponding to the energy distributions of the secondary electrons in the crystal. Such discontinuities are not indeed to be expected, since the form of the observed pulse amplitude distributions indicates that the average number of electrons released at the cathode of the photo-multiplier by the scintillation produced by a 1 MeV. secondary electron in calcium tungstate is approximately three. It will be seen from figure 11 that under these conditions the fine structure of the pulse amplitude distribution is completely lost because of the photo-multiplier statistics.

In order to observe this fine structure, it is necessary to use an experimental arrangement of higher optical efficiency. For this purpose, use was made of the device shown in figure 13 (inset B),

in which the crystal is mounted almost in contact with the envelope of the photo-multiplier tube. The photo-multiplier assembly was mounted on the optical bench as in the previous experiments.

The photo-multiplier was usually uncooled in these measurements, its inter-dynode potential being 108 volts. The amplifier was operated at an attenuation of 20 dB. or more; under these conditions, the background counting rate due to thermionic emission at the photo-cathode was small at pulse discriminator settings of greater than 15 volts. Counting rates were observed on the rate-meter, the pulse-height distributions being obtained by differentiation of the observed curves of counting rate against pulse-discriminator setting. Sources of approximately 1 millicurie, measured as already described, were used at distances from the crystal of the order of 10 cm.

The method of measuring the distributions was as follows:- with no crystal in the holder, a calibrated source was mounted on the optical bench at a measured distance from the light tight cap of the holder. A copper filter of suitable thickness was interposed between the source and the holder to

exclude beta-radiation. Observations were then made of the background counting rates at 1 volt intervals of pulse discriminator setting. A mounted crystal was next placed in the holder, and observations of the variation in counting rate as a function of pulse discriminator setting again made. All counting rates were corrected for resolving time losses, and the true counting rates due to scintillations in the crystal appropriate to 1 millicurie of activity at 1 metre distance deduced from the known strength of the source, corrected where necessary for radio-active decay. A correction was included here for absorption of radiation in the copper filter, but no correction was needed for the very slight shielding effect of the crystal on the photo-multiplier tube.

The integral curve of true counting rate against pulse discriminator setting was then differentiated by taking its increment over each 1 volt step in pulse discrimination. This differentiation would have been avoided, and the experimental errors due to random fluctuations in counting rate reduced, if a pulse-height analyser could have been used in

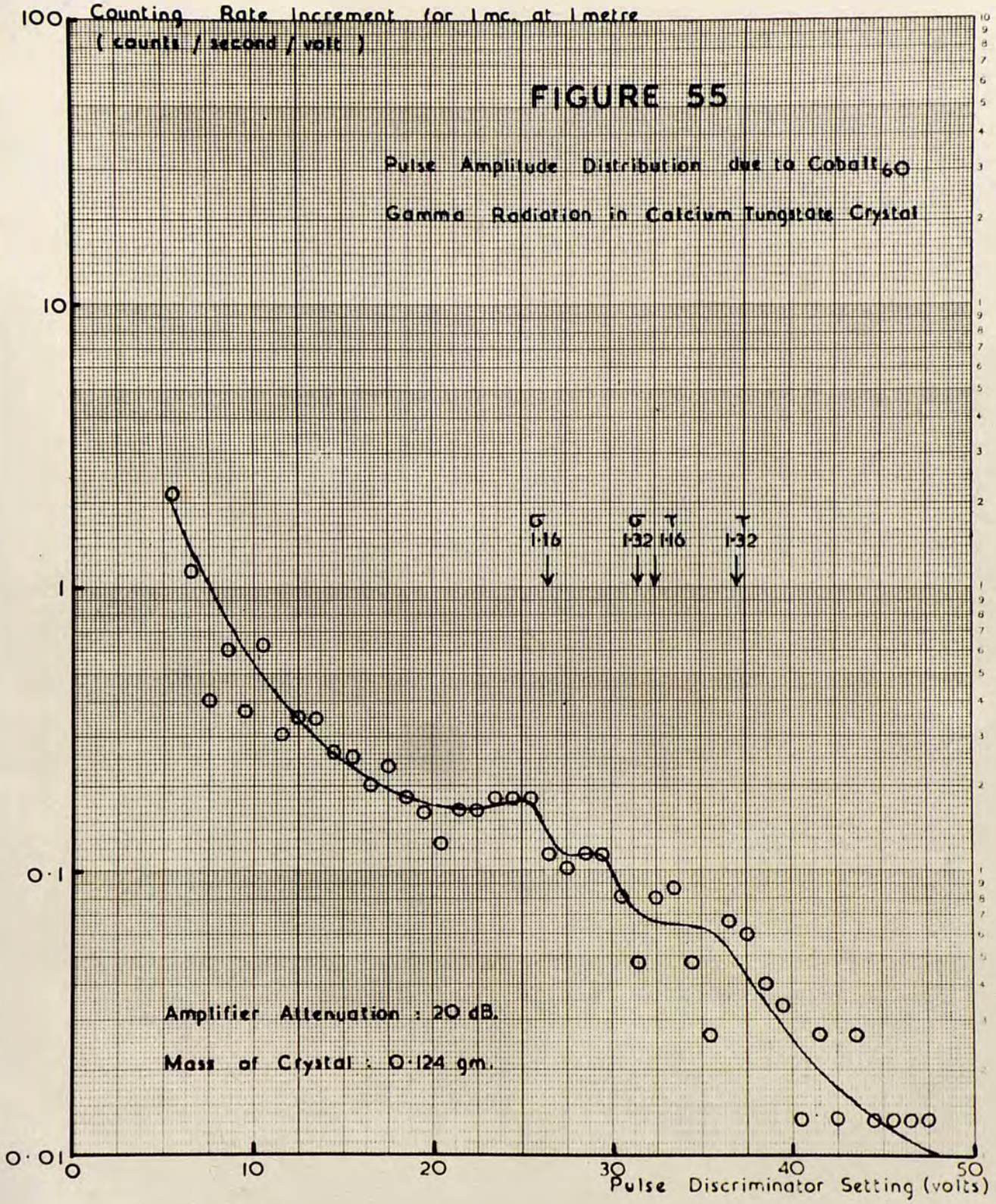

FIGURE 55

Pulse Amplitude Distribution due to Cobalt$_{60}$ Gamma Radiation in Calcium Tungstate Crystal

place of the ratemeter. Unfortunately, such an instrument was not at the time available.

(b) Experimental Results:

A typical distribution, obtained at an amplifier attenuation of 20 dB. (nominal) and ratemeter resolving time of 100 microseconds (nominal) with a small crystal of calcium tungstate of mass 0.124 gms. irradiated by $cobalt_{60}$ gamma-radiation, is shown in figure 55. There is some evidence of discontinuities in the distribution due to the photo-electric absorption and Compton scattering of the two gamma-rays at 1.16 and 1.32 MeV. The arrows give the theoretical positions of the photo-electron peaks and Compton edges calculated from the observed position of the 1.32 MeV. photo-electron peak, assuming a linear relationship between secondary electron energy and pulse amplitude.

Figures 56 and 57 show pulse-amplitude distribution due to $sodium_{24}$ and $iodine_{131}$ gamma-radiation in the same calcium tungstate crystal, the former at an amplifier attenuation of 26 dB. and the latter at 20 dB. The theoretical positions of the peaks and edges indicated on these distributions are also based on the observed position of the 1.32 MeV. peak in the

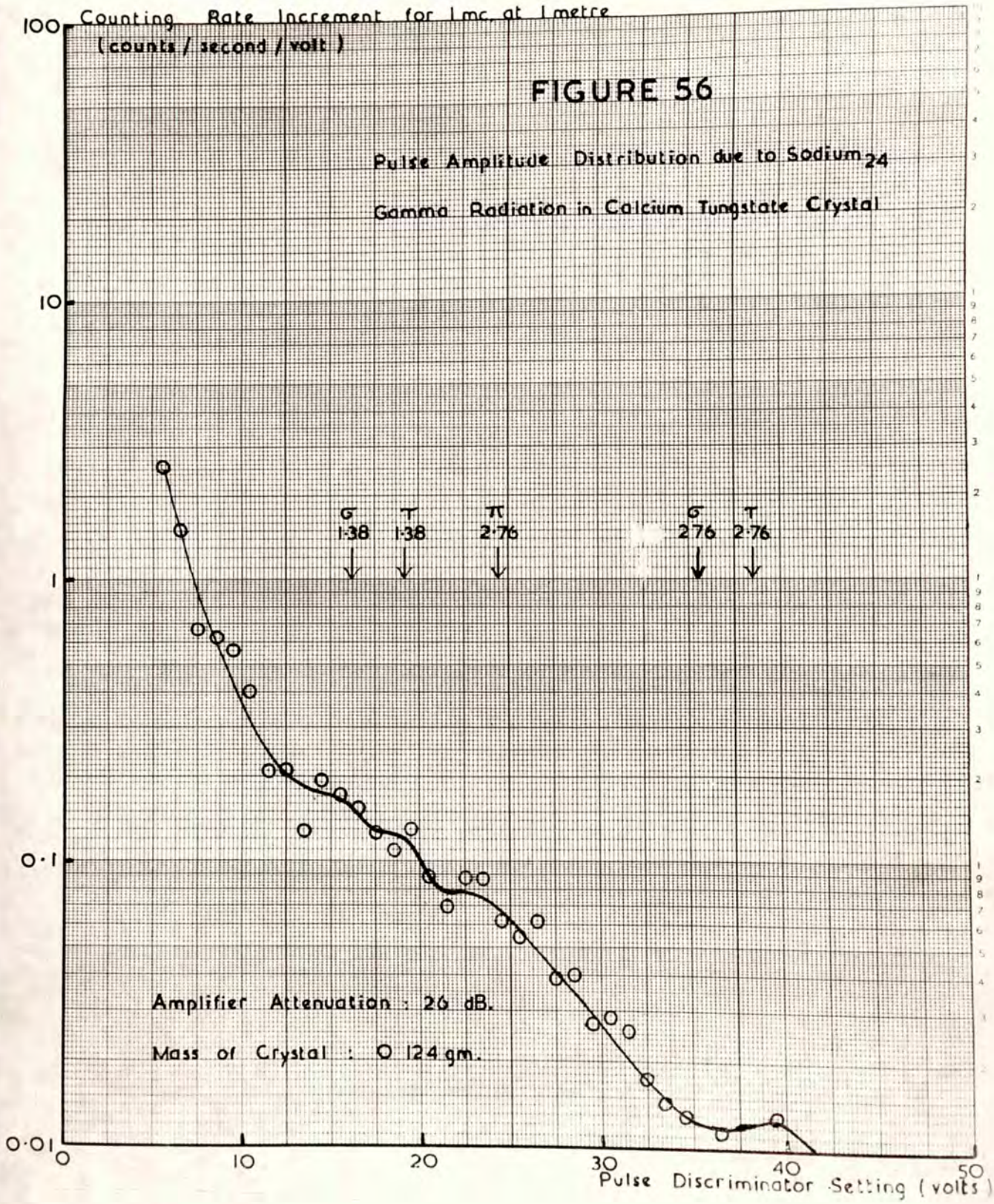

FIGURE 56

Pulse Amplitude Distribution due to Sodium 24 Gamma Radiation in Calcium Tungstate Crystal

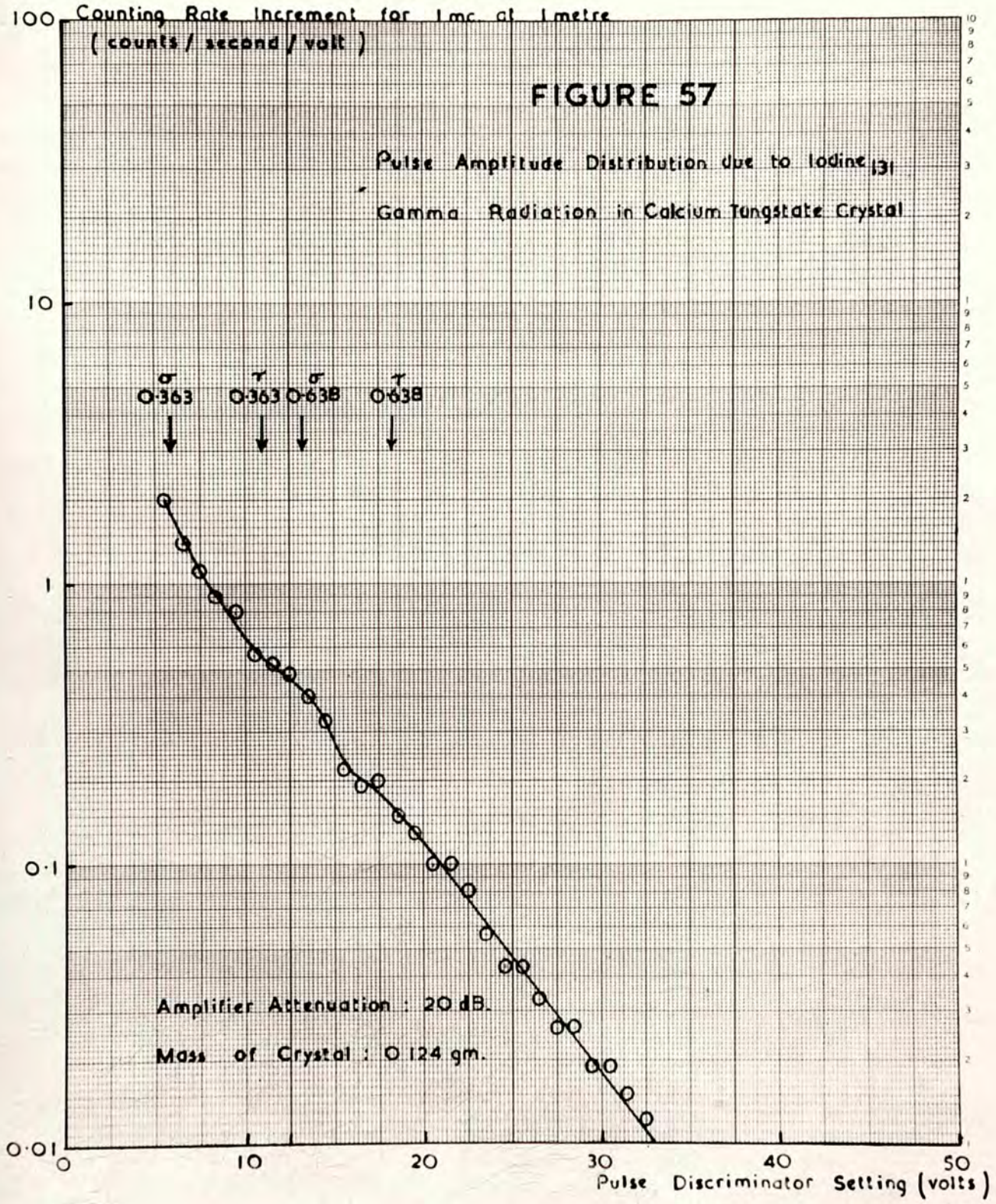

FIGURE 57

Pulse Amplitude Distribution due to Iodine $_{131}$ Gamma Radiation in Calcium Tungstate Crystal

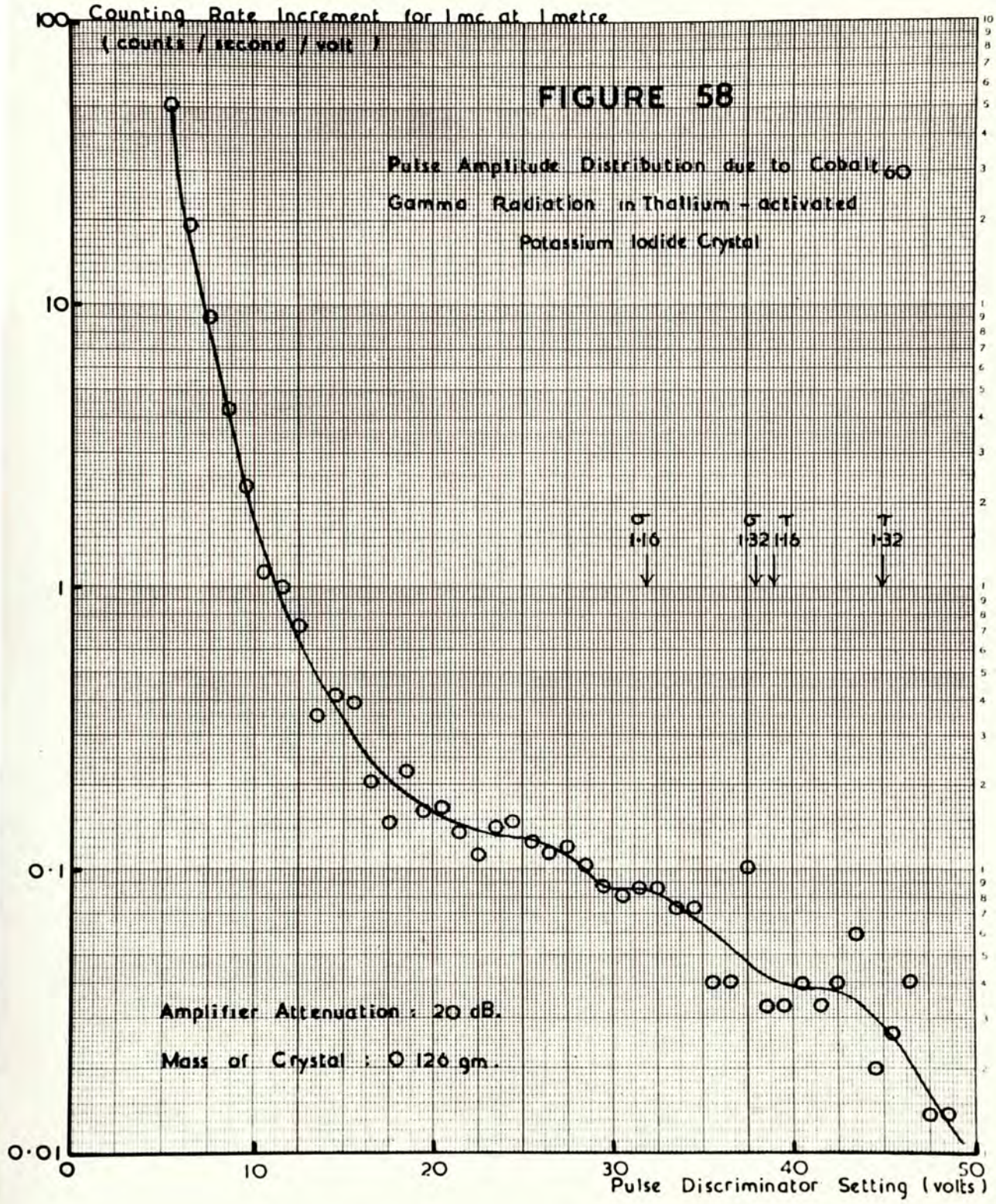

FIGURE 58

Pulse Amplitude Distribution due to Cobalt 60 Gamma Radiation in Thallium - activated Potassium Iodide Crystal

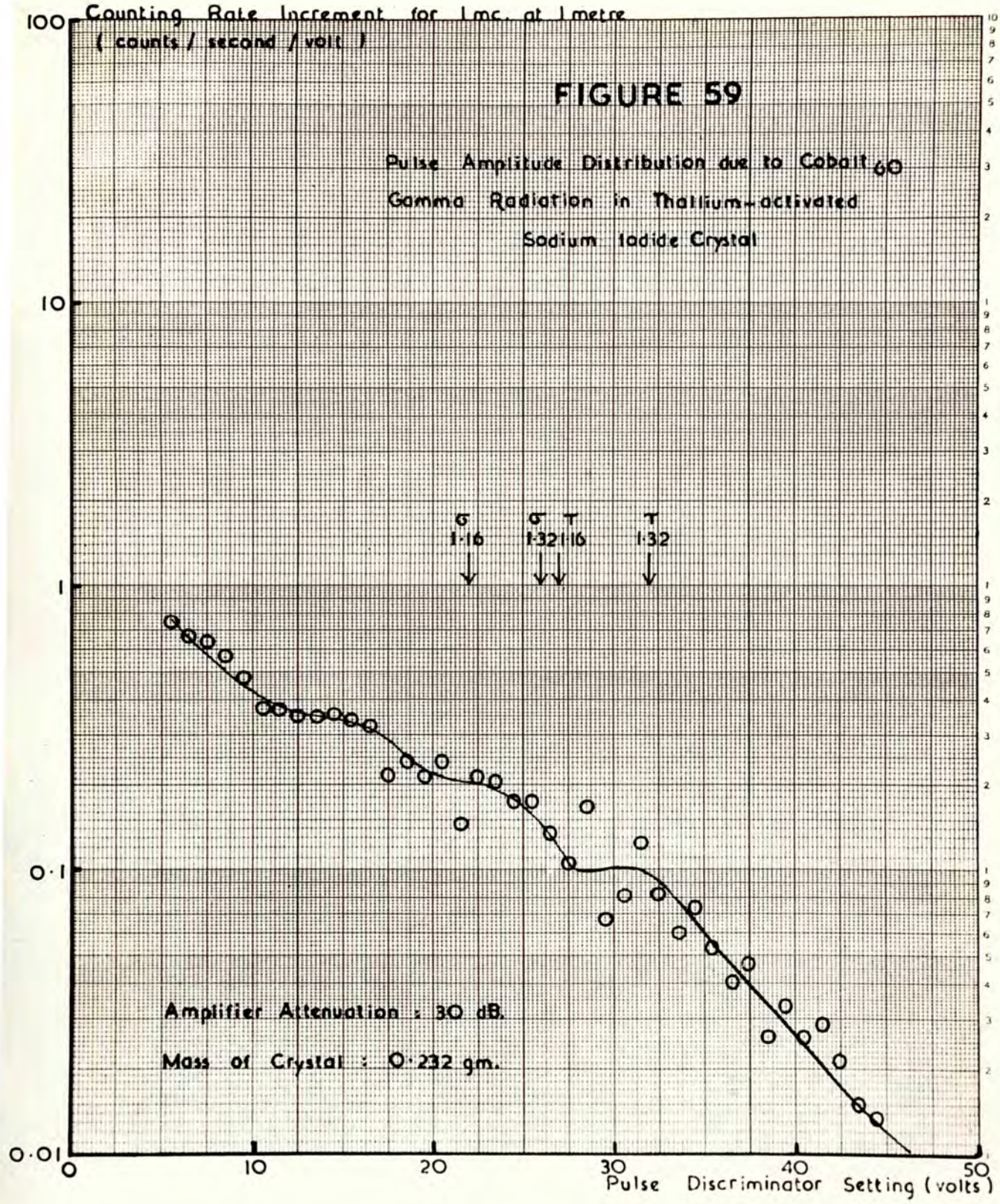

FIGURE 59

Pulse Amplitude Distribution due to Cobalt 60 Gamma Radiation in Thallium-activated Sodium Iodide Crystal

distribution for cobalt$_{60}$. Similar distributions were obtained in crystals of larger size, but the discontinuities were then less easy to observe, probably because of the variation in optical efficiency of the system towards events occurring at different points within the crystal.

In figure 58, is seen the corresponding distribution obtained at an amplifier attenuation of 20 dB. with a 0.126 gm. crystal of thallium-activated potassium iodide exposed to cobalt$_{60}$ gamma-radiation. In this case the phosphorescence of the luminophor produces a sharp rise in the distribution at pulse discriminator settings below 20 volts. A similar distribution for a 0.232 gm. crystal of thallium-activated sodium iodide is shown in figure 59., these measurements being made at an attenuation of 30 dB., because of the higher luminescent efficiency of the crystal.

It is of interest that the gradient of the early portion of these distributions is similar to that due to the photo-multiplier tube stimulated by a low intensity of continuous light (figure 26) confirming the single-photon character of the phosphorescent emission.

(c) Discussion:

It is known from the experimental data of figures 25 and 26 that a single electron arriving at the first dynode of the photo-multiplier produces a pulse of 17 volts amplitude at an amplifier attenuation of 10 dB. From the observed position of the 1.32 MeV. photo-electron peak in figure 55 it can be deduced that a 1 MeV. photo-electron released in the crystal causes the arrival at the first dynode of approximately 5.2 electrons. A comparison of the general form of the distribution with those of figure 11 supports this deduction.

It is apparent that for gamma-ray spectroscopy with the scintillation counter, a considerably higher optical efficiency is required than is realised in the experimental arrangement used here. This is difficult to achieve with the type I P 21 photo-multiplier tube. Using an R.C.A. type 5819 photo-multiplier, which has the photo-sensitive surface deposited on the glass envelope, permitting an highly efficient optical coupling with the crystal, and a thallium-activated sodium iodide luminophor backed by a reflector, Hofstadter and MacIntyre

(1950 a, b, c, d, e, f.) have recently obtained distributions analogous to the curve of figure 11 for $(m_1 \cdot m_2 \cdot m_3 \cdot m_4) = 1000$. Using this system they have been able successfully to analyse the gamma-spectra of many radio-isotopes. Johannson (1950 a, b.), has obtained distributions similar to those of the author, using a type I P 21 tube in conjunction with a thallium-activated sodium iodide crystal.

From the data of figures 55 - 59, it is possible to assess the relative efficiencies of the various luminophors used. The values of Table XVII are based on the observed positions of the 1.32 MeV. photo-electron peak due to cobalt$_{60}$ gamma-radiation, having due regard for the different levels of amplifier attenuation used, calcium tungstate being taken as unity. No correction has been made for the response of the photo-multiplier cathode.

Table XVII

Relative Efficiencies of Crystalline Luminophors.

Calcium Tungstate	1.0
Potassium Iodide/Thallium	1.2
Sodium Iodide/Thallium	1.7

An approximate estimate of the absolute efficiency of the various luminophors used can be made as follows: The cathode of the I P 21 photo-multiplier has an area of 1.9 cm^2 (Morton and Mitchell 1948), and the distance from the mid-point of the crystal to the photo-sensitive surface in the arrangement used was approximately 1 cm. Assuming a uniform emission of light in all directions from the crystal, the optical efficiency (m_2), was thus approximately 0.1. The mean quantum efficiency (m_3), of the photo-cathode of the type I P 21 tube over the range of visible light concerned is also approximately 0.1. The factor (m_4), has already been shown to be 0.66, where the whole of the photo-cathode is illuminated (figure 35). Hence for a 1 MeV. secondary electron in thallium-activated sodium iodide:

$$m_1 \cdot 0{\cdot}1 \cdot 0{\cdot}1 \cdot 0{\cdot}66 = 5{\cdot}1 \cdot 1{\cdot}7$$

$$m_1 \simeq 1500$$

This value may be compared with the figure quoted by Hofstadter and MacIntyre (1950 d, e.) of approximately 1000 photo-electrons released at the photo-cathode of a type 5819 photo-multiplier by the

scintillation due to a 1 MeV. secondary electron in thallium-activated sodium iodide. The optical efficiency of the system used by these workers was said to be near to unity. Hence, assuming a mean quantum efficiency for the type 5819 tube of 0.1 also, their results indicate a photon yield (m_1) in the luminophor of 10,000 due to a 1 MeV. secondary electron. The apparent disagreement in these two results can be explained in part by the improved response of the type 5819 tube, but derives more from the assumption made on page 147 that light is emitted uniformly in all directions from the crystal. Owing to internal reflection and refraction effects, a considerable fraction of the photons produced in the crystal may fail to escape from it, and this effect will reduce the effective optical efficiency of the system.

Because of the difficulty in designing a system of high optical efficiency with the type I P 21 photo-multiplier, these studies were discontinued until tubes of improved design became available.

5. MEASUREMENT OF VARIATION OF EFFICIENCY WITH TEMPERATURE IN CRYSTALLINE LUMINOPHORS:

(a) Method of Measurement:

The experimental arrangements just described for the investigation of pulse amplitude distributions could also be used to investigate the temperature characteristics of the efficiencies of crystalline luminophors. A crystal of the luminophor to be studied was mounted inside the photo-multiplier case, and irradiated by a constant flux of gamma-radiation from a cobalt$_{60}$ source. An integral curve of counting rate as a function of pulse discriminator setting was plotted in the manner already described. The pulse discrimination control of the ratemeter was then set at a level at which the photo-multiplier background was small but the counting rate due to the crystal still large, and cooling with liquid nitrogen commenced. The observed counting rate either increased or decreased as cooling progressed, according as the temperature characteristic was negative or positive. From the curve of counting rate against pulse discriminator setting already plotted, the effect of cooling on pulse amplitude could be deduced. By repeating the procedure in the absence of any crystal, the

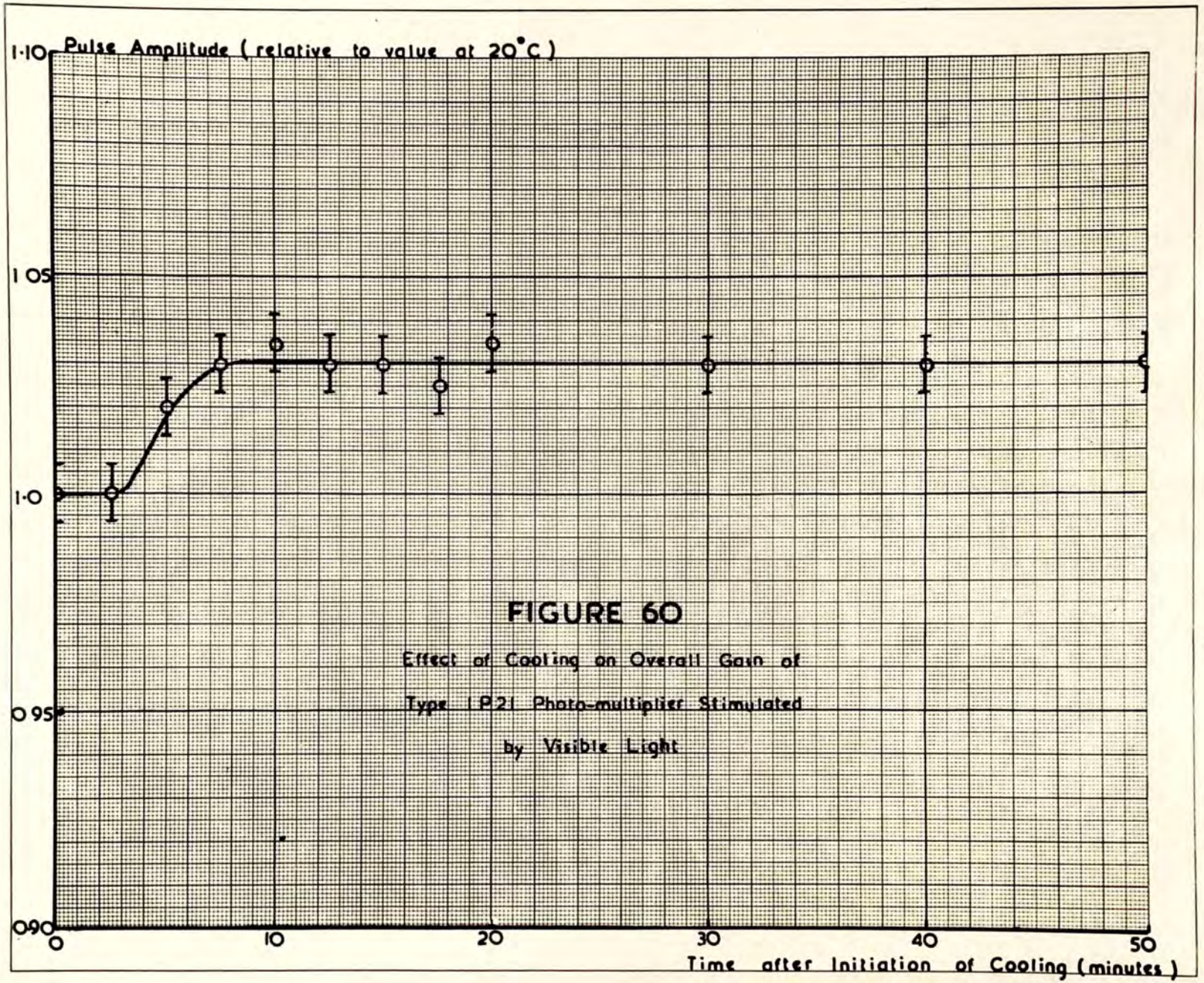

FIGURE 60

Effect of Cooling on Overall Gain of Type IP21 Photo-multiplier Stimulated by Visible Light

appropriate correction for background effects could be deduced. Similar measurements could be made with the photo-multiplier stimulated with continuous light, using the pinhole collimator and light guide assembly in the manner described on page 101.

(b) Experimental Results and Discussion:

Figure 60 shows the effect of cooling on the amplitude of the pulses produced by single photons incident upon the cathode of the photo-multiplier. The light source was a white cardboard diffuser placed on the axis of the collimator and illumined by a 40 watt incandescent light bulb several metres distant; an Ilford "Spectrum Blue" filter was interposed between source and collimator. The pulse amplitude at room temperature is taken as unity, and appropriate corrections made for the reduction in photo-multiplier background on cooling.

There is seen to be a rapid rise of some 4% in pulse amplitude shortly after the commencement of cooling. The magnitude of this effect, and its early occurrence, suggest that it is not due to changes in the photo-multiplier temperature but

rather to the change in resistamce on cooling of the load resistor (R 11 in figure 16) which is located inside the photo-multiplier mounting. Support for this explanation is given by the fact that the photo-multiplier background has not changed significantly after ten minutes cooling, whereas the effect under discussion is by that time almost complete. The temperature coefficient of resistivity of cracked carbon is stated to be of the order of - 0.0004 per ^{o}C., so that a change in temperature of 100^{o} C. would produce an effect of the order of magnitude required.

The fact that no significant change in pulse amplitude occurs on further cooling after this effect is complete indicates that the temperature coefficients of the photo-cathode quantum efficiency (m_3) and inter-stage gain (R) are either negligibly small, or act in opposite senses.

Figure 61 shows similar curves for the effect of cooling on pulse amplitude for each of the four luminophors studied - calcium tungstate, anthracene, and thallium-activated potassium and sodium iodides - excited by cobalt$_{60}$ gamma-radiation. In deriving

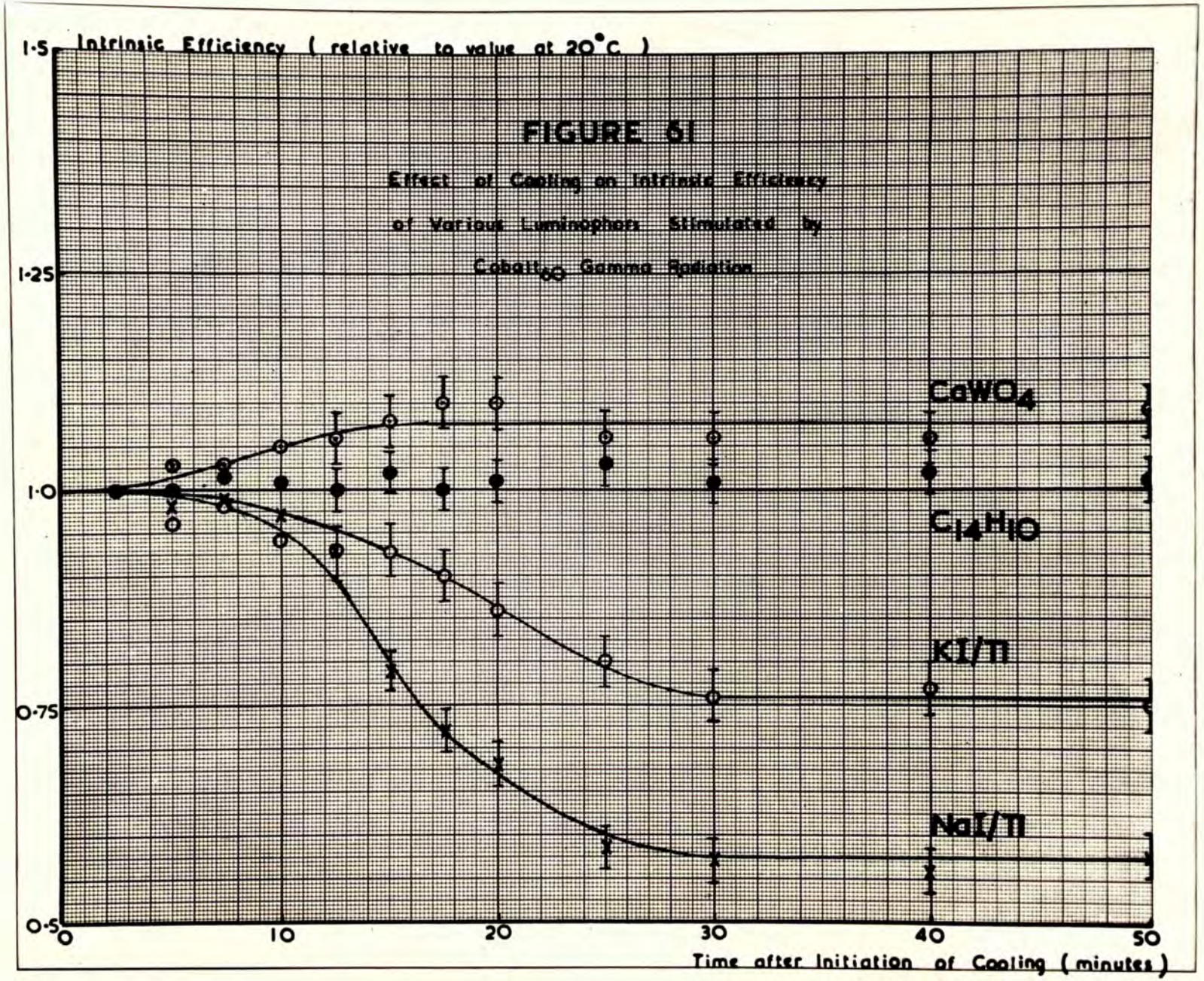

FIGURE 61

Effect of Cooling on Intrinsic Efficiency of Various Luminophors Stimulated by $Cobalt_{60}$ Gamma Radiation

the curves of relative amplitude, a correction has been included for the effect of cooling on the photo-multiplier load resistor, the observed values of relative amplitude, corrected for background effects, being divided by the appropriate ordinates of figure 60.

It will be seen that the pulses obtained in calcium tungstate increase slightly in amplitude on cooling to liquid nitrogen temperature, those in anthracene remain constant within the limits of experimental error, while those in the thallium-activated alkali-halides fall rapidly. These observations are in agreement with the theoretical predictions of Krőger (1948) regarding pure and impurity-activated luminophors. In pure luminophors, a fall in temperature is accompanied by a reduction in thermal quenching of excited centres and so by an increase in luminescent efficiency. In impurity -activated systems however, this is accompanied by a reduced rate of release of electrons from trapping sites and so by a reduction in efficiency.

The results for calcium tungstate are also in good agreement with experimental observations reported by the same author (Krőger 1948). Published data do not appear to be available for the effect of cooling on the efficiency of the other luminophors studied.

It is clear from these results that the efficiency of a scintillation counter utilising a calcium tungstate or anthracene crystal will be but slightly affected if the crystal be cooled. On the other hand, the cooling of crystals of the alkali-halide type is definitely contra-indicated, and where such crystals are used and it is desired to cool the photo-multiplier, a light guide must be used.

6. MEASUREMENT OF SPECTRAL DISTRIBUTION OF LIGHT EMITTED BY CRYSTALLINE LUMINOPHORS.

(a) Method of Measurement:

The spectral distributions of the light emitted under gamma-radiation by the crystalline luminophors studied were examined by means of a Zeiss medium dispersion quartz spectrograph. The low intensity

of the emitted light necessitated a long exposure (of the order of 14 days) with the slit of the spectrograph wide open. The technique adopted for these measurements was as follows:- The spectrograph was set up in a well tested dark room. The largest available crystal of the luminophor to be studied was mounted in close proximity to the wide open slit of the instrument, and a disc source of cobalt ^{60} of strength 1.5 millicuries approximately, was placed behind and almost in contact with the crystal. The plate was then exposed for the required period, after which the source and crystal were removed and mercury discharge reference spectra recorded on either side of the luminophor spectrum. The plate was then developed in the usual manner.

Control exposures in the absence of any crystal showed that the direct effect of gamma-radiation on the plate was negligible, as also was the luminescence produced in the quartz lenses and prisms by the radiation. Only one luminophor spectrum was recorded on each plate.

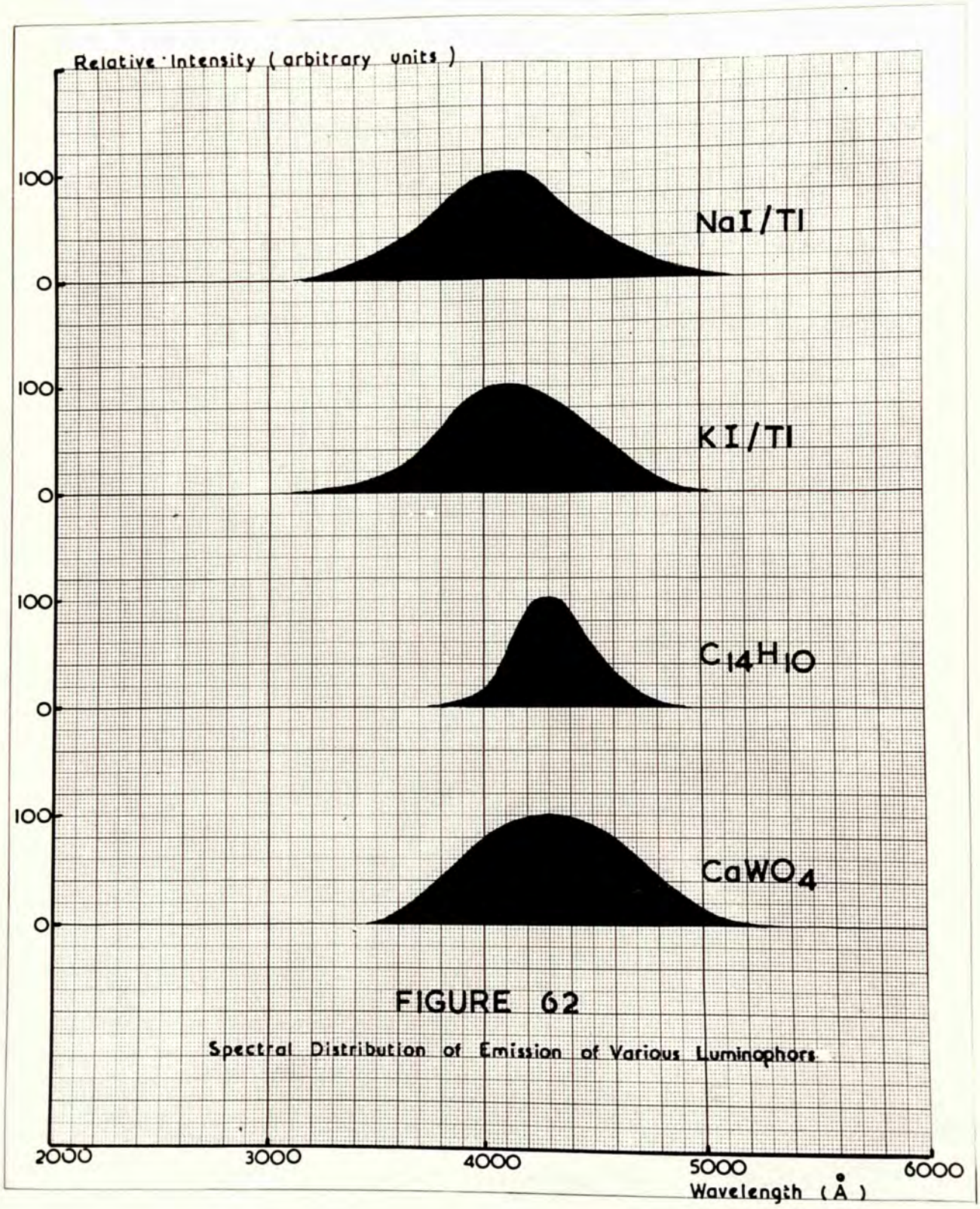

FIGURE 62

Spectral Distribution of Emission of Various Luminophors

The spectra were examined with a micro-densitometer, and the blackening plotted as a function of wavelength. Because of the difficulty in estimating the radiation flux through the crystal, it was not possible to make absolute measurements of intensity of emission. The distributions were therefore plotted on an arbitrary scale, taking the peak intensity of emission as 100 in each case.

(b) Experimental Results and Discussion:

Results are shown in figure 62 for the four luminophors studied. It will be seen that calcium tungstate and anthracene emit almost entirely in the visible region, but that the emission of the alkali-halide luminophors extends into the near ultra-violet. Only in the case of the latter luminophors therefore, would any advantage be gained from the use of a photo-multiplier tube with a quartz envelope.

The form of the distributions for calcium tungstate and anthracene agree well with those already reported by Kröger (1948) and Garlick (1949). Spectral distributions for thallium-activated potassium and sodium

iodide have not been published, but Hofstadter has reported that the distributions of these luminophors show maxima at 4100 Å (see Table II).

7. COMPARATIVE STUDIES ON LUMINESCENCE INDUCED IN LIQUID LUMINOPHORS BY GAMMA-RADIATION.

(a) Introduction:

One of the limiting factors in the design of practical scintillation counters is the difficulty in growing large single crystals of luminophors. For this reason, the possibility of using a liquid luminescent medium contained in a cell of the required dimensions has been considered by many workers. Following the report by Ageno, Chiozzotto and Querzoli (1950) that solutions of naphthalene in xylene solution irradiated by gamma-quanta showed a weak luminescence many such systems have been investigated. Reynolds et al (1950) showed that p-terphenyl in xylene solution had a luminescent efficiency one half that of crystalline anthracene. In a comprehensive series of investigations, Kallmann and Furst (1950) compared the effects observed in a

very large number of solutions of organic compounds, pointing out that the emission of light in such systems could only be explained by a transport of excitation energy between the solvent molecules and those of the fluorescent substance.

In experiments similar to those of Kallmann and Furst, a large number of liquid systems was also examined by the author for luminescence under gamma-irradiation. The results of these experiments are reported below.

(b) Methods of Measurement:

The experimental arrangement adopted for these investigations was that shown in figure 13 (inset C). The uncooled photo-multiplier tube was mounted horizontally, and a thin cylindrical glass phial, 5 cm. long and 1.5 cm. in diameter, containing a 1 ml. sample of the liquid to be tested was introduced into the side tube. The latter was closed by a light tight cap, on top of which was placed a metal disc source of $cobalt_{60}$, containing approximately 1.5 millicuries of activity. The photo-multiplier

inter-dynode potential was 108 volts. The amplifier was operated at an attenuation of 20 dB. Counting rates were obaerved in the ratemeter, the pulse discriminator control being set at 10 volts and the resolving time at 100 microseconds.

A "figure of merit" was assigned to each liquid tested this being the counting rate in counts/second observed with a 1 ml. sample measured in the manner described above, and corrected for counting losses in the ratemeter and for background effects in the glass phial and the photo-multiplier. Since it was the number of scintillations per second, and not the total intensity of emitted light which was measured, this "figure of merit" was not necessarily linearly proportional to the luminescent efficiency of the medium, the relationship between these two quantities depending on the form of the curve of counting rate as a function of pulse amplitude.

The measurements expended over a period of no more than six weeks; no corrections were thus necessary for radio-active decay of the cobalt$_{60}$ source, the activity of which changed by less than 1.5% during this period.

(c) Experimental Results:

All the pure liquids studied, including pure distilled water, showed a slight but measureable luminescence under gamma-irradiation. The magnitude of this effect varied only slightly over a wide range of colourless liquids, and could not easily be related to their chemical constitution and physical properties. Table XVIII lists experimental values for the figures of merit of a number of these pure solvents.

Table XVIII

Figures of Merit of Pure Liquids.

Liquid	Figure of Merit.
Benzene	910
Xylene	910
Water (distilled)	620
Water + sodium carbonate (10 gm/litre)	640
Di-ethyl ether	430
Acetone	420

The behaviour of organic luminophors in solution was found to be very strongly influenced by the choice of solvent. This is well illustrated by the experimental results shown in figure 63, where the figures of merit of solutions of p -terphenyl in

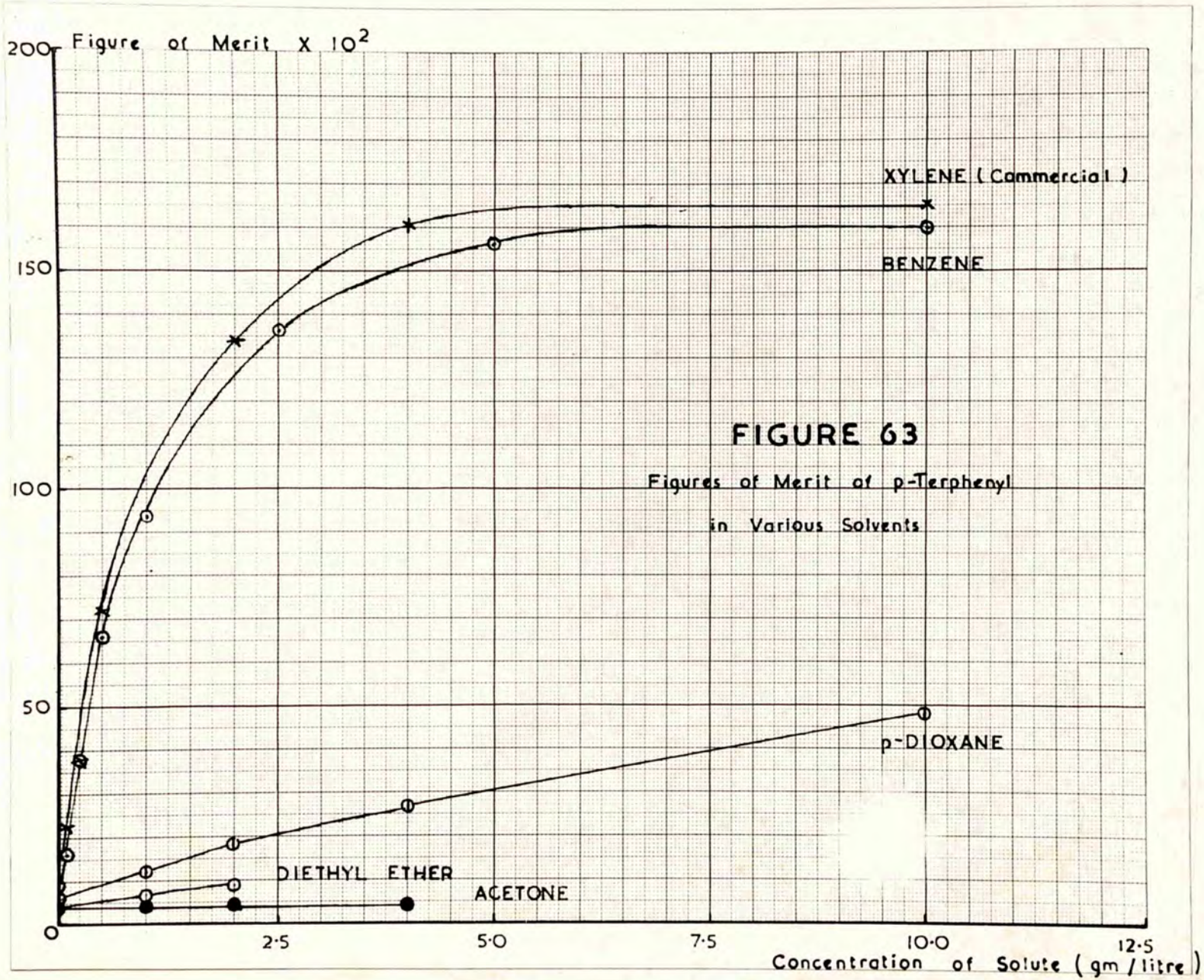

FIGURE 63

Figures of Merit of p-Terphenyl in Various Solvents

various solvents are plotted as a function of concentration of solute. There is seen to be little difference in behaviour between solutions of this substance in benzene or xylene. In p-dioxane however, the figure of merit is considerably reduced; while in diethyl-ether the luminescence is almost completely suppressed. In acetone solution, there is no evidence whatever of luminescent emission due to p-terphenyl.

For comparative studies of various luminophors, benzene was chosen as solvent, firstly because solubilities were in general greater in this liquid than in toluene or xylene, and secondly because it was readily available in a highly purified state. "ANALAR" thiophene-free benzene was used throughout these studies, although no significant change in the observed figures of merit resulted from the use of the "crystallisable" grade of the solvent. Results in xylene solution, on the other hand, were found to be greatly influenced by the isomeric composition and state of purity of the solvent.

The relationship between figure of merit and concentration of solute was studied for a large

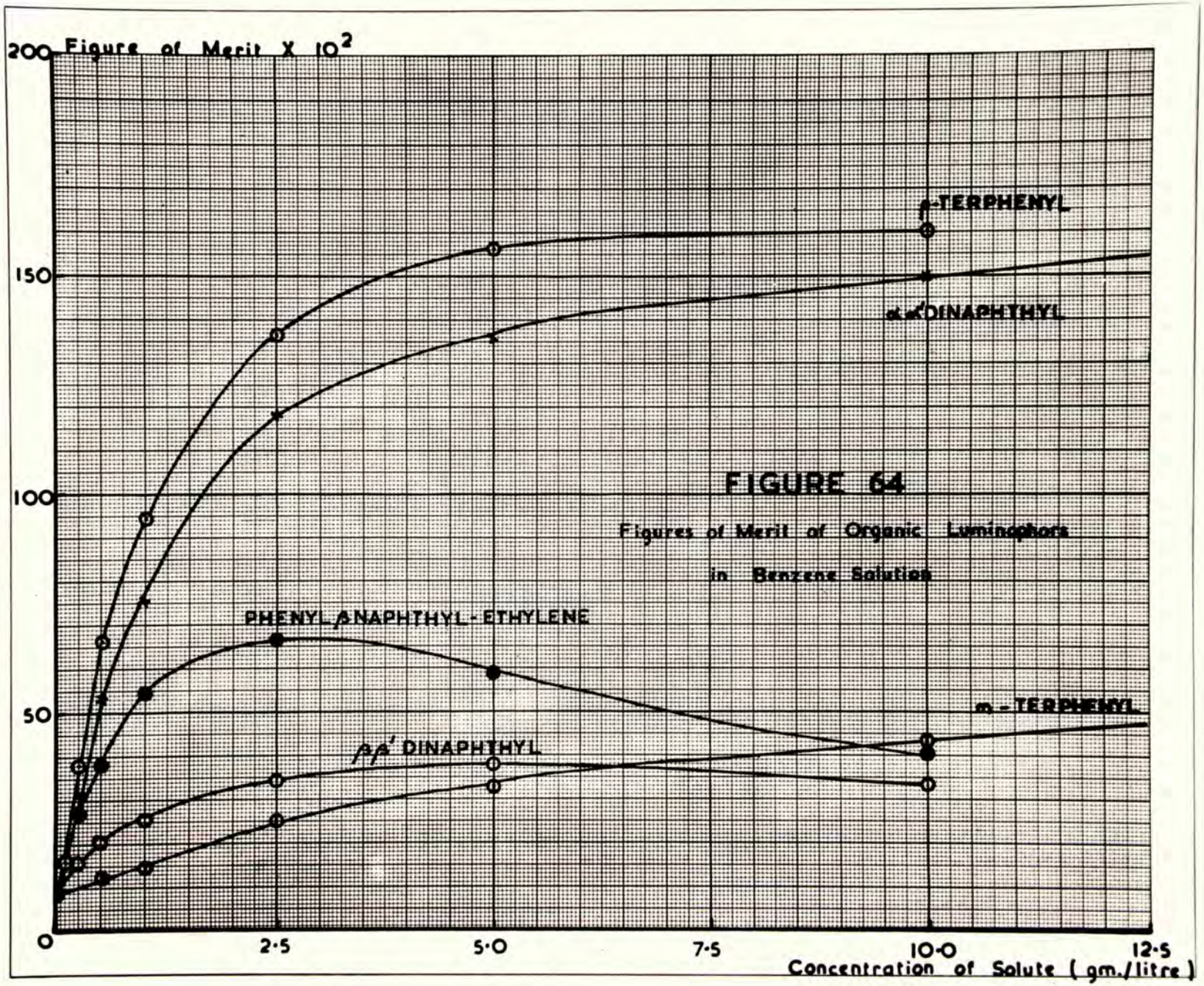

FIGURE 64

Figures of Merit of Organic Luminophors in Benzene Solution

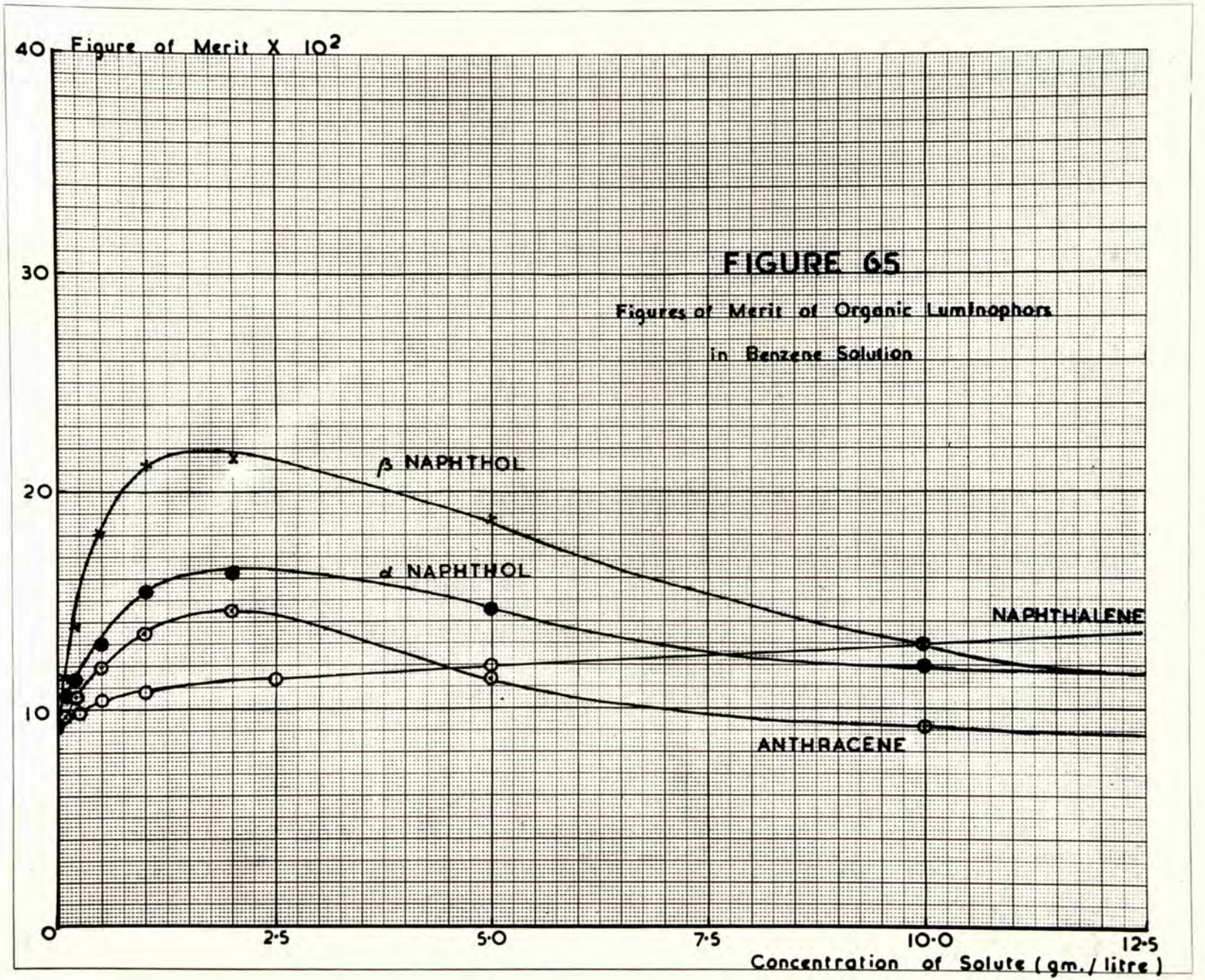

FIGURE 65

Figures of Merit of Organic Luminophors in Benzene Solution

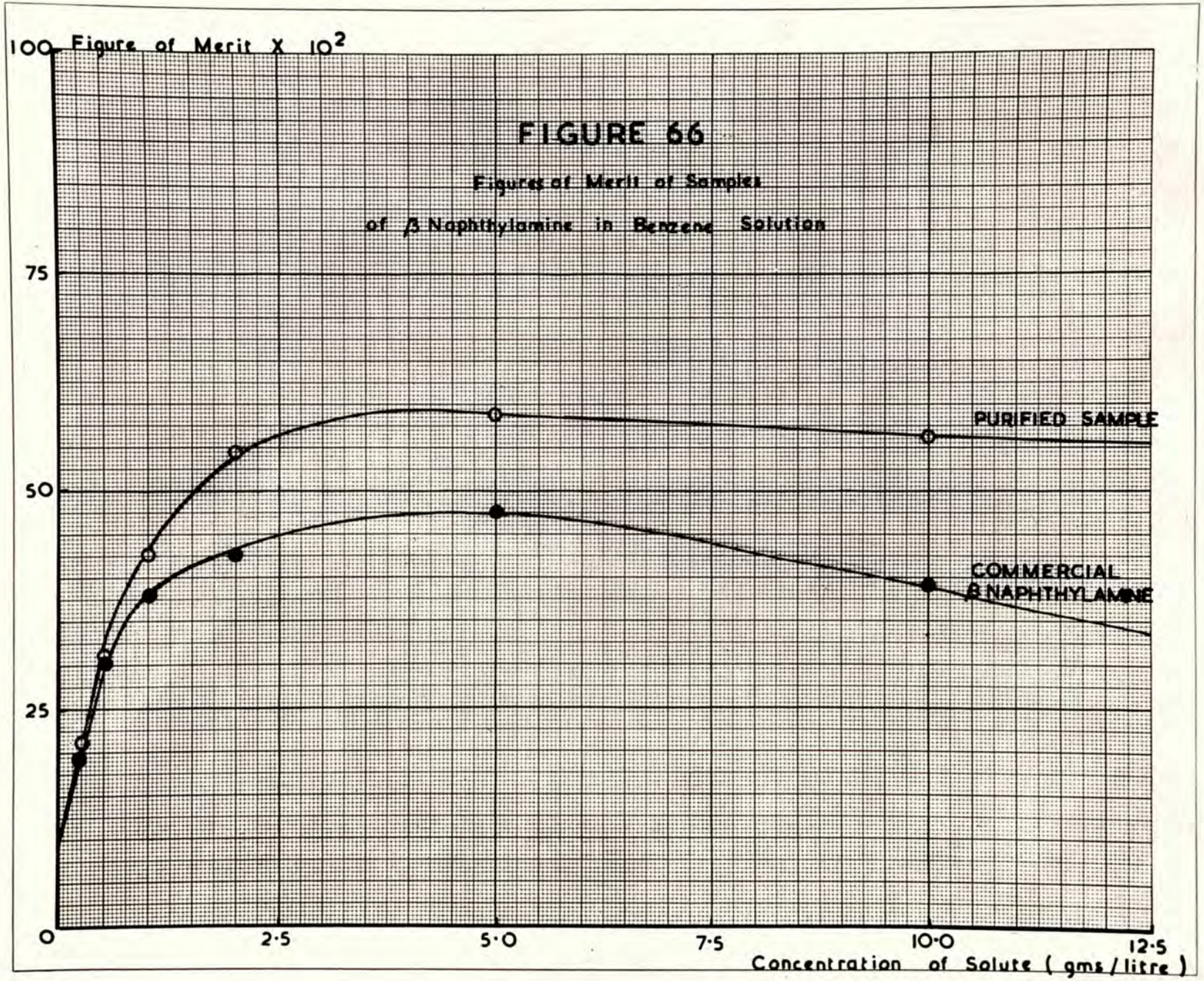

FIGURE 66

Figures of Merit of Samples

of β Naphthylamine in Benzene Solution

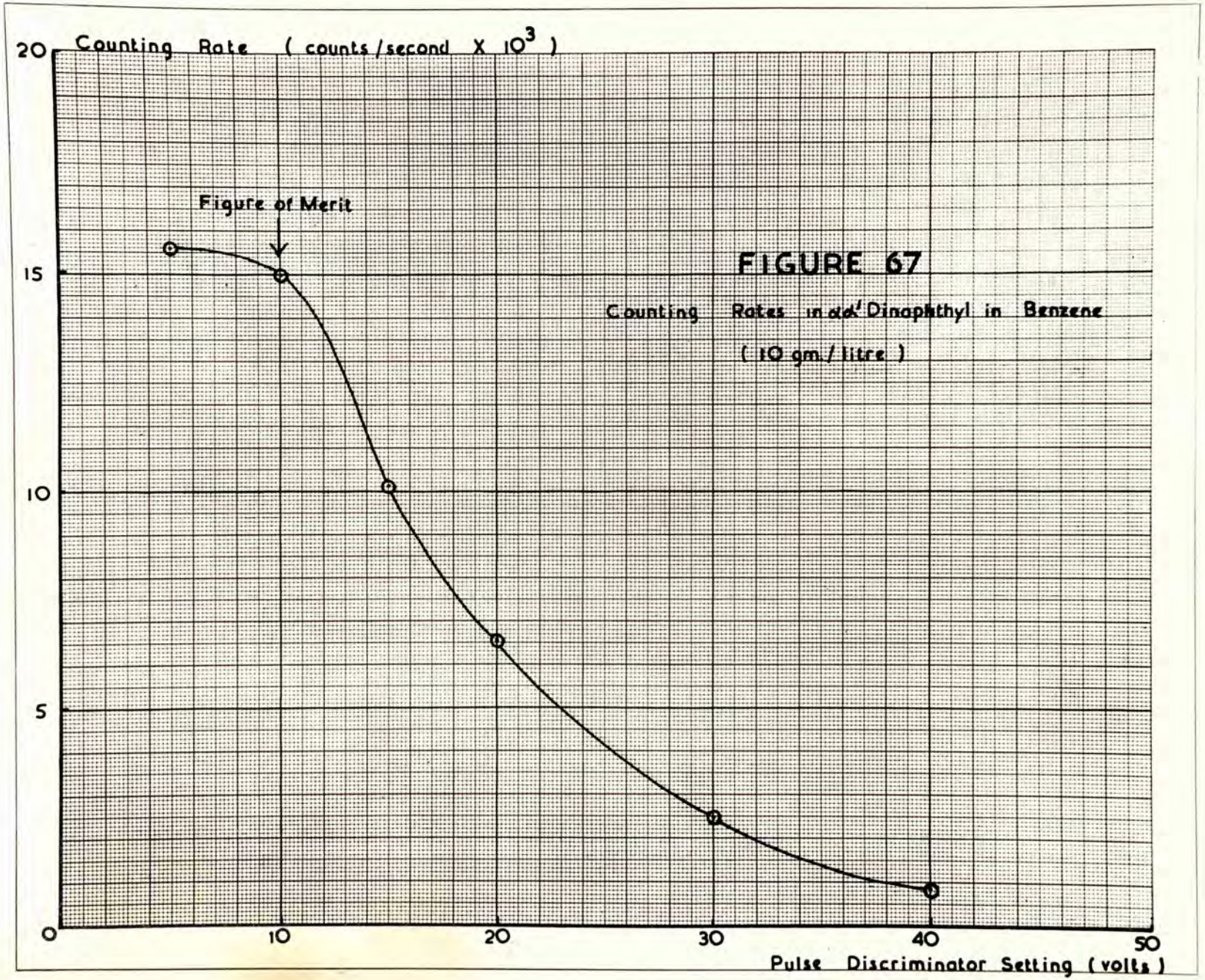

FIGURE 67

Counting Rates in $\alpha\alpha'$ Dinaphthyl in Benzene

(10 gm. / litre)

number of organic luminophors in benzene solution. Some results typical of these studies are summarised in figures 64, 65 and 66. The substances studied could be divided into two groups according to behaviour. In the first, exemplified by naphthalene, m -terphenyl, p -terphenyl, and αα'-dinaphthyl, the figures of merit increased continuously up to the saturation concentration of the solute. In the second, exemplified by anthracene, α - and β -naphthol, and α - and β -naphthylamine, the figures of merit rose initially, but passed through a maximum at an optimum concentration of solute, falling at higher concentrations. It will be observed that the unsubstituted aromatic hydrocarbons studied, with the exception of anthracene, fall into the first group, whereas compounds with a substituent group in the aromatic nucleus are classified in the second.

But the experimental results show that the variation of figure of merit with concentration may be profoundly influenced by the degree of purity of the solute. This is well shown by the data of figure 66, in which the curve of figure of merit as a function of concentration for a commercial sample

of β-naphthylamine is compared with that for a highly purified sample of the compound. In view of these results, all the luminophors studied, regardless of their origin, were first purified by a single recrystallisation from benzene; if this process produced a significant change in the observed figure of merit for a saturated solution, a second recrystallisation from benzene was carried out.

Table XIX summarises the behaviour of some of the systems investigated. The highest efficiency was obtained from a saturated solution of $\alpha\alpha'$-dinaphthyl in benzene; such a solution has a figure of merit rather higher than that of p-terphenyl in xylene or in benzene, the best system previously reported. More recent experiments have shown that by the use of ternary systems incorporating $\alpha\alpha'$-dinaphthyl, still higher figures of merit may be realised.

The use of $\alpha\alpha'$-dinaphthyl in solution as a luminophor for scintillation counters does not appear to have been reported elsewhere, although Prichotko and Shabaldas (1941) have studied the emission spectrum of this compound under ultra-violet excitation.

Table XIX

Figures of Merit of Liquid Luminophors.

System	Optimum Concentration of solute (gm./litre)	Figure of merit at optimum concentration.
αα'-Dinaphthyl/benzene	Saturation	16,400
p -Terphenyl/benzene	Saturation	15,600
m -Terphenyl/benzene	Saturation	9,400
Phenyl -naphthylethylene/ benzene	2.7	6,700
β -Naphthylamine/benzene	5.0	5,950
α -Naphthylamine/benzene	2.8	5,050
ββ'-Dinaphthyl/benzene	6.0	3,900
ββ' -Dinaphthylethane/ benzene	Saturation	3,200
1.3.5. Triphenylbenzene/ benzene	Saturation	2,500
β -Naphthol/benzene	1.5	2,200
α -Naphthol/benzene	2.5	1,700
Naphthalene/benzene	Saturation	1,460
Anthracene/benzene	2.2	1,460

(d) Discussion:

The experimental results for pure liquids are similar to those of Kallmann and Furst (1950).

These workers attributed the observed effects to the presence of very small amounts of fluorescent materials present in the liquids as impurities. Their hypothesis would seem, however, to be invalidated by the observation that the figure of merit is of the same order for a wide range of colourless liquids, and is not significantly affected by progressive purification (for example, in water or in benzene).

Studies to be described in a later sub-section (sub-section IV.9) suggest that these effects may be satisfactorily explained in terms of the Čerenkov effect, and are therefore dependent neither on the chemical composition of the liquids nor on their physical properties, except density and transmissibility to light.

The results for solutions of organic luminophors are in general agreement with those of Ageno, Chiozzotto and Querzoli (1949), Reynolds et al. (1950), and Kallmann and Furst (1950), taking into account the different experimental arrangements used. It

is of interest, however, to record that Kallmann and Furst observed maxima in the curves of relative intensity of emitted light as a function of concentration of solute, for all the systems which they studied, including naphthalene in benzene (maximum at 3 gms./litre), naphthalene in xylene (maximum at 12 gms./litre), and p-terphenyl in benzene (maximum at 4.5 gms./litre). These observations are contrary to those of the author which indicate a continuous increase in figure of merit up to saturation concentration of these systems. Ageno et al. (1950) also report a continuous increase in luminescent intensity for naphthalene in xylene.

The theoretical interpretation of the observed variation in luminescent efficiency with concentration of solute has been discussed in detail by Kallmann and Furst (1950). They showed that their experimental results could be explained qualitatively in terms of the following competitive processes:-

(i) Absorption of incident energy in solvent molecules with the production of excited solvent molecules.

(ii) Quenching of excitation energy of solvent molecules by conversion into heat.

(iii) Transport of excitation energy from solvent to solute molecules.

(iv) Quenching of excitation energy of solute molecules by internal conversion or by interaction with solvent, (described as "internal quenching".)

(v) Quenching of excitation energy of solute molecules by interaction with other solute molecules, or with molecules of impurities present in the solute, (described as "self-quenching".)

(vi) Emission of light by solute molecules.

At high concentrations of solute, a seventh process must also be considered, in addition to process (iii) as a source of excited solute molecules:-

(vii) Absorption of incident energy in solute molecules.

Only in the case of processes (iii) and (v) does the probability of the reaction depend on the concentration of the solute. The quenching processes (iv) and (v) may occur in two quite distinct ways. Firstly, there may be a direct transfer of energy from the excited molecule to a quenching molecule in its immediate vicinity. Theprobability of such a

transfer occurring will not be greatly dependent on the volume of the liquid and shape of the containing vessel. Secondly, light may be emitted by the excited molecule only to be reabsorbed by a quenching molecule which may be far removed from the original excited molecule. This process may be profoundly influenced by the shape and size of the system.

On this theory, the initial sharp rise in luminescent efficiency with concentration is explained by the dominance of process (iii); in this region, the curve of efficiency as a function of concentration should be linear. At medium solute concentrations, the efficiency tends towards a maximum value, which is reached when all the available energy in the solvent is being transported to solute molecules. At still higher concentrations, self-quenching effects become important, and cause the luminescent efficiency to fall.

Because of the discrepancy referred to above between the experimental results of Kallmann and Furst and those of Ageno et al. and of the author it

is of interest to consider these self-quenching effects in greater detail. Two explanations are suggested. The first is the possible use by Kallmann and Furst of samples of luminophors containing small amounts of impurities. The second, and more probable, explanation arises from the fact that these workers used a type I P 28 photo-multiplier as detector, whereas Ageno et al. and the author used a type I P 21 tube. Since the former is sensitive to radiation in the near ultra-violet, while the latter is not so, the observed effects could be explained in terms of the self-quenching of light emitted in this portion of the spectrum. In other words, light emitted in this spectral region may be reabsorbed by other solute molecules, the importance of the effect increasing with concentration. As both naphthalene and p-terphenyl are known to emit in the ultra-violet, there is good reason to accept this explanation, and in the case of naphthalene further evidence in its support may be adduced from the published data of Pringsheim (1949). Pringsheim shows that the emission of naphthalene in solution

extends from 3000 - 3650 Å, whereas the long wave limit of its absorption spectrum is at 3300 Å approximately.

Without giving a detailed account of the precise mechanisms by which the processes of energy transport, quenching, and emission take place, a theoretical analysis of the data of figures 64 - 66 is possible in terms of a general theory of luminescent emission recently developed by Johnson and Williams (1950a). These workers showed that the luminescent efficiency η of any system either solid or liquid, consisting of emission centres randomly distributed in a matrix could be represented by an expression of the form:-

$$\eta \propto \frac{c(1-c)^z}{\left[c + \frac{\sigma}{\sigma'}(1-c)\right]} \qquad 4.7.$$

where c is the molecular concentration of emission centres

σ/σ' is the ratio of the probability of processes of type (ii) above to that of type (iii)

z is a parameter representing self quenching, and corresponds to the mean number of

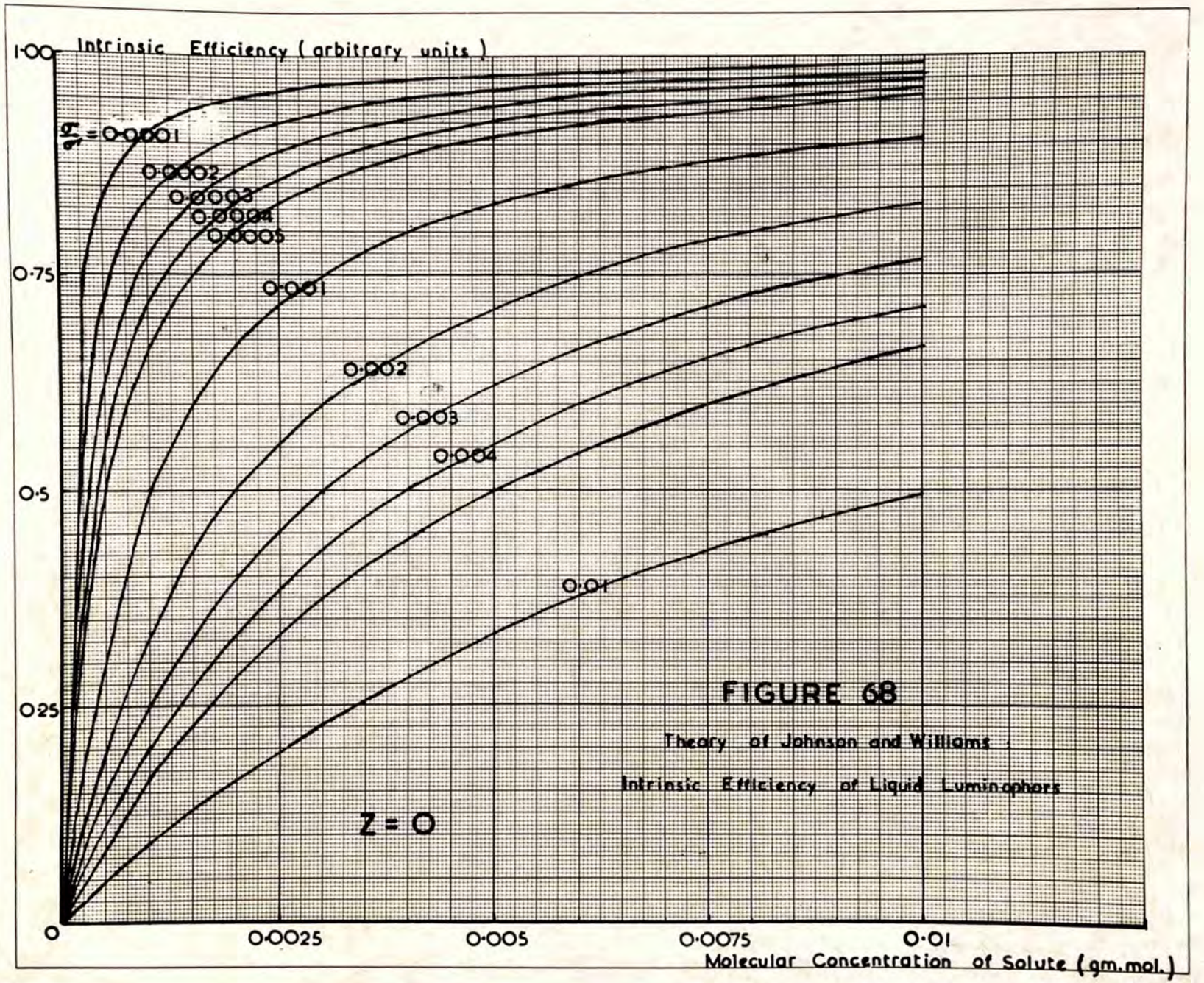

FIGURE 68

Theory of Johnson and Williams

Intrinsic Efficiency of Liquid Luminophors

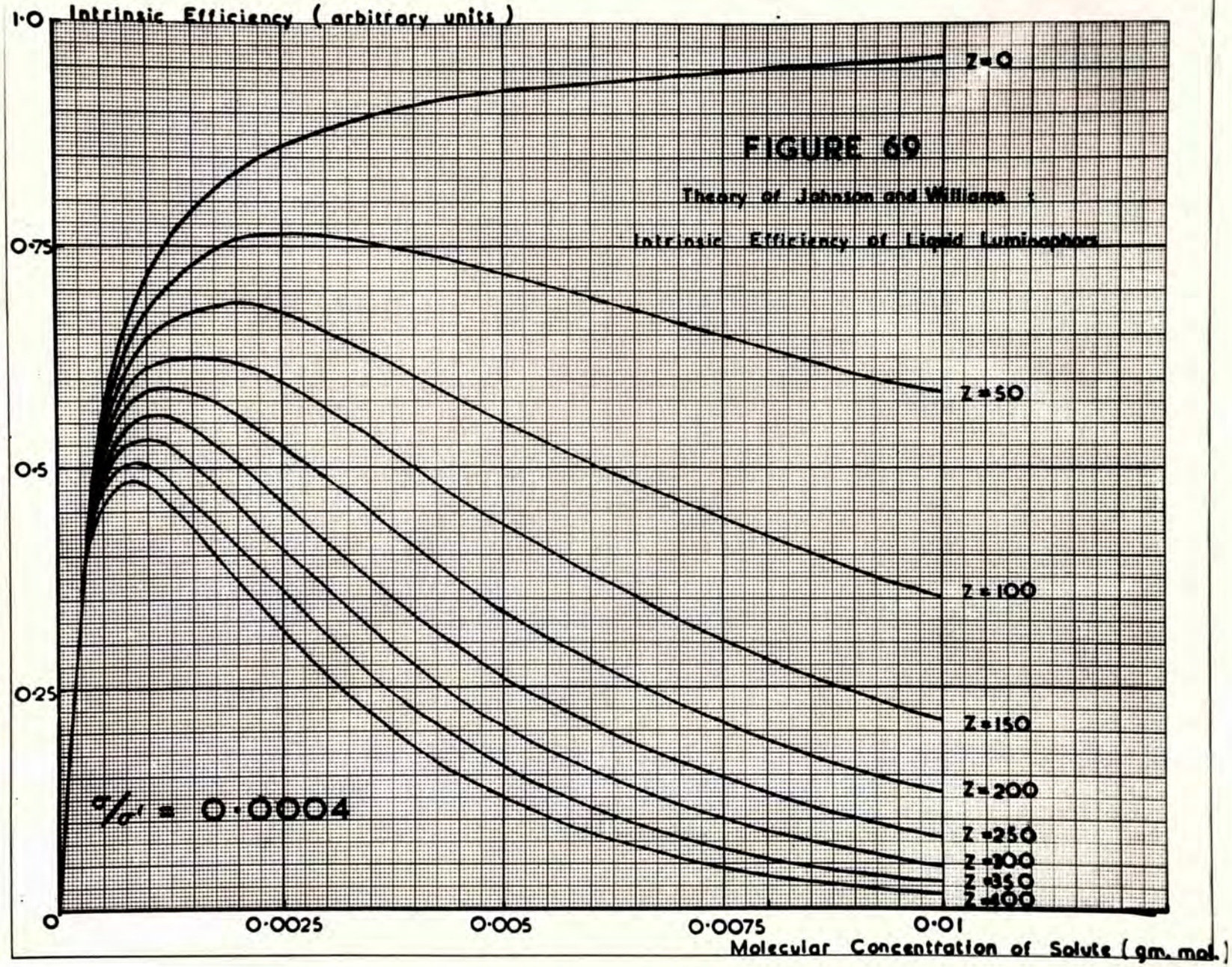

FIGURE 69

Theory of Johnson and Williams :

Intrinsic Efficiency of Liquid Luminophors

positions surrounding a given emission centre which, if occupied by a second emission centre, quench luminescence.

Expression 4.7. assumes that process (vii) is negligible. This assumption is not valid at high concentrations of solute or activator, and in systems where self quenching is negligible the efficiency at high concentrations must be expressed as a linear combination of the efficiencies of the two excitation mechanisms (iii) and (vii):-

$$\eta = f_1 \eta_1 + (1 - f_1) \eta_2 \qquad 4.8.$$

If κ is the ratio of the capture cross-sections in solute and solvent, equation 4.8. becomes:-

$$\eta \propto \left[\frac{\kappa c}{c(\kappa - 1) + 1} \right] k + \left[\frac{1 - c}{c(\kappa - 1) + 1} \right] \left[\frac{c}{c + \frac{\sigma}{\sigma'}(1 - c)} \right] \qquad 4.9.$$

where k is a constant determined by the relative probabilities of processes (iv) and (vi), and of (iii) and (vii).

Figures 68 and 69 show calculated curves derived from expression 4.7. assuming various values for the parameters σ/σ', and Z. The curves of figure 68 assume that no self quenching

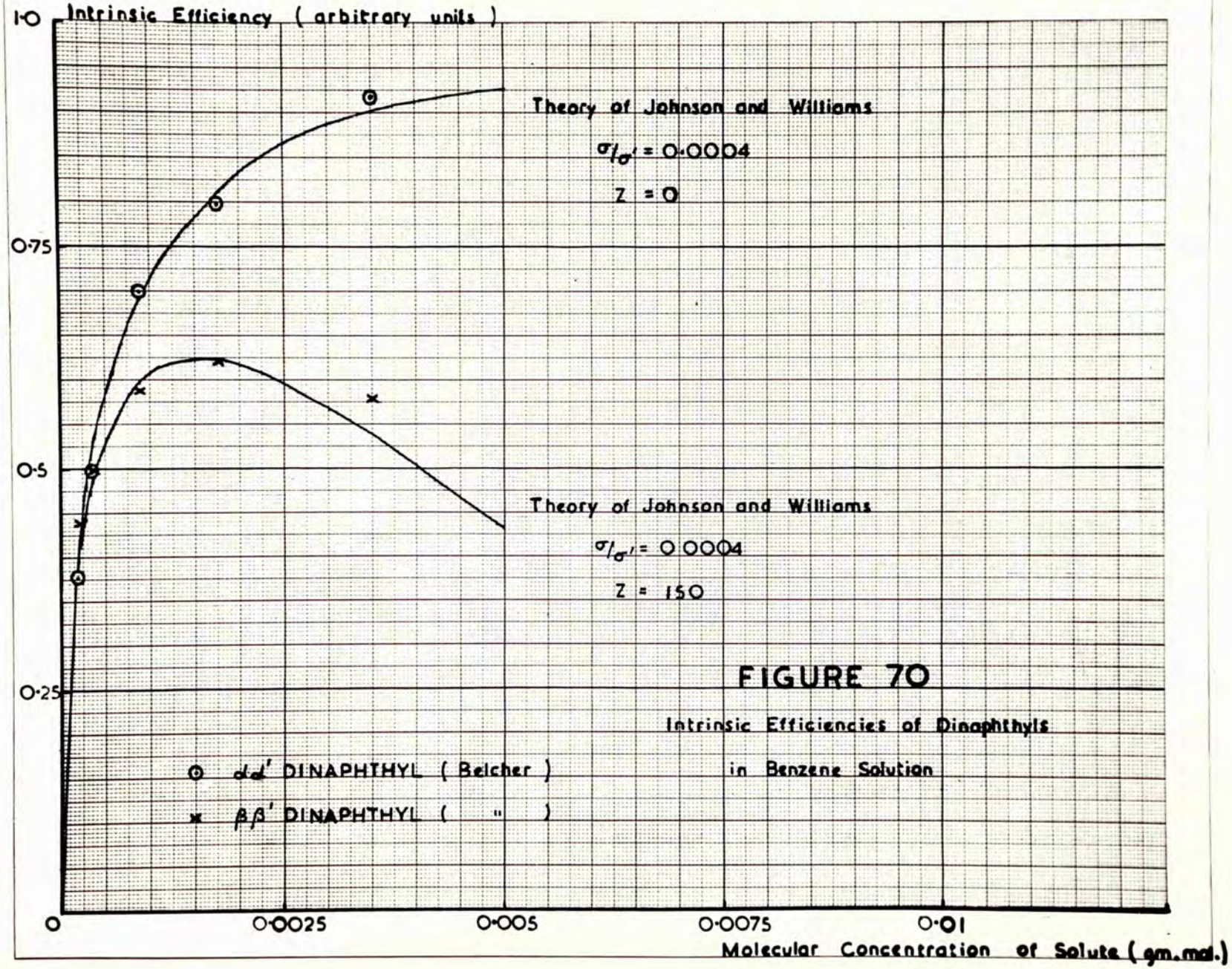

FIGURE 70

Intrinsic Efficiencies of Dinaphthyls in Benzene Solution

occurs and that $Z = 0$, those of figure 69 are for $\sigma/\sigma' = 0.0004$ and various degrees of self quenching.

A direct comparison of the experimental curves of figures 68 and 69 with those of figures 64 and 66 is not possible because the former are not curves of true luminescent efficiency but curves of figure of merit. However, by using the data of figure 67 to convert values of figure of merit into luminescent efficiency, and expressing all concentrations as gm. molecules of solute/gm. molecule of solvent, such a comparison can be made, and approximate values of the parameters σ/σ', and Z assigned in each case. In figure 70, this has been done for $\alpha\alpha'$-dinaphthyl and $\beta\beta'$-dinaphthyl in benzene solution.

In Table XX, the results of a number of such analyses are presented.

Table XX.

Luminescent Efficiency of Liquid Luminophors.

System	σ/σ'	Z
α-Naphthol/Benzene	0.0004±0.0001	120 ± 20
β-Naphthol/Benzene	"	120 ± 20
α-Naphthylamine/Benzene	"	90 ± 15
β-Naphthylamine (Commercial)/ Benzene	"	60 ± 15
β-Naphthylamine (Purified)/ Benzene	"	30 ± 10
$\alpha\alpha'$-diNaphthyl/Benzene	"	0 ± 5
$\beta\beta'$-diNaphthyl/Benzene	"	150 ± 30
p-Terphenyl/Benzene	"	0 ± 5
m-Terphenyl/Benzene	"	0 ± 5
Anthracene/Benzene	"	300 ± 100
Anthracene/Xylene*	0.0004	270
Naphthalene/Xylene*	0.0004	0

*Results of Johnson and Williams (1950b).

The values of σ/σ', and Z for naphthalene and anthracene in xylene obtained by Johnson and Williams (1950b) from an examination of the experimental data of Ageno et al. (1949) and Kallmann and Furst (1950) have been included

in the table for comparison. Because of uncertainty in the conversion of figure of merit into true efficiency, the derived values of the parameters are subject to errors of the order indicated. More accurate measurements would require an experimental arrangement measuring total intensity of emitted light rather than scintillation rate.

The parameter σ/σ', is seen to be constant within the limits of experimental error for a given solvent, and is not significantly different in benzene and xylene.

8. MEASUREMENT OF ABSOLUTE COUNTING RATES IN LIQUID LUMINOPHORS.

(a) Methods of Measurement:

Measurements similar to those already described in sub-section IV.3. on crystalline luminophors were made on solutions of p -terphenyl in benzene contained in quartz cells of known dimensions. These measurements were made using the photo-multiplier cooled with liquid nitrogen, in conjunction with the device shown in figure 13, (inset D). The inter-dynode potential was as before, 108 volts, the amplifier was operated at full gain, and counting rates were measured with the scaler operating at a pulse discrimination of 5 volts.

The liquid samples were contained in cylindrical quartz cells of internal diameter 1.4 cm., and wall thickness 2 mm. Three such cells, having internal lengths of 1 cm., 2 cm., and 4 cm. respectively, were available. When placed on the perspex knife edges of the light guide assembly, they were coaxial with the light guide itself. Filling with liquid was accomplished through two small side tubes fused into the cylindrical surface of each cell.

Measurements were carried out as follows:- the background counting rate due to the photo-multiplier in the absence of any source or cell was first measured. A cell filled with ρ -terphenyl solution was then placed on the knife edges and pushed back until it was just in contact with the end of the light-guide. The background rate was then again measured. A gamma-source of known strength was next mounted on the optical bench at a suitable distance from the cell, and the counting rate measured. The cell was withdrawn slightly, and a disc of black paper, of diameter slightly more than the maximum diameter of the light-guide assembly was introduced between the cell and the light-guide. Counting rates were again measured with and without the source in position. The cell was then removed, emptied of solution, and replaced, whereupon the last four measurements were repeated. From the measured counting rates, corrected for the finite resolving time of the scaler, the true maximum counting rate due to scintillations produced in the volume of the solution could be obtained, corrected for background effects and for scintillations produced in the quartz walls of the cell and the light guide.

This seemingly complex procedure was necessary in order to eliminate errors due to the shielding effect of the volume of liquid filling the cell on the light-guide and photo-multiplier tube, and the luminescence of the empty cell under gamma-irradiation.

From the known strength of the source and its distance from the mid-point of the cell, the counting rate appropriate to 1 mc. of activity was thus determined. The rate of production of secondary electrons in the medium corresponding to this gamma-flux was calculated in the manner described in sub-section II.2. using linear gamma-absorption coefficients for benzene derived from figure 5. (Since the concentration of ρ-terphenyl solution used was only 10 gm./litre it is permissible to ignore the effect of the solute in this calculation.) No correction was necessary for absorption in the copper beta filter, since none was used; its function was fulfilled by the end wall of the quartz cell. An appropriate correction was made for gamma absorption in this wall. The Dural cap of the

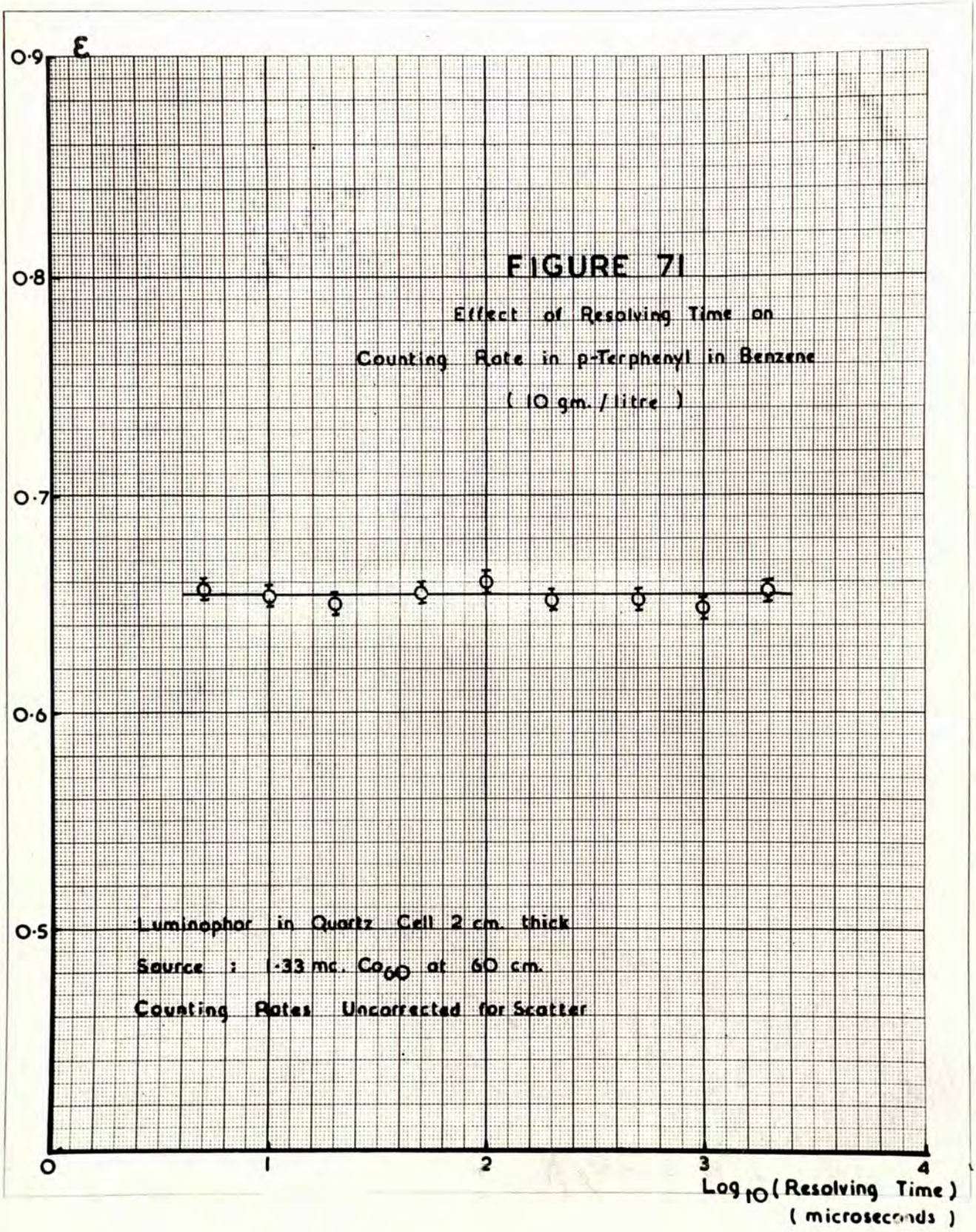

FIGURE 71

Effect of Resolving Time on Counting Rate in p-Terphenyl in Benzene (10 gm. / litre)

light-guide assembly was sufficiently thin not to necessitate a correction.

The value of ε , the ratio of the observed maximum true counting rate to the calculated rate of production of secondary electrons could thus be obtained.

(b) Experimental Results:

Initial studies were concerned with investigating the relationship between observed counting rate and scaler resolving time. Figure 71 summarises the results obtained with the 2 cm. cell and a cobalt ^{60} source; no significant change in the ratio ε is observed over the whole range of resolving times studied, suggesting that the decay time of the luminophor is very short ($<$ 1 microsecond).

Table XXI

Maximum True Counting Rates in p -Terphenyl in Benzene due to 1 millicurie of various Radio-isotopes at 1 metre.

1 cm. quartz cell.

	Observed Counting Rate Counts/second.	Calculated Rate Of Production of secondary electrons. electron/second	ε
Sodium 24	46.9	36.8	1.28
Cobalt 60	39.3	46.6	0.84
Bromine 82	59.1	83.1	0.71
Iodine 131	22.5	130.3	0.17
Gold 198	22.0	131.4	0.17

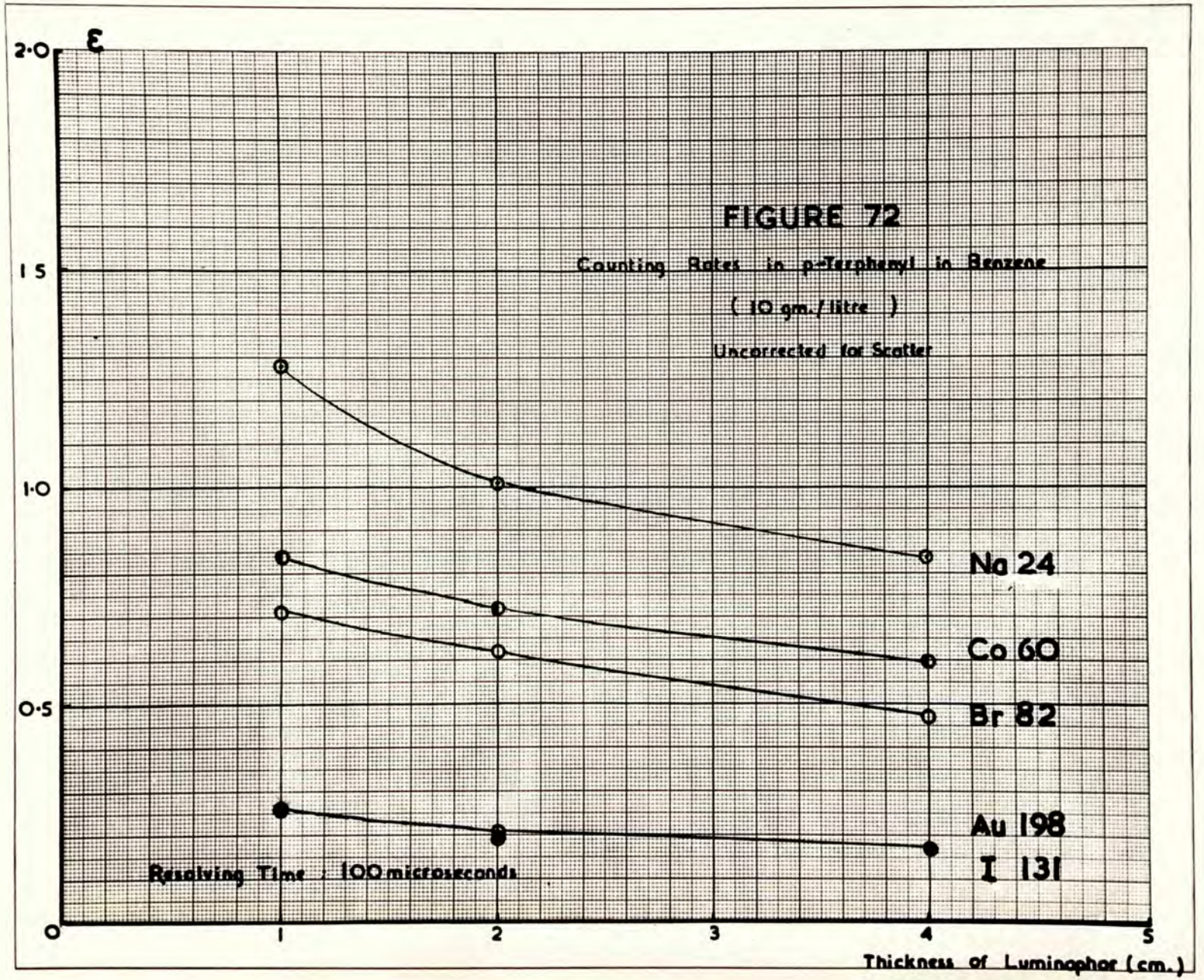

FIGURE 72

Counting Rates in p-Terphenyl in Benzene

(10 gm./litre)

Uncorrected for Scatter

Table XXI summarises the results of more detailed studies made at a scaler resolving time of 100 microseconds with the 1 cm. cell. Similar measurements were made with the 2 cm. and 4 cm. cells, the variation in with cell thickness being shown in figure 72. These results conform to the same general pattern as has been established in sub-section IV.3. for crystalline luminophors. The ratio ε falls with increasing thickness of the luminophor, and with decreasing gamma-ray energy. However, it will be seen that its value for $sodium_{24}$ rises significantly above unity even though it has already been established that the decay time of the luminophor is very short, so that the possibility of multiple counting of secondary electrons can be discounted.

This apparent anomaly may be explained in terms of the scattering of gamma-radiation and secondary electrons from the quartz walls of the cells into the sensitive volume of the luminophor. An accurate correction for this effect is difficult to make, but its approximate magnitude can be estimated in the following way:-

Since only a small fraction of the scattered gamma-quanta will be absorbed in the luminophor, consider first only the secondary electrons crossing the interface. It has been shown by Sinclair (1950) that the number of electrons emerging per second from the surface of am infinite medium containing a uniformly distributed radio-active source of monoenergetic beta-particles is given by the formula:-

$$\text{Number of particles escaping per cm.}^2\text{ per second} = \frac{R.N}{8} \qquad 4.10.$$

where R = range of electrons in medium in cm.

N = rate of production of beta-particles per cm.^3 of medium.

Applying this general formula to the case of a cylindrical cell, of thickness greater than R, and considering both the end walls and curved surface:-

$$\text{Number of particles escaping per second} = \frac{R.N}{8}\left(2\pi r_1 h + 2\pi r_1^2\right) \qquad 4.11.$$

where r_1 = internal radius of cell

h = internal length of cell.

Sinclair's expression applies properly only to a random, non-directional emission of monoenergetic beta-particles, while in the case of the Compton

scattering of gamma-quanta, the recoil electrons are emitted mainly in the forward direction, and are not of course mono-energetic. The error due to the former effect will be small when averaged over the whole cell. For the non-homogeneity of the electrons, it is more difficult to correct, but an approximate application of Sinclair's equation to the problem is possible if it is assumed that the secondary electrons produced by a given gamma-ray all have energy equal to the calculated mean energy of electrons in the medium. This can be evaluated for quartz from the data of Appendix I. The rate of production of electrons per cm^3 is expressed as the ratio of the rate of absorption of gamma-quanta in the walls of the cell to the total volume of the cell. For a radio-isotope with a complex decay scheme, the effect due to the various gamma-quanta are evaluated separately, and each weighted according to the probability of emission. The total effect is then found by summation.

Sinclair's expression thus becomes, for S mc. of a radio-isotope at x cm. distance:

Number of secondary electrons escaping per second

$$= \frac{3.7.10^7 . s . (2\pi r_1 h + 2\pi r_1^2)}{4\pi x^2 \left[(\pi r_2^2 - \pi r_1^2)(h+2t) + 2\pi r_1^2 t \right]} \sum_\gamma \frac{R_\gamma}{8} \left[(\pi r_2^2 - \pi r_1^2)(1 - e^{-\mu_\gamma (h+2t)}) + \pi r_1^2 (1 - e^{-2\mu_\gamma t}) \right] . f_\gamma$$

$$= \frac{3.7.10^7 . s . r_1 . (h + r_1)}{16 x^2 \left[h (r_2^2 - r_1^2) + 2t r_2^2 \right]} \cdot \sum_\gamma R_\gamma \left[(r_2^2 - r_1^2)(1 - e^{-\mu_\gamma (h+2t)}) + r_1^2 (1 - e^{-2\mu_\gamma t}) \right] . f_\gamma$$

4.12.

where r_1 = internal radius of cell

r_2 = external radius of cell

h = internal length of cell

t = thickness of cell

R_γ = range in cell medium of secondary electrons of energy equal to mean energy of secondary electrons produced in medium by gamma-quanta of energy E_γ .

and s , x , μ_γ , f_γ , have the significance attached to them in equation 2.2.

This expression has been evaluated for 1 mc. of each radio-isotope at 1 metre distance and for each of the three quartz cells used. The values of μ for quartz used were derived from Appendix I. The values of R were derived from the collected

data of Kamen for the ranges of homogeneous electrons in unit density material quoted in Appendix II, assuming a density of 2.66 for quartz. Appropriate corrections for internal conversion and self-absorption in the source were included in the values for f_γ .

The results of these calculations are shown in Table XXII.

Table XXII

Counting Rate Correction for Secondary Electrons Scattered from Walls of Quartz Cells due to 1 millicurie of various Radio-isotopes at 1 metre.

	Counting Rate in 1 cm. cell counts/second	Counting Rate in 2 cm. cell counts/second	Counting Rate in 4 cm. cell counts/second
Sodium 24	11.2	18.0	31.3
Cobalt 60	6.0	9.5	16.6
Bromine 82	6.0	9.5	16.6
Iodine 131	0.4	0.7	1.2
Gold 198	0.4	0.7	1.2

Since many of the scattered electrons entering the sensitive volume of the luminophor will have low energy, and consequently will have a low probability of producing a count in the scaler, the values of this table constitute an upper limit to the correction for scattering that may be applied to the observed

counting rates of Table XXI ; this is particularly true for the low energy gamma-radiation from iodine$_{131}$ and gold$_{198}$. On the other hand, the contribution of the scattered gamma-quanta, which has not been taken into account, will offset this effect to some extent. The estimated corrections for sodium$_{24}$ are probably not in error by more than 25%.

Table XXIII

Maximum True Counting Rates in p -Terphenyl in Benzene due to 1 millicurie of various Radio-isotopes at 1 metre.

Corrected for Scatter.

(1 cm. quartz cell)

	Observed Counting Rate counts/second	Calculated Rate of Production of Secondary Electrons counts/second.	ε
Sodium 24	46.9	48.0	0.98
Cobalt 60	39.3	52.6	0.75
Bromine 82	59.1	89.1	0.66
Iodine 131	9.83	37.9	0.26
Gold 198	9.82	37.5	0.26

If the observed counting rates of Table XXI are submitted to corrections based on the Table XXII , the results shown in Table XXIII are obtained. It will be

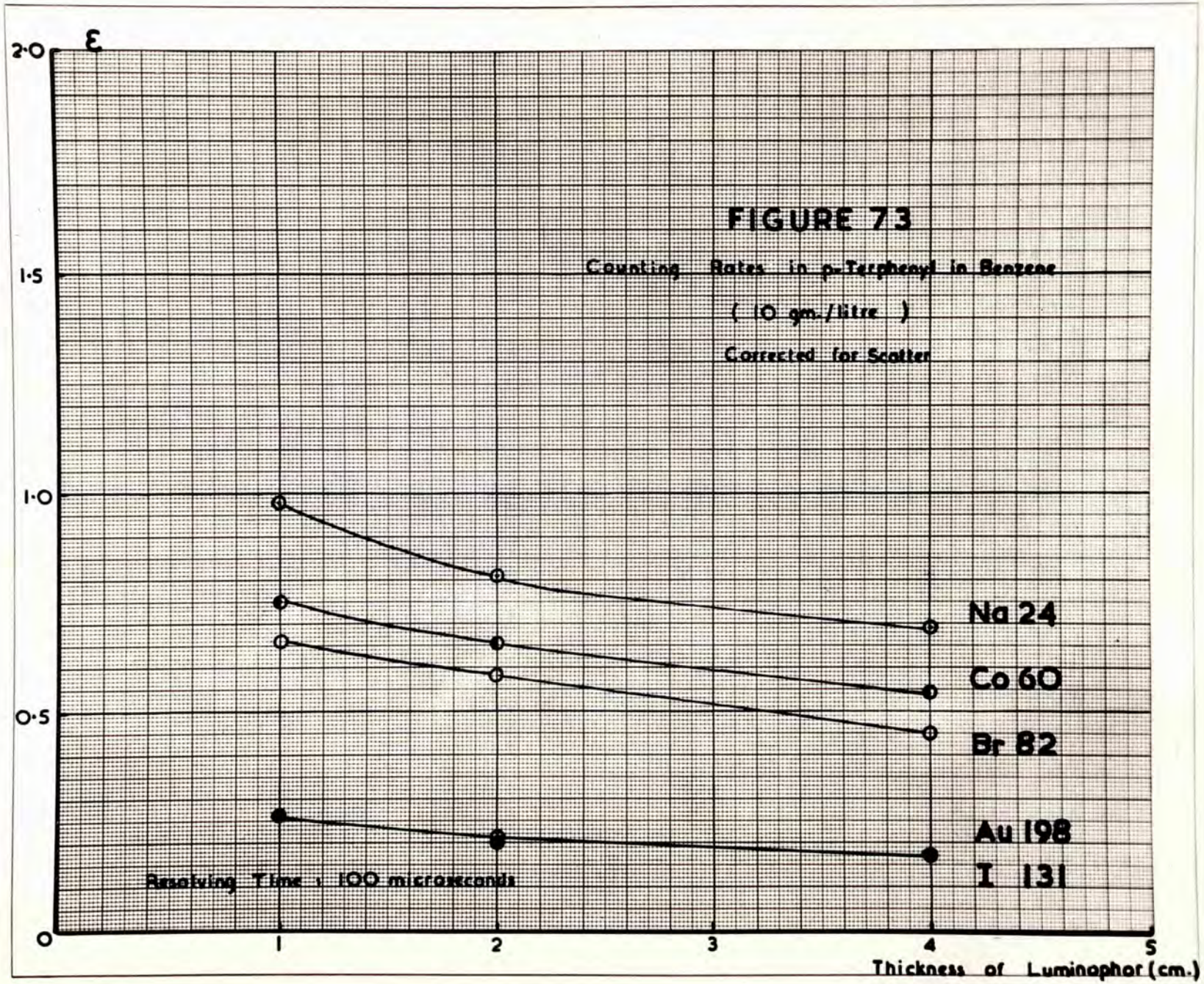

FIGURE 73

Counting Rates in p-Terphenyl in Benzene

(10 gm./litre)

Corrected for Scatter

seen that the effects due to the walls of the cells are entirely sufficient to explain the anomalies in the original results. The corrected values of the ratio ε are in all cases less than unity, but approach this level in the case of sodium$_{24}$. The rapid fall in ε at low gamma-ray energies may be explained by the predominance of Compton absorption in the case of the liquid luminophors, whereas with calcium tungstate, absorption in the energy range 0.1 - 0.5 MeV. takes place largely by the photo-electric process. The smaller scintillations produced by the much less energetic Compton recoil electrons may be expected to have a lower probability of recording on the scaler.

9. STUDIES ON THE ČERENKOV EFFECT IN SCINTILLATION COUNTERS.

(a) Introduction:

The observation of scintillations in pure liquids such as water and benzene (page 159), and in Perspex (page 119), irradiated by gamma-quanta suggested that some mechanism other than the excitation-emission process described in sub-section II.4. must contribute to their luminescence. Following the reports of Jelley (1950) that the passage of cosmic-ray

μ-mesons through distilled water was accompanied by the production of light pulses due to the Čerenkov effect, and that these pulses could be counted with a photo-multiplier, fast amplifier, and scaler, experiments were carried out to determine whether the pulses observed under gamma-irradiation could also be attributed to this effect.

Čerenkov (1934) showed that the passage through matter of fast beta-particles or secondary electrons from Compton encounters, was accompanied by the emission of light extending from the visible region of the spectrum into the ultra-violet. He showed further that this emission was not isotropic but occurred along a cone at a particular angle to the direction of the incident particle, this angle being characterised by the energy of the particle. The theory of the effect has been reviewed by Robin (1950) and was first developed on a classical basis by Frank and Tamm (1937). These workers demonstrated that the emission of light was due to the deceleration of the particle in its passage through matter and could only occur when its velocity was greater than the phase velocity of light within the medium. They showed the angle θ between the direction of the incident electron and that of the emitted light to be given by:-

$$\frac{c}{n} = v \cos\theta \qquad 4.13.$$

where v = velocity of particle

n = refractive index of medium

Writing $\frac{v}{c} = \beta$, it follows from equation 4.13 that:-

$$\cos\theta = \frac{1}{\beta n}$$

β is of course related to the energy E_e of the electron expressed in MeV., by the well-known relationship:-

$$E_e = 0.51 \left[\frac{1}{(1-\beta^2)^{\frac{1}{2}}} - 1 \right]$$

For emission to occur, it is thus necessary that $\beta n > 1$; this sets a lower limit on the energy of electrons which can emit light by such a process. At this limit θ becomes equal to zero. The cone of emission of Čerenkov radiation thus contracts as the electron is slowed down in its passage through matter, vanishing at the instant when the velocity of the electron becomes $\frac{c}{n}$.

Frank and Tamm calculated the total energy, W , radiated over a short length l of the track of the electron, over which v may be assumed constant. This they found to be given by:

$$W = \frac{e^2 l}{c^2} \int_{\beta n > 1} \omega . d\omega . \left(1 - \frac{1}{\beta^2 n^2}\right) \qquad 4.14.$$

where ω is the frequency of the emitted radiation.

From this expression, the number of photons with wavelengths between λ_1 , and λ_2 emitted in a length dl of track is given by:-

$$N = 2\pi\alpha\left(\frac{1}{\lambda_2} - \frac{1}{\lambda_1}\right)\left(1 - \frac{1}{\beta^2 n^2}\right) dl \qquad 4.15$$

$$= \text{constant} \cdot \left(1 - \frac{1}{\beta^2 n^2}\right) \cdot dl$$

where $\alpha = \frac{e^2}{hc}$, the fine structure constant.

Early experimental studies on the Čerenkov effect were made with collimated beams of beta-particles incident upon thin films of transparent materials, using photographic recording techniques. The velocity of the incident electrons could be assumed unchanged after passage through these thin films; it was therefore possible to verify equation 4.13. directly. Using an arrangement of this type, and 2 MeV. electrons from an accelerating tube, Collins and Reiling (1938) showed the dependence of θ on refractive index in various materials. In a similar manner, Wyckoff and Henderson (1943) investigated the relationship between θ and electron energy for electrons in the energy range 240 - 815 keV. passing through a mica film.

The angular distributions of emitted light obtained by these workers showed broad maxima at the values of θ predicted by the theory of Frank

amd Tamm, but with a spread of many degrees about these values. This spread was attributed by Wyckoff and Henderson to scattering of electrons within the film. More recently, however, it has been pointed out by Li (1950) that an angular spread of emitted light about the values of predicted by the classical theory is to be expected from a relativistic approach to the problem.

Getting (1947) first suggested the use of a photo-multiplier to detect Čerenkov radiation. Dicke (1947) has described the use of a liquid nitrogen cooled type I P 28 tube in conjunction with an amplifier and scaler to observe the pulses produced in Perspex irradiated by X-rays from a 20 MeV. betatron, but did not study the angular distribution of the emission. No reports have yet appeared describing the extension of the technique to the study of the Cerenkov effect produced by secondary electrons from gamma-rays.

(b) Methods of Measurement:

It was decided to study this effect in Perspex, because of the very widespread use of this material in the fabrication of light-guides for scintillation counters. An experimental arrangement similar to

that already described in connection with the measurement of absolute counting rates in liquid luminophors (page 174) was used. The photo-multiplier tube was cooled with liquid nitrogen and used in conjunction with the quartz cell mounting of figure 13 (inset D). Inside the latter, however, a cylindrical perspex plug, 4 cm. in length and 1.8 cm. in diameter (equal to the maximum diameter of the light guide), was placed in the position previously occupied by the quartz cells containing the liquid samples. This plug had one basal blane covered with black paper, the other basal plane and the cylindrical surface being highly polished. By measuring the total counting rate with the polished basal plane presented towards, and in contact with, the polished end of the light guide, and then reversing the plug and measuring the background, the true counting rate due to luminescent effects in the plug could be measured. This procedure eliminated errors due to the shielding effect of the plug on the light guide and photo-multiplier, which would have been introduced had the background been measured by removing the plug completely. Since the true counting rates due to luminescence in the plug

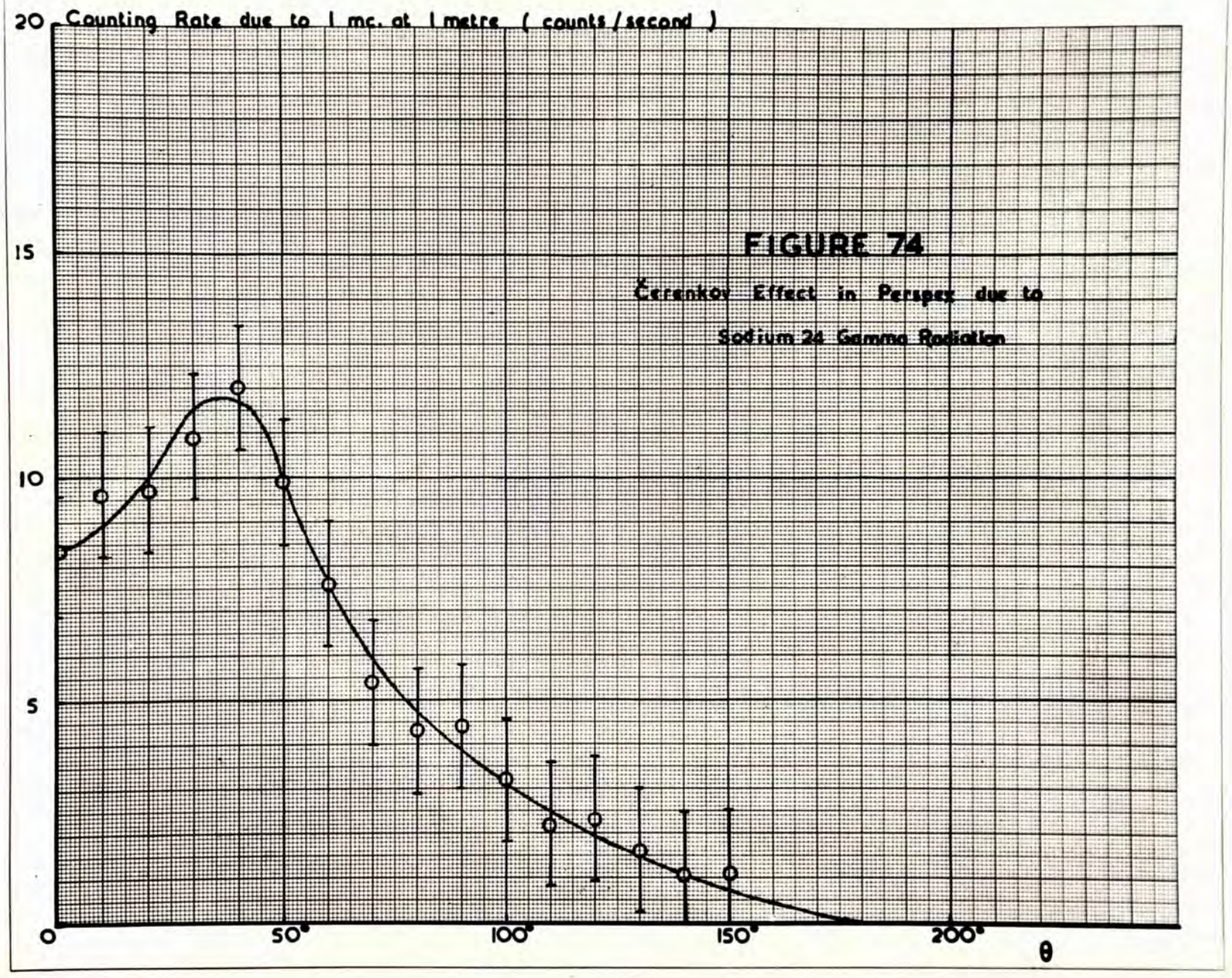

FIGURE 74

Čerenkov Effect in Perspex due to Sodium 24 Gamma Radiation

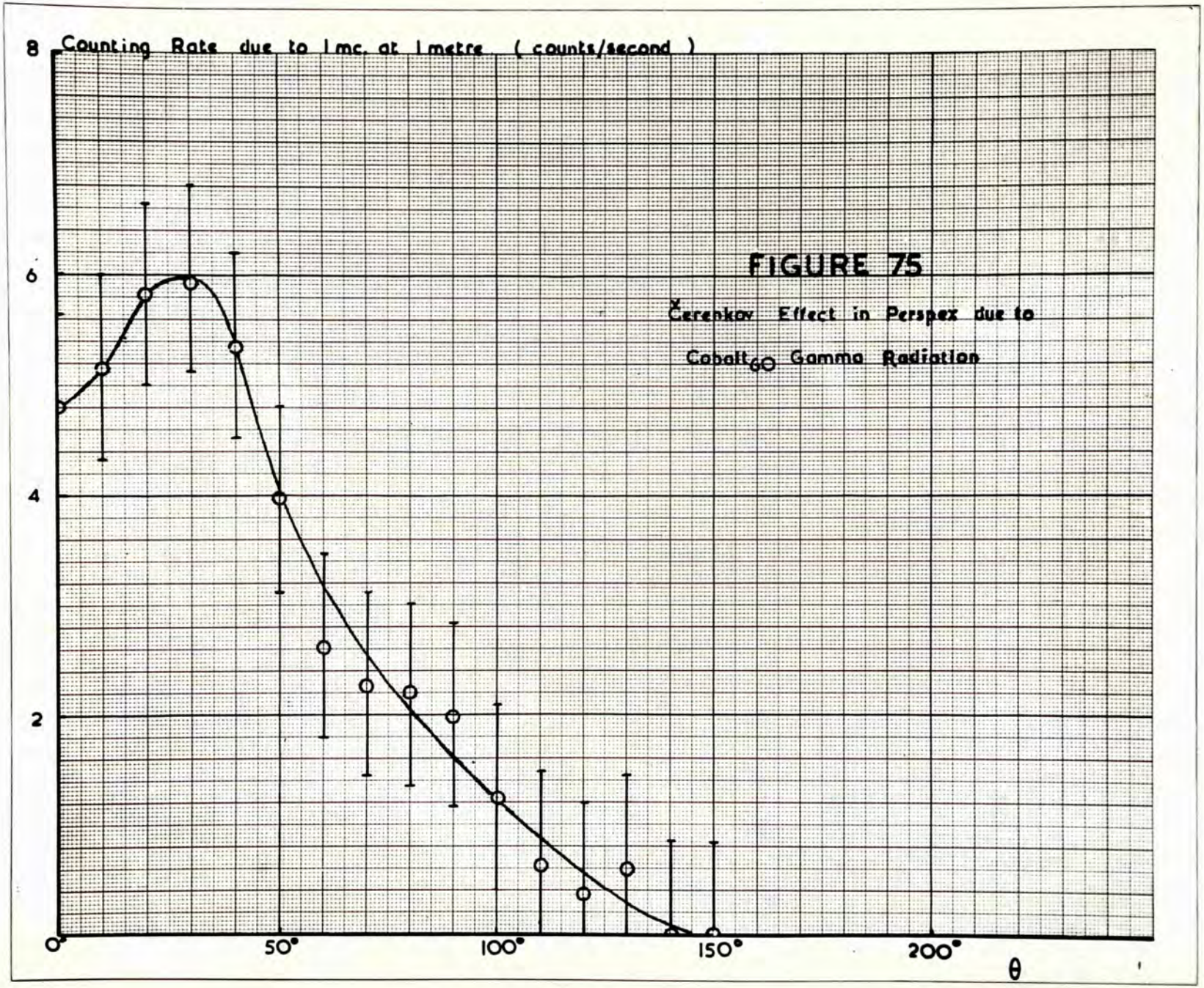

FIGURE 75

Čerenkov Effect in Perspex due to Cobalt$_{60}$ Gamma Radiation

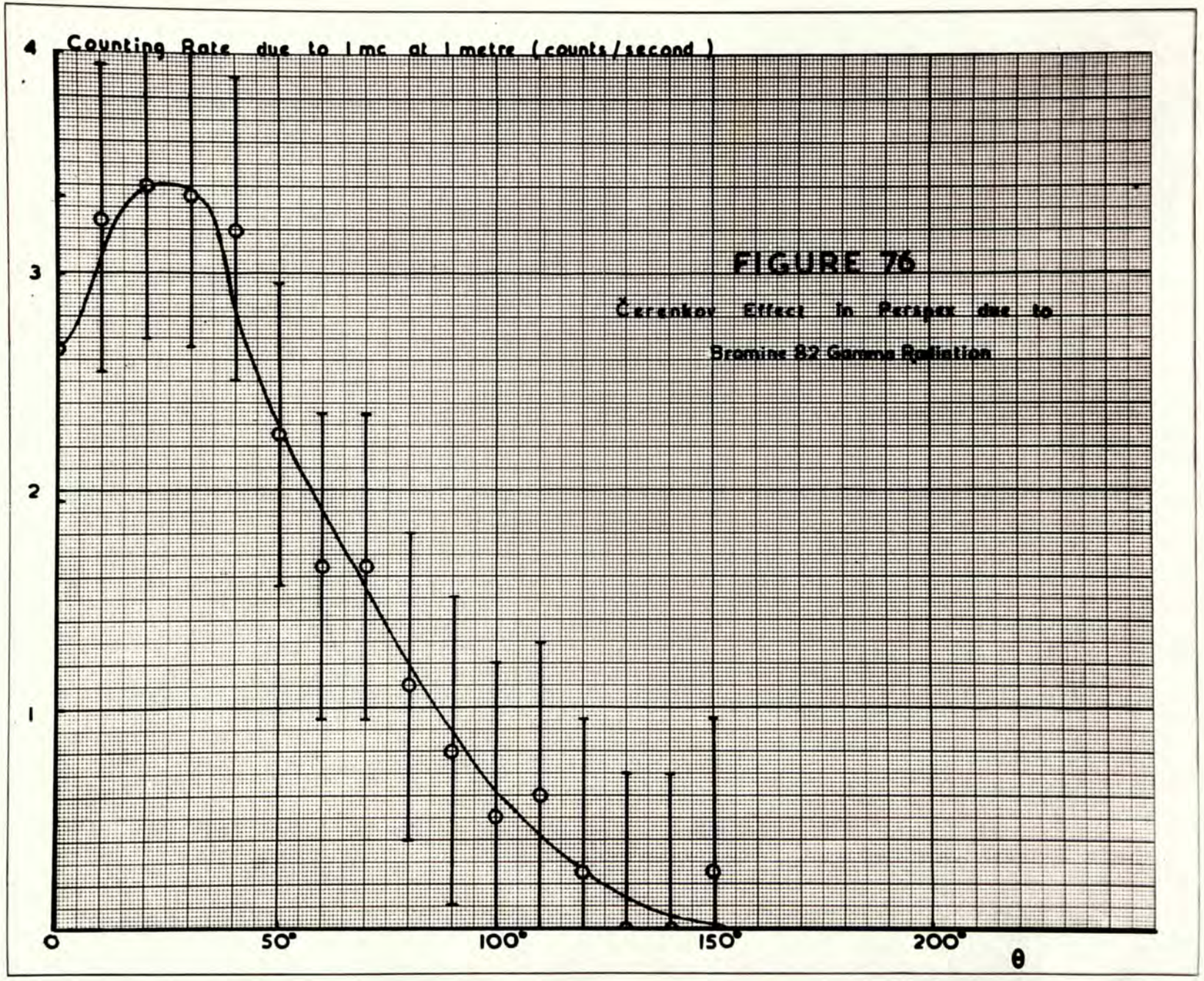

FIGURE 76

Čerenkov Effect in Perspex due to Bromine 82 Gamma Radiation

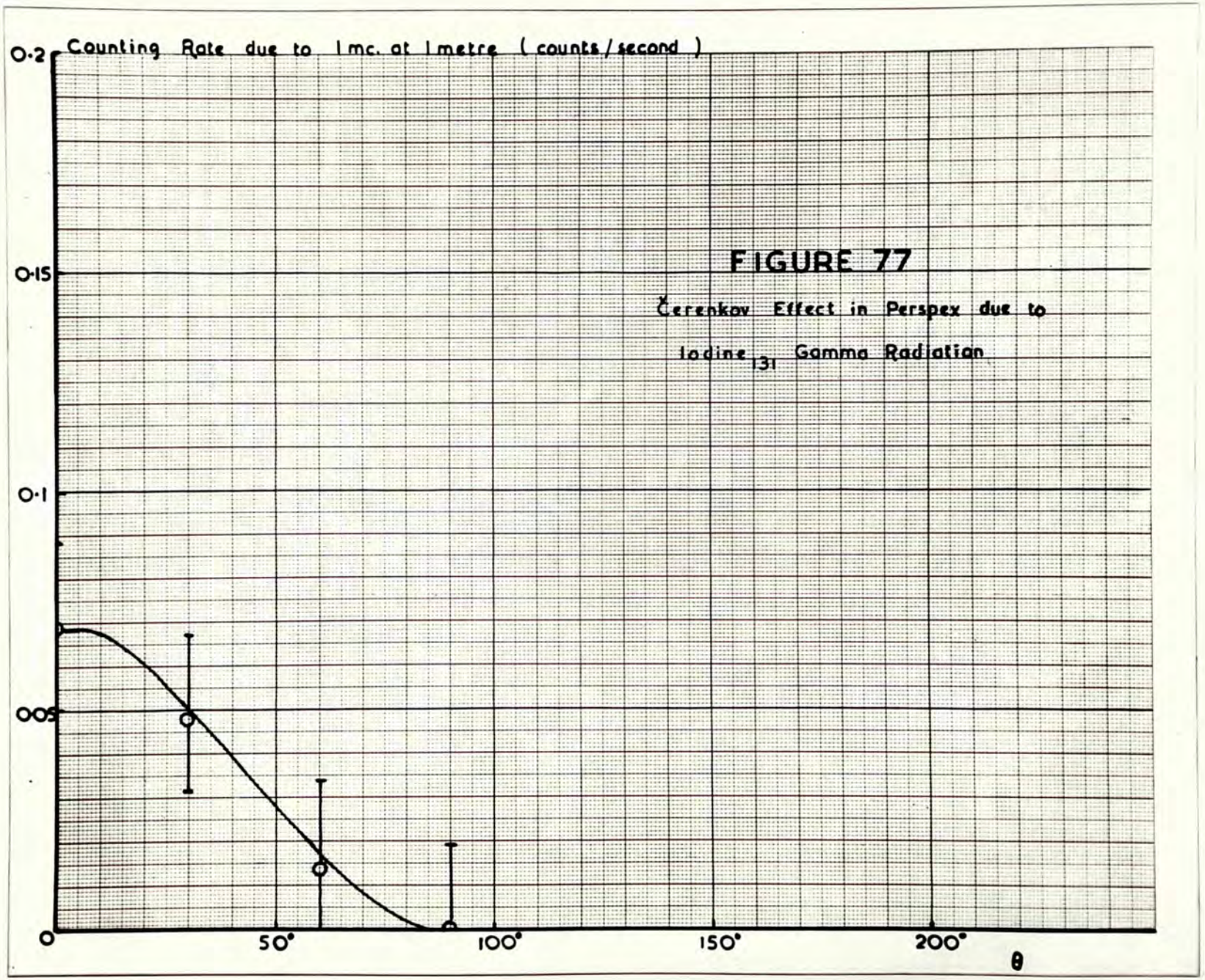

FIGURE 77

Čerenkov Effect in Perspex due to Iodine$_{131}$ Gamma Radiation

amounted to no more than 20% of the total counting rate, such errors would have been very significant.

The photo-multiplier tube was operated at an inter-dynode potential of 108 volts, and the amplifier at full gain. Counting rates were measured with the ratemeter, the pulse discriminator control being set at 5 volts, and the resolving time at 100 microseconds.

Measurements were made of the variation in counting rate when radio-active sources were moved in a circle at a known fixed distance from the mid-point of the perspex slug; this distance being between 10 and 50 cms. The sources used were calibrated in the manner already described (sub-section III.5) and were of the order of 1 millicurie. The counting rates corresponding to 1 millicurie of activity at 1 metre distance were then deduced from the observed rates.

(c) Experimental Results:

Measurements were made with sources of the four radio-isotopes sodium$_{24}$, cobalt$_{60}$, bromine$_{82}$ and iodine$_{131}$. The variation in counting rate with angular position of the source for these four isotopes is shown in figures 74 - 77, all counting rates being corrected to correspond to 1 millicurie of activity

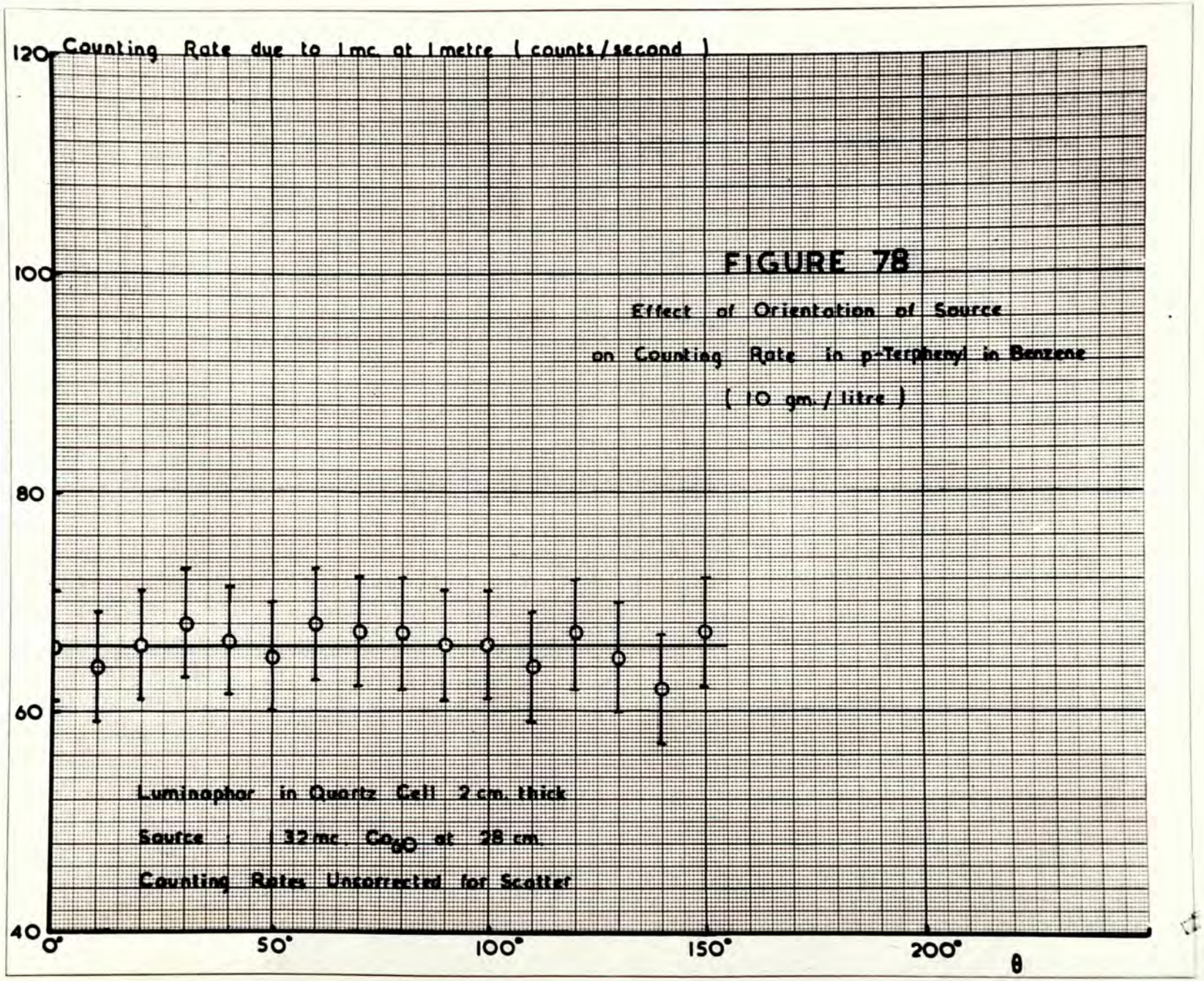

FIGURE 78

Effect of Orientation of Source on Counting Rate in p-Terphenyl in Benzene (10 gm. / litre)

at 1 metre. In figure 78, a set of results for a quartz cell filled with p -terphenyl in benzene solution is presented for comparison. Whereas in the latter case, there is no evidence of any directional effects, the counting rates observed in perspex are in all cases extremely dependent upon the position of the source.

The general form of these results is not incompatible with the proposition that the luminescence excited in Perspex by gamma-radiation is due entirely to the Cerenkov effect. An accurate analysis of the observed distributions in terms of the theory of Frank and Tamm is difficult however. In the first place, the secondary electrons produced by gamma-radiation are not mono-energetic, but have an energy distribution of the form shown in figure 6. In the second place they are not necessarily ejected parallel to the incident gamma-quanta, although in the case of gamma-radiation in the energy range studied here, most of the Compton recoils will travel in the forward direction. Each secondary electron may be expected to emit light until its energy has reached the lower limit for the effect. The angle between the emitted light and the track of the electron will vary between

an initial value of $\cos^{-1}(1/3n)$ given by equation 4.13. and a final value of zero, when its velocity has fallen to c/n. At this point its energy will be $0.51\left(\frac{1}{(1-1/n^2)^{1/2}}-1\right)$ MeV. Since n for Perspex is 1.50, the lower energy limit for the Cerenkov effect in this material is:-

$$0.51\left[\frac{1}{(1-\frac{1}{1.5^2})^{1/2}}-1\right] \text{ MeV.} \qquad 4.16.$$

or, in other words, 0.175 MeV.

The angular distribution of the emitted light will be still further modified by the optical properties of the slug, which acts as a short section of light guide. Nevertheless, an approximate check of the observed distributions in terms of the theory of Frank and Tamm may be attempted along the following lines:-

Assume that all the secondary electrons produced by a given gamma-ray are mono-energetic and of energy equal to their mean secondary electron energy in the medium, $\overline{E_e}$, calculated as described on page 26. Then, whatever be the angular distribution of the emission, the <u>total</u> intensity of emitted light can be seen from equation 4.14. to be:-

$$I = N_e \int_{l_1}^{l_2} \text{constant}.\left(1-\frac{1}{\beta^2 n^2}\right).dl. \qquad 4.17.$$

where N_e = rate of production of secondary electrons in the medium by the gamma-ray in question.

ℓ_1 = total range of an electron of energy in the medium

ℓ_2 = residual range of an electron of energy 0.175 MeV. in the medium.

Where a radio-isotope emits more than one gamma-ray per disintegration, the total intensity of emitted light will be the sum of the effects due to each separate gamma-ray, weighted according to its probability, f_γ , of emission:-

$$I = \sum_\gamma I_\gamma \cdot f_\gamma$$

Evaluating the integral $\int_{\ell_1}^{\ell_2} (1 - \frac{1}{\beta^2 n^2}) \cdot d\ell$. by graphical methods it is possible to calculate the expected relative values for I for each of the radio-isotopes studied. These relative values can then be compared with the relative <u>areas</u> under the curves of figures 74 - 77.

In Table XXIV, the data necessary for the calculations are summarised. The values of $\overline{E_e}$ were calculated from the data of Appendix I for Perspex;

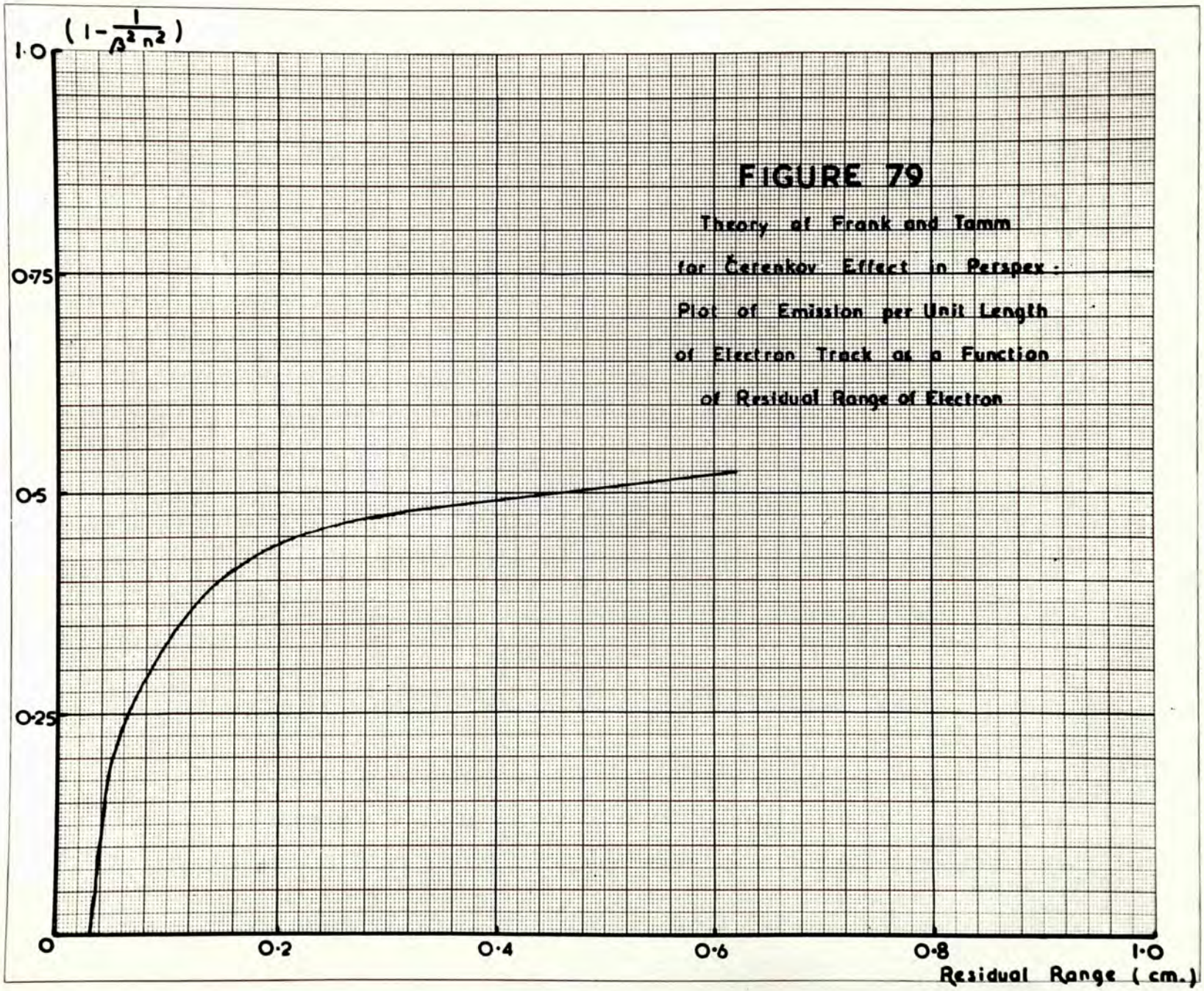

FIGURE 79

Theory of Frank and Tamm for Čerenkov Effect in Perspex - Plot of Emission per Unit Length of Electron Track as a Function of Residual Range of Electron

those of ℓ_1, ℓ_2 were derived from the collected data of Kamen (1950) for the ranges of homogeneous electrons in unit density material, assuming a density of 1.18 for Perspex. N_e was calculated for each gamma-ray as described in sub-section II.2. From these data, the plot of $\left(1 - \frac{1}{\beta^2 \sigma^2}\right)$ against residual electron range shown in figure 79 could be drawn; graphical integration then made possible the evaluation of relative values for I.

In Table XXV, the predicted values obtained in this way of the total intensity of emitted light due to 1 mc. of each radio-isotope at 1 metre distance, relative to the predicted value for cobalt$_{60}$ which is taken as unity, are compared with the values derived from the experimental curves of figures 74 - 77. The agreement between the two sets of values is surprisingly good considering the approximations made in calculation, and adds great weight to the contention that the effects observed in Perspex are due entirely to Čerenkov radiation.

Table XXIV

Čerenkov Effect due to Gamma Radiation in Perspex.

Gamma Quantum Energy (E_γ)	Mean Secondary Electron Energy ($\bar{E}_e$)	β	Mean Secondary Electron Range (ℓ_1)	$(1-\frac{1}{\beta^2 n^2})$	$\int_{\ell_1}^{\ell_2}(1-\frac{1}{\beta^2 n^2}).d\ell$	Rate of Production of Secondary Electrons, (N_e)	$N_e \int_{\ell_1}^{\ell_2}(1-\frac{1}{\beta^2 n^2})d\ell$
0.283	0.080	0.48	0.008	0	0	280	0
0.363	0.105	0.53	0.017	0	0	267	0
0.55	0.195	0.69	0.034	0.066	0	234	0
0.638	0.240	0.73	0.042	0.166	0.002	221	4
0.79	0.315	0.78	0.076	0.270	0.009	201	18
1.16	0.530	0.87	0.161	0.413	0.040	174	70
1.32	0.620	0.885	0.195	0.432	0.054	167	90
1.35	0.640	0.89	0.200	0.439	0.056	163	91
1.38	0.655	0.895	0.204	0.445	0.058	160	93
2.76	1.560	0.965	0.620	0.523	0.258	114	295
	0.175	0.667	0.029	0	0	0	0

Table XXV

Total Intensity of Čerenkov Effect in Perspex due to Gamma-Radiation from Various Radio-Isotopes.

(relative to effect due to Cobalt$_{60}$ radiation)

	I/I_{C_o} Observed	I/I_{C_o} Calculated
Sodium 24	2.1	2.4
Cobalt 60	1.0	1.0
Bromine 82	0.58	0.68
Iodine 131	0.0061	0.0038

SECTION V : DISCUSSION:

The theoretical and experimental studies just described have demonstrated some of the problems which are encountered when an attempt is made to use the scintillation counter as an absolute measuring instrument for gamma-radiation. These studies have shown that where the scintillations produced are large, and the optical efficiency of the detecting system is high, it is possible to relate the observed counting rates to the rates of absorption of radiation in the luminophor. But if the scintillations are of weak intensity, and the optical efficiency low, statistical effects in the optical system and in the photo-multiplier tube greatly modify this relationship. Similar considerations are found to apply when an attempt is made to relate the amplitude distributions of the pulses produced in the counter to the energy distributions of the secondary electrons produced in the luminophor.

The theoretical analysis of these statistical processes given in sub-section II.6. has accounted satisfactorily for the experimental results of sub-section IV.1., for stimulation of the photo-multiplier

both by single photons of visible light and by artificial light pulses containing many photons. These results have very clearly demonstrated the fundamental importance of statistical effects in measuring devices based on photo-multiplier tubes.

The studies of absolute counting rate in crystalline luminophors described in sub-section IV.3. have shown that an upper limit is imposed on the counting rate observed under scatter-free conditions by the rate of production of secondary electrons in the luminophor, calculated as described in sub-section II.2., provided that the decay period of the luminophor is less than the resolving time of the counting equipment. Such conditions can be satisfied in the case of calcium tungstate. With the experimental arrangements used, this upper limit is approached in the case of the gamma-radiation from sodium$_{24}$ and cobalt$_{60}$, but in the case of the lower energy radiation from bromine$_{82}$, iodine$_{131}$ and gold$_{198}$, many of the scintillations produced in the luminophor fail to record because of the statistical processes already mentioned. It is clear that for absolute measurements of gamma-radiation flux, a system of higher optical efficiency is required; such a system is difficult to

achieve however with the type I P 21 photo-multiplier or an equivalent type. The greatest need here is for improved photo-multiplier design; during the period of these studies, only the type I P 21 tube was available; but photo-multipliers such as the R.C.A. type 5819 and the E.M.I. type 5311, which have the photo-cathode deposited on the glass envelope, are now in production. These tubes are not easily adapted to an experimental arrangement in which liquid nitrogen cooling can be used, but a considerable increase in optical efficiency can be achieved by their use.

Anomalously high counting rates were obtained in thallium-activated alkali halide luminophors, and these effects were shown to be explicable in terms of delayed phosphorescence produced by electron trapping levels in the luminophor. In practical scintillation counters of high optical efficiency, these effects can be overcome by the use of a relatively high level of pulse discrimination, since the phosphorescent pulses consist only of single photons. It is no doubt for this reason that the phosphorescent effects in thallium-activated sodium iodide have not been recorded by other workers. But in counters with long

light guides designed as probe units for biological or clinical measurements, in which the optical efficiency is reduced and cooling of the photo-multiplier is necessary in order to achieve high counting effieiencies, such effects may profoundly modify the observed counting rates (Belcher and Evans 1951).

The experimental studies of pulse amplitude distribution in crystalline luminophors described in sub-section IV.4. show general agreement with the theoretical distributions of section II, but are seen to be very dependent upon photo-multiplier statistics. Some evidence of discontinuities in the distributions due to photo-electron peaks and recoil electron edges is shown, but in order to observe these discontinuities with certainty, an experimental arrangement of higher optical efficiency is required. Further work in this field would require a photo-multiplier having the photo-cathode deposited on the glass envelope, in contact with which the luminophor could be mounted, backed by a reflector. A pulse analyser of the "kick-sorter" type should be used in place of the pulse discriminating ratemeter, in order to eliminate the errors involved

in the differentiation of a curve of integral counting rate. With such a system, spectrographic studies of radio-isotopes would be possible, and have in fact been made by Hofstadter and his co-workers.

Regarding the experimental studies on the temperature effects and emission spectra of crystalline luminophors described in sub-sections IV.5. and IV.6., little is to be said; for the most part they serve only to confirm already published work, although it is of interest to note that the overall gain of the type I P 21 photo-multiplier appears independent of temperature. The comparative studies of sub-section IV.7. on luminescence in liquid luminophors, on the other hand, suggest a number of interesting fields for future work. Whilst it seems unlikely that any crystalline luminophors will be developed that are superior to those already known, it is quite clear that liquid systems of considerably higher efficiency than p-terphenyl in xylene (Reynolds 1950), or $\alpha\alpha'$-dinaphthyl in benzene (Belcher 1951) may be devised. While the low density and low mean atomic number of such systems make them

unsuitable for applications in which high counting rates are required from a luminophor of small sensitive volume, for many types of scintillation counter they may be preferred to crystalline luminophors. For example, for work with high-energy gamma-radiation, a large sensitive volume is required to contain the range of the energetic secondary electrons. This could readily be obtained with a liquid system. Again, in directional counters a tube containing the liquid system can be placed behind a collimating aperture, and will act as both luminophor and light guide, giving nearly 100% counting efficiency. Moreover, the short decay time of these luminophors makes them particularly suited to research applications.

The studies described in sub-section IV.7. confirm and extend the published work of Kallmann and Furst (1950) on liquid luminophors. Further comparative studies might well reveal binary or ternary liquid systems of still higher luminescent efficiency. Of greater interest perhaps, are the implications of these results with regard to the chemical and biological effects of ionising radiations.

Little is known regarding the precise mechanism of luminescence in these systems, although it is clear that this mechanism must involve absorption of energy in the solvent followed by transport of energy from excited solvent molecules to the solute. The experimental results of figure 63 show that this transport is extremely dependent on the nature of the solvent, and indicate that polar solvents such as acetone or diethyl-ether are less effective vehicles than non-polar solvents such as benzene. Further studies in a wide range of solvents with and without added impurities, together with spectrographic studies of the distributions of the emitted light and chemical studies of radiation effects on the solvents might lead to a better understanding of the mechanism of luminescence in liquid systems, and of the fundamental energy transport processes on which many of the chemical and biological effects of radiation depend.

The experimental results of sub-section IV.8. show that the absolute counting rates in liquid luminophors are limited by the rates of production of secondary electrons, provided that appropriate

corrections are included for scatter from the walls of the containing vessel. This effect is shown to make a significant contribution to the observed counting rates.

The results of section IV.9. show that the luminescence observed in Perspex under gamma-radiation may be attributed to the Čerenkov effect. It would be of interest to extend these measurements to other classes of transparent materials, for example to the pure solvents studied in sub-section IV.7., and to higher energy radiation than that from sodium$_{24}$ gamma-rays. The possibility of using the Čerenkov effect for the measurements of high-energy radiation in the 10 - 100 MeV. energy range suggests that a study of the luminescence induced by gamma-rays of such energies might be profitable.

Finally, it may be mentioned that the methods of measurement used in these studies are readily adaptable to other fields of research in which the measurement of very low intensities of light is involved. In the study of chemically-induced luminescence, and of low luminescent processes, to quote only two examples, the techniques described may make possible the observation of lower light intensities than has hitherto been possible.

SECTION VI : ACKNOWLEDGEMENTS:

The author wishes to acknowledge his indebtedness to Professor W. V. Mayneord, Director of the Physics Department, Royal Cancer Hospital, without the benefit of whose advice and encouragement these studies could not have been made. He also wishes to record his grateful thanks to Mr. N. Veall of the Post-Graduate Medical School, Hammersmith, Dr. G. H. J. Garlick of Birmingham University, and Mr. J. Sharpe of A.E.R.E. Harwell, all for gifts of luminophors; to Dr. W. K. Sinclair of the Royal Cancer Hospital for the provision of facilities for the measurement of gamma-sources; to Mr. H. C. Hodt and Mr. H. J. Hodt for assistance with the construction of apparatus; to Mr. Gilbert-Purssey for help in the preparation of the diagrams; and finally to Miss P. Leach for the typescript.

List of References.

AGENO, M., CHIOZZOTTO, M., QUERZOLI, R.,
Atti. Accad. Naz. Lincei, 6, 453, 1949a.
Atti. Accad. Naz. Lincei, 6, 626, 1949b.

AGENO, M., CHIOZZOTTO, M., QUERZOLI, R.,
Phys. Rev., 79, 720, 1950.

ALBURGER, D. E.,
Phys. Rev., 76, 435, 1949.

ALLEN, J. S.,
Phys. Rev., 55, 966, 1939.

BECQUEREL, H.,
C. R., 129, 912, 1899.

BEERS, Y.,
Rev. Sci. Instr., 13, 72, 1942.

BELCHER, E. H.,
Nature, 166, 742, 1950a.
Nature, 166, 846, 1950b.

BELCHER, E. H.,
Nature, 167, 314, 1951.

BELCHER, E. H., EVANS, H. D.,
J. Sci. Instr., 28, 71, 1951.

BELL, P. R.,
Phys. Rev., 73, 1405, 1948.

BETHE, H., HEITLER, W.,
Proc. Roy. Soc. (London), A 146, 83, 1934.

BLAU, M., DREYFUS, B.,
Rev. Sci. Instr., 16, 245, 1945.

BLIZARD, E. P., DE BENEDETTI, S.,
Rev. Sci. Instr., 20, 81, 1949.

BLOCH, F.,
Z. für Phys., 52, 555, 1928.

BORST, L. B., FLOYD, J. J.,
Phys. Rev., 74, 989, 1948.

BOWEN, E. J.,
"Chemical Aspects of Light",
Oxford University Press, 1946.

CASSEN, B., CURTIS, L. R.,
Science, 110, 94, 1949.

CAVANAGH, P. E.,
Nature, 165, 889, 1950.

ČERENKOV, P. A.,
C. R. Sci. U.R.S.S., 2, 451, 1934.

COLLINS, G. B.,
Phys. Rev., 74, 1543, 1948.

COLLINS, G. B., REILING, V. G.,
Phys. Rev., 54, 499, 1938.

COLTMAN, J. W., MARSHALL, F. H.,
Phys. Rev., 72, 528, 1947.

COMPTON, A. H.,
Phys. Rev., 21, 482, 1923.

COOKE-YARBOROUGH, E. C.,
J. Sci. Instr., 26, 96, 1949.

CORK, J. M., KELLER, H. B., SAZYNSKI, J.,
RUTLEDGE, W. C., STODDARD, A. E.,
Phys. Rev., 75, 1621, 1949.

CROOKES, W.,
Proc. Roy. Soc. (London), A 71, 405, 1903.

DE BENEDETTI, S., MACGOWAN, F. K., FRANCIS, J. E.,
Phys. Rev., 73, 1404, 1948.

DEUTSCH, M.,
Massachusetts Institute of Technology Technical
Report No. 3., Dec. 1947.

DEUTSCH, M., ELLIOT, L. G, ROBERTS, A.,
Phys. Rev., 68, 193, 1945.

DEUTSCH, M., SIEGBAHN, K.,
Phys. Rev., 77, 680, 1950.

DICKE, R. H.,
Phys. Rev., 71, 737, 1947.

DOWNING, J. R., DEUTSCH, M., ROBERTS, A.,
Phys. Rev., 61, 686, 1947.

DU MOND, J. W. M., LIND, D. A., WATSON, B. B.,
Phys. Rev., 73, 1392, 1948.

ELLIOT, J. P., LIEBSON, S. H., MYERS, R. D.,
RAVILIOUS, C. F.,
Rev. Sci. Instr., 21, 631, 1950.

ENGSTRÖM, R. W.,
J. Opt. Soc. Amer., 37, 420, 1947a.
Rev. Sci. Instr., 18, 587, 1947b.

EVANS, R. D., EVANS, R. O.,
Rev. Mod. Phys., 20, 305, 1948.

FARMER, E. C., MOORE, H. B., GOODMAN, C.,
Phys. Rev., 76, 454, 1949.

FLAMMERSFELT, A.,
Z. für Phys., 112, 729, 1939.

FLOYD, J. J., BURST, L. B.,
Phys. Rev., 75, 1106, 1949.

FOWLER, R. H., HULME, W. R., MACDOUGALL, J.,
BUCKINGHAM, R. A.,
Proc. Roy. Soc. (London), A 149, 131, 1935.

FRANK, I., TAMM, I.,
C.R. Sci. U.R.S.S., 3, 109, 1937.

FRENKEL, J.,
Phys. Rev., 37, 17, 1931.

FRERICHS, R., WARMINSKY, R.,
Naturwiss., 33, 251, 1946.

GARLICK, G. F. J.,
"Luminescent Materials",
Oxford University Press, 1949.

GARLICK, G. F. J., GIBSON, A. F.,
Nature, 158, 704, 1946.

GARLICK, G. F. J., GIBSON, A. F.,
Proc. Phys. Soc., 50, 574, 1948.

GETTING, I. A.,
Phys. Rev., 71, 123, 1947.

GILLESPIE, A. B.,
A.E.R.E. Report, No. G/R 118, 1947.

GILLESPIE, A. B.,
A.E.R.E. Report, No. G/R 168, 1948.

GILLETTE, R. H.,
Rev. Sci. Instr., 21, 294, 1950.

GITTINGS, H. T., TASCHEK, R. F., RONZIO, A. R.,
JONES, E., MASILUN, W. J.,
Phys. Rev., 75,205 , 1948.

GÖRLICH, P.,
Z. für Phys., 101, 335, 1936.

GRAY, L. H.,
Proc. Roy. Soc. (London), A 156, 578, 1936.

HIRZEL, O., WÄFFLER, H.,
Hebr. Phys. Acta, 19, 216, 1946.

HOFSTADTER, R.,
Phys. Rev., 74, 100, 1948.

HOFSTADTER, R.,
Nucleonics, 4 (4), 2, 1949a.
Nucleonics, 4 (5),29, 1949b.
Phys. Rev., 75, 796, 1949c.

HOFSTADTER, R.,
Nucleonics, 6 (5), 70, 1950.

HOFSTADTER, R., LIEBSON, S. H., ELLIOT, J. O.,
Phys. Rev., 78, 81, 1950.

HOFSTADTER, R., MACINTYRE, J. A.,
Phys. Rev., 78, 617, 1950a.
Phys. Rev., 78, 619, 1950b.
Phys. Rev., 79, 389, 1950c.
Nucleonics, 7 (3), 32, 1950d.
Phys. Rev., 80, 631, 1950e.

JELLEY, J. V.,
Proc. Phys. Soc., A 64, 82, 1951.

JENSEN, E. H., LASLETT, L. J., PRATT, W. W.,
Phys. Rev., 75, 458, 1949a.
Phys. Rev., 76, 430, 1949b.

JENTSCHKE, W.,
Phys. Rev., 73, 77, 1948.

JOHANSSON, S. A. E.,
Nature, 165, 396, 1950a.
Ark. für Fys., 2, 171, 1950b.

JOHNSON, P. D., WILLIAMS, F. E.,
J. Chem. Phys., 18, 1477, 1950a.
Phys. Rev., 81, 146, 1950b.

JOHNSON, R. P.,
J. Opt. Soc. Amer., 29, 387, 1939.

JORDAN, W. H., BELL, P. R.,
Nucleonics, 5 (4), 30, 1949.

JORGENSEN, T.,
Amer. J. Phys., 16, 285, 1948.

JURNEY, E. T.,
Phys. Rev., 74, 1049, 1948.

KALLMANN, H.,
Z. für Naturforsch., 2a, 439, 1947a.
Z. für Naturforsch., 2a, 642, 1947a.
Natur und Technik., July 1947,c.

KALLMANN, H.,
Phys. Rev., 75, 623, 1949.

KALLMANN, H., ACCARDO, C. A.,
Rev. Sci. Instr., 21, 48, 1950.

KALLMANN, H., FURST, M.,
Phys. Rev., 79, 857, 1950.

KAMEN, M. D.,
"Radio-active Tracers in Biology",
Academic Press Inc., New York, 1948.

KERN, B. D., MITCHELL, A. C. G., ZAFFARANO, D. J.,
Phys. Rev., 76, 94, 1949.

KLEIN, O., NISHINA, Y.,
Z. für Phys., 52, 853, 1929.

KRAUSHAAR, W. L., THOMAS, J. E., HENRI, V. P.,
Phys. Rev., 78, 486, 1950.

KRÖGER, F. A.,
"Some Aspects of the Luminescence of Solids",
Elsevier, Amsterdam, 1948.

LEVY, P. W., GREULING, E.,
Phys. Rev., 73, 83, 1948.

LI YIN - YUAN,
Phys. Rev., 80, 104, 1950.

LIEBSON, S. H., BISHOP, M. E,. ELLIOT, J. O.,
Phys. Rev., 80, 907, 1950.

LIEBSON, S. H., ELLIOTT, J. O.,
Phys. Rev., 78, 65, 1950.

LIFSCHUTZ, H., DUFFENDACK, O..S.,
Phys. Rev., 53, 941, 1938a.
Phys. Rev., 54, 714, 1938b.

LIND, D. A., BROWN, J., DU MOND, J.,
Phys. Rev., 76, 591, 1949.

LIND, D. A., BROWN, J., KLEIN, D., MULLER, D.,
DU MOND, J. W. M.,
Phys. Rev., 75, 1544, 1949.

LUNDBY, A.,
Phys. Rev., 80, 477, 1950.

MACINTYRE, W. J.,
Phys. Rev., 75, 1439, 1949.

MACINTYRE, W. J.,
Phys. Rev., 81, 1018, 1951.

MADGWICK, E.,
Proc. Cambridge Phil. Soc., 23, 970, 1927.

MANDEVILLE, C. E., ALBRECHT, H. O.,
Phys. Rev., 79, 1010, 1950a.
Phys. Rev., 80, 117, 1950a.
Phys. Rev., 80, 299, 1950c.
Phys. Rev., 80, 300, 1950d.

MANDEVILLE, C. E.,
Nucleonics, 7, (4), 92, 1950e.

MANDEVILLE, C. E., SCHERB, M. V.,
Nucleonics, 7, (5), 34, 1950f.

MARSHALL, F. H., COLTMAN, J. W., BENNETT, A. I.,
Rev. Sci. Instr., 19, 744, 1948.

MARSHALL, J. S., WARD, A. G.,
Can. J. Research, 15, 29, 1937.

MAYNEORD, W. V.,
Nat. Research,Council of Canada Report No. C.R.M. 315, 1946.

MAYNEORD, W. V., BELCHER, E. H.,
Brit. J. Radiology, Supplement No. 2, 1950a.
Nature, 165, 930, 1950b.

MAYNEORD, W. V., ROBERTS, J. E.,
Brit. J. Radiology, 10, 365, 1937.

METZGER, F., DEUTSCH, M.,
Phys. Rev., 74, 1640, 1948.

MITCHELL, A. C.G.,
Rev. Mod. Phys., 20, 296, 1948.

MITCHELL, A. C. G.,
Rev. Mod. Phys., 22, 36, 1950.

MOE, D., OWEN, G. E., COOK, C. S.,
Phys. Rev., 75, 1270, 1949.

MOON, R. J.,
Phys. Rev., 73, 1210, 1948.

MORRISH, A. H., DEKKER, A. J.,
Phys. Rev., 80, 1030, 1950.

MORTON, G. A.,
R.C.A. Review, 10, 525, 1949.

MORTON, G. A., MITCHELL, J. A.,
R.C.A. Review, 9, 632, 1948.

MORTON, G. A., ROBINSON, K. W.,
Nucleonics, 4, (2), 25, 1949.

NIER, A. O.,
Phys. Rev., 77, 789, 1950.

OWEN, G. E., MOE, D., COOK, C. S.,
Phys. Rev., 74, 1879, 1948.

PAPP, G.,
Rev. Sci. Instr., 19, 568, 1948.

PEACOCK, C. L., WILKINSON, R. G.,
Phys. Rev., 74, 297, 1948.

PEIERLS, R.,
Ann. der Phys. (Leipzig), 13, 905, 1932.

POST, R. F., SHIREN, N. S.,
Phys. Rev., 78, 80, 1950.

PRICHOTKO, A. F., SHABALDAS, K. G.,
Bull. Acad. Sci. U.S.S.R., 5, 120, 1941.

PRINGLE, R. W., ROULSTON, K. I., BROWNELL, G. M.,
Nature, 165, 527, 1950a.

PRINGLE, R. W., ROULSTON, K. I., TAYLOR, H. W.,
Rev. Sci. Instr., 21, 216, 1950b.

PRINGLE, R. W.,
Atomics, 1, 49, 1950c.

PRINGSHEIM, P.,
"Fluorescence and Phosphorescence",
Interscience Inc., New York, 1949.

PUTMAN, J. L.,
A.E.R.E. Report N/R 318, 1949.

RAJCHMAN, J. A., SNYDER, R. L.,
Electronics, 13, 2, 1940.

RAMLER, W. J., FREEDMAN, M..S.,
Rev. Sci. Instr., 21, 784, 1950a.
Rev. Sci. Instr., 21, 922, 1950b.

RANDALL, J. T.,
Trans. Faraday Soc., 35, 2, 1939.

RANDALL, J. T., WILKINS, M. H. F.,
Proc. Roy. Soc. (London), A 184, 366, 1945.

RAVILIOUS, C. F., ELLIOTT, J. O., LIEBSON, S. H.,
Phys. Rev., 77, 851, 1950.

REGENER, E.,
Verh. des. Deut. Phys. Ges., 19, 78, 1908.

REYNOLDS, G. T., HARRISON, F. B., SALVINI, G.,
Phys. Rev., 78, 488, 1950a.

REYNOLDS, G. T.,
Nucleonics, 6, (5), 68, 1950b.

ROBERTS, A., BROWNING, J. R., DEUTSCH, M.,
Phys. Rev., 60, 544, 1941.

ROBIN, S.,
J. de Phys. et le Rad., 11, 17D, 1950.

ROBINSON, J. E. , TER-POGOSSIAN, M. , COOK, C. S.,
Phys. Rev., 75, 1099, 1949.

RODDA, S.,
J. Sci. Instr., 26, 65, 1949.

RUARK, A. E., BRAMMER, F. E.,
Phys. Rev., 52, 322, 1937.

RUTHERFORD, E.,
"Radio-active Substances and their Radiations",
Cambridge University Press, 1913.

SAUTER, F.,
Z. für Naturforsch., 4a, 682, 1949.

SCHILLINGER, E. J., WALDMAN, W. C., MILLER, B.,
Phys. Rev., 75, 900, 1949.

SCHONLAND, B. F.J.,
Proc. Roy. Soc. (London), 108A, 187, 1925.

SEABORG, G. T., PERLMAN, I.,
Rev. Mod. Phys., 20, 585, 1948.

SEITZ, F.,
Trans. Faraday Soc., 35, 74, 1939.

SEITZ, F., MÜLLER, D. W.,
Phys. Rev., 78, 605, 1950.

SIEGBAHN, K.,
Phys. Rev., 70, 127, 1947.

SIEGBAHN, K., HEDGRAN, A.,
Phys. Rev., 75, 523, 1949.

SIEGBAHN, K., HEDGRAN, A., DEUTSCH, M.,
Phys. Rev., 76, 1263, 1949.

SINCLAIR, W. K.,
Dissertation, London, 1950.

SINCLAIR, W. K., HOLLOWAY, A. F.,
Nature, 167, 365, 1951.

SIRI, W. E.,
"Isotopic Tracers and Nuclear Radiations",
McGraw-Hill, New York, 1949.

SKINNER, S. M.,
Phys. Rev., 48, 438, 1935.

SMALLER, B., MAY, J., FREEDMAN, M.,
Phys. Rev., 79, 940, 1950.

SMELTZER, J. C.,
Rev. Sci. Instr., 21, 669, 1950.

SOLOMON, A. K.,
Phys. Rev., 79, 403, 1950.

SREB, J. H.,
Phys. Rev., 81, 469, 1951.

TIMMERHAUS, K. D., GILLER, E. B., DUFFIELD, R. B.,
DRICKAMER, H. G.,
Nucleonics, 6 (6), 37, 1950.

VAN HEERDEN, P. J.,
Dissertation, Utrecht, 1945.

WOOLDRIDGE, D. E., AHEARN, A. J., BURTON, J. A.,
Phys. Rev., 71, 913, 1947.

VON HIPPEL, A.,
Z. für Phys., 101, 680, 1936.

WEISS, J.,
Nature, 152, 176, 1942.

WIEGAND, C.,
Rev. Sci. Instr., 21, 975, 1950.

WYCKOFF, H. O., HENDERSON, J. E.,
Phys. Rev., 64, 1, 1943.

WYNN-WILLIAMS, E. E., WARD, F. A. B.,
Proc. Roy. Soc. (London), A 131, 391, 1931.

ZWORYKIN, V. K., MORTON, G. A., MALTER, L.,
Proc. Inst. Radio Engrs., 24, 361, 1936.

APPENDIX I : LINEAR ABSORPTION COEFFICIENTS IN VARIOUS MATERIALS FOR GAMMA-RADIATION IN THE ENERGY RANGE 0.08 - 3 MeV.

Explanatory Note:

The values for the linear absorption coefficients presented in these tables have been calculated by the author from the corresponding values for lead, using the relationships quoted in sub-section II.2.:-

$$\tau_M = \tau_{Pb} \cdot \frac{\rho_M}{\rho_{Pb}} \cdot \frac{A_{Pb}}{A_M} \cdot \left(\frac{Z_M}{Z_{Pb}}\right)^4$$

$$\sigma_M = \sigma_{Pb} \cdot \frac{\rho_M}{\rho_{Pb}} \cdot \frac{A_{Pb}}{A_M} \cdot \left(\frac{Z_M}{Z_{Pb}}\right)$$

$$\sigma_{a_M} = \sigma_{a_{Pb}} \frac{\rho_M}{\rho_{Pb}} \cdot \frac{A_{Pb}}{A_M} \cdot \left(\frac{Z_M}{Z_{Pb}}\right)$$

$$\pi_M = \pi_{Pb} \cdot \frac{\rho_M}{\rho_{Pb}} \cdot \frac{A_{Pb}}{A_M} \cdot \left(\frac{Z_M}{Z_{Pb}}\right)$$

$$\mu_M = \tau_M + \sigma_M + \pi_M$$

The coefficients for lead used in these calculations have been derived from the published data of Siri

(1949), with the exception of the values for at energies less than 0.5 MeV. The latter were obtained from unpublished calculations by Mayneord (private communication).

The values for the mean energies of the secondary electrons have been deduced from those for the linear absorption coefficients, using the relationship also quoted in sub-section II.2:-

$$\bar{E}_e = \frac{E_\gamma(\tau + \sigma_a) + (E_\gamma - 1.02)\pi}{\tau + \sigma + \pi} = \frac{\sum E_e}{\mu}$$

Lead, Pb :- $\rho = 11.35$ gm./cm^3.

Energy E_γ MeV.	σ_a^{-1} cm.	σ^{-1} cm.	τ^{-1} cm.	π^{-1} cm.	μ^{-1} cm.	ΣE_e MeV./cm	$\bar{E}_e$ MeV.
0.08	0.160	1.38	113	-	114	9.05	0.0794
0.1	0.180	1.31	61.0	-	62.3	6.12	0.0982
0.2	0.240	1.10	9.70	-	10.8	1.99	0.184
0.3	0.265	0.950	3.50	-	4.45	1.13	0.254
0.4	0.270	0.860	1.65	-	2.51	0.768	0.307
0.5	0.270	0.780	0.950	-	1.73	0.610	0.353
1	0.250	0.570	0.220	-	0.790	0.470	0.595
2	0.210	0.400	0.070	0.035	0.505	0.595	1.18
3	0.180	0.310	0.040	0.110	0.460	0.880	1.91

Anthracene, $C_{14}H_{10}$:- $\rho = 1.25$ gm./cm.^{3}

Energy E_γ MeV.	σ_a $^{-1}$ cm.	σ $^{-1}$ cm.	τ $^{-1}$ cm.	π $^{-1}$ cm.	μ $^{-1}$ cm.	ΣE_e MeV./cm.	$\bar{E}_e$ MeV.
0.08	0.0235	0.203	0.0058	-	0.209	0.00234	0.0112
0.1	0.0264	0.192	0.0031	-	0.195	0.00295	0.0151
0.2	0.0352	0.161	0.0005	-	0.161	0.00714	0.0443
0.3	0.0389	0.139	0.0002	-	0.139	0.0117	0.0844
0.4	0.0396	0.126	0.0001	-	0.126	0.0159	0.126
0.5	0.0396	0.114	-	-	0.114	0.0198	0.174
1	0.0367	0.0837	-	-	0.0837	0.0367	0.439
2	0.0308	0.0587	-	0.0003	0.0590	0.0619	1.05
3	0.0264	0.0455	-	0.0011	0.0466	0.0803	1.75

Benzene, C_6H_6 :- $\rho = 0.880$ gm./cm.^{3}

Energy E_γ MeV.	σ_a^{-1} cm.	σ^{-1} cm.	τ^{-1} cm.	π^{-1} cm.	μ^{-1} cm.	ΣE_e MeV./cm.	$\bar{E}_e$ MeV.
0.08	0.0168	0.145	0.0040		0.149	0.00166	0.0111
0.1	0.0190	0.138	0.0022	-	0.140	0.00212	0.0151
0.2	0.0253	0.116	0.0003	-	0.116	0.00512	0.0441
0.3	0.0279	0.100	0.0001	-	0.100	0.00840	0.0840
0.4	0.0284	0.0906	-	-	0.0906	0.0114	0.125
0.5	0.0284	0.0821	-	-	0.0821	0.0142	0.173
1	0.0263	0.0600	-	-	0.0600	0.0263	0.439
2	0.0221	0.0421	-	0.0002	0.0423	0.0444	1.05
3	0.0190	0.0327	-	0.0007	0.0334	0.0584	1.75

Calcium Tungstate, $CaWO_4$:- $\rho = 6.06$ gm./cm.^{3}

Energy E_γ MeV.	σ_a $^{-1}$ cm.	σ $^{-1}$ cm.	τ $^{-1}$ cm.	π $^{-1}$ cm.	μ $^{-1}$ cm.	ΣE_e MeV./cm.	$\bar{E}_e$ MeV.
0.08	0.0944	0.815	29.0	-	29.8	2.32	0.0780
0.1	0.106	0.773	15.6	-	16.4	1.57	0.0960
0.2	0.142	0.649	2.49	-	3.14	0.526	0.168
0.3	0.156	0.561	0.897	-	1.46	0.316	0.217
0.4	0.159	0.508	0.423	-	0.931	0.233	0.250
0.5	0.159	0.460	0.244	-	0.704	0.201	0.286
1	0.148	0.337	0.0564	-	0.393	0.204	0.519
2	0.124	0.236	0.0179	0.0123	0.266	0.296	1.11
3	0.106	0.183	0.0103	0.0385	0.231	0.424	1.84

Copper, Cu :- $\rho = 8.94$ gm./cm.^{3}

Energy E_γ MeV.	σ_a $^{-1}$ cm.	σ $^{-1}$ cm.	τ $^{-1}$ cm.	π $^{-1}$ cm.	μ $^{-1}$ cm.	ΣE_e MeV./cm.	$\bar{E}_e$ MeV.
0.08	0.145	1.25	4.54	-	5.79	0.375	0.0647
0.1	0.163	1.19	2.45	-	3.64	0.263	0.0740
0.2	0.218	0.999	0.390	-	1.39	0.122	0.0875
0.3	0.241	0.862	0.141	-	1.00	0.115	0.115
0.4	0.245	0.781	0.066	-	0.846	0.124	0.147
0.5	0.245	0.708	0.038	-	0.746	0.141	0.190
1	0.227	0.517	0.009	-	0.526	0.236	0.449
2	0.191	0.363	0.003	0.011	0.377	0.399	1.06
3	0.163	0.281	0.001	0.035	0.316	0.562	1.78

Perspex, $C_5H_8O_2$:- ρ = 1.18 gm./cm.^{3}

Energy E_γ MeV.	σ_a cm.$^{-1}$	σ cm.$^{-1}$	τ cm.$^{-1}$	π cm.$^{-1}$	μ cm.$^{-1}$	ΣE_a MeV/cm.	$\bar{E}_a$ MeV.
0.08	0.0227	0.196	0.0079	-	0.204	0.00245	0.0120
0.1	0.0255	0.186	0.0042	-	0.190	0.00297	0.0156
0.2	0.0340	0.156	0.0007	-	0.157	0.00694	0.0443
0.3	0.0376	0.135	0.0002	-	0.135	0.0113	0.0839
0.4	0.0383	0.122	0.0001	-	0.122	0.0154	0.126
0.5	0.0383	0.111	-	-	0.111	0.0191	0.173
1	0.0354	0.0808	-	-	0.0808	0.0354	0.438
2	0.0298	0.0567	-	0.0003	0.0570	0.0599	1.05
3	0.0255	0.0439	-	0.0011	0.0450	0.0787	1.75

Potassium Iodide, KI :- ρ = 3.13 gm./cm^3

Energy E_γ MeV.	σ_a $cm.^{-1}$	σ $cm.^{-1}$	τ $cm.^{-1}$	π $cm.^{-1}$	μ $cm.^{-1}$	ΣE_a MeV./cm.	$\bar{E}_a$ MeV.
0.08	0.0484	0.417	6.90	-	7.32	0.556	0.0760
0.1	0.0544	0.396	3.73	-	4.13	0.378	0.0917
0.2	0.0725	0.332	0.592	-	0.924	0.133	0.144
0.3	0.0801	0.287	0.214	-	0.501	0.0882	0.176
0.4	0.0816	0.260	0.101	-	0.361	0.0730	0.202
0.5	0.0816	0.236	0.0580	-	0.294	0.0698	0.237
1	0.0755	0.172	0.0134	-	0.185	0.0889	0.480
2	0.0634	0.121	0.0043	0.0057	0.131	0.141	1.08
3	0.0544	0.0937	0.0024	0.0179	0.114	0.206	1.81

Silica, SiO_2 :- ρ = 2.66 gm./cm.^{3}

Energy E_γ MeV.	σ_a $^{-1}$ cm.	σ $^{-1}$ cm.	τ $^{-1}$ cm.	π $^{-1}$ cm.	μ $^{-1}$ cm.	ΣE_e MeV./cm.	$\bar{E}_e$ MeV.
0.08	0.0473	0.408	0.0950	-	0.503	0.0114	0.0226
0.1	0.0532	0.388	0.0508	-	0.439	0.0104	0.0237
0.2	0.0710	0.325	0.0081	-	0.333	0.0158	0.0476
0.3	0.0784	0.281	0.0029	-	0.284	0.0244	0.0859
0.4	0.0799	0.254	0.0014	-	0.255	0.0325	0.128
0.5	0.0799	0.231	0.0008	-	0.232	0.0403	0.174
1	0.0739	0.169	0.0002	-	0.169	0.0741	0.438
2	0.0621	0.118	0.0001	0.0014	0.119	0.126	1.05
3	0.0532	0.0917	-	0.0043	0.0960	0.168	1.75

Sodium Iodide, NaI :- $\rho = 3.67$ gm./cm^3.

Energy E_γ MeV.	σ_a $^{-1}$ cm.	σ $^{-1}$ cm.	τ $^{-1}$ cm.	π $^{-1}$ cm.	μ $^{-1}$ cm.	ΣE_e MeV./cm.	$\bar{E}_e$ MeV.
0.08	0.0558	0.481	8.82	-	9.30	0.710	0.0764
0.1	0.0627	0.457	4.76	-	5.22	0.482	0.0924
0.2	0.0836	0.383	0.757	-	1.14	0.168	0.147
0.3	0.0923	0.331	0.273	-	0.604	0.110	0.181
0.4	0.0941	0.300	0.129	-	0.429	0.0892	0.208
0.5	0.0941	0.272	0.0742	-	0.346	0.0841	0.243
1	0.0871	0.199	0.0172	-	0.216	0.104	0.483
2	0.0732	0.139	0.0055	0.0068	0.151	0.164	1.09
3	0.0627	0.108	0.0031	0.0214	0.132	0.240	1.82

Water, H_2O :- $\rho = 1.00$ gm./cm^3.

Energy E_γ MeV.	σ_a $^{-1}$ cm.	σ $^{-1}$ cm.	τ $^{-1}$ cm.	π $^{-1}$ cm.	μ $^{-1}$ cm.	ΣE_e MeV./cm.	$\bar{E}_e$ MeV.
0.08	0.0198	0.170	0.0104	-	0.180	0.00241	0.0134
0.1	0.0222	0.162	0.0056	-	0.168	0.00278	0.0165
0.2	0.0296	0.136	0.0009	-	0.137	0.00610	0.0445
0.3	0.0327	0.117	0.0003	-	0.117	0.00990	0.0846
0.4	0.0334	0.106	0.0002	-	0.106	0.0134	0.126
0.5	0.0334	0.0964	0.0001	-	0.0965	0.0167	0.173
1	0.0309	0.0704	-	-	0.0704	0.0309	0.439
2	0.0259	0.0494	-	0.0003	0.0497	0.0521	1.05
3	0.0223	0.0383	-	0.0011	0.0394	0.0691	1.75

APPENDIX II : RANGE-ENERGY DATA FOR MONO-ENERGETIC ELECTRONS IN UNIT-DENSITY MATERIAL.

Explanatory Note:

The values for the ranges in this table have been derived from the collected data of Kamen (1948) for extrapolated ranges of homogeneous electrons in aluminium.

Energy E_c MeV.	Extrapolated Range R_e cm.
0.113	0.0171
0.150	0.0264
0.191	0.0383
0.232	0.0541
0.276	0.0686
0.531	0.184
0.797	0.319
1.078	0.472
1.37	0.629
1.65	0.790

APPENDIX III : MAXIMUM ENERGIES OF COMPTON RECOIL ELECTRONS:

Explanatory Note:

The values for maximum recoil electron energy in this table have been calculated using the relationship quoted in sub-section II.2.:-

$$E_{e\,max} = \frac{E_\gamma}{1 + \frac{0.51}{2E_\gamma}}$$

Gamma-Quantum Energy E_γ MeV.	Maximum Recoil Electron Energy $E_{e\,(max)}$ MeV.
0.363	0.213
0.41	0.250
0.55	0.375
0.638	0.457
0.79	0.60
1.16	0.95
1.32	1.11
1.35	1.14
1.38	1.16
2.76	2.52

APPENDIX IV : METHOD OF CALCULATION OF RATE OF PRODUCTION OF SECONDARY ELECTRONS IN A LUMINOPHOR OF KNOWN DIMENSIONS SUBJECTED TO A KNOWN FLUX OF GAMMA-RADIATION:-

This appendix illustrates the method of setting out the calculation referred to in sub-section II.2. of the rates of production of secondary electrons in a luminophor of known dimensions subjected to gamma-radiation from sources of 1 millicurie of various radio-isotopes at 1 metre. The crystal in this case was of calcium tungstate, cylindrical in form and of mass 0.1244 gm. The complete calculation is shown only for bromine$_{82}$, the rates for other radio-isotopes being calculated in an analogous manner.

Calcium Tungstate: 0.1244 gm.

Mass of crystal = 0.1244 gms.

Average radius of crystal = 0.218 cm.

Density of crystal = 6.06 gm./cm^3.

Hence, thickness of crystal (t) $= \frac{0.1244}{\pi (0.218)^2 . 6.06}$

$= 0.1375$ cm.

			0.4972
		$(0.218)^2$	$\bar{2}.6770$
0.1244	$\bar{1}.0948$	6.06	0.7825
	$\bar{1}.9567$		$\bar{1}.9567$
0.1375	$\bar{1}.1381$		

Number of gamma-quanta incident on crystal per second, assuming one gamma-quantum emitted per disintegration

$$= \frac{3.7.10^7.\pi.(0.218)^2}{4\pi(100)^2}$$

$$= 43.95 \text{ sec}^{-1}$$

$3.7.10^7$	7.5682
$(0.218)^2$	$\bar{2}.6770$
	6.2452
4.10^4	4.6021
43.95	1.6431

Bromine 82.

E_γ	0.55	0.79	1.35
$\log \mu_\gamma$	$\bar{1}.8062$	$\bar{1}.6902$	$\bar{1}.5410$
$\log t$	$\bar{1}.1381$	$\bar{1}.1381$	$\bar{1}.1381$
$\log \mu_\gamma t$	$\bar{2}.9443$	$\bar{2}.8283$	$\bar{2}.6791$
$\log (\log e)$	$\bar{1}.6378$	$\bar{1}.6378$	$\bar{1}.6378$
$\log (\log e^{\mu_\gamma t})$	$\bar{2}.5821$	$\bar{2}.4661$	$\bar{2}.3169$
$\log e^{\mu_\gamma t}$	0.0382	0.0292	0.0207
$\log e^{-\mu_\gamma t}$	$\bar{1}.9618$	$\bar{1}.9708$	$\bar{1}.9793$
$e^{-\mu_\gamma t}$	0.9158	0.9350	0.9535
$(1 - e^{-\mu_\gamma t})$	0.0842	0.0650	0.0465
$\log (1 - e^{-\mu_\gamma t})$	$\bar{2}.9253$	$\bar{2}.8129$	$\bar{2}.6675$
log 43.95	1.6431	1.6431	1.6431
$\log f_\gamma$	0.0000	0.0000	0.0000
Correction for beta filter	$\bar{1}.9828$	$\bar{1}.9854$	$\bar{1}.9893$
Correction for absorption in source	$\bar{1}.9900$	$\bar{1}.9900$	$\bar{1}.9900$
$\log N_e$	0.5412	0.4314	0.2899
N_e	3.48	2.70	1.95

Hence Total Rate of Production of Secondary Electrons

$= 3.48 + 2.70 + 1.95$

$= 8.13$ electrons/second.

PAPERS SUBMITTED.

Scintillation Counting of Gamma-Rays;
Mayneord, W. V., Belcher, E. H.,
'Nature' (London), 165, 930, 1950.

Abnormal Efficiencies in the Scintillation Counting of Gamma Rays;
Belcher, E. H.,
'Nature' (London), 166, 742, 1950.

Measurements of Gamma-Ray Energies with the Scintillation Counter;
Belcher, E. H.,
'Nature' (London), 166, 826, 1950.

Scintillations Produced in Liquids by High-Energy Radiation: Dinaphthyl as a Scintillating Medium;
Belcher, E. H.,
'Nature' (London), 167, 314, 1950.

A Directional Scintillation Counter for Clinical Measurements;
Belcher, E. H., Evans, H. D.,
J. Sci. Instr., 28, 71, 1951.

(*Reprinted from Nature, Vol.* 165, *p.* 930, *June* 10, 1950)

Scintillation Counting of Gamma-Rays

We have investigated the significance of absolute counting-rate in the scintillation measurement of gamma-rays from radium-226, iodine-131, cobalt-60 and sodium-24.

Experiments have been carried out using synthetic crystals of calcium tungstate, chosen for its high density and high absorption coefficient for gamma-rays, in conjunction with a 1*P*21 *R.C.A.* electron-multiplier connected to the crystal via a 'Perspex' light guide. The multiplier tube is cooled in liquid nitrogen. Pulses from the multiplier are amplified (amplifier type 1008 : maximum gain 16,000) and led into a scaler (type 1009) incorporating a discriminator. A thin camera shutter and adjustable iris diaphragm placed between the crystal and 'Perspex' rod enables the scintillations produced in the crystal to be distinguished from spurious effects in the light-guide and photo-multiplier. These effects prove to be of great importance at low pulse discrimination.

The intensity of the gamma-radiation at the crystal was estimated in a standard carbon ionization chamber of known absolute calibration. From the theoretical relationship between ionization current and energy flux for gamma-rays of varying energies, the number of quanta falling on the crystal could be calculated. The number of quanta absorbed in the

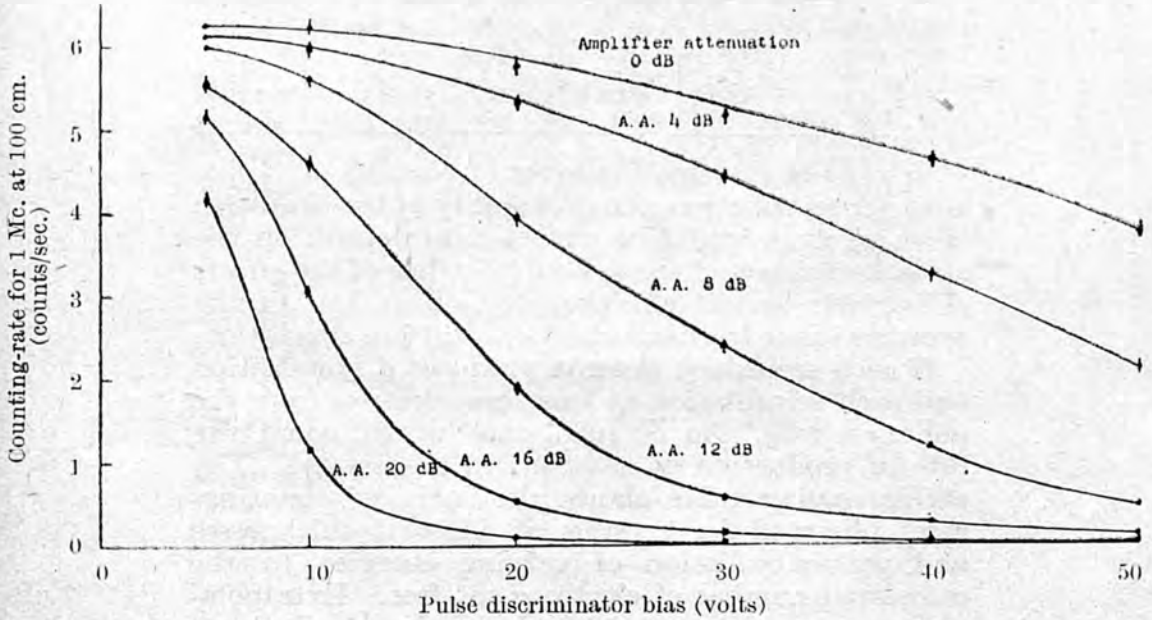

Fig. 1

crystal was then estimated from linear absorption coefficients for calcium tungstate, derived from Klein–Nishina, Fowler–Hulme and Heitler theories for scattering, photo-electric and pair-production coefficients respectively. This number of absorbed quanta will correspond to the number of secondary electrons released in the crystal and hence may be related to the observed counting-rate. The secondary electrons will have a range of energies and produce light flashes of varying sizes.

Fig. 1 shows the effects of applying discrimination at various levels to amplifier gain to the pulses produced by cobalt-60 gamma-rays in a crystal of mass 0·330 gm. The results indicate that the counting-rates tend to a maximum limiting value at zero discrimination, the decrease in counting-rate with discrimination being much sharper at low amplification.

Fig. 2 shows the effects of varying the photo-multiplier voltage at zero discrimination and maximum amplifier gain for crystals of equal cross-section but different thicknesses. It will be noted that the counting-rate is approximately constant in the region of highest voltage available. At high pulse-discrimination the counting-rate is, as frequently reported, sharply dependent on photo-multiplier voltage and low amplifier-gain. The measurements appear to indicate that we are observing all the scintillations which set free at least one electron from the photo-multiplier cathode.

RATIO OF OBSERVED TO CALCULATED COUNTING-RATES

Mass of crystal (gm.)	0·124	0·330	0·495	0·617
Sodium-24	1·13	0·90	0·80	0·73
Cobalt-60	0·91	0·63	0·52	0·46
Iodine-131	0·79	0·56	0·44	0·39

In view of the small number of photons of visible light per scintillation, the probability of the liberation of an electron would be expected to depend on the optical efficiency of the system. Studies of the effects of varying optical efficiency by adjustment of the aperture of the iris diaphragm confirm this suggestion.

If each secondary electron produces a scintillation and each scintillation at least one electron from the photo-cathode, the counting-rate would equal the rate of production of electrons in the crystal. The accompanying table shows the ratio of counting-rates observed for crystals of different thicknesses and gamma-radiation of varying energies to the calculated number of electrons set free. Extrapolation to zero thickness yields observed and calculated rates in approximate agreement. At finite thicknesses some secondary electrons are not observed

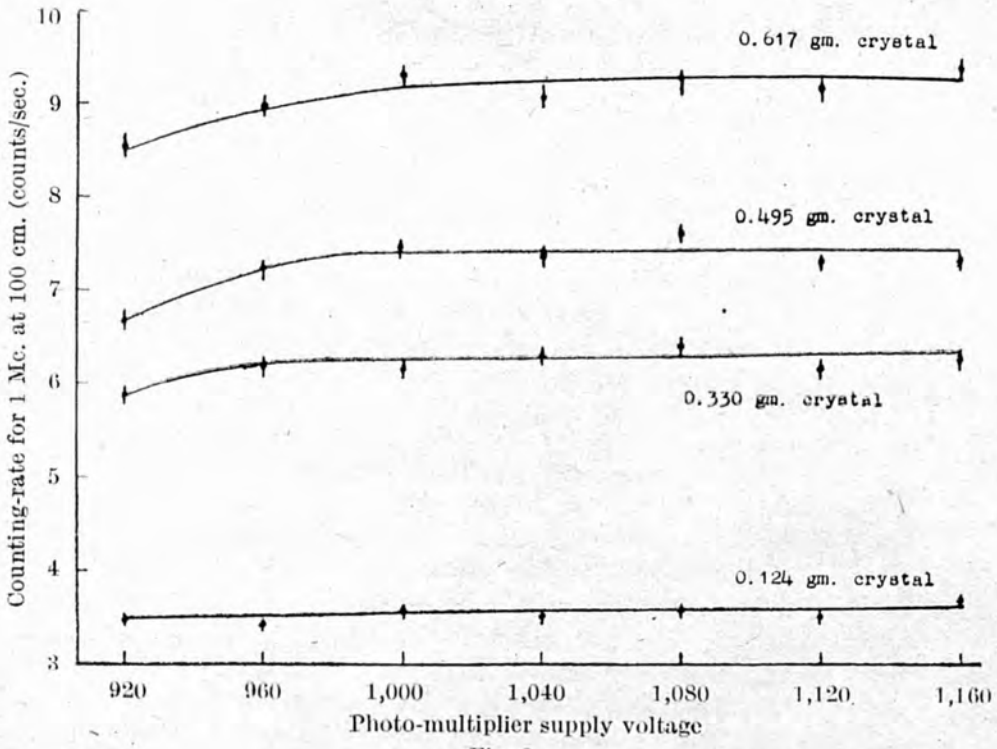

Fig. 2

owing to the absorption of light quanta in the crystal. The experiments, therefore, show that under appropriate experimental conditions the observed counting-rates in a scintillation counter exposed to gamma-rays have absolute significance, and in calcium tungstate are approximately equal to the number of electrons set free in the crystal. This result is in accordance with the known approximately 100 per cent efficiency for counting alpha- or beta-particles.

We wish to acknowledge the kindness of Mr. N. Veall, who loaned the synthetic calcium tungstate crystals used, and of our colleague, Mr. W. K. Sinclair, who measured the activity of the radioactive sources.

W. V. Mayneord
E. H. Belcher

Physics Department,
Royal Cancer Hospital,
London, S.W.3.
Feb. 23.

[1] Kallman, H., and Broser, I., *Z. Naturforsch.*, **2***a*, 439 and 642 (1947).
[2] Moon, R. J., *Phys. Rev.*, **73**, 1210 (1948).
[3] Kallman, H., *Phys. Rev.*, **75**, 623 (1949).
[4] Jordan, W. H., and Bell, P. R., *Nucleonics*, 30 (October 1949).

Printed in Great Britain by Fisher, Knight & Co., Ltd., St. Albans

(*Reprinted from Nature, Vol.* 166, *p.* 826, *November* 11, 1950)

Measurement of Gamma-Ray Energies with the Scintillation Counter

THE use of the scintillation counter as a gamma-ray spectrometer has been described by Pringle, Roulston and Taylor[1], Johannson[2], MacIntyre and Hofstadter[3], Cavanagh[4] and other workers. However, the resolutions obtained have in general been poor, and quantitative measurements of gamma-ray energies and relative intensities difficult to make.

Lack of resolution may be attributed to three main effects. First, the optical efficiency of the system will vary through the volume of the crystal, and the number of photons incident upon the photomultiplier cathode will not be constant for scintillations of equal size produced at different positions in the crystal. Secondly, some secondary electrons may escape from the crystal before expending all their energy; mono-energetic secondary electrons thus may not produce scintillations of uniform size. Finally, the size of pulse at the photomultiplier output will be subject to large statistical variations where only a few photons are incident upon the photocathode per scintillation.

These effects may be reduced by the use of small crystals of high density in a system the optical efficiency of which is as high as possible. Calcium tungstate is particularly suitable having a density of 6·06 gm./c.c., and the accompanying graph shows the differential curve of counting-rate against pulse-discriminator setting obtained when a small (0·124 gm.) crystal of this material placed in direct contact

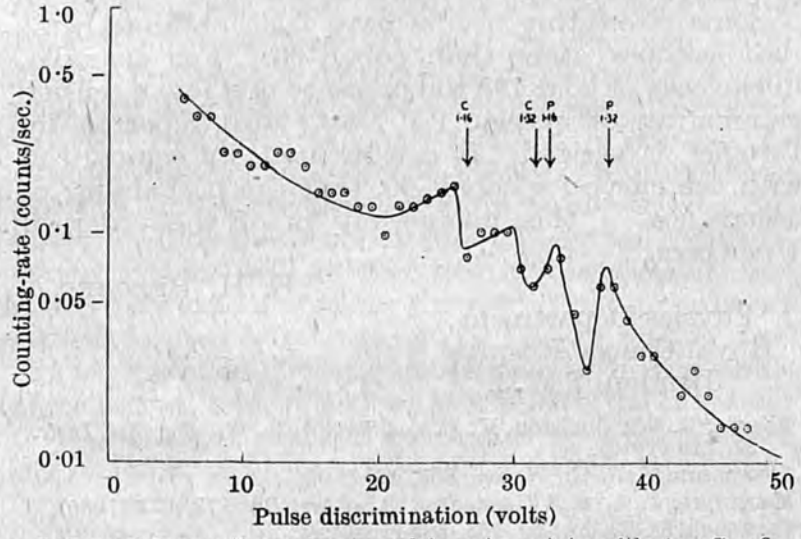

Differential counting-rates in calcium tungstate with 1 mC. of cobalt-60 at 1 m. Photomultiplier voltage 1,080; amplifier gain 1,600; mass of crystal 0·1244 gm.; resolving time 200 μsec.

with the envelope of an uncooled 1*P*21 photomultiplier was irradiated with the gamma-radiation of cobalt-60. The pulses at the photomultiplier output were amplified in a linear amplifier (type 1008) operating at a gain of 1,600, and recorded in a counting-rate meter (type 1037*A*) incorporating a pulse discriminator circuit calibrated directly in volts. The integral curve of counting-rate against pulse-discriminator setting was differentiated by taking the increment in counting-rate over each one-volt step in pulse discrimination. All counting-rates are corrected for background effects.

The twin peaks and edges due to the photo-electric absorption and Compton scattering of the two gamma-rays of energy 1·16 and 1·32 MeV. are clearly resolved. The arrows give the theoretical position of these peaks and edges calculated from the observed position of the 1·32-MeV. photo-electron peak, assuming a linear relationship between secondary electron energy and pulse size. The rise in the curve at low pulse discrimination may be attributed to degenerate radiation scattered from the photomultiplier housing and crystal mounting.

Similar measurements have been made using a small crystal of thallium-activated potassium iodide. Owing to the lower density (3·13), resolution is reduced, and a large increase in counting-rate appears below 20 volts discrimination owing to the single-photon phosphorescent emission of this material; it is of interest that the gradient of this portion of the curve is similar to that of the noise background of the photomultiplier, showing that it represents the emission of single electrons at the photocathode. This confirms the single-photon character of the phosphorescent emission of the luminophor[5].

Some interesting results have been obtained with radioisotopes other than cobalt-60. For example, in the case of gold-198 the presence of a low-intensity gamma-ray of energy 1·1 MeV., also reported by Pringle[6], is verified. It is estimated, by comparison with the curve for cobalt-60, that the probability of occurrence of this gamma-ray is of the order of 1 per cent.

E. H. Belcher

Physics Department,
Royal Cancer Hospital,
London, S.W.3.

[1] Pringle, R. W., Roulston, K. I., and Taylor, H. W., *Rev. Sci. Instr.*, **21**, 216 (1950).
[2] Johannson, S. A. E., *Nature*, **165**, 396 (1950).
[3] MacIntyre, J. A., and Hofstadter, R., *Phys. Rev.*, **78**, 617 (1950).
[4] Cavanagh, P. E., *Nature*, **165**, 889 (1950).
[5] Belcher, E. H., [**166**, 742 (1950)].
[6] Pringle, R. W., *Nature*, **166**, 11 (1950).

Printed in Great Britain by Fisher, Knight & Co., Ltd., St. Albans

(*Reprinted from Nature, Vol.* 166, *p.* 742, *October* 28, 1950)

Abnormal Efficiencies in the Scintillation-counting of Gamma-Rays

In an earlier communication, Mayneord and Belcher[1] have shown that, under appropriate conditions of high gain and low pulse-discrimination, the counting-rates for scintillations observed in a small calcium tungstate crystal irradiated by gamma-radiation approximate to the rates of absorption of gamma-ray quanta in the crystal calculated from theoretical linear absorption coefficients.

Similar observations on small crystals of thallium-activated potassium iodide show, however, that the counting-rates in this material may be many times greater than the calculated absorption-rates. This anomalous behaviour of thallium-activated potassium iodide, first reported by Freedman, Smaller and May[2], has been studied using experimental arrangements identical to those already described[1].

Fig. 1 shows the ratios, R, of the observed maximum counting-rates to the calculated rates of absorption of gamma-quanta derived from Klein–Nishina, Fowler–Hulme and Heitler theories, plotted as a function of crystal mass for crystals of equal cross-section, but varying thickness. Appropriate corrections have been made for background effects and scaler dead-time. Measurements were made for the gamma-radiation from various radioisotopes.

It will be seen that the observed rates are considerably greater than those calculated, and that the ratio of the two increases with increase in energy of the exciting radiation. Further studies have shown that this effect is due to electron-trapping levels in the luminophor lattice; each gamma-quantum absorbed may thus produce a delayed phosphorescent emission consisting of single photons, in addition to a short-duration fluorescent pulse containing many photons. Of these single photon pulses, a fraction, determined by the resolving time and optical efficiency of the system, will be recorded in the counter.

We may expect that the number of phosphorescent centres excited by a single gamma-quantum absorbed in the crystal will depend on the energy of its secondary electron, and indeed will be linearly proportional to this energy. This is confirmed in Fig. 2, where the ratio, R, of observed to calculated counting-rates for various radioisotopes in a crystal of mass 0·126 gm. is plotted against the calculated mean energy, $\overline{E}_e$, of the secondary electrons produced in the crystal. As expected, the experimental values fall approximately on a straight line, which when

extrapolated intersects the vertical axis at unity, showing that the number of phosphorescent pulses, $R - 1$, counted for each quantum absorbed is linearly proportional to $\bar{E}_e$. The slight deviation from linearity in the case of the high-energy radiation of sodium-24 may be interpreted as being due to the escape from the crystal of some of the more energetic secondary electrons produced by this isotope before they have expended all their energy in exciting phosphorescent centres ; the fall in the ratio of observed to calculated counting-rate apparent in Fig. 1 in the case of the smallest crystal studied may also be explained in terms of this effect.

Studies on the effect of scaler resolving time on counting-rate in thallium-activated potassium iodide show that the phosphorescent emission obeys a non-exponential decay law ; it falls to half its initial value in 2·5 msec., but persists for many minutes after the initial excitation event. Further observations on synthetic calcium tungstate indicate that this material also shows an impurity-activated phosphorescent emission, but of low intensity and of

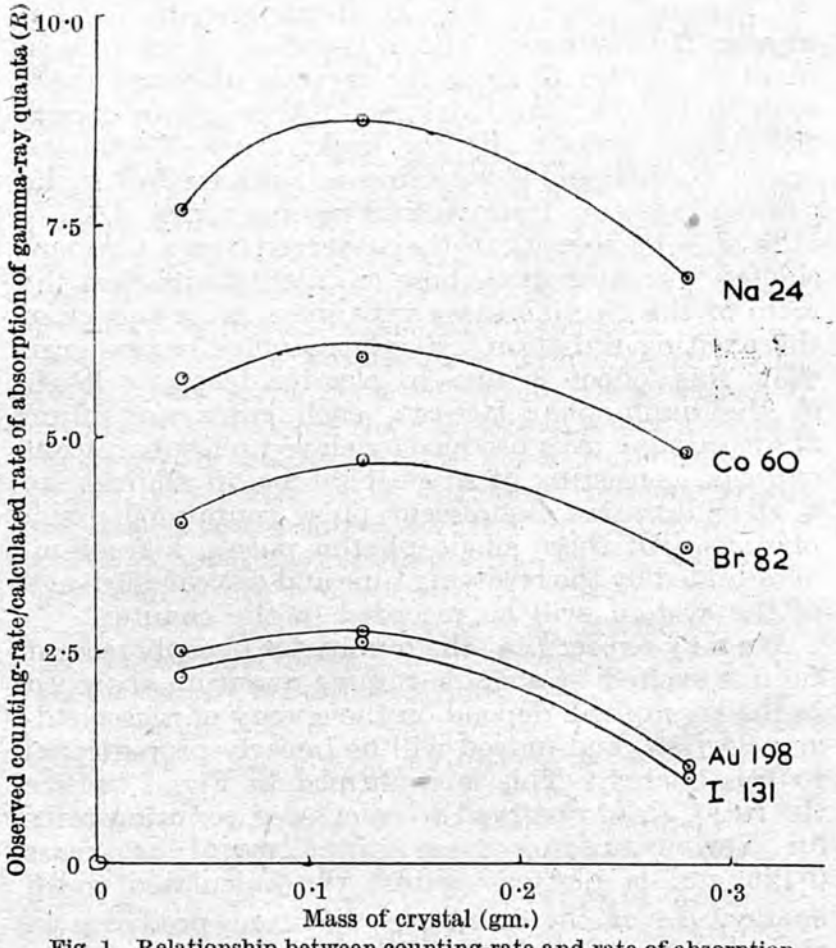

Fig. 1. Relationship between counting-rate and rate of absorption of gamma-ray quanta in thallium-activated potassium iodide. Resolving time, 10 μsec.; photo-multiplier voltage, 1,080; amplifier gain, 16,000

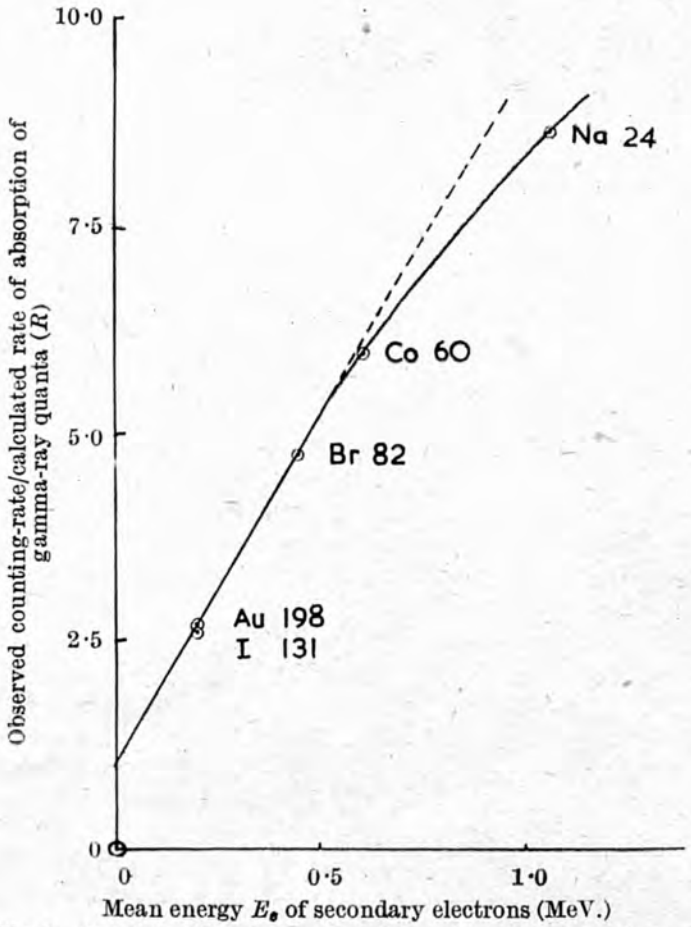

Fig. 2. Relationship between counting-rate and energy of secondary electrons in thallium-activated potassium iodide. Resolving time, 10 μsec.; photo-multiplier voltage, 1,080; amplifier gain, 16,000; mass of crystal, 0·126 gm.

short duration. The decay in this case appears exponential, with a half-life of 20 μsec. (to be compared with the approximate figure of 100 μsec. quoted by Garlick[3]). Thus, it is not appreciable at counter resolving times greater than 100 μsec. Samples of purified anthracene and of anthracene-activated naphthalene have also been examined; but contrary to the reports of Cross[4] no phosphorescent emission has been detected in the samples tested.

Thanks are due to Mr. J. Sharpe, of the Atomic Energy Research Establishment, Harwell, for the gift of thallium-activated potassium iodide crystals, and to Dr. G. F. J. Garlick, of the University of Birmingham, for a sample of purified anthracene.

E. H. Belcher

The Royal Cancer Hospital,
Fulham Road, London, S.W.3.

Aug. 3.

[1] Mayneord, W. V., and Belcher, E. H., *Nature*, **165**, 930 (1950).
[2] Freedman, M., Smaller, B., and May, J., *Phys. Rev.*, **77**, 759 (1950).
[3] Garlick, G. F. J., "Luminescent Materials", 94 (Oxf. Univ. Press, 1949).
[4] Cross, W. G., *Phys. Rev.*, **78**, 185 (1950).

Printed in Great Britain by Fisher, Knight & Co., Ltd., St. Albans.

(*Reprinted from Nature, Vol.* 167, *p.* 314, *February* 24, 1951)

Scintillations Produced in Liquids by High-Energy Radiation: αα′ Dinaphthyl as a Scintillating Medium

In efforts to find a suitable liquid medium to replace the crystalline luminophors at present used in scintillation counters for gamma-ray measurements, a wide variety of solutions of organic compounds known or suspected to have fluorescent properties has been examined.

In these experiments, a small sample (1 ml.) of each liquid to be tested was placed in a flat-bottomed cylindrical phial of resistance glass which was then mounted in a light-tight housing in close proximity to the photo cathode of a 1*P*21 photomultiplier tube, and irradiated by gamma-rays from a standard source (1·5 mC.) of cobalt-60 at a fixed distance (6 cm.) from the sample. The resulting pulses were amplified in a linear amplifier (type 1008) and counted in a rate-meter (type 1037*A*).

A 'figure of merit' was assigned to each liquid tested, this being the observed counting-rate in counts per second due to the 1-ml. sample under standard conditions of amplifier gain and pulse discrimination corrected for counter resolving-time and background effects.

The more important results are summarized in the accompanying table. All the pure solvents examined showed slight but measurable luminescence, which must in some cases be attributed to small amounts of impurities either present in the solvents before irradiation or formed in them by chemical radiation effects. The figure of merit of many solutions showed a maximum value at a certain optimum concentration of solute, falling at higher concentration owing to quenching effects. In yet other solutions, the figure of merit increased continuously up to the saturation concentration of the solute. For comparison, approximate figures of merit for samples of crystalline calcium tungstate and of anthracene of mass equal to that of the liquid samples are included in the table.

Of the systems investigated, αα′ dinaphthyl in benzene is the most promising and will be seen to be superior to *p*-terphenyl in benzene, the use of which in this connexion has been suggested by Reynolds *et al.*[1] and by Kallmann and Furst[2]. A saturated solution of αα′ dinaphthyl in benzene has a figure of merit greater than that of synthetic crystalline calcium tungstate and half that of crystalline anthracene;

FIGURES OF MERIT OF SCINTILLATING LIQUIDS

System	Optimum concentration of solute (gm./litre)	Figure o merit at optimum concentration
$\alpha\alpha'$ Dinaphthyl/benzen	Saturation	16,400
p-Terphenyl/benzene	Saturation	15,600
m-Terphenyl/benzene	Saturation	9,400
Phenyl β-naphthylethylene/benzene	2·7	6,700
β-Naphthylamine/benzene	5·0	5,950
α-Naphthylamine/benzene	2·8	5,050
$\beta\beta'$ Dinaphthyl/benzene	6·0	3,900
$\beta\beta'$ Dinaphthylethane/benzene	Saturation	3,200
1.3.5. Triphenylbenzene/benzene	Saturation	2,500
β-Naphthol/benzene	1·5	2,200
α-Naphthol/benzene	2·5	1,700
Naphthalene/benzene	Saturation	1,460
Anthracene/benzene	2·2	1,460
Benzene	—	910
Water (distilled)	—	620
Calcium tungstate (crystalline		12,000
Anthracene (crystalline)		37,000

these figures refer, of course, to the counting-rates produced by the gamma-radiation of cobalt-60. It should be emphasized that for gamma-radiation of other energies the relative counting-rates may be different owing to differences in density and mean atomic number of the luminophors. In particular, the counting-rates for low-energy gamma-rays in the energy-range 0·1–0·5 MeV. will be low in the case of the liquid systems studied. Further experiments are being carried out on $\alpha\alpha'$ dinaphthyl and its derivatives, and a full account of the work will be published elsewhere.

I wish to express my thanks to Prof. W. V. Mayneord, director of the Physics Department, for permission to carry out this work, and to Mr. J. Everett, of the Chester Beatty Research Institute, Royal Cancer Hospital, for providing samples of a number of organic compounds, including the dinaphthyls.

E. H. BELCHER

The Royal Cancer Hospital,
Fulham Road,
London, S.W.3.
Nov. 17.

[1] Reynolds, G. T., Harrison, F. B., and Salvini, G., *Phys. Rev.*, **78**, 488 (1950).
[2] Kallmann, H., and Furst, M., *Phys. Rev.*, **79**, 857 (1950).

Printed in Great Britain by Fisher, Knight & Co., Ltd., St. Albans.

Reprinted from the *Journal of Scientific Instruments*, VOL. 28, pp. 71–75, MARCH 1951

A directional scintillation counter for clinical measurements

By E. H. BELCHER, M.A., and H. D. EVANS, B.Sc., Ph.D., A.Inst.P., Physics Department, Royal Cancer Hospital, London, S.W.3

[*Paper received* 27 *October*, 1950]

A scintillation counter designed for clinical measurements is described. The instrument incorporates a liquid nitrogen cooled photo-multiplier and a thallium activated potassium iodide crystal separated from the photo-multiplier by a Perspex light guide. Details are given of the absolute counting rates obtainable with five radio-isotopes commonly used in clinical work and also of the directional properties of the instrument. The counting efficiency for the gamma radiation from iodine 131, expressed as counts/quantum incident on the crystal, is 31·6%.

The scintillation counter as a device for observing alpha particles was first described as long ago as 1905 by Crookes; its extension to the measurement of gamma radiation, made possible by the development in recent years of the photo-multiplier tube as a sensitive detector of low intensity light flashes, has been described by numerous workers.[1–8] In this application it possesses several advantages over instruments based on Geiger-Müller counters or ionization chambers, notably in its increased sensitivity and in the small size of the sensitive volume within which the radiation flux is measured. Gamma counting efficiencies of 30% are easily obtainable, while those of Geiger-Müller counters rarely exceed 5%. The small size of the detecting element permits the design of improved directional counters for the localization of radioactive materials in the human body. This paper describes the construction and characteristics of such a directional scintillation counter, designed and built at the Royal Cancer Hospital. This instrument has been used continually for clinical measurements in the Physics Department of that hospital for the past nine months, during which time it has proved entirely reliable. In Table 1, the counting rates obtained in the counter when irradiated with the gamma radiation from point sources of 1 mc of four commonly used radioactive isotopes at one metre distance in air, are compared with the corresponding rates in a Geiger-Müller tube of standard type (G.E.C. gamma counter Type G.4). All values are fully corrected for background and resolving time.

Table 1. *Comparison of counting rates*

Isotope	*Counting Rate (unshielded)* *Scintillation Counter*	*Geiger-Müller Counter*
I^{131}	77·4 counts/sec	4·58 counts/sec
Br^{82}	296·0 counts/sec	36·8 counts/sec
Co^{60}	206·0 counts/sec	35·0 counts/sec
Na^{24}	278·0 counts/sec	59·0 counts/sec

The increased sensitivity of the scintillation counting instrument is clearly apparent.

DESIGN

The counter was designed for clinical work and therefore incorporates certain features, such as mobility, which would be unnecessary in a laboratory instrument. One of the chief difficulties to be overcome is the high "noise" background of the photo-multiplier. To achieve maximum efficiency, sufficient amplification must be employed to record every scintillation in the crystal which releases a single electron at the cathode of the multiplier; this clearly also permits counting of every thermal electron released at the cathode. The "noise" background of the tube at room temperature, under these conditions, is of the order of 6 000 to 8 000 counts/sec, and it is therefore impractical to count low levels of activity against it. The most obvious method of reducing the background is to cool the tube, and in the instrument described this is the course which has been adopted, liquid nitrogen being used as the refrigerant. At this temperature (— 196° C) the thermal background of the tube amounts to rather less than 1 count/sec. Cooling, however, introduces a complication, namely that for clinical purposes the part of the counter in contact with the skin must be at room temperature. The problem is readily solved by mounting the crystal at the end of a Perspex light-guide, and introducing a thermally insulating section in the surrounding light-tight tube. This arrangement also meets the requirement of providing the probe of fairly small dimensions necessary for clinical work. It should be noted that if the crystal is situated very close to the photo-multiplier the tube need not be cooled since the efficiency of light-collection is then much higher and the background can be reduced by raising discriminator voltage. The photo-multiplier itself is sensitive to gamma radiation and Perspex scintillates to a limited extent. Lead shielding must therefore be provided for both.

The choice of crystal is largely a matter of compromise.[9] The material should be of high density and should contain atoms of high atomic number so that its absorption coefficient for gamma radiation is high. The crystal should be large and transparent to its own light radiation, the wavelength of which should lie near the maximum sensitivity of the tube (i.e. of about 4 200 A). A polycrystalline mass can be used, but its efficiency is obviously less than that of a single crystal, due to scattering, refraction and reflexion at interfaces. A suitable material, used in early experiments, is calcium tungstate; its density is fairly high (6·06 gm/c.c.), but it is difficult at present to obtain large crystals other than in the form of rods, about 3 mm in diameter. Natural calcium tungstate (scheelite) generally consists of a mass

of small, almost opaque crystals and thicknesses above 1 or 2 mm are not efficient on account of the absorption of light.

Naphthalene and anthracene are both well known as luminophors and with care can be produced in large single crystals. Their efficiencies for counting gamma rays are, however, relatively small owing to their low densities and mean atomic numbers. The most suitable materials used so far are the alkali halides which can be activated by the addition of a small percentage of thallium halide; it is possible to grow large crystals by a method outlined by Taylor.[10] A crystal of potassium iodide (with $\frac{1}{2}\%$ thallium iodide) is used in the instrument described. This material has a density of 3·13 gm/c.c. and a fairly high absorption coefficient for low energy gamma radiation owing to the presence of iodine atoms. The presence of small amounts of the beta and gamma active isotope K40 in naturally occurring potassium is a distinct disadvantage producing a background of some 30 counts/sec in a crystal of dimensions 10 × 11 × 7 mm. Sodium iodide[11] is clearly an improvement in this respect, but being highly deliquescent cannot be used unless protected from the air.

With regard to photo-multiplier tubes, the choice lies basically between the R.C.A. type 1P21 (or the Mazda type 27 M.1) and the E.M.I. types 5311 and 5060. The former is a nine stage tube with a gain of the order of 10^6 and the latter have eleven stages with a gain of the order of 10^8. The R.C.A. type 1P21 was chosen for the present application on account of its smaller dimensions.

CONSTRUCTION

A sectioned diagram of the counter is shown in Fig. 1, and an external view in Fig. 2. The crystal *A* (Fig. 1) is potassium iodide, 10 mm in diameter and 7 mm thick, cut from a single crystal 10 × 11 × 7 mm. It is cemented to the polished end of a $\frac{1}{2}$ in diameter Perspex rod *B* by means of Canada Balsam, and an aluminium foil reflector is cemented on the face remote from the rod. A lens turned on the other end of the rod focuses the light on the cathode of the photo-multiplier *C* which is mounted on a special Perspex base *K*, supported by a brass cylinder through the top of which pass two brass tubes carrying the cables *P* and *R*. The resistor chain *L* and output capacitor *M* are fitted directly to the base. This whole assembly slides into a second container, the joint being made air-tight and light-tight by a Neoprene washer *N*; the Perspex rod enters this container near its lower end and the light-tight enclosure is completed by the Duralumin tube *E* (in which the rod is centred by polished Duralumin rings) and the Keramot thermal insulator *G*. The multiplier enclosure is entirely surrounded by a liquid nitrogen jacket *H*. The vertical brass tubes mentioned earlier carry the output cable *P* and the e.h.t. cable *R* above the level of the liquid nitrogen, and the rubber sleeves *S* prevent seepage of condensed water into the multiplier enclosure. The liquid nitrogen container is suspended from the Keramot ring *U* which supports and centres it in the outer case of the instrument; the space *V* is filled with cotton wool lagging to reduce the liquid nitrogen evaporation rate. The crystal is surrounded by a lead shield and collimator *D*, the end of the tube *E* being closed by a thin Duralumin cap. The photo-multiplier and Perspex rod are shielded from direct gamma radiation by the lead screens shown in Fig. 2.

The apparatus was designed primarily for the attempted localization of cerebral tumours by injection of di-iodofluorescein containing I^{131}.[12, 13] In this application the pointer of the Perspex cap *F* and the detachable Duralumin arm shown in Fig. 2 indicate the axis of the cone of collimation of the instrument, thus permitting accurate positioning along fixed lines through the human head. However, the apparatus is readily adaptable to other types of investigation. The counter

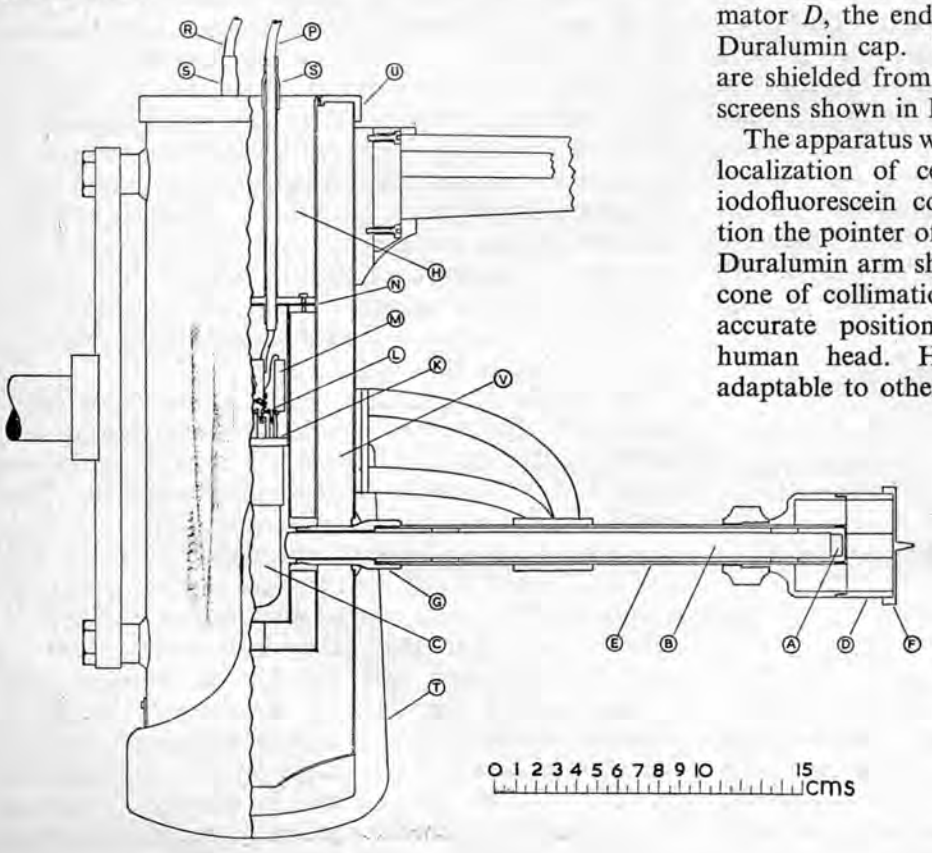

Fig. 1. Scintillation counter

A, crystal; *B*, Perspex light-guide; *C*, photo-multiplier; *D*, lead collimator; *E*, Duralumin tube; *F*, Perspex cap; *G*, thermal insulator; *H*, liquid nitrogen container; *K*, photo-multiplier base; *L*, resistor chain; *M*, output capacitor; *N*, Neoprene washer; *P*, output cable; *R*, e.h.t. supply cable; *S*, rubber sleeve; *T*, lead screening; *U*, Keramot ring; *V*, lagging.

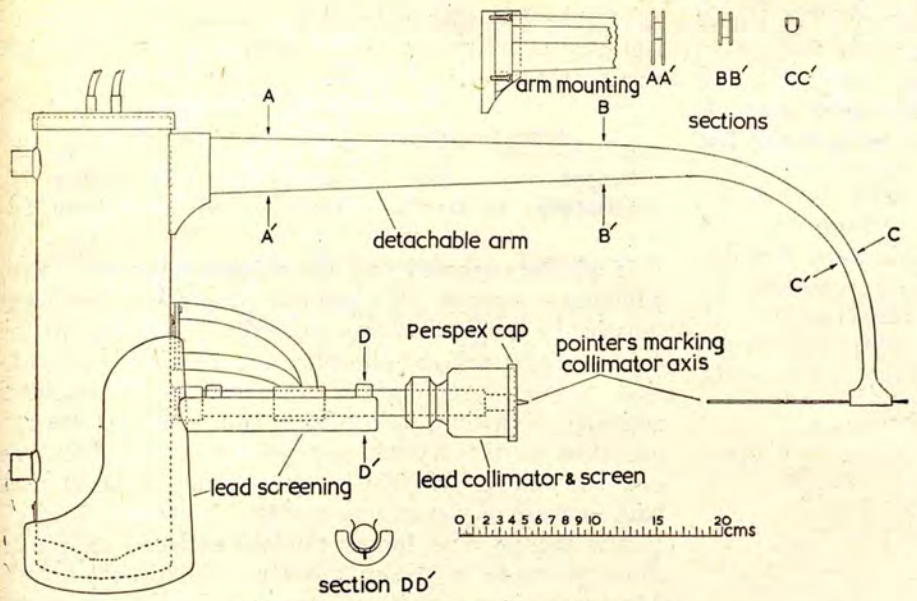

Fig. 2. Scintillation counter, external view

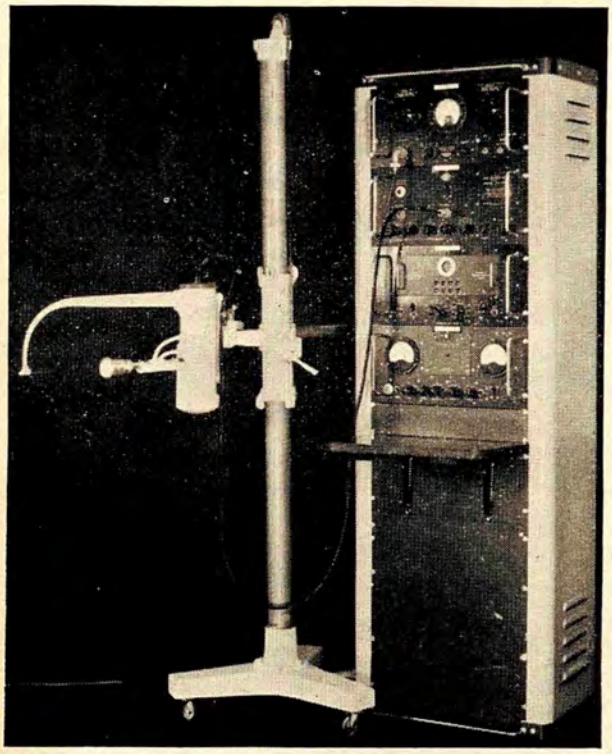

Fig. 3. The complete apparatus

is fitted to a mobile stand (Fig. 3) allowing vertical and horizontal movements and a rotation about the vertical pillar.

The electronic equipment is shown schematically in Fig. 4, the units being fitted into the rack shown on the right of Fig. 3. Connexions between the counter and the rack units are made by two 8 ft lengths of $\frac{1}{4}$ in diameter, 70 Ω screened cable. The circuit of the multiplier resistance chain is shown in Fig. 5. The output capacitor in the refrigerated enclosure does not appear to be affected by the low temperature and it has not proved necessary to provide a drying agent in this space; the coolest part of the enclosure is the outer wall, on to which water vapour probably freezes during the first few minutes of cooling without affecting the optical surfaces.

PERFORMANCE

The gain of the 1P21 photomultiplier, working at 100 V per stage, is stated by the makers to be 2×10^6. The amplifier type 1008 works at a gain of 16 000 times, and the discriminators in scaler and

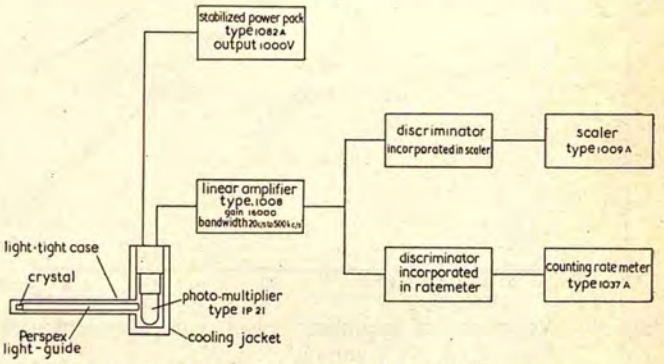

Fig. 4. Schematic diagram of scintillation counter

The type numbers refer to electronic units designed and supplied by the Atomic Energy Research Establishment, Harwell.

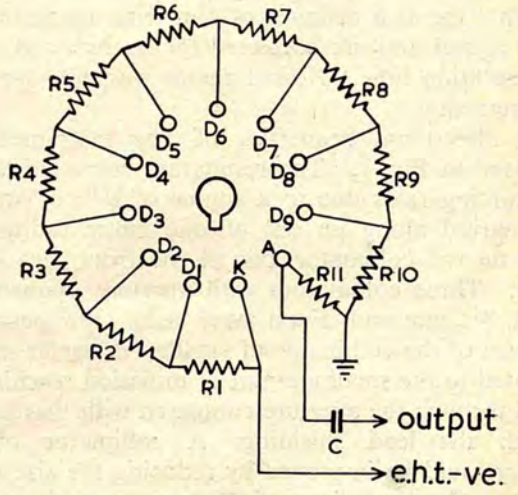

Fig. 5. Photomultiplier base

R_1 to R_{10}, 4·7 MΩ. R_{11}, 47 kΩ. C, 0·001 μF.

ratemeter are set at their minimum value of 5 V. Under these conditions, the total background of the instrument amounts to approximately 30 counts/sec when no active material is in the vicinity; the photomultiplier accounts for less than 1 count/sec, the remainder being largely due to the activity of K40 in the crystal.

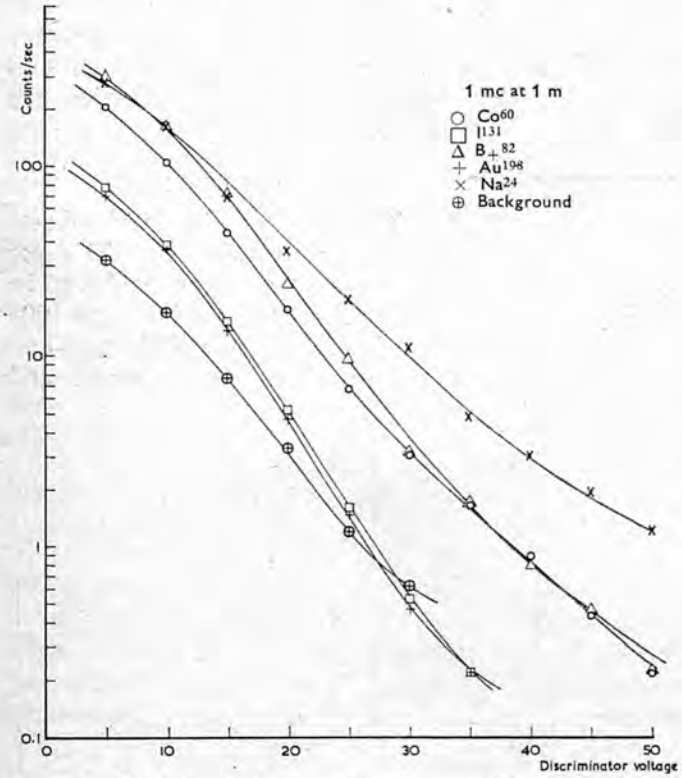

Fig. 6. Variation of counting rates with discriminator voltage

The variation of counting rate with discriminator voltage for five radioactive isotopes is shown in Fig. 6; the curves show the counting rates due to sources of strength 1 mc at a distance of 1 m from the front face of the crystal and are corrected for background effects and resolution time. No collimator was used for these measurements.

The directional properties of the instrument are illustrated in Fig. 7. The results are corrected to give the counting rates due to a source of I^{131}, of strength 1 mc moved along an arc of one metre radius, with centre on the collimator axis at the front face of the crystal. Three collimators with aperture diameters of 12 mm, 8·5 mm and 5 mm were used; the poor performance of the collimator of smallest diameter may be attributed to the small amount of radiation reaching the crystal through the aperture compared with that passing through the lead shielding. A collimator of this aperture could be improved by reducing the size of the crystal to the dimensions of the aperture or by using a material of higher atomic number than lead (e.g. uranium) for screening.

The absolute efficiencies of the counter for four radioisotopes, expressed as counts/quantum incident on the crystal, are given in Table 2.

Table 2. *Absolute efficiencies of the counter*

Isotope	I^{131}	Br^{82}	Co^{60}	Na^{24}
Efficiency	31·6%	42·6%	44·5%	60·1%

It will be observed that the efficiency increases with gamma-ray energy, although the absorption coefficient falls in the range of energy studied. This is due to the existence of a delayed phosphorescent emission in addition to the instantaneous fluorescence of thallium activated potassium iodide;[14, 15] thus each gamma ray absorbed in the crystal may produce more than one count in the scaler. The magnitude of this effect rises with increase of gamma-ray energy. The pulse distribution is therefore no longer random and due allowance must be made in the calculation of statistical errors. Moreover, since the phosphorescence persists for several minutes, care must be taken to avoid exposing the crystal to a sudden heavy flux of radiation which will result in an apparent rise in background. This effect is negligible at counting rates below about 1 000 counts/sec.

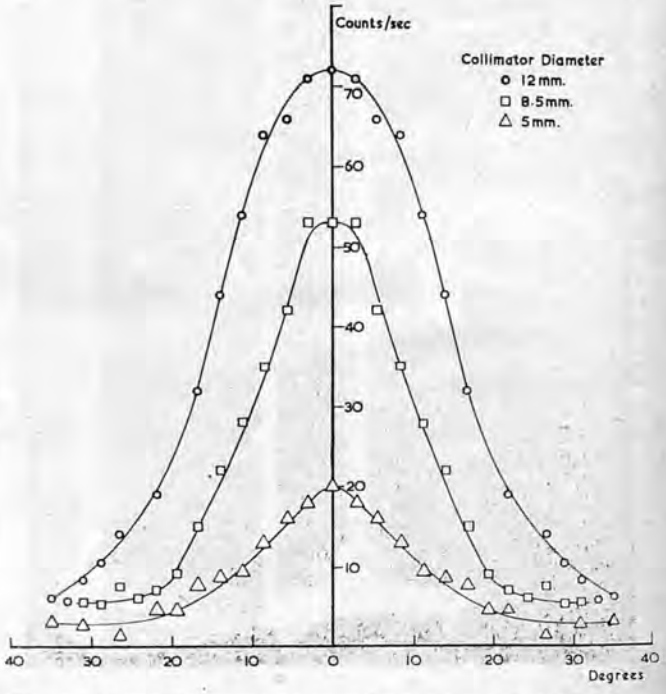

Fig. 7. Polar diagrams of counter for 1 mc of I^{131} at 1 m

ACKNOWLEDGMENTS

The authors wish to express their thanks to Professor W. V. Mayneord for his interest, advice and encouragement throughout the course of this work, to Mr. H. C. Hodt and Mr. H. J. Hodt for the construction of the instrument, and to the Medical Research Council which supported these investigations.

REFERENCES

(1) COLTMAN, J. W. *Proc. Inst. Radio Engrs.*, **37,** p. 671 (1949).
(2) JORDAN, W. H., and BELL, P. R. *Nucleonics*, **5** (4), p. 30 (1949).
(3) CURRAN, S. C., and CRAGGS, J. D. *Counting Tubes* (London: Butterworths Ltd.)
(4) MAYNEORD, W. V., and BELCHER, E. H. *Supplement to Brit. J. Radiol.*, p. 259 (1950).
(5) MORTON, G. A., and MITCHELL, J. A. *Nucleonics*, **4** (1), p. 16 (1949).
(6) ROBINSON, L. B., and ARNOLD, J. R. *Rev. Sci. Instrum.*, **20,** p. 549 (1949).
(7) MAYNEORD, W. V., and BELCHER, E. H. *Nature, Lond.*, **165,** p. 930 (1950).
(8) HOYT, R. C. *Rev. Sci. Instrum.*, **20,** p. 178 (1949).
(9) *Nucleonics*, **6** (5), p. 70 (1950).
(10) TAYLOR, D. *J. Sci. Instrum.*, **27,** p. 81 (1950).
(11) HOFSTADTER, R. *Phys. Rev.*, **75,** p. 796 (1949).
(12) BELCHER, E. H., and EVANS, H. D. In the press. *Brit. J. Radiol.*
(13) DE WINTER, J. G. In the press. *Brit. J. Radiol.*
(14) FREEDMAN, M., SMALLER, B., and MAY, J. *Phys. Rev.*, **77,** p. 759 (1950).
(15) BELCHER, E. H. *Nature, Lond.*, **166,** p. 742 (1950).

UNWIN BROTHERS LIMITED, WOKING AND LONDON